

AD-A075 748

AEROSPACE CORP EL SEGUNDO CA SPACE SCIENCES LAB

F/G 4/1

A SURVEY OF CURRENTLY IMPORTANT EMPIRICAL THERMOSPHERIC MODELS, (U)

SEP 79 D R HICKMAN , B K CHING , C J RICE

F04701-78-C-0079

UNCLASSIFIED

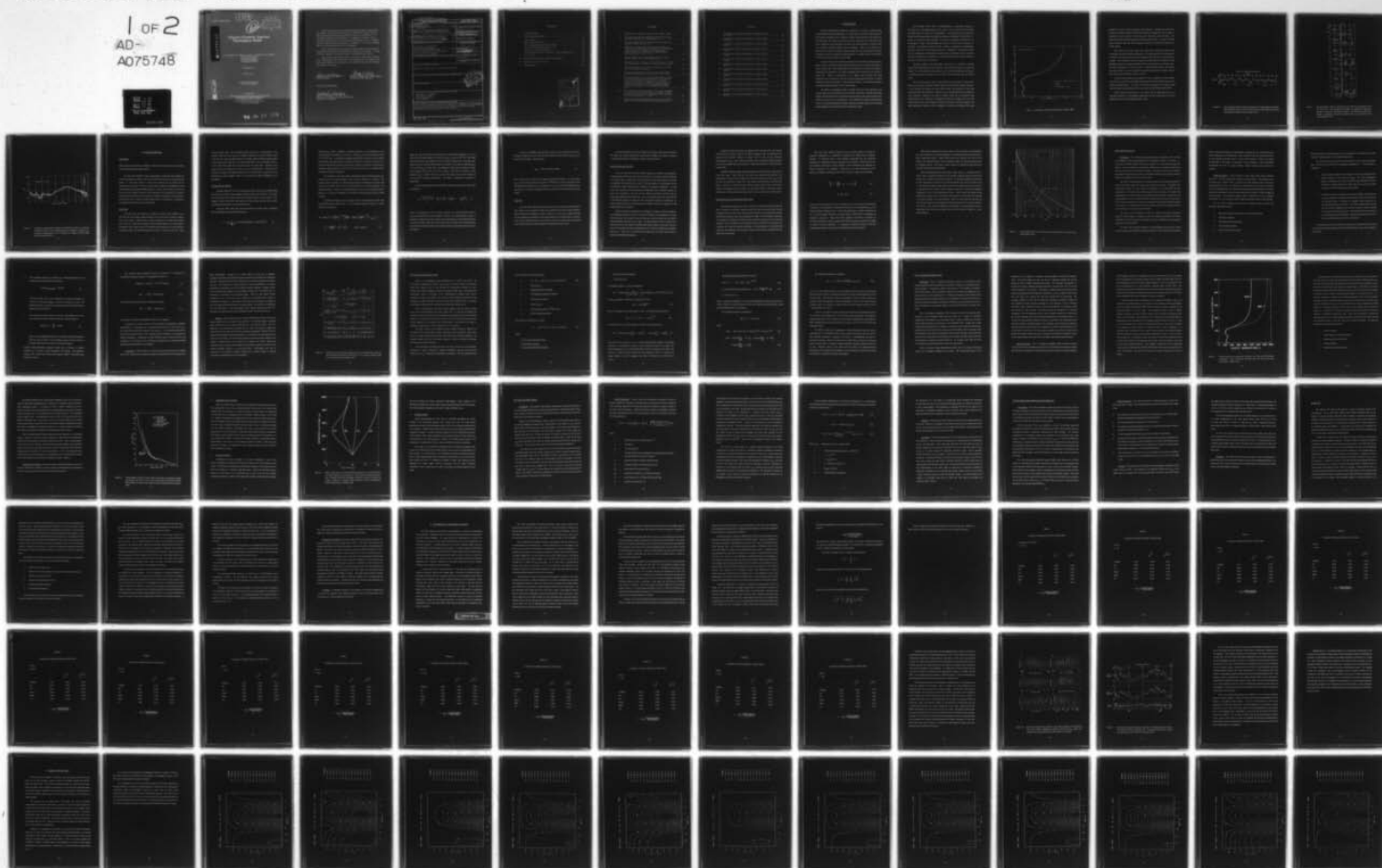
TR-0079(4960-04)-2

SAMS0-TR-79-57

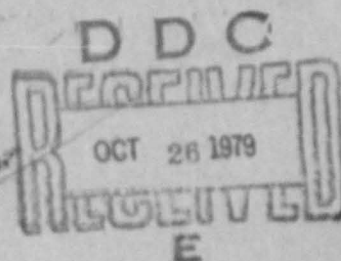
NL

1 OF 2

AD-A075748



LEVEL 11



AD A075748

A Survey of Currently Important Thermospheric Models

D. R. HICKMAN, B. K. CHING, C. J. RICE, L. R. SHARP, and J. M. STRAUS

Space Sciences Laboratory
Laboratory Operations
The Aerospace Corporation
El Segundo, Calif. 90245

14 September 1979

Interim Report

APPROVED FOR PUBLIC RELEASE;
DISTRIBUTION UNLIMITED

DDC FILE COPY

Prepared for
SPACE AND MISSILE SYSTEMS ORGANIZATION
AIR FORCE SYSTEMS COMMAND

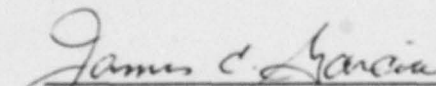
Los Angeles Air Force Station
P.O. Box 92960, Worldway Postal Center
Los Angeles, Calif. 90009

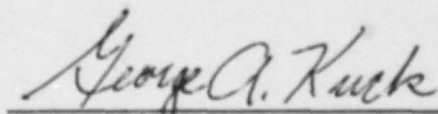
79 10 26 023

This interim report was submitted by The Aerospace Corporation, El Segundo, CA 90245, under Contract No. F04701-78-C-0079 with the Space and Missile Systems Organization, Deputy for Technology, P. O. Box 92960, Worldway Postal Center, Los Angeles, CA 90009. It was reviewed and approved for The Aerospace Corporation by G. A. Paulikas, Director, Space Sciences Laboratory. Lieutenant J. C. Garcia, SAMSO/DYXT, was the project officer for Technology.

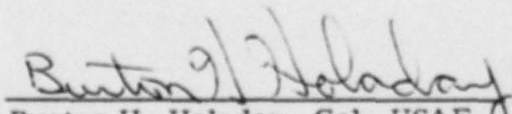
This report has been reviewed by the Information Office (OI) and is releasable to the National Technical Information Service (NTIS). At NTIS, it will be available to the general public, including foreign nations.

This technical report has been reviewed and is approved for publication. Publication of this report does not constitute Air Force approval of the report's findings or conclusions. It is published only for the exchange and stimulation of ideas.


James C. Garcia, Lt, USAF
Project Officer


George A. Kuck, Maj, USAF, Chief
Technology Plans Division

FOR THE COMMANDER


Burton H. Holaday, Col, USAF
Director of Technology Plans and Analysis
Deputy for Technology

UNCLASSIFIED

SECURITY CLASSIFICATION OF THIS PAGE (When Data Entered)

19 REPORT DOCUMENTATION PAGE		READ INSTRUCTIONS BEFORE COMPLETING FORM
1. REPORT NUMBER SAMS0-TR-79-57	2. GOVT ACCESSION NO.	3. RECIPIENT'S CATALOG NUMBER
4. TITLE (and Subtitle) A SURVEY OF CURRENTLY IMPORTANT EMPIRICAL THERMOSPHERIC MODELS	5. TYPE OF REPORT & PERIOD COVERED Interim report	6. PERFORMING ORG. REPORT NUMBER TR-0079(4960-04)-2
7. AUTHOR(s) David R. Hickman, Barbara K. Ching, Carl J. Rice, Lawrence R. Sharp, and Joe M. Straus	8. CONTRACT OR GRANT NUMBER(s) F04701-78-C-0079	9. PROGRAM ELEMENT, PROJECT, TASK AREA & WORK UNIT NUMBERS 12 189
10. PERFORMING ORGANIZATION NAME AND ADDRESS The Aerospace Corporation El Segundo, Calif. 90245	11. CONTROLLING OFFICE NAME AND ADDRESS Space and Missile Systems Organization Air Force Systems Command Los Angeles, Calif. 90009	12. REPORT DATE 14 September 1979
13. MONITORING AGENCY NAME & ADDRESS (if different from Controlling Office)	14. NUMBER OF PAGES 184	15. SECURITY CLASS. (of this report) Unclassified
16. DISTRIBUTION STATEMENT (of this Report) Approved for public release; distribution unlimited		15a. DECLASSIFICATION/DOWNGRADING SCHEDULE
17. DISTRIBUTION STATEMENT (of the abstract entered in Block 20, if different from Report)		
18. SUPPLEMENTARY NOTES		
19. KEY WORDS (Continue on reverse side if necessary and identify by block number) Atmospheric Composition Atmospheric Density Model Atmospheres Thermosphere		
20. ABSTRACT (Continue on reverse side if necessary and identify by block number) A description of currently important empirical thermospheric models is given, and the relative advantages of each are discussed. In addition, a comprehensive set of contour plots of total density is presented to allow more detailed examination of quantitative aspects of the models.		

DD FORM 1473
(FACSIMILE)

4107 512

UNCLASSIFIED
SECURITY CLASSIFICATION OF THIS PAGE (When Data Entered)

JLB

CONTENTS

I.	INTRODUCTION	7
II.	MODEL DESCRIPTIONS	15
	Early Models	15
	CIRA 1972/Jacchia 1971	25
	The McDonnell Douglas Model, MDAC	32
	The U.S. Standard Atmosphere, 1976	37
	The OGO-6 and ESRO-4 Models	47
	The Mass Spectrometer-Incoherent Scatter (MSIS) Model	52
	Jacchia 1977	55
III.	DISCUSSION AND COMPARISON OF MODELS	61
IV.	DENSITY CONTOUR PLOTS	85
V.	REFERENCES	185

Accession For	
NTIS GSA&I	<input checked="checked" type="checkbox"/>
DOC TAB	<input type="checkbox"/>
Unannounced	<input type="checkbox"/>
Justification	
By	
Distribution/	
Availability Codes	
Dist	Avail and/or special
A	

FIGURES

1.	Atmospheric temperature profile (from COESA, 1966)	9
2.	The semiannual density variation as derived from drag analysis on Satellite 1966 44A (Explorer 32)	11
3.	The geomagnetic effect as derived from the drag of six satellites in May and June 1967	12
4.	Atmospheric temperatures obtained on November 30, 1967, by Carru and Waldteufel (1969) by use of Thomson-scatter techniques, compared with temperatures predicted by the J71 models for a height of 300 km (solid line) (from Jacchia, 1971).	13
5.	Jacchia-Walker-Bruce model (solid lines) compared with the Jacchia 1965 model (dashed lines)	24
6.	Thirty-day means of density residuals from the J71/CIRA 1972 model for nine satellites covering a full solar cycle	31
7.	Kinetic temperature vs geometric altitude for the 1962 and 1976 Standard Atmospheres	40
8.	Density-height profiles of several model and standard atmospheres showing the evolution from 1947 to 1976.	43
9.	Range of deviations of the density-altitude profiles from the 1976 standard for various degrees of solar activity: (A) for lowest exospheric temperature at sunspot minimum; (B) average conditions at sunspot minimum; (C) average conditions at average sunspot maximum; and (D) exceptionally active conditions (from COESA, 1976)	45
10.	Ratio of the measured N_2 density to the model N_2 density as a function of time from perigee, geographic latitude, local time, $F_{10.7}$ solar flux, magnetic index A_p and day of year (from Hedin et al., 1972)	81
11.	Observed and computed densities, reduced to a standard height of 530 km for satellite 1964 76A (Explorer 24)	82

TABLES

1.	Comparison of Measured Densities of Model Values, 135-300 km	67
2.	Comparison of Measured Densities to Model Values, 135 km	68
3.	Comparison of Measured Densities to Model Values, 140 km	69
4.	Comparison of Measured Densities to Model Values, 150 km	70
5.	Comparison of Measured Densities to Model Values, 160 km	71
6.	Comparison of Measured Densities to Model Values, 170 km	72
7.	Comparison of Measured Densities to Model Values, 180 km	73
8.	Comparison of Measured Densities to Model Values, 200 km	74
9.	Comparison of Measured Densities to Model Values, 220 km	75
10.	Comparison of Measured Densities to Model Values, 240 km	76
11.	Comparison of Measured Densities to Model Values, 260 km	77
12.	Comparison of Measured Densities to Model Values, 280 km	78
13.	Comparison of Measured Densities to Model Values, 300 km	79

I. INTRODUCTION

Empirical thermospheric models are employed for a number of practical uses including satellite ephemeris prediction. For users who are unfamiliar with the field of thermospheric modeling it can be difficult to choose among the many models which have been developed. This report is intended to help such a user select the model best suited for his requirements by presenting a summary of the characteristics of a number of the most important empirical models of the thermosphere. With a view toward use in satellite orbit studies, the primary emphasis is placed on total mass density rather than temperature or number densities of individual species. An earlier report by Bruce (1965) summarized empirical models in use as of 1965.

The next section of this report will describe the most important empirical thermospheric models. A synopsis of early models is followed by a more complete description of those in current use. These descriptions will be followed by a section which provides a comparison and discussion of the relative advantages and limitations of the models in current use. Finally, a comprehensive set of figures which illustrate the model predictions of total density as a function of solar and geophysical parameters at several altitudes of interest will be given. These figures will allow a more detailed comparison of specific quantitative aspects of the various models.

The effects of aerodynamic drag on satellite orbits are most important in the altitude region from 120 to 400 km above the surface of the earth. Satellites which have perigee altitudes below 120 km suffer such great deceleration that their lifetimes before reentry are so short as to be impractical. For satellites with perigee altitudes above 400 km, the orbital perturbations caused by drag are relatively small, and the resulting gradual change in orbital elements can be accounted for easily.

The atmosphere above 120 km is characterized by a spectacular increase in temperature with increasing altitude, as seen in Fig. 1, and it is this feature from which the region derives its name, the "thermosphere." At high altitude the temperature finally levels off, approaching a limiting value known as the "exospheric temperature." A number of models have been developed in an effort to represent the behavior of the thermosphere. These models generally fall into one of two classes, theoretical or empirical. The theoretical models attempt to achieve a description of thermospheric behavior in terms of the basic physical processes. Although it is through such models that an understanding of thermospheric dynamics must be obtained, for many uses these theoretical models are not suitable due to their complexity and the large amounts of computer memory and time they require.

Empirical models of the thermosphere make little or no attempt to describe correctly the underlying physics, but rather try to provide density values in a convenient manner. It is these empirical models which are most suitable for applications such as use in operational systems concerned with the effects of aerodynamic drag on satellite orbits.

Prior to 1957 there had been a limited number of rocket probes of the thermosphere, but there were insufficient data to determine the systematic density variations. An Air Research and Defense Command (ARDC) model was developed in 1956 which utilized the data from these probes. However, only the average density and temperature were presented. Analysis of the decay of satellite orbits due to aerodynamic drag allowed study of the variations of atmospheric density near perigee and it was soon confirmed that there were substantial variations of density at satellite altitudes. The major variations in density are due to changes in the amount of heating of the upper

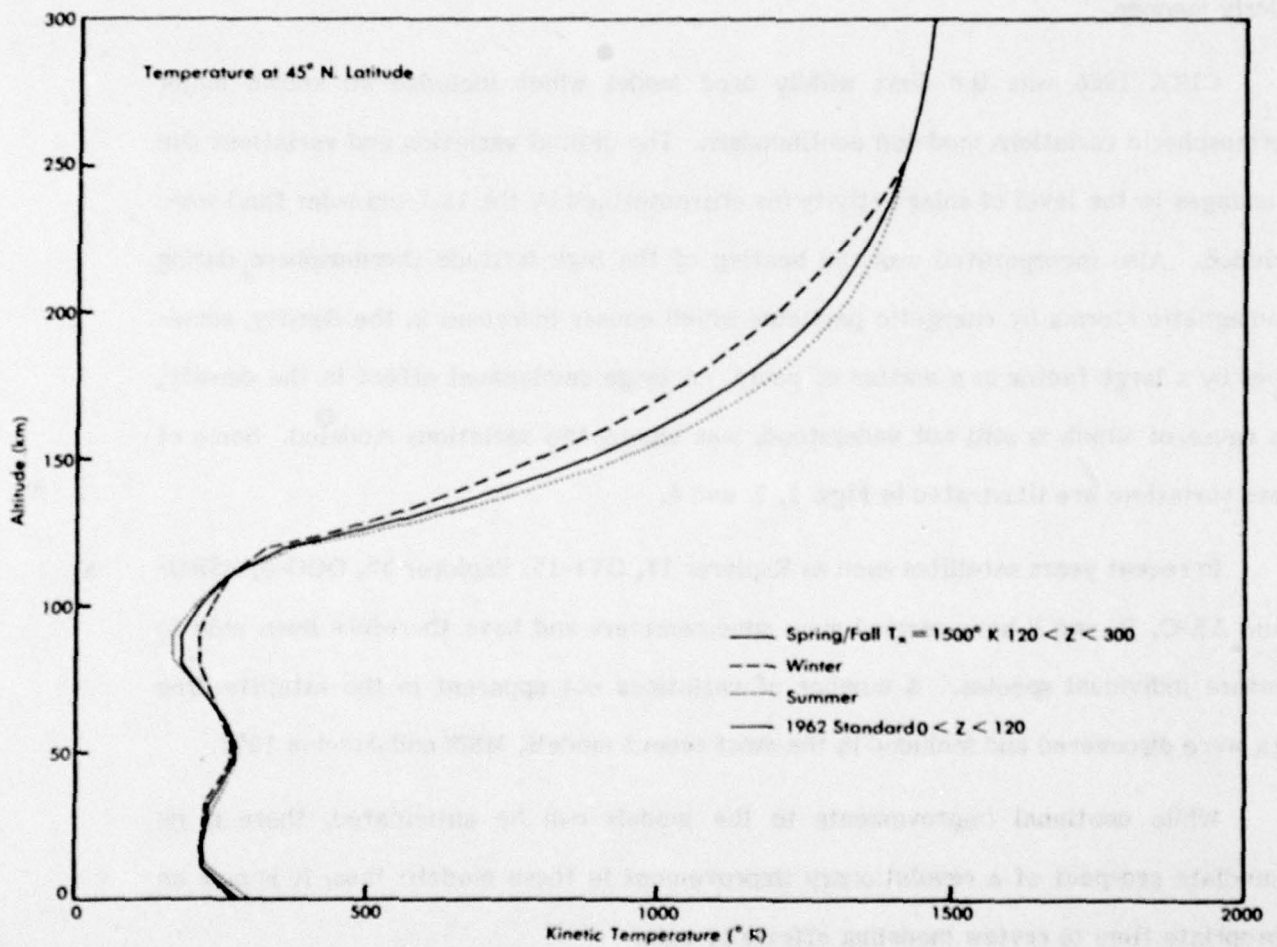


Figure 1. Atmospheric temperature profile (from COESA, 1966).

atmosphere by solar extreme ultraviolet (EUV) radiation. Although near 120 km the variations in density are small, at 400 km the density may change by over two orders of magnitude from the minimum to the maximum of the eleven year solar cycle. The simple ARDC 1956 model was therefore of obviously limited value. A number of models based on satellite data were later developed to describe the observed variations in an orderly manner.

CIRA 1965 was the first widely used model which included all known major thermospheric variations modeled continuously. The diurnal variation and variations due to changes in the level of solar activity (as characterized by the 10.7-cm solar flux) were included. Also incorporated was the heating of the high latitude thermosphere during geomagnetic storms by energetic particles which causes increases in the density, sometimes by a large factor in a matter of hours. A large semiannual effect in the density, the cause of which is still not understood, was among the variations modeled. Some of these variations are illustrated in Figs. 2, 3, and 4.

In recent years satellites such as Explorer 17, OV1-15, Explorer 32, OGO-6, ESRO-4 and AE-C, D, and E have carried mass spectrometers and have therefore been able to measure individual species. A number of variations not apparent in the satellite drag data were discovered and included in the most recent models, MSIS and Jacchia 1977.

While continual improvements to the models can be anticipated, there is no immediate prospect of a revolutionary improvement in these models; thus, it is now an appropriate time to review modeling efforts to date.

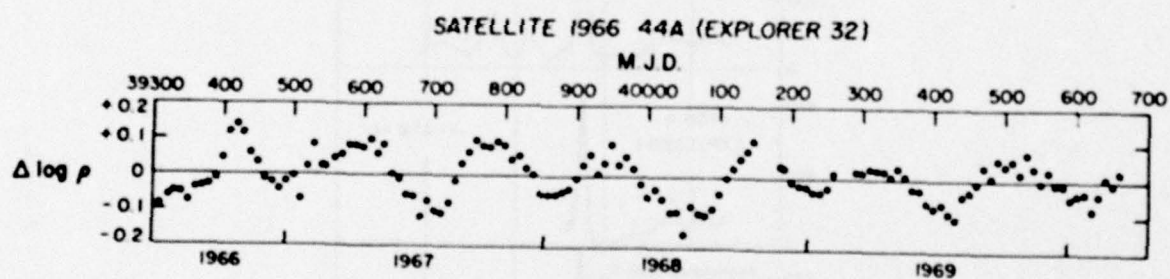


Figure 2. The semiannual density variation as derived from drag analysis on Satellite 1966 44A (Explorer 32). All other variations have been suppressed by using the appropriate equations (from Jacchia, 1971).

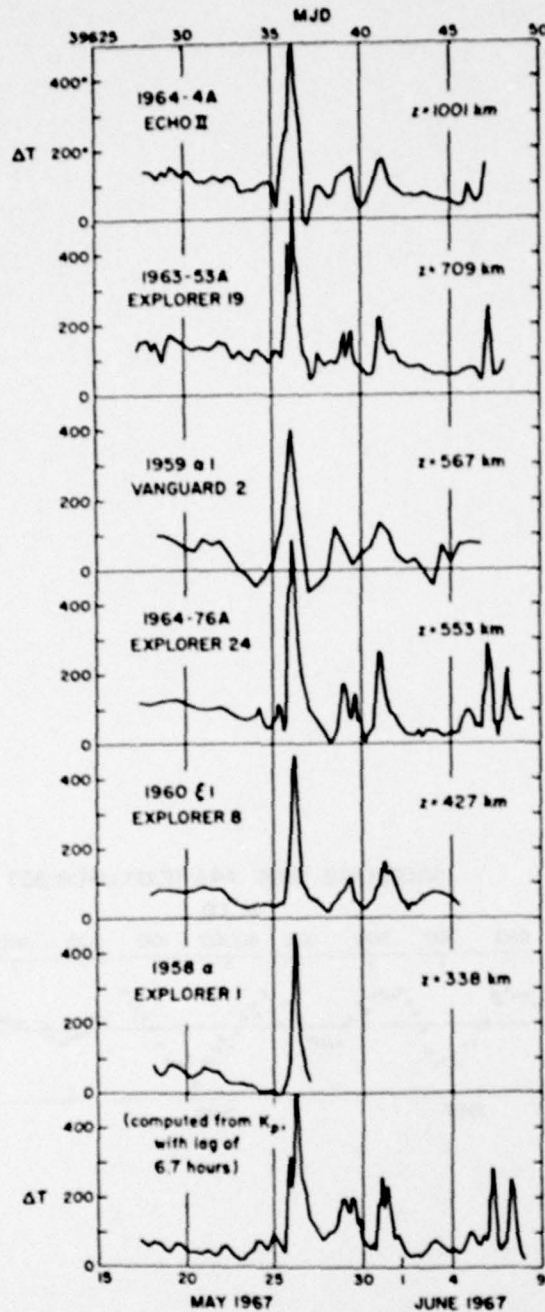


Figure 3. The geomagnetic effect as derived from the drag of six satellites in May and June 1967. ΔT represents the change in exospheric temperature required to represent the observed density. The lowest panel shows the change in exospheric temperature computed from K_p by using the model (from COSPAR, 1972).

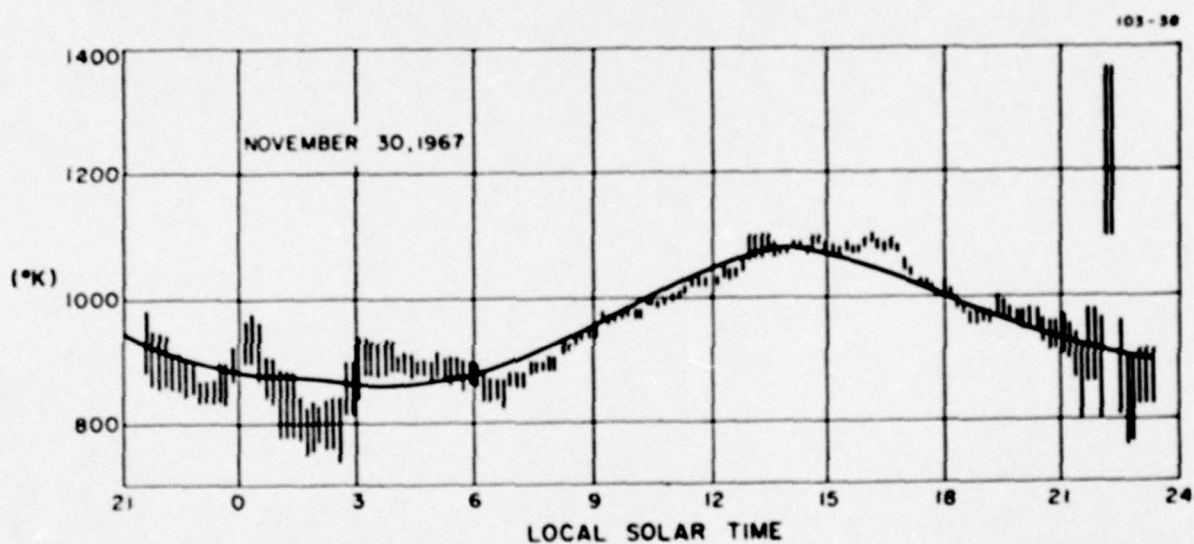


Figure 4. Atmospheric temperatures obtained on November 30, 1967, by Carru and Waldteufel (1969) by use of Thomson-scatter techniques, compared with temperatures predicted by the J71 models for a height of 300 km (solid line) (from Jacchia, 1971).

II. MODEL DESCRIPTIONS

Early Models

(ARDC 1959; Jacchia 1960 and 'DENSEL; CIRA 1961; Harris-Priester and CIRA 1965; Jacchia 1965 and Jacchia-Walker-Bruce)

The basis and limitations of some thermospheric models that were developed in the decade following the launch of the first artificial earth satellite are discussed in this section. A fairly large number of models were developed in that period, but the discussion will be limited to those that either achieved international recognition or were used frequently for Aerospace/SAMSO programs. A few of these models are still in use. Some of the early models attempted a "full" description of the atmosphere; i.e. pressure, temperature, and composition were specified in addition to the density. Since, however, such attempts were not based on actual measurements of temperature or composition, our discussion shall be limited only to the density.

ARDC 1959

The ARDC 1959 (Air Research and Defense Command) model (Minzner et al., 1959) was the first standard upper-atmospheric model that utilized satellite measurements of the density. Densities were, of course, deduced by the orbital decay method, and so only very coarse time and space resolution was provided by the measurements. Accordingly, only a single profile of the density was presented out to 700 km altitude. Although the data base covered altitudes from 170 km to 650 km, there was a large

interval between about 350 and 600 km where there were no measurements. The satellite orbits used were mostly of moderate inclination and covered different local times; thus, the model was representative of "average" global conditions during a period of high solar activity (1957-58). The density profile above 150 km was higher than that of the ARDC 1956 model (which was based only on rocket data). Initially it was suspected that the difference was due to errors of measurement. Today, with our increased knowledge of atmospheric behavior, we can believe that the major part of the difference was most probably related to real solar-cycle induced variability of the atmosphere.

Jacchia 1960 and 'DENSEL

Jacchia's (1960) first model of thermospheric density was based on satellite drag data from four satellites having perigee altitudes between 210 and 650 km. The model took into account both diurnal effects and variations related to solar activity. Geomagnetic activity effects had been observed in orbital decay data but were not sufficiently well-understood to be modeled at that time.

Unlike the ARDC 1959 model, which was presented in tabular form, the Jacchia 1960 model density was expressed analytically by

$$\rho = \rho_0 \frac{F_{20}}{100} \left\{ 1 + 0.19 [\exp(0.0055 z) - 1.9] \cos^6 \frac{\psi}{2} \right\} \quad (1)$$

where $\log \rho_0 = -16.021 - 0.001985 z + 6.363 \exp(-0.0026 z)$. In this expression, ρ is the density in gm/cm^3 at altitude z in km ($200 \leq z \leq 700$); F_{20} is the 20-cm solar flux in units of $10^{-22} \text{W/m}^2\text{-Hz}$. ψ represents the angular distance from the maximum of the diurnal density bulge, which was placed at the subsolar latitude at a local time of about 14 hr. (Note that Jacchia used the 20-cm solar flux as an index of the degree of solar activity. Subsequent studies utilized the 10.7-cm flux, which was found to be somewhat better correlated with density variations.)

The simplicity of the model made it particularly useful for production-type calculations (as in orbit determination) where numerical efficiency is required. The Lockheed Missile and Space Co. (1961) recognized this and incorporated the Jacchia 1960 model with the ARDC 1959 model at lower altitudes for use in orbital analyses. The Lockheed product is known as "Lockheed-Jacchia" by users of the Aerospace TRACE program; it is the same as 'DENSEL in the Advanced Orbital Ephemeris System (AOES) software.

In 'DENSEL, the density up to an altitude of 140 km is represented by ARDC 1959; above 200 km Jacchia 1960 is used. In the intervening region (140-200 km) a smooth transition is provided by

$$\rho = 2.889 \times 10^{-12} \left(\frac{140.8}{z} \right)^{7.18} \left[\frac{200-z}{59} + 0.0085 \left(\frac{z-140.8}{59} \right)^{4/3} F_{10.7} \right] \times$$

$$\left[1 + \frac{z-140.8}{283} \cos^6 \left(\frac{\psi}{2} \right) \right] \quad (140 < z < 200 \text{ km}) \quad (2)$$

where ρ , z and ψ have the same meaning as in the previous expressions. It is to be noted that the model utilizes the 10.7-cm flux ($F_{10.7}$ in units of $10^{-22} \text{ W/m}^2\text{-Hz}$) rather than the 20-cm flux. The usage of the 10.7-cm flux is maintained even in the region 200-700 km, where the Jacchia 1960 formulation is adopted. This is done by replacing F_{20} in Eq. (1) by $0.85 F_{10.7}$, where 0.85 is the appropriate scaling factor between the solar-cycle averages of the 20-cm and 10.7-cm fluxes. While Eq. (2) provides a smooth transition from the ARDC 1959 to the Jacchia 1960 model, the slope of the density at the end points is usually discontinuous. This feature is generally not important in applications.

At very high orbital altitudes (700-1850 km) 'DENSEL represents the density with the expression

$$\rho = \frac{2.60 \times 10^{-5} F_{10.7}}{h^5} \left[\cos^6 \left(\frac{\psi}{2} \right) \left(1 - \frac{6 \times 10^6}{h^3} \right) + \frac{6 \times 10^6}{h^3} \right] \quad (3)$$

where h is the altitude in nmi ($h = z/1.852$). Equation (3) is only approximate, based on the very limited data that were available at the time. For orbital studies, however, it generally is adequate since the air drag is very small relative to other perturbing forces. In the light of more recent data we now know that eq. (3) does not accurately describe the global and seasonal variation of the density (which is predominantly made up of He in that regime).

A feature of 'DENSEL which should be noted is that a formula for the time-dependent behavior of the 10.7-cm flux is used whenever actual values of $F_{10.7}$ are not provided to the program. This is given by

$$F_{10.7} = 150 + 80 \cos (2\pi d/4020) \quad (4)$$

where d is the time in days from the previous solar-cycle maximum. As can be seen, $F_{10.7}$ in Eq. (4) varies between 70 and $230 \times 10^{-22} \text{ W/m}^2\text{-Hz}$. Thus, the predicted values encompassing the maximum are on the high side. It is to be noted that 'DENSEL does not include any of the known atmospheric variations other than the diurnal and solar cycle effects.

CIRA 1961

The CIRA 1961 (COSPAR International Reference Atmosphere) model consisted of three tables of the atmospheric variables that represented the daily average conditions, daytime maximum and nighttime minimum conditions. No other time or space variation of the atmosphere was described. The model purported to be representative of medium solar activity conditions, but since the data base consisted of orbital decay observations in the 1958-60 period, it should be regarded as a high solar activity model.

The lower boundaries of the three models that comprise CIRA 1961 are different. The daily mean model extended from ground level to 800 km; the daytime maximum model started at 200 km, the nighttime minimum model at 170 km.

Harris-Priester and CIRA 1965

The work of Harris and Priester (1962a,b) represents a milestone in thermospheric modeling studies since theirs was a first major attempt to describe the upper atmosphere on a physical basis. Rather than fit the observational data with profiles or empirical formulas that had no physical basis, they fit the data subject to the constraints of the thermospheric energy equation under conditions of hydrostatic equilibrium. In other words, they solved the one-dimensional time-dependent heat conduction equation to obtain the temperature, and with this the different constituent profiles could be computed assuming diffusive equilibrium. Once the temperature and the concentrations of the different species are known, all other atmospheric variables are determined. To fit the computed density to the observations, the boundary conditions or properties of the energy sources can be adjusted.

Harris and Priester encountered some difficulty in trying to match the observations using only the solar EUV flux as the source of heating. The amplitude of the daily density variation was too large, the time of maximum was several hours too late, and the required heating efficiency was too high. All these problems could be removed if a second heat source were added; this hypothetical source needed to be similar to the EUV source in its strength and vertical distribution, but the maximum heating was required at about 9 a.m. local time. It was qualitatively argued that the second source could be related to corpuscular energy input.

Using this second heat source to supplement EUV heating, Harris and Priester (1962a) produced a diurnal model of the upper atmosphere that was appropriate for equatorial and temperate latitudes at equinox and for solar activity conditions corresponding to $F_{10.7} = 200$. Shortly thereafter, Harris and Priester (1962b) extended their model to include solar cycle variations. Tables were published in NASA document D-1444 (1962).

COSPAR (Congress on Space Research) adopted the Harris-Priester models for the CIRA 1965 model. Under this title 120 tables were published that described the thermospheric structure from 120-800 km for 10 levels of solar activity ($65 \leq F_{10.7} \leq 225$) and with 2-hr increments of local time. The tables, as described above, were based on theory. However, to account for other observed density effects, such as the 27-day variation, geomagnetic activity effects and semiannual changes, empirically derived corrections to the exospheric temperature need to be used in conjunction with the tables.

Jacchia 1965 and the Jacchia-Walker-Bruce Model

With satellite drag data from half a solar cycle (1958-1964), Jacchia (1965) was able to construct an improved empirical model that took into account solar activity (including both 11-yr and 27-day cycles), diurnal variations, and geomagnetic activity. Although the published model was accompanied by tables of the atmospheric quantities, the composition, temperature and density could be directly computed for any set of given conditions. This is in contrast to the CIRA 1965 model, in which one had no choice but to interpolate the tables for arbitrary conditions. The formulation of the Jacchia-1965 model was also continuous over the globe, whereas CIRA 1965 was essentially only for middle and low latitudes.

With this model Jacchia initiated the now common practice of using the exospheric temperature as a parameter to synthesize the density data at different altitudes. To elaborate, given a lower boundary temperature and the exospheric temperature, a temperature profile is assumed to be determined. Then, given a set of lower boundary conditions on number densities of the constituents, the equations for diffusive equilibrium are integrated to determine the vertical distributions of the different atmospheric constituents, which may be summed to obtain the total density:

$$\frac{dn_i}{n_i} = - \frac{m_i g}{kT(z)} dz - (1 + \alpha_i) \frac{dT}{T} \quad (5)$$

$$\rho = \sum_i n_i m_i \quad (6)$$

where n_i is the concentration of the i th constituent, m_i is its mass, g is the acceleration of gravity, z is the altitude, k is Boltzmann's constant, T is the temperature, α_i is the thermal diffusion coefficient and ρ is the total mass density. In essence, then, given a set of lower boundary conditions, a density profile is determined by specifying the exospheric temperature. Thus, rather than manipulate the density to simulate the different atmospheric variations, Jacchia 1965 utilizes exospheric temperature changes to produce the density variations. The appropriate temperature changes, which were analytically formulated, were derived by fitting the model to observations.

When Jacchia published his model in 1965, it was stated that the concentrations were to be computed by numerical integration of the diffusion equation using the appropriate temperature profile. Walker (1965) pointed out, however, that with a minor change in the mathematical form of the temperature profile, the diffusion equation could be integrated directly. This feature is quite important in applications where numerical efficiency and economy are imperative.

The Jacchia-Walker-Bruce model (Bruce, 1966), which is a standard option for TRACE users, is basically Jacchia-1965 with densities computed using the closed-form solution of the integral of the diffusion equation. An additional modification introduced by Bruce eliminates the cross-over of the density profiles near 150 km as shown in Fig. 5. This crossing of density profiles, which means that on opposite sides of the cross-over (or isopycnic) point the density varies in opposite senses as a function of exospheric temperature, is due to the conservation of mass. In other words, the density at high altitudes can increase only at the expense of the density at low altitudes if the pressure at the lower boundary is to remain constant. While it is quite likely that such behavior does exist somewhere in the atmosphere, observations indicate that it is below about the 120-km level. Thus, Bruce's modification, while leading to nonconservation of mass, or equivalently, flow across the boundary, does force the model to behave in a more realistic fashion.

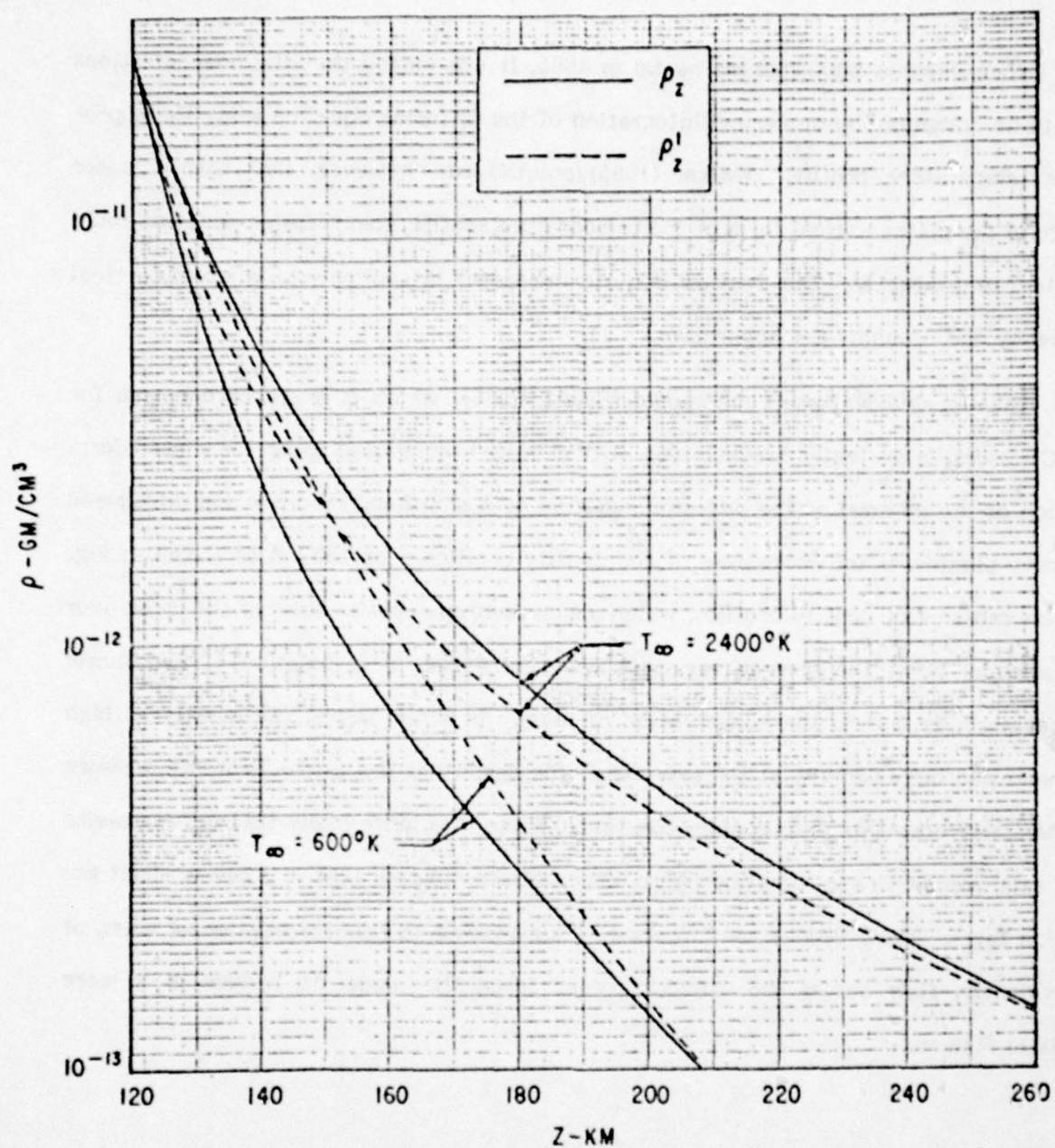


Figure 5. Jacchia-Walker-Bruce model (solid lines) compared with the Jacchia 1965 model (dashed lines).

CIRA 1972/JACCHIA 1971

Introduction. The COSPAR International Reference Atmosphere 1972, or CIRA 1972, (COSPAR, 1972) consists principally of two independent models: A model of G. V. Groves for the altitude range 25-125 km and a model of L. G. Jacchia for the range 110-2000 km. The two models differ considerably, including the use of different parameters; they also do not match in the region of overlap. Our concern in this report is with the high altitude model of Jacchia, which is essentially identical with the model commonly referred to as Jacchia 1971 or J71 (Jacchia, 1971).

The model is based primarily on satellite-drag data, with composition adjusted to reflect theoretical results and in situ mass spectrometer results. In particular the controversial analysis of atomic oxygen measurements by von Zahn (1970) has been incorporated. As a static model which assumes diffusive equilibrium, J71 builds on the foundations laid by Nicolet (1965), Jacchia (1965), and Jacchia (1970). Perhaps the most notable change in J71 is in moving the constant boundary conditions from 120 km down to 90 km, which has the effect of moving the resultant notorious isopycnic layer from near 150 km down to a height well below normal satellite altitudes, thus making the Bruce-type correction in a more self-consistent fashion.

The 150 km level is employed in effect as a reference level; the temperature profile at lower altitudes is "adjusted to give the required total density at 150 km" (COSPAR, 1972) after setting the composition at 150 to correspond to the composition suggested by von Zahn (1970).

The CIRA 1972 model also represents a model different from the more "mathematical" models, such as MSIS (to be discussed below), for which the choice of functional

forms is dictated by questions of orthogonality, completeness, etc., with the final parameters determined by a fitting routine. In the CIRA 1972 model the mathematical forms and the specific parameters enter in ways which attempt to reflect the current understanding of the physics and chemistry of the atmosphere, or which specifically demonstrates the form of a given variation, thereby isolating certain features or variables.

Model Formulation. The J71 model is a static model which assumes diffusive equilibrium. The basic independent variable is the temperature. All temperature profiles begin from a constant value $T_0 = 183^{\circ}\text{K}$ at the base altitude of 90 km and have an inflection point at 125 km. The choice of the functional form of the profile is dictated as much by computational as by theoretical and experimental considerations. The chosen profiles yield continuous first and second derivatives with respect to height through the inflection point. The temperature-height profile is characterized by the exospheric temperature, T_{∞} , the temperature which is approached asymptotically at high altitudes.

The J71 model recognizes several types of variations which are dealt with explicitly. Specifically they are:

1. Solar cycle variations and shorter-term solar activity effects.
2. The diurnal variation.
3. Geomagnetic activity variations.
4. The semiannual variation.
5. Seasonal-latitudinal variations.

(More rapid density variations (waves) are also recognized to be present but as being incapable of being handled in a static model of this type.)

The above five sources of variations are accounted for in the model in two distinct ways. The first is as a variation of the exospheric temperature T_{∞} . The variations so modeled are:

1. The solar activity effects, which employ for their input parameters the readily available 10.7-cm solar flux ($F_{10.7}$). The model distinguishes between a contribution from active areas and a disk component, which are modeled by a slightly delayed (1.71 days) value of $F_{10.7}$ and by a running average over 6 solar rotations ($\bar{F}_{10.7}$), respectively.
2. The diurnal variation is represented by a sub-solar "bulge." The ratio of the maximum exospheric temperature at the sub-solar point to the minimum at the anti-solar point is a constant 1.3, although Jacchia points out the considerable uncertainty on this point. The diurnal variation has both local time and latitude dependence (and seasonal variability implicitly through the movement of the sub-solar point). The hours of minimum and maximum of the daily density are independent of latitude and altitude and occur at 02.87 and 14.08 hours local solar time, respectively.

The second way in which the sources of variation are incorporated into the model is via a direct percentage variation of the local ambient density. The sources modeled in this way are:

1. The semiannual variation is expressed as a separable function of time (expressed in days) and altitude in the manner

$$\log_{10} \rho_{\text{semiannual}} = f(z) g(t) \quad (7)$$

The function $g(t)$, which is not sinusoidal, has maximum excursions of -0.519 and $+0.478$ and averages to zero over the period of a year. The height function $f(z)$ is relatively small below 200 km with a broad maximum peaking at 0.353 near 800 km.

2. The seasonal-latitudinal variations in the lower thermosphere arise in J71 as an attempt to fit lower boundary conditions. The form chosen is

$$\Delta \log_{10} \rho = S \frac{\phi}{|\phi|} P \sin^2 \phi \quad (8)$$

where ϕ is the geographic latitude, S is a function of altitude which has a maximum value of 0.166 at 110 km, falling to zero by 170 km, and P is a sinusoidal function with the maximum at the winter solstice.

Another seasonal-latitudinal variation, namely that of helium, is modeled separately as a function of solar declination and latitude. The maximum, $\Delta \log_{10} n(\text{He}) = 0.420$, occurs over the winter pole at solstice. The summer polar minimum is -0.230 .

The variations with geomagnetic activity are modeled by a combination of temperature and density variations. The suggested formulas are:

$$\Delta \log_{10} \rho = 0.012 K_p + 1.2 \times 10^{-5} \exp(K_p) \quad (9)$$

$$\Delta T_{\infty} = 14^{\circ} K_p + 0.02 \exp(K_p). \quad (10)$$

An alternative version employs only a temperature variation

$$\Delta T_{\infty} = 28^{\circ} K_p + 0.03 \exp(K_p). \quad (11)$$

A time lag of 6.7 hours for the appropriate value of K_p is suggested.

In practice, the model is used by first determining the appropriate exospheric temperature, T_{∞} , according to the various parameters (local time, time of year, $F_{10.7}$, etc.) which directly affect this quantity. The value of T_{∞} then completely determines a given density-height profile for the individual species according to the equations for diffusive equilibrium. Adjustments to these individual density profiles are then made according to the formulas for the semiannual, geomagnetic, and seasonal-latitudinal effects which operate directly on the density.

Limitations. CIRA 1972/J71 is a static model derived primarily from insights gained from examination of satellite drag data; its limitations derive in large part from

these circumstances. Because it is a static model it is best able to represent atmospheric variability with relatively long time scales like, for example, the semiannual variation. Variations with shorter time scales, such as the diurnal variation, are modeled less well. For example, the diurnal response of various constituents in the upper atmosphere, in particular N_2 and O, have different phases resulting in a change in phase of the overall diurnal response as the atmosphere changes from a dominantly N_2 to a dominantly O atmosphere with increasing height. While J71 does contain diurnal asymmetry, it has a very simple form, constant at all altitudes, and is subject to considerable uncertainty. At even shorter time scales the more dynamic K_p response is still more poorly modeled, particularly for high K_p values. This difficulty is exacerbated when the comparison is made with in situ mass or density measurements with their inherently more rapid response than the drag data used for the model formulation.

Accuracy. Figure 6, taken from the CIRA 1972 publication (COSPAR, 1972), gives density residuals from the model for nine satellites. The residuals appear to average about 15-25% over the time period 1958-1970, i.e., an entire solar cycle. This is in agreement with values derived comparing the J71 model with in situ ion gauge data below 300 km for the period 1973-1975 (Rice and Sharp, unpublished). Because of lack of available low altitude data when formulating J71, the model at low altitudes may not be correct in all its details. For example, the phase of the diurnal variation changes at low altitude, a feature which is not modeled by J71 (Sharp et al., 1978). Because the amplitude of such variations also decreases at low altitudes, however, the effect on the overall percentage accuracy is not extremely great. Nevertheless, care must be exercised at low altitudes if specific details such as diurnal behavior or relative composition are significant for the use considered.

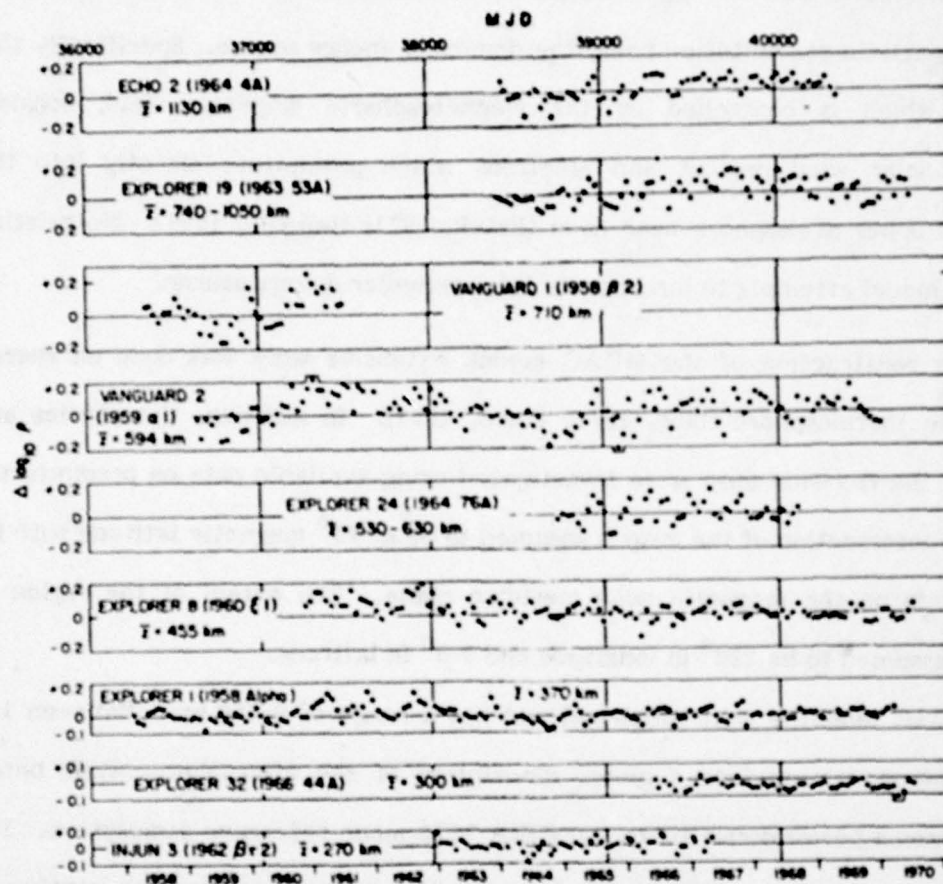


Figure 6. Thirty-day means of density residuals from the J71/CIRA 1972 model for nine satellites covering a full solar cycle. \bar{Z} is an average effective height for each satellite (from COSPAR, 1972).

The McDonnell Douglas Model, MDAC

MDAC is an atmospheric model developed by W. P. Olson et al. (1975). The motivation for developing the MDAC model arose as a result of studies of the dayside cusps which indicated that at high latitudes the thermospheric densities are quite variable, with particle precipitation being the dominant energy source. Specifically this precipitation, which is controlled by the magnetospheric magnetic field, consists principally of solar wind protons and electrons which precipitate directly into the ionosphere and upper atmosphere near noon (Frank, 1971; Heikkila, 1971). No existing thermospheric model attempts to incorporate this particular energy source.

Prior to construction of the MDAC model, extensive work was done on energy sources for the thermosphere (Moe, 1971; Olson, 1971). In addition, the physics and morphology of the day-side cusp were investigated using available data on precipitating particles. The intersection of the cusp is assumed to be at 75° magnetic latitude with its central longitude on the magnetic noon meridian plane. The extent of the region of interaction is assumed to be 180° in longitude and $3-5^{\circ}$ in latitude.

The MDAC model is semi-empirical and has a range of 0-450 km. Between 120 and 450 km the model provides a global description of the atmosphere, while below 120 km it utilizes a power series fit to the CIRA 1972 mean reference atmosphere. The boundary between the lower- and upper-atmospheric models is everywhere continuous and the slopes are closely matched.

The total density returned by the model is the sum of two terms: the corpuscular heating term ($\Delta\rho_c$) is described in magnetic coordinates, while the EUV and other sources term (ρ_{μ}) is described in geographical coordinates. The two contributions are

then combined in the following manner:

$$\rho = \rho_{\mu} + \Delta\rho_c = \rho(z, \lambda, \phi, T, D, F, P) \text{ in gm/cm}^3 \quad (12)$$

z = altitude in km

λ = geographic latitude in degrees

ϕ = east geographic longitude in degrees

T = universal time in hours

D = day of the year

F = decimetric solar flux in $10^{-22} \text{ W/m}^2\text{-Hz}$

P = particle heating parameters.

The first term is expressed as a product

$$\rho_{\mu} = \rho_0(z, F) B(z, \lambda, t) J(z, \lambda, D) Q(z, D) \quad (13)$$

where

ρ_0 is the mean equatorial density

B is the diurnal variation

J is the seasonal-latitudinal variation

Q is the semi-annual variation

t is the local time.

For average conditions ρ_0 can be expressed as

$$\rho_0 = \rho(120) \exp \left[\frac{120 - z}{1.737 \sqrt{z-103}} \right] \text{ where } \rho(120) = 2.7 \times 10^{-11} \text{ gm/cm}^3. \quad (14)$$

The $F_{10.7}$ variation is introduced by replacing 1.737 with

$$0.99 + 0.518 \left(\frac{F + \bar{F}}{110} \right)^{\frac{1}{2}} \quad (15)$$

where \bar{F} is averaged over the preceding 3 months. The diurnal variation is given by

$$B(z, \lambda, t) = \left[1 + (f(t) - 1) \cos \lambda \right]^{\mu(z)}. \quad (16)$$

The function $f(t)$ is the diurnal variation in density at the equator given by

$$f(t) = 0.994 + 0.545 \cos \left[\frac{\pi}{12} (t - 14.745) \right] + 0.102 \cos \left[\frac{\pi}{6} (t - 1.838) \right]. \quad (17)$$

The function $\mu(z)$ is given by $1.1 \times (1 - \exp(-(z-120)/150))$ which satisfies the following conditions. It reproduces the values at 450 km observed by Hedin et al. (1974). The height dependence fits the LOGACS data (Bruce, 1972) near local noon at 186 km and the data of Ching and Carter (1974) near local midnight at 230 km. In addition the diurnal variation is made to approach zero where it interfaces with CIRA 1972 at 120 km.

The latitudinal-seasonal dependence is given by

$$J(z, \lambda, D) = 1 - \alpha(1 - \cos(\lambda - \lambda_s))^m \mu(z) \quad (18)$$

$$\lambda_s \text{ is the latitude of the subsolar point, } 23.5 \sin \frac{2\pi(D - 81)}{365} \text{ deg.} \quad (19)$$

$$\alpha = 0.25 \text{ and } m = 2.5.$$

This is a compromise equation to fit the latitude dependence observed by Hedin et al. (1974) at 450 km, the LOGACS data at 186 km, and observations indicating only a small latitude dependence due to UV heating.

The semiannual variation is expressed as

$$Q(z, D) = 1 + R(z) G(D) \quad (20)$$

where

$$R(z) = -0.02 + 0.27 \times 10^{-2} z - 0.85 \times 10^{-6} z^2 - 0.59 \times 10^{-9} z^3, \quad (21)$$

$$\begin{aligned} G(D) = & 0.143 \cos \left[\frac{2\pi}{365} (D - 4) \right] + 0.239 \cos \left[\frac{4\pi}{365} (D - 109) \right] \\ & + 0.044 \cos \left[\frac{6\pi}{365} (D - 66) \right]. \end{aligned} \quad (22)$$

The corpuscular heating term is given by

$$\Delta \rho_c = \rho_\mu \exp \left[-(z-120)/50 \right] C(\lambda_m, t_m, P) \quad (23)$$

where λ_m is the magnetic latitude, t_m is the magnetic local time and P the cusp heating parameters which include the particle precipitation intensity and size parameters of the heating region. The function is given a scale height of 50 km in order to have zero heating at 120 km and approach a maximum heating near 170 km. This is done because, although protons can penetrate to about 110 km, the peak energy loss per km is at ~169 km (Olson, 1971, 1972).

Function C represents a density bulge which encircles the geomagnetic pole and is most intense at local magnetic noon. The amplitude, extent and location of the bulge are adjustable parameters which depend on solar wind and magnetospheric characteristics. These adjustable values have been nominally set to give a best fit to the LOGACS data during quiet times.

The MDAC model has the advantage of being functionally simple and computationally fast. The FORTRAN version of this model (as provided by Olson, et al.) has been carefully optimized to minimize the number of multiplications and calls to elementary functions. Since the model does not include the K_p variation, its utility is limited to quiet times. In addition it predicts densities which are in general about 10% too low. However, since it does include the heat source from charged particle precipitation into the high latitude regions, it can be valuable as a baseline in the study and prediction of densities in the polar thermosphere.

The U. S. Standard Atmosphere, 1976

Introduction. The U. S. Standard Atmosphere, 1976, is the atmospheric model adopted officially by the United States Committee on Extension to the Standard Atmosphere (COESA). It replaces an earlier model known as "U.S. Standard Atmosphere, 1962" (COESA, 1962). The new standard is defined and described with graphs and complete tables in the official publication "U. S. Standard Atmosphere, 1976" (COESA, 1976) published jointly by the National Oceanic and Atmospheric Administration (NOAA), the National Aeronautics and Space Administration (NASA), and the United States Air Force. The new standard is also described together with abbreviated tables by Minzner et al. (1976).

The U. S. Standard Atmosphere, 1976, attempts to set forth an idealized representation of the atmosphere which will have utility for a number of scientific, engineering, meteorological, and commercial needs. As such it differs from the other recent models discussed in this document in two significant ways. Firstly, only a single model profile is produced which is "designed to represent mean mid-latitude conditions as presently known for heights within and below the thermosphere and to represent mean solar conditions in and below the exosphere" (COESA, 1976). Secondly, the altitude range covered by the model extends from ground level (actually from 5000 meters below sea level) upwards to exospheric altitudes (1000 km). The complete CIRA 1965 and CIRA 1972 models do not extend below 30 km and 25 km, respectively.

Both of the above unique characteristics derive from the manner in which the concept of a "standard atmosphere" has evolved. The century-long history of the

development of and changes in "standard" model atmosphere is well told by Minzner (1977). The initial impetus for their use was as a calibration standard for aneroid barometers used as height measuring instruments. The subsequent development of aviation and its rapid expansion following World War I increased the need for and the accuracy required of such models. Development of higher flying aircraft and rockets during and following World War II greatly increased the need for a higher altitude model and at the same time increased the data base available for its construction. The launching of Sputnik I in 1957 and the subsequent proliferation of satellites circling the earth produced a similar situation extending out to the exosphere. The U. S. Standard Atmosphere, 1962, incorporated much of this early satellite data in producing a model which reached to 700 km altitude. The primary impetus for issuing the U. S. Standard Atmosphere, 1976, was recognition that the "mean" conditions chosen for the 1962 model were, in fact, strongly biased toward conditions representative of high solar activity. As a result, the thermospheric temperature profile, in particular, was considerably hotter and hence densities considerably greater than subsequent measurements have supported. Differences between the 1962 and 1976 standards are confined to altitudes above 51 km. In this report, our interest is with the upper atmosphere, which for this model can be defined as the region above 86 km where a change in computational techniques is made. The following discussion will refer only to this higher region unless stated otherwise.

Model Formulation. The U. S. Standard Atmosphere, 1976, is intended to represent year-round mean atmospheric properties for a mid-latitude location during moderate solar conditions. Quoting the COESA Working Group with respect to the upper altitudes:

"The atmosphere shall also be considered to rotate with the earth, and be an average over the diurnal cycle, semi-annual variation, and the range of conditions from active to quiet geomagnetic, and active to quiet sunspot conditions. Above the turbopause (above 110 km) generalized forms of the hydrostatic equations apply" (COESA, 1976). This definition leaves open the determination of just what average conditions actually obtain in the earth's atmosphere, a difficulty which grows with increasing altitude. This subject will be discussed further when we examine the model's limitations.

The primary parameter for defining the U. S. Standard Atmosphere, 1976, is the temperature vs. altitude profile, as it has been for every accepted reference atmosphere since the constant temperature (50°F) British standard atmosphere published by the Astronomer Royal G. B. Airy in 1867. The temperature profile is used to achieve continuity between the various altitude regimes where differing computational techniques must be employed. The actual form of the temperature profile chosen must be a reasonably accurate representation of the average measured profile and at the same time be of a form suitable for use with the computational formulas. Prior to the 1976 model, the temperature profiles consisted of segments linear in either temperature T or molecular scale temperature MT with respect to either geometric or geopotential height. The 1976 model also employs linear temperature segments up to 86 km. Above 86 km the 1976 standard uses a temperature profile consisting of four (non-linear) segments chosen so that the first derivative of temperature with respect to geometric height is continuous over the entire region 86-1000 km. The exospheric temperature which is approached asymptotically at high altitude is 1000°K, 500°K below the exospheric temperature used in the 1962 standard. The 1962 and 1976 profiles of kinetic temperature are shown in Figure 7.

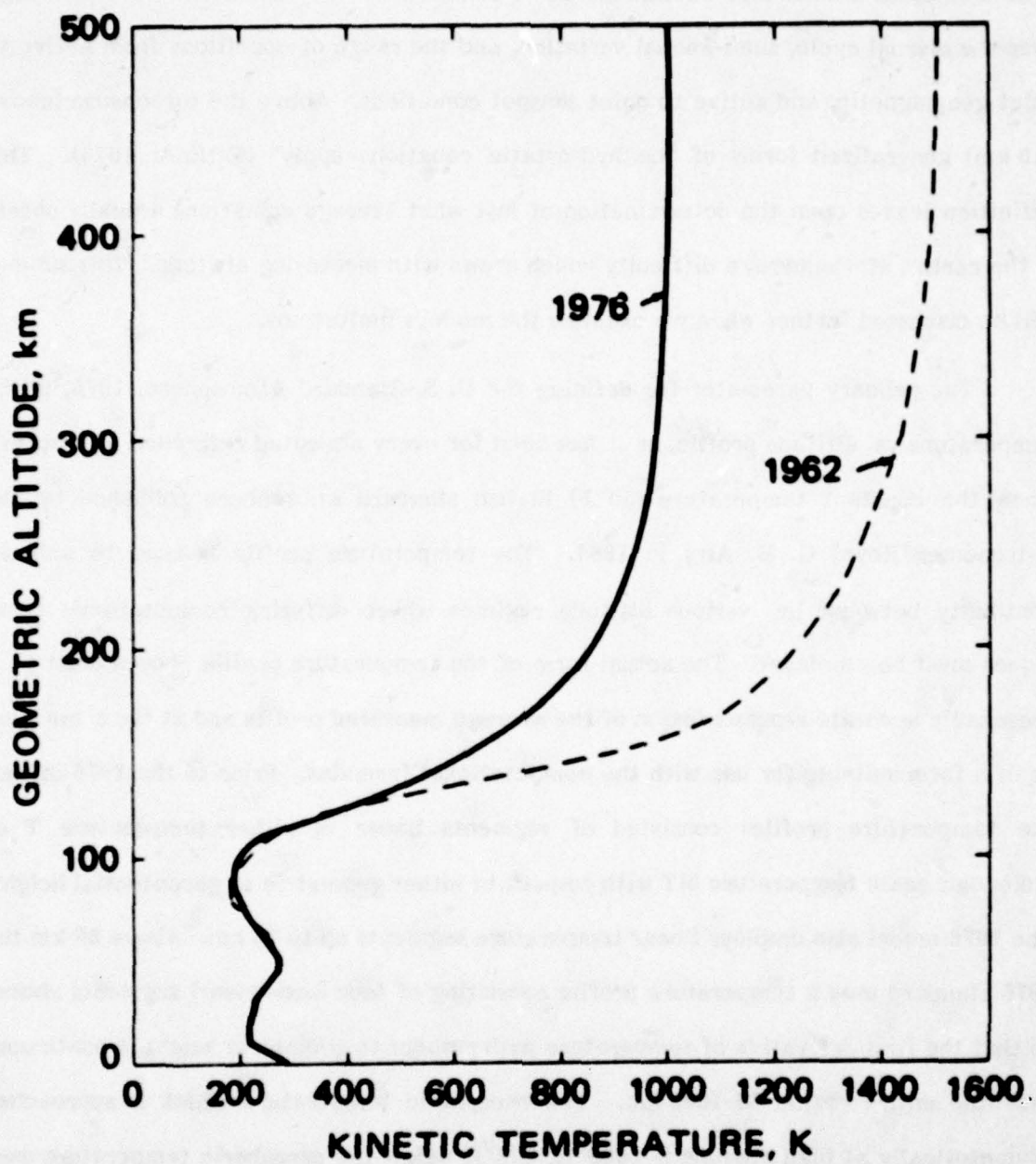


Figure 7. Kinetic temperature vs geometric altitude for the 1962 and 1976 Standard Atmospheres. Note in particular the differences near 100 km and above 120 km (from COESA, 1976).

The computations are performed differently in the regions below and above 86 km. Below the 86 km the model assumes ground level mixing ratios (except for trace constituents such as ozone which are handled separately) and hydrostatic equilibrium. Above 86 km the simplified hydrostatic equation no longer applies, and diffusion and vertical transport as well as effects of atmospheric chemistry must be considered. The transition to a purely diffusive regime is accomplished gradually in the region 86-115 km. It is therefore necessary to consider each constituent separately; many of the atmospheric properties which are calculated directly below 86 km, such as pressure, viscosity, etc., must be determined as the sum of the contributions of the various constituents at higher altitudes. A number of processes known to occur in this height range are taken into account by a combination of tractable analytical formulas and empirically determined constants to reproduce experimental data. Since small adjustments in parameters propagate their effects to higher altitudes, the choice of a particular parameter value (or even functional form) is often the result of an iterative procedure. The processes considered in formulating the model are

1. Vertical transport
2. Height-dependent molecular diffusion
3. Height-dependent eddy diffusion
4. Thermal diffusion
5. Dissociation and recombination.

The altitude profiles for the various species considered, N_2 , O, O_2 , Ar, He, and H, should be determined simultaneously as a coupled set of equations using the predetermined temperature profile. In practice, in order to reduce computation time, an iterative procedure was used, starting with N_2 and proceeding in the order in which the species are named above. The rationale for this is explained in Part 1 of the published model (COESA, 1976). The parameters chosen for the 1976 model have the eddy diffusion coefficient set to zero above 115 km, the thermal diffusion and vertical velocity terms small or zero above 120 km, and complete diffusive equilibrium obtaining above 150 km. Hydrogen is an exception to the above; it is only determined for altitudes 150-1000 km, with diffusive equilibrium obtaining essentially above 500 km.

After the number-density altitude profiles have been obtained for the individual species, a number of other atmospheric properties are determined by combining the profiles with the previously determined temperature profile. These include pressure, total number and mass densities, density and pressure scale heights, mean air-particle speed, mean free path, mean collision frequency, speed of sound, dynamic and kinematic viscosity, and the coefficient of thermal conductivity. All of these parameters are either tabulated or shown graphically in the published model. The density-height profile for the 1976 standard and several earlier standards are shown in Figure 8.

Accuracy and Limitations. When considering a reference atmosphere such as the 1976 U.S. Standard the question of accuracy involves somewhat different considerations than for a more complete model such as CIRA 1972 or Jacchia 1977.

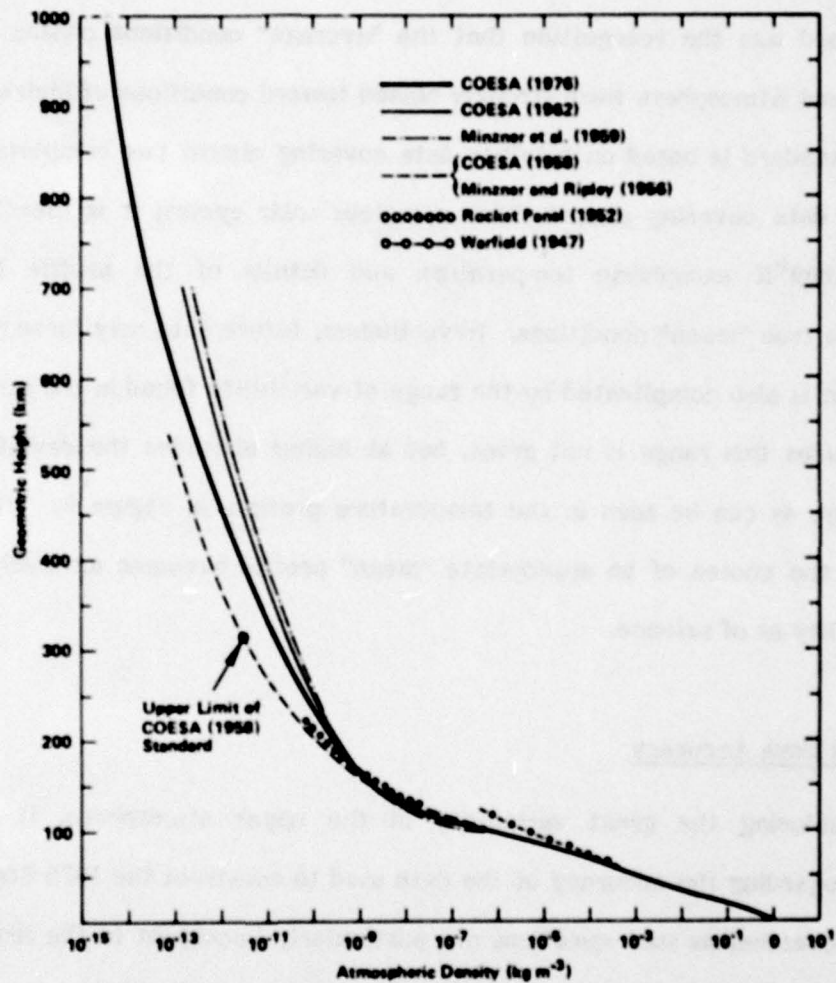


Figure 8. Density-height profiles of several model and standard atmospheres showing the evolution from 1947 to 1976. Note in particular altitudes above about 250 km where the range is more than an order of magnitude (from Minzner, 1977).

a. Appropriate Mean Conditions

Since the model is meant to represent mean conditions, the first question must be: How appropriately are the mean conditions selected and how well do the selected data represent this mean condition. As noted previously, a primary impetus for issuing the 1976 Standard was the recognition that the "average" conditions chosen for the 1962 U. S. Standard Atmosphere were strongly biased toward conditions of high solar activity. The 1976 Standard is based on satellite data covering almost two complete solar cycles and rocket data covering almost three complete solar cycles; it is therefore probable that the 1000°K exospheric temperature and details of the profile fairly closely approximate true "mean" conditions. Nevertheless, future data may force re-evaluation. The problem is also complicated by the range of variability found in the atmosphere. At lower altitudes this range is not great, but at higher altitudes the deviations increase dramatically, as can be seen in the temperature profiles in Figure 9. With such large variations, the choice of an appropriate "mean" profile becomes as much a matter of taste or utility as of science.

b. Data Base Accuracy

Considering the great variability in the upper atmosphere, it may be that questions regarding the accuracy of the data used to construct the 1976 Standard are not crucial. Nevertheless such questions are particularly important in the range 86-150 km where the transition to a diffusive model takes place. Much of the chemistry and the dynamics of this region is not well-known and in many cases the few available measurements appear to conflict with requirements imposed by measurements at higher

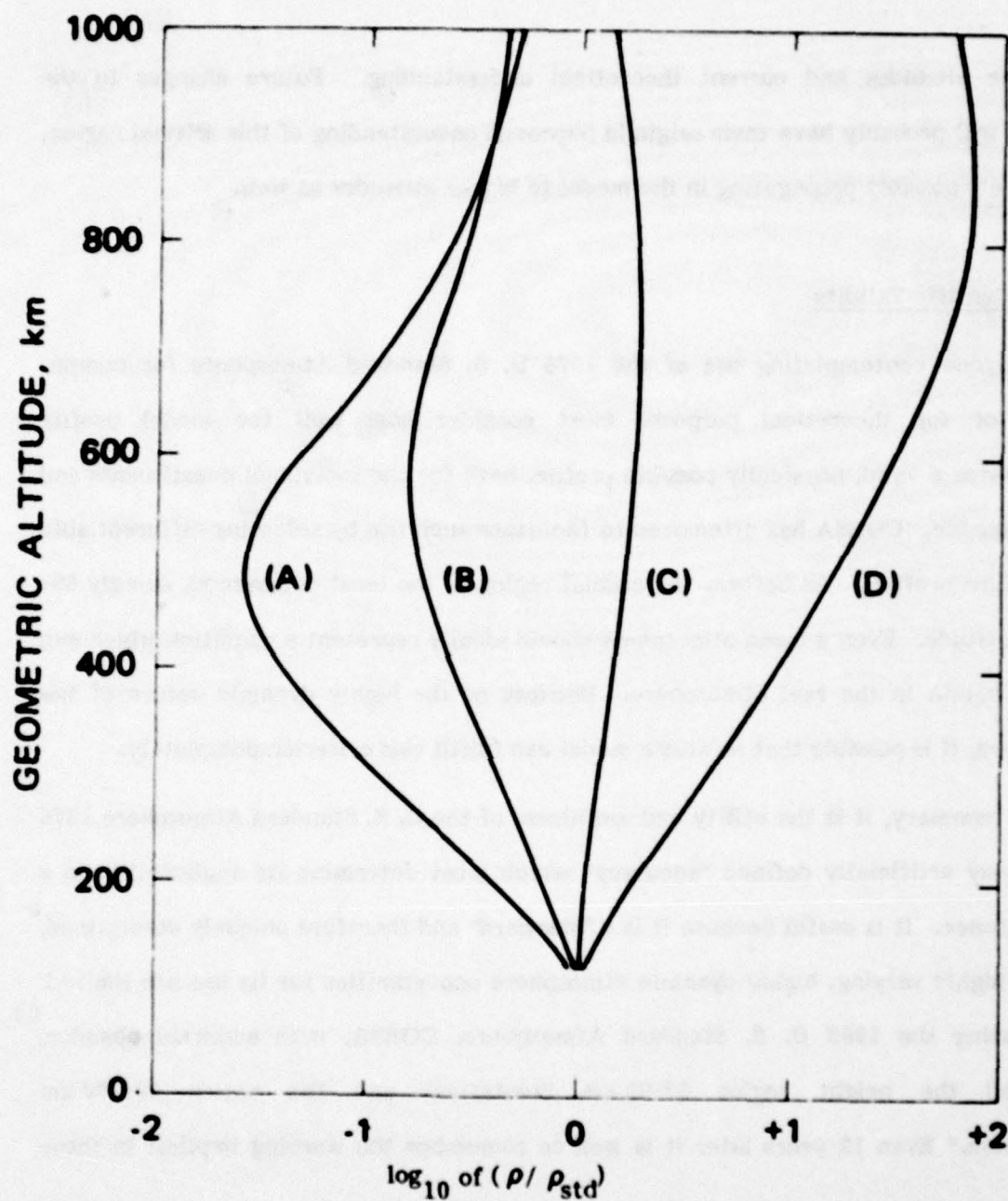


Figure 9. Range of deviations of the density-altitude profiles from the 1976 standard for various degrees of solar activity: (A) for lowest exospheric temperature at sunspot minimum; (B) average conditions at sunspot minimum; (C) average conditions at average sunspot maximum; and (D) exceptionally active conditions (from COESA, 1976).

and lower altitudes and current theoretical understanding. Future changes to the Standard will probably have their origin in improved understanding of this critical region, with effects possibly propagating in the model to higher altitudes as well.

c. Scientific Validity

Anyone contemplating use of the 1976 U. S. Standard Atmosphere for computational or for theoretical purposes must consider how well the model profile approximates a valid, physically possible profile, both for the individual constituents and as an ensemble. COESA has attempted to facilitate such use by selecting differentiable temperature profiles. As before, the crucial region is the least understood, namely 85-150 km altitude. Even a mean atmosphere should ideally represent a condition which can actually obtain in the real atmosphere. Because of the highly dynamic nature of the atmosphere, it is possible that no static model can fulfill this criterion completely.

In summary, it is the utility and usefulness of the U. S. Standard Atmosphere 1976 and not any artificially defined "accuracy" which must determine its applicability in a given instance. It is useful because it is a "standard" and therefore uniquely determined, but in a highly varying, highly dynamic atmosphere opportunities for its use are limited. When issuing the 1962 U. S. Standard Atmosphere, COESA, with admirable candor, designated the height region 32-90 km "tentative" and the region 90-700 km "speculative." Even 15 years later it is well to remember the warning implicit in these words.

The OGO-6 and ESRO-4 Models

Introduction. Two models of thermospheric temperature, density and composition have been derived entirely from data taken by satellite-borne mass spectrometers. Since these models are identical in their mathematical formulation, differing only in their data bases, they will be described together.

Hedin et al. (1974) developed a global model of the thermosphere above 120 km for quiet geomagnetic conditions from measurements of the density of N_2 , O and He taken by the mass spectrometer on the OGO-6 satellite. This satellite was launched on 5 June 1969 into an 82° inclination orbit with 398 km perigee and 1100 km apogee and operated until July 1971. During this period, the latitude of perigee of the satellite moved six times around the earth and through ten diurnal cycles. Values of the mean $F_{10.7}$ flux varied from 108 to 168, the overall average being near 150; the average value of A_p was 4. The data used in the model covered the altitude range 400-600 km.

Data taken by the mass spectrometer on board the ESRO-4 satellite during geomagnetically quiet times were used by von Zahn et al. (1977) to develop a global model of the thermosphere above 120 km. The ESRO-4 satellite was launched on 22 November 1972 into a 91° inclination orbit with initial perigee at 245 km and apogee at 1177 km and operated until 15 April 1974. Data from 228 days during this period were used as the data base. Values of $F_{10.7}$ ranged from ~ 70 to ~ 125 , with a mean value of 92; the average value of A_p was 7. The data used in the model covered the altitude range 240-320 km. The ESRO-4 model thus complements the OGO-6 model with measurements at lower altitudes and lower levels of solar activity.

Model Formulation. In both models, the composition is described in terms of density variations at a reference altitude z_0 (450 km for OGO-6 and 275 km for ESRO-4) with an altitude dependence which assumes isothermal conditions at higher altitudes at any given time and location. A spherical harmonic expansion (in geographic latitude-local time coordinates) is used to fit the density data at z_0 (in a least-squares sense) with the following formula:

$$n(z, L) = n(z_0) \exp \left[G(L) - 1 \right] \exp - \left[\frac{Mg_0 (z-z_0) (R_E + z_0)}{R T_\infty(L) (R_E + z)} \right] \quad (24)$$

where

- n = number density of a particular gas, cm^{-3}
- z = altitude, km
- z_0 = reference altitude
- L = variable representing the geographical and geophysical parameters upon which density is assumed to depend
- G = spherical harmonic expansion described below
- M = molecular weight of a particular gas, g/mole
- R_E = polar radius of the earth, 6357 km
- g_0 = acceleration of gravity at the reference altitude
- R = gas constant, $8.314 \times 10^{-3} \text{ gm-km}^2/\text{mole sec}^2 \text{ deg}$
- T_∞ = exospheric temperature, $^\circ\text{K}$.

The function $G(L)$ contains the information on the variation of density with selected geographic and solar activity parameters. It is written as a series of spherical harmonics whose coefficients for each gas have been determined using the mass spectrometer data and are tabulated in the model. The spherical harmonics represent the following kinds of variations of density in the thermosphere: variations with solar activity ($F_{10.7}$), variations with geomagnetic activity (A_p), variations with time of the year (including annual and semiannual terms), variations with local time and latitude (including diurnal, semidiurnal and terdiurnal terms). A total of 37 coefficients for each thermospheric constituent is involved. The input parameters required by the model are latitude, local time and altitude of the point in question, day of the year, the values of $F_{10.7}$ both one day before the day in question and averaged over three solar rotations, and the geomagnetic activity index A_p , with a six hour lag in the OGO-6 model, and a latitude-dependent lag of $4.8 - |\phi|/45^\circ$, where ϕ is the geographic latitude, in the ESRO-4 model.

The merit of a model based on a spherical harmonic analysis is that these functions form a complete set that can, in principle, represent any degree of complexity in the data by a systematic increase in the number of terms used. Furthermore, since the spherical harmonics are approximate eigenfunctions of the thermosphere, relatively few terms should be required. The form of the dependence of density on $F_{10.7}$ is similar to that of the Jacchia 1971 model, except that allowance is made for a possible non-linearity in the correlation with the 27-day $F_{10.7}$ variation; such an effect has been suggested by some data from ground-based observations. The dependence of density on A_p included in these models is small; the possibility of a latitude variation of the geomagnetic activity effect has been included.

Once the density distributions at the reference altitude and T_{∞} are determined using equation (24), the following formulas are used to evaluate the densities and temperatures at all other altitudes:

$$T(z, L) = T_{\infty}(L) - \left[T_{\infty}(L) - T_{120} \right] \exp \left[-s(z-120) \right] \quad (25)$$

$$n(z, L) = n(120) D(z, T_{\infty}(L), s) \quad (26)$$

$$D(z, T(L), s) = \left[\frac{1-a}{1-ae^{-\sigma\xi}} \right]^{1+\alpha+\gamma} \exp(-\sigma\gamma\xi) \quad (27)$$

where T_{120} = temperature at 120 km altitude, 355°K

s = temperature gradient parameter, 0.022 km^{-1}

σ = $s + 1.5 \times 10^{-4}$

a = $1 - T_{120}/T_{\infty}(L)$

ξ = $(z - 120)(R_E + 120)/(R_E + z)$

γ = $Mg_{120}/\sigma R T_{\infty}(L)$

α = thermal diffusion coefficient.

The expression for $T(z, L)$ leads to a temperature which increases with increasing altitude above the 120 km level, asymptotically approaching the exospheric temperature $T_{\infty}(L)$ at great heights. The formulations of equations (26) and (27) are based on the assumption of hydrostatic equilibrium above the 120 km level, where variations in all quantities other than the temperature and the N_2 density are allowed.

Accuracy. The accuracy of these models is on the order of the experimental error for He and O (20% for O and larger for He) and about three times the experimental error for N_2 . The root-mean-square error of the models (with respect to the data which were used in their generation) is on the order of 15-20%.

Limitations. There are two aspects of the mass spectrometer models which limit their usefulness. These limitations are basically due to characteristics of the data bases used in their generation. Since each model used data from only about two years of satellite operation, the coverage in latitude and local time at specified values of $F_{10.7}$ and A_p is not really adequate for producing a definitive model. (This is especially evident with respect to A_p , leading to a restriction of the models to quiet geomagnetic conditions.) The second limitation is related to the coverage in altitude. Since the data used in the models were taken above a particular altitude, no actual measurements of density below these altitudes could be used. The model predictions at lower altitudes are thus extrapolations of the model under the assumption of hydrostatic equilibrium. Hydrostatic equilibrium for an individual gas species probably does not occur below ~200 km altitude, except in the case of molecular nitrogen. Thus, these models may be suspect at all altitudes below those at which data were taken, and certainly are unreliable below ~200 km.

The Mass Spectrometer-Incoherent Scatter (MSIS) Model

Introduction. The OGO-6 and ESRO-4 models were the first empirical models of the upper atmosphere to be based on data taken by satellite-borne mass spectrometers. These models suffer from restricted data bases, however, and are useful only when values of atmospheric properties are required for the ranges of altitude, solar and geomagnetic activity, etc., which were included in these data bases.

Since the launch of these two satellites, a number of additional spacecraft carrying mass spectrometers have been placed into earth orbit. These satellites, taken in combination, provide a significant improvement in data coverage. For example, measurements of atmospheric density and composition are now available over a wide range of altitudes (~140-600 km), and for a range of $F_{10.7}$ of $\sim 75-180 \times 10^{-22} \text{ W/m}^2 \text{ Hz}$. Furthermore, a large data base of upper-atmospheric temperature measurements has been compiled at several ground-based incoherent scatter radar sites; these data provide complementary information in the form of direct measurements of temperature with good local time coverage at particular latitudes over a wide range of solar activity and all seasons.

The mass spectrometer-incoherent scatter (MSIS) model (Hedin et al., 1977a,b) makes use of measurements of upper-atmospheric composition from mass spectrometers on five satellites (AE-B, OGO-6, San Marco 3, Aeros A and AE-C) and neutral temperatures inferred from incoherent scatter measurements at four ground stations (Arecibo, Puerto Rico; Jicamarca, Peru; Millstone Hill, Mass.; and St. Santin, France). The overall data set covers the time period from the end of 1965 to mid-1975 (effectively a complete 11 year solar cycle), values of $F_{10.7}$ of 75-180, values of A_p up to ~ 100 , and is most applicable to the altitude range 200-600 km.

Model Formulation. The model formulation is virtually identical to that of the OGO-6 and ESRO-4 models. The following exceptions allow more versatility in the MSIS model:

- 1) The temperature and N_2 density at 120 km are functions of L , the variable representing the geographical and geophysical input parameters.
- 2) The temperature gradient parameter s is a function of L .
- 3) The variation with daily geomagnetic index A_p is nonlinear, allowing the model to be applied to moderately disturbed times.
- 4) A time-independent North-South asymmetry is allowed in the densities.
- 5) Because of the likelihood of noticeable departures from hydrostatic equilibrium in the diurnal and magnetic activity components of the density below 200 km, some of the terms in the function $G(L)$ are multiplied by a function of altitude which approximates the effects of a vertical diffusion velocity.
- 6) Many parameters in the function $G(L)$ as formulated in the OGO-6 and ESRO-4 models were found to be of little significance and are set to zero in the MSIS model.

Accuracy. The uncertainty in the absolute average exospheric temperature in the model is about 15-20°K. The coefficient of temperature variation with $F_{10.7}$ is 3% higher than in the Jacchia 1971 model and 10% higher than that in the OGO-6 model.

The MSIS model N_2 density at 120 km is 25% below that in the Jacchia 1971 model. The average temperature gradient parameter $s = 0.0255$ gives a temperature gradient at 120 km of 16.7°K/km , which is higher than the 10°K/km of the Jacchia 1971 model, but which agrees with the incoherent scatter measurements.

The various atmospheric species can be crudely ranked as to the absolute error in the model representation of the mean density profile above 150 km: N_2 (~15%), O (~20%), He (~20%), Ar (~25%), H (~50%) and O_2 (~50%). Fortunately, the atmospheric gas above 150 km is composed primarily of those species whose errors are the lowest.

At 120 km, the total density is 30% below that of the Jacchia 1971 model, primarily because of the lower N_2 density, which is closer to that measured by rocket-borne mass spectrometers than is that in the Jacchia 1971 model. At altitudes above 205 km, the MSIS model average density is about 15% above that of the Jacchia 1971 model, well within errors of absolute calibration and analysis for both mass spectrometers and orbital drag studies.

Limitations. The MSIS model is believed to provide a better representation of global temperature and composition variations than do other existing global models. The limitations of the model arise primarily from incomplete data at low altitudes and during times of disturbed magnetic conditions.

Jacchia 1977

The Jacchia 1977 model is the latest in a series of empirical models of the thermosphere. The previous (1971) Jacchia model enjoyed widespread use, but the analysis of mass spectrometer data from OGO-6 revealed that revision was necessary. Analysis of these data showed that the phase of the diurnal variation was a function of altitude and, more important, at a fixed altitude the phases of the diurnal variations of the individual gases were different. A major goal of the model was to reproduce the relative concentrations of N_2 and O at 450 km as derived from OGO-6 while agreeing with the total density determined by satellite drag.

Jacchia 1977 is really two sets of models, the static models and a model which includes known thermospheric variations. The static models are indexed by exospheric temperature, from which a temperature profile is determined. The profile starts with a constant value of 188°K at 90 km, and an altitude gradient of zero, rises to an inflection point at a fixed altitude of 125 km, and then continues to rise, asymptotically approaching the selected exospheric temperature at high altitudes. In addition to temperature, the static models give number densities as a function of altitude for N_2 , O_2 , Ar, O, He, and H. A fraction by volume for each gas at 90 km which agrees with the sea level value (except for a correction to the helium fraction which is required in order to obtain proper thermospheric helium results) is specified. Between 90 and 100 km a temporary empirically determined mean molecular weight profile is given and used, along with the temperature profile, to integrate the barometric equation for total mass density. The departure from constant mean molecular weight is ascribed entirely to the

dissociation of O_2 ; the relative number densities of N_2 , Ar, and He are held constant at the 90 km values. Small corrections are then applied to the O and O_2 profiles in order to bring them into better agreement with experimental measurements. The final mean molecular weight profile is computed from the number densities thus determined. Above 100 km the individual number densities decrease with altitude at a rate determined by a diffusion equation which includes thermal diffusion (He and H) and vertical flux (H only) terms as well as the usual molecular diffusion and gravity terms. For H the boundary condition is specified at 500 km and is a function of exospheric temperature, unlike the other gases for which the boundary conditions are determined at 100 km as described above.

The Jacchia 1977 model which includes thermospheric variations is an elaboration of the static models and attempts to model several types of variation:

1. Variation with the solar cycle
2. Variation with the daily change in activity on the visible disk of the sun
3. The daily, or diurnal, variation
4. Variation with geomagnetic activity
5. Seasonal-latitudinal variations
6. The semi-annual variation.

The discussion of the model in this report is necessarily brief, and the complete description (Jacchia, 1977) should be consulted for details.

The mean exospheric temperature is determined by a function of the daily $F_{10.7}$ solar flux (evaluated at a time delayed an amount depending on local time) and a Gaussian weighted average of $F_{10.7}$ (using a time constant of 71 days).

The diurnal variation of the temperature about its mean value is given by a function of solar declination, latitude, and local time. For use in determining number density profiles, a set of "pseudo-temperature" profiles are introduced, one for each constituent. The equations which describe these pseudo-temperature curves all have the same form, but the phase of the local time variation is different for the pseudo-temperature associated with each of the individual constituents. This is done so that, when integrating the diffusion equation above 100 km, the times of peak density of the various constituents can be at different hours of the day. The phases of the various pseudo-temperatures are related in such a way as to result in the peak in total density always occurring at the same local time, independent of altitude.

Variations with geomagnetic activity (characterized by the planetary index K_p) are divided into three categories. The first category, the "thermal component," is accounted for by an increase in temperature at all altitudes. The amount of atmospheric heating which causes this temperature increase is characterized by K_p evaluated at a time which allows for a delay due to the propagation time of the heating from the polar regions to the point of interest. This delay time increases with decreasing invariant magnetic latitude. A correction to the temperature profile at all altitudes is determined by the delayed K_p value and the invariant magnetic latitude. This corrected temperature profile, of course, is used when integrating the barometric and diffusion equations. It

might be noted that this change greatly complicates use of the model because the resulting temperature profile is not the same as the static model temperature profile with the same exospheric temperature. This means that for $K_p \neq 0$ it is not sufficient to calculate the exospheric temperature, consult the static model tables corresponding to that exospheric temperature, and then modify the tabulated densities as prescribed by the model.

The second component of the variations due to geomagnetic activity is the "effect of a change in the height of the homopause." This is accounted for by a correction to the individual number densities which increases the abundance of Ar and O₂ while decreasing the abundance of O and He; no correction is made to N₂ or H.

The third component is the "equatorial wave" which describes the "piling up" of the atmosphere near the equator due to meridional flow driven by the polar region heating. This latitude-dependent correction increases all constituents by the same fractional amount.

The seasonal-latitudinal variations are divided into a "thermospheric" and a "mesospheric" variation. The thermospheric term adjusts each gas by an amount proportional to the product of solar declination and sine of the latitude of the point of interest.

Although in the troposphere and stratosphere, as well as the upper thermosphere, the temperature is warmer in summer than winter, in the mesosphere the temperature is warmer in winter than in summer. A corresponding behavior (with opposite phase) is expected for the density. The mesospheric seasonal-latitudinal correction is of no importance above 170 km.

The semi-annual variation is accounted for in the same manner as in the Jacchia 1971 model where the density of all constituents is modified by a percent which is the product of a function of altitude and a function of day of the year.

Limitations of the Model. The great majority of the data which have been used to develop the model is from altitudes above 250 km. The model may therefore not represent variations in the lower thermosphere as well as variations in the higher altitude regions. The model is not well suited for use without a computer because of its complexity. Relative to other recent models, Jacchia 1977 is not well suited for use on a computer either. The modification of the basic form of the temperature profile because of geomagnetic activity requires either numerical integration of the barometric and diffusion equations for each data point of interest, or storage of a vast amount of pre-computed data. The introduction of psuedo-temperatures and the later correction of densities destroys much of the aesthetic value which might have been derived from basing density profiles on the diffusion equation. One might well ask whether the great complexity relative to other models is adequately justified by any compensating significant increase in accuracy. Computational ease and efficiency have apparently not been given much weight in the development of the model.

Accuracy. No adequate discussion of the accuracy of the model is presented by its author, but comparison with experimental data (see the next section) leads to an estimated r.m.s. error for densities of about 19%.

III. DISCUSSION AND COMPARISON OF MODELS

Two major factors which determine the usefulness of a model are its convenience and its accuracy. Although the need for accuracy is obvious, the need for convenience is often not clearly recognized. To a large extent, the requirements for a model to be convenient for use are the same whether calculations are to be made manually or by an electronic computer. A notable exception is in the use of extensive tables, which are more appropriate for the human than the computer. A classic example is the evaluation of an elementary trigonometric function which a human might look up in a table of pre-calculated values; the storage space which would be taken up by such a table in a computer is too valuable for such use, and the elementary functions are therefore calculated from a formula. Hereafter we will assess convenience in terms of implementation of the model for use by a computer.

A model should have a simple structure. It can then be implemented with a compact code which requires little storage space. This desire for simple structure is somewhat in conflict with the complicated behavior of the thermosphere which tends to require more complexity in the model if adequate accuracy is to be maintained. Simple structure also usually leads to fast execution time; however a structure which is conceptually simple can lead to slow execution in some cases. The most common instance of this difficulty is in the semi-empirical models which specify a temperature profile and then give a differential equation (involving temperature) which must be solved to obtain density profiles. The differential equation is solved by numerical integration, a simple but time-consuming process. If the equation can be integrated analytically (as is the case when using a "Bates-Walker" approach), the usefulness of the model is improved.

The model must provide the required parameters. Most modern models provide temperature and densities of the major species. If only total density is required, this detailed output may have been purchased at some cost in terms of efficiency. The input parameters required by the model must be available. Such indices as $F_{10.7}$ and K_p have been used in spite of their well-known inadequacies largely because of their availability.

That a model must be accurate is obvious. Less obvious is how the accuracy is to be characterized for a particular use. A perfect description of the atmosphere is the ideal, but some kinds of inaccuracies are unimportant for specific applications. A satellite system designer who is required to estimate the orbital lifetime until reentry of a satellite designed for a two year lifetime may be quite satisfied with a model having the correct mean value when averaged over a month's time span even if the errors averaged over a single orbit are quite large. On the other hand, a tracking station operator may attach no importance at all to the long-term mean behavior of the atmosphere (which can be empirically adjusted for in day-to-day operations) if the model could only accurately predict the short-term variations.

Now we will try to make some assessment concerning the usefulness of the models presented in this report. Models produced prior to 1970 were developed from data bases with significant limitations. Most of the data were from satellites with perigee altitudes above 250 km and were based on drag calculations which only give total density. The only advantage these models have over more recent models is their greater simplicity and the many years of experience which some groups have had in using them. More recent models are more suitable except for those situations where only total density is required and some loss of accuracy can be tolerated in exchange for small, fast computer code or where the cost of replacing present software greatly exceeds the benefits achievable by the use of better (but still far from perfect) models.

The OGO-6 and ESRO-4 models have the same structure as the MSIS model but were based on more limited data, and these two models can probably be regarded as obsolete.

The McDonnell Douglas model (MDAC) has as its most interesting and potentially important feature a specific incorporation of high latitude heating effects. The present version of the model, unfortunately, does not specify how the parameters which describe this heating are to be derived from available geophysical data, and only "typical" values for these parameters are given. Thus, the model's greatest potential asset is presently one of its greatest weaknesses, and until the model is developed further it cannot be recommended for general use.

The best models for general use are probably Jacchia 1971 (or the nearly identical CIRA 1972) and MSIS. Jacchia 1971/CIRA 1972 is an internationally recognized model which is familiar to most workers in the field. It is thoroughly documented, and an excellent FORTRAN version of the computer code has been published in the CIRA 1972 report. It is primarily based on drag data from satellites with perigee altitudes above 200 km. It does not incorporate some of the most recent knowledge of the behavior of individual species and thus is especially of value when only total density at altitudes above 200 km is required. The model requires numerical integration of the diffusion equation which is a time-consuming procedure; in order to avoid this difficulty some users have developed modified versions of the model which give approximately the same results but are computationally more efficient.

Jacchia's 1977 model, although still limited in the amount of low altitude data on which it is based, does describe the diurnal behavior of the individual species in a manner

consistent with recent observations. The major objection to this model is its complexity and resulting inconvenience of use. It appears that development of the model was guided almost entirely by considerations of accuracy.

The data base used to develop the MSIS model includes low altitude data and mass spectrometer determined measurements of individual species. Numerical integration is not required, resulting in a reasonably fast computer code. There is no published version of the computer code. The Goddard group has provided a FORTRAN version of the model upon request, but there are some difficulties with this code. It appears to have been developed over a period of time and is not as "clean" or well written as the CIRA 1972 code. It is written in a non-ANSI dialect of FORTRAN which is not acceptable at some computer installations without non-trivial modifications. Despite these limitations, it is probably the best presently available model for general use, especially for use at altitudes below 200 km and where individual species data are required. As the model is based on only a fraction of the Atmosphere Explorer data, publication of a revised version in the near future would not be surprising. If we may be guided by memory of the replacement of the OGO-6 model by the MSIS model, we may anticipate that a revised version of the MSIS model would have a structure nearly identical to the present version.

A specific comparison of a number of models with measured data is given in Tables 1-13. The data consist of in-situ measurements of total density made by cold cathode ion gauges carried on board NASA's AE-C, D, and E satellites. Data were from December 1973 to November 1974 (AE-C), October 1975 to January 1976 (AE-D), and November 1975 to October 1976 (AE-E). Measurements were made in an altitude range of approximately 135 to 300 km. For every experimental determination of density, each of the models was used to calculate a density using values of geophysical and solar

parameters appropriate for the time and location of the experimental measurement. The quantity

$$r = \log_e \left(\frac{\text{measured density}}{\text{model density}} \right)$$

was then used to compute three statistics which may be used to examine the ability of the models to predict thermospheric density. Let us denote by r_i this quantity calculated for the i -th density determination in the data base.

The mean, or average, error of a model is characterized by

$$\bar{r} = \frac{1}{n} \sum_{i=1}^n r_i ,$$

where n is the number of points used. The r.m.s. error is characterized by

$$\sqrt{\overline{r^2}} = \left(\frac{1}{n} \sum_{i=1}^n r_i^2 \right)^{\frac{1}{2}} ,$$

and the r.m.s. error after removing the mean error is characterized by

$$\sqrt{\overline{r^2} - \bar{r}^2} = \left[\frac{1}{n} \sum_{i=1}^n (r_i - \bar{r})^2 \right]^{\frac{1}{2}} .$$

Table 1 presents these statistics computed for the entire data base. Tables 2-13 give the same statistics computed using data from a number of specific altitudes.

TABLE 1

Comparison of Measured Densities to Model Values

All altitudes (135-300 km)

n = 32, 720

	\bar{r}	$\sqrt{\bar{r}^2}$	$\sqrt{\bar{r}^2 - \bar{r}^2}$
'DENSEL	0.152	0.283	0.239
J65	-0.186	0.258	0.180
J71	0.058	0.173	0.163
MDAC	0.230	0.307	0.203
MSIS	0.001	0.163	0.163
J77	0.054	0.182	0.174

$$r = \log_e \left(\frac{\text{measured density}}{\text{model density}} \right)$$

TABLE 2

Comparison of Measured Densities to Model Values

135 km

n = 331

	\bar{r}	$\sqrt{\bar{r}^2}$	$\sqrt{\bar{r}^2 - \bar{r}^2}$
'DENSEL	0.236	0.289	0.166
J65	-0.089	0.191	0.169
J71	-0.040	0.150	0.145
MDAC	-0.017	0.150	0.149
MSIS	0.110	0.170	0.130
J77	-0.052	0.199	0.192

$$r = \log_e \left(\frac{\text{measured density}}{\text{model density}} \right)$$

TABLE 3

Comparison of Measured Densities to Model Values

140 km

n = 939

	\bar{r}	$\sqrt{\bar{r}^2}$	$\sqrt{\bar{r}^2 - \bar{r}^2}$
'DENSEL	0.215	0.271	0.166
J65	-0.060	0.181	0.171
J71	0.009	0.136	0.136
MDAC	0.047	0.146	0.138
MSIS	0.089	0.160	0.133
J77	0.010	0.178	0.178

$$r = \log_e \left(\frac{\text{measured density}}{\text{model density}} \right)$$

TABLE 4

Comparison of Measured Densities to Model Value

150 km

n = 1655

	\bar{r}	$\sqrt{\bar{r}^2}$	$\sqrt{\bar{r}^2 - \bar{r}^2}$
'DENSEL	0.171	0.234	0.159
J65	-0.108	0.191	0.158
J71	0.034	0.143	0.139
MDAC	0.108	0.185	0.150
MSIS	0.057	0.135	0.122
J77	0.031	0.165	0.162

$$r = \log_e \left(\frac{\text{measured density}}{\text{model density}} \right)$$

TABLE 5

Comparison of Measured Densities to Model Value

160 km

n = 2059

	\bar{r}	$\sqrt{\bar{r}^2}$	$\sqrt{\bar{r}^2 - \bar{r}^2}$
'DENSEL	0.178	0.238	0.159
J65	-0.132	0.200	0.150
J71	0.057	0.152	0.141
MDAC	0.164	0.231	0.163
MSIS	0.041	0.130	0.123
J77	0.050	0.168	0.161

$$r = \log_e \left(\frac{\text{measured density}}{\text{model density}} \right)$$

TABLE 6

Comparison of Measured Density to Model Values

170 km

n = 1371

	\bar{r}	$\sqrt{\bar{r}^2}$	$\sqrt{\bar{r}^2 - \bar{r}^2}$
'DENSEL	0.223	0.275	0.161
J65	-0.133	0.200	0.149
J71	0.082	0.169	0.148
MDAC	0.216	0.276	0.172
MSIS	0.037	0.140	0.135
J77	0.069	0.166	0.151

$$r = \log_e \left(\frac{\text{measured density}}{\text{model density}} \right)$$

TABLE 7

Comparison of Measured Densities to Model Values

180 km

n = 1367

	\bar{r}	$\sqrt{\bar{r}^2}$	$\sqrt{\bar{r}^2 - \bar{r}^2}$
'DENSEL	0.256	0.308	0.172
J65	-0.149	0.214	0.154
J71	0.091	0.178	0.152
MDAC	0.253	0.310	0.178
MSIS	0.029	0.145	0.142
J77	0.076	0.175	0.158

$$r = \log_e \left(\frac{\text{measured density}}{\text{model density}} \right)$$

TABLE 8

Comparison of Measured Densities to Model Values

200 km

n = 1982

	\bar{r}	$\sqrt{\bar{r}^2}$	$\sqrt{\bar{r}^2 - \bar{r}^2}$
'DENSEL	0.286	0.340	0.184
J65	-0.188	0.245	0.156
J71	0.099	0.185	0.156
MDAC	0.312	0.365	0.188
MSIS	0.025	0.152	0.150
J77	0.091	0.189	0.165

$$r = \log_e \left(\frac{\text{measured density}}{\text{model density}} \right)$$

TABLE 9

Comparison of Measured Densities to Model Values

220 km

n = 1100

	\bar{r}	$\sqrt{\bar{r}^2}$	$\sqrt{\bar{r}^2 - \bar{r}^2}$
'DENSEL	0.084	0.238	0.223
J65	-0.266	0.324	0.186
J71	0.039	0.185	0.181
MDAC	0.277	0.350	0.214
MSIS	-0.068	0.185	0.172
J77	0.033	0.188	0.185

$$r = \log_e \left(\frac{\text{measured density}}{\text{model density}} \right)$$

TABLE 10

Comparison of Measured Densities to Model Values

240 km

n = 804

	\bar{r}	$\sqrt{\bar{r}^2}$	$\sqrt{\bar{r}^2 - \bar{r}^2}$
'DENSEL	-0.108	0.251	0.226
J65	-0.332	0.375	0.174
J71	-0.006	0.182	0.182
MDAC	0.252	0.332	0.215
MSIS	-0.145	0.226	0.174
J77	-0.009	0.178	0.178

$$r = \log_e \left(\frac{\text{measured density}}{\text{model density}} \right)$$

TABLE 11

Comparison of Measured Densities to Model Value

260 km

n = 675

	\bar{r}	$\sqrt{\bar{r}^2}$	$\sqrt{\bar{r}^2 - \bar{r}^2}$
'DENSEL	-0.213	0.300	0.212
J65	-0.316	0.358	0.169
J71	0.023	0.182	0.181
MDAC	0.290	0.360	0.214
MSIS	-0.141	0.224	0.174
J77	0.035	0.184	0.180

$$r = \log_e \left(\frac{\text{measured density}}{\text{model density}} \right)$$

TABLE 12

Comparison of Measured Densities to Model Values

280 km

n = 625

	\bar{r}	$\sqrt{\bar{r}^2}$	$\sqrt{\bar{r}^2 - \bar{r}^2}$
'DENSEL	-0.262	0.337	0.211
J65	-0.283	0.331	0.172
J71	0.068	0.192	0.179
MDAC	0.337	0.399	0.215
MSIS	-0.112	0.206	0.172
J77	0.091	0.200	0.178

$$r = \log_e \left(\frac{\text{measured density}}{\text{model density}} \right)$$

TABLE 13

Comparison of Measured Densities to Model Values

300 km

n = 582

	\bar{r}	$\sqrt{\bar{r}^2}$	$\sqrt{\bar{r}^2 - \bar{r}^2}$
'DENSEL	-0.297	0.367	0.215
J65	-0.245	0.307	0.184
J71	0.122	0.225	0.189
MDAC	0.378	0.441	0.228
MSIS	-0.078	0.187	0.170
J77	0.151	0.240	0.187

$$r = \log_e \left(\frac{\text{measured density}}{\text{model density}} \right)$$

Perhaps the most notable (and most discouraging) feature of Table 1 is the lack of substantial improvement in model development since 1971. In fact, except for an overall multiplicative factor due to being based on data taken at times near maximum solar activity, one might well conclude that there has been little improvement since 1965. If individual species were examined instead of total density, the progress of the last several years would presumably be more apparent. J71, MSIS and J77 all give similar accuracy when used to predict total density and are significantly superior to 'DENSEL, J65 and MDAC. For predicting number densities of individual species it may be anticipated that the performance of J71 would be poorer than that of MSIS and J77.

After nearly twenty years of thermospheric modeling work, it is interesting to ask about the accuracy of the models. This is a question not often discussed in any significant detail by the authors of the various models. An indication of the limits of recent models is seen in Figure 10, taken from the OGO-6 model report. The comparison seen is between the model prediction and the data on which the model is based. If compared with other data it would undoubtedly be found that the agreement would be even worse. Some of the scatter in Figure 10 is attributable to measurement error, but it seems clear that much of it is due to limitations of the model. Figures such as this clearly demonstrate the limitations of present-day models. Although this performance may seem rather poor in view of the ever greater accuracy demanded by users, a glance at Figure 11 may serve as a reminder that the remaining errors are not especially large when compared with the great variations present in the upper atmosphere. If one could predict the stock market behavior as accurately as thermospheric density, his future financial security would be well assured.

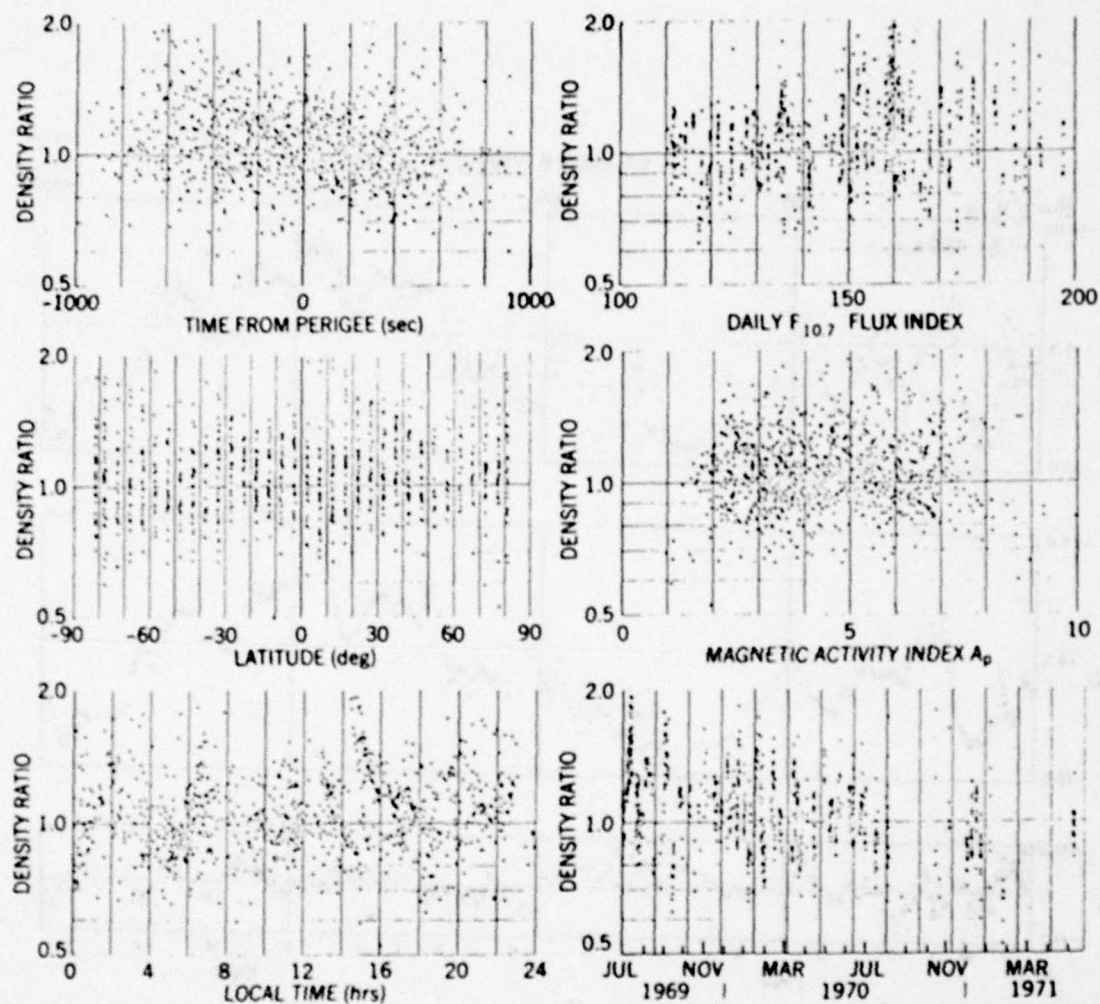


Figure 10. Ratio of the measured N_2 density to the model N_2 density as a function of time from perigee, geographic latitude, local time, $F_{10.7}$ solar flux, magnetic index A_p and day of year (from Hedin et al., 1972).

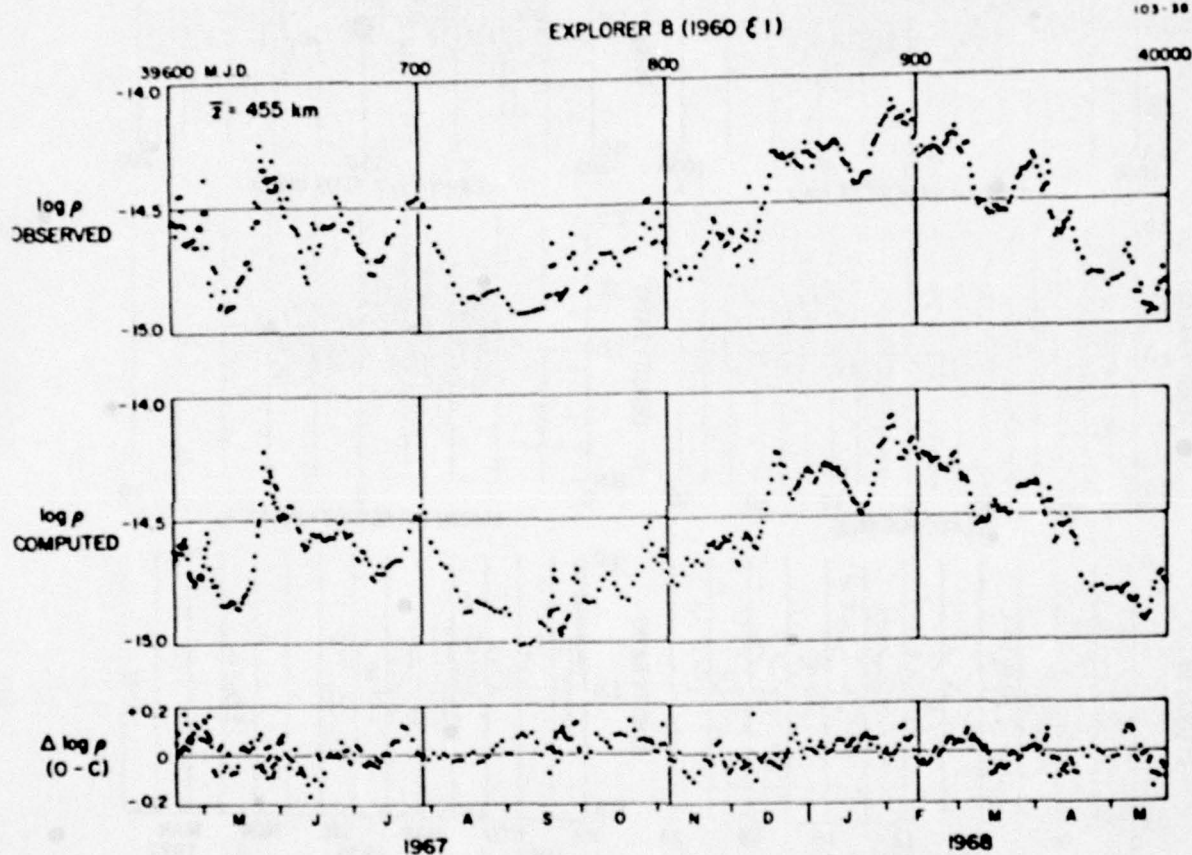


Figure 11. Observed and computed densities, reduced to a standard height of 530 km for satellite 1964 76A (Explorer 24). Computed densities were derived using the Jacchia 1971 model (from Jacchia, 1971).

Why is it that models do not do a better job of predicting thermospheric density? Part of the answer lies in the selection of parameters to characterize conditions in the thermosphere. For example, the amount of EUV heating is often measured by the 10.7-cm solar flux. The 10.7-cm flux itself cannot significantly heat the upper atmosphere. It has been established, however, that there is a reasonable correlation between the EUV flux and the 10.7-cm flux. This correlation is only approximate and may not be adequate for use in accurate models. However, the 10.7-cm flux is measured regularly and hence is readily available; better a "fair" index than none at all. A similar situation exists with respect to the energetic particle heating which occurs during geomagnetic storms. This heating is related to disturbances in the earth's magnetic field, but the relationship is undoubtedly not adequate for high accuracy models. There is a need for new parameters to be made available which more directly characterize phenomena which affect the thermosphere. Although this need has been recognized for over a decade, no significant new parameters have emerged.

Even if such improved parameters were available, it is not clear that extremely accurate models are possible. Gravity waves and other transient disturbances affect the density in a seemingly random fashion. It may be that ultimately we will be able accurately to predict the average state of the atmosphere but not be able to predict short-term (e.g. on a time scale shorter than a few hours) departures from this average state. In the language of the meteorologist it may be that we can predict the "climate" but not the "weather." It is not clear at present what the ultimate accuracy of models can be. There is still much to be done in developing the theoretical understanding of thermospheric behavior, particularly the interaction of the thermosphere with the next lower altitude region, the mesosphere.

Although there is no immediate prospect of a revolutionary improvement in the accuracy of thermospheric models, there are nevertheless good reasons for believing that prediction of thermospheric behavior may undergo significant improvement in the long run. Unlike tropospheric weather prediction, there does not exist the problem of local geography causing small-scale local differences. Propagation times for disturbances are of the order of hours which helps to smooth out perturbations quickly. The coupling between the mesosphere and the thermosphere and the unknown behavior of the atmosphere in the region near 90 km is a problem, as is the lack of routine monitoring of the state of the entire thermosphere by the equivalent of present meteorological satellites which monitor the troposphere and stratosphere. As remote sensing techniques are developed and applied to the mesosphere and lower thermosphere, we may reasonably expect that there will be steady, though probably not spectacular, progress toward higher accuracy models.

IV. DENSITY CONTOUR PLOTS

Contour plots with isopleths of constant total mass density are shown in this section for the most important models in current use: 'DENSEL, Jacchia 1971, MDAC, MSIS, and Jacchia 1977. The OGO-6 and ESRO-4 models are assumed to have been replaced by MSIS. As the emphasis for this report is on the lower thermospheric regions where satellite drag is important, the models have been evaluated at 140 and 180 km to show the low altitude behavior, and at 400 km to give an indication of the behavior at higher altitudes.

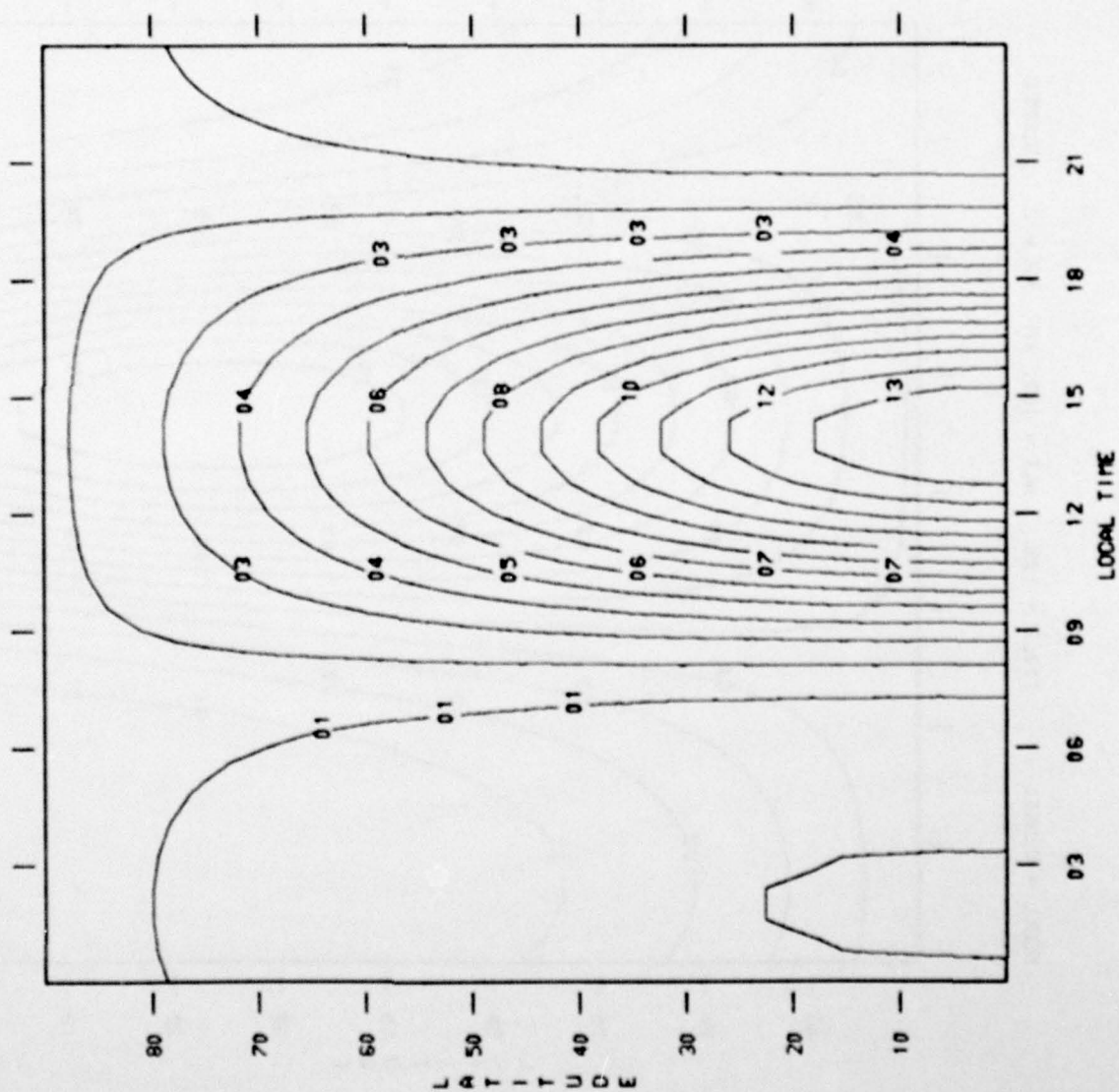
The contour lines are labeled with a two digit code, and the densities corresponding to the various code numbers are given in a table to the right of each plot. It should be noted that each plot is scaled independently and that in two different plots, contour lines with the same label may correspond to different densities. The primary coordinates of local time (in hours) and latitude (in degrees) are given on the axes of the plot for the northern hemisphere. The values of various other parameters are given in the heading above the plot. Equinox, Summer, and Winter denote the dates March 21, July 21, and December 21, respectively.

Although to the greatest extent possible, the plots have been made for identical conditions for each of the models, some accommodation has been made to the varying requirements of the models. The value labeled F 10.7 has been used for both $\bar{F}_{10.7}$ (the long term average) and $F_{10.7}$ (the daily value). There is no density variation for 'DENSEL at 140 km, so contour plots at that altitude are not shown. MSIS requires specification of A_p rather than K_p . A value of $A_p = 7$ has been used for the plots labeled $K_p = 2$.

In some cases both geomagnetic and geographic latitude are required. The plots given were produced by setting both the geomagnetic and geographic latitude to the same value corresponding to the indicated latitude.

It is interesting to note that the computer version of the model obtained from Jacchia's group does not apply the method described in Jacchia 1977 for correcting the temperature profile for geomagnetic activity, but rather uses the static model temperature profile which has the correct exospheric temperature. At the time of this writing, Jacchia's group did not have a computer routine which corresponded exactly to the model description (private communication). The lower altitudes are most likely to be affected by this change, although it is anticipated that differences should not be large.

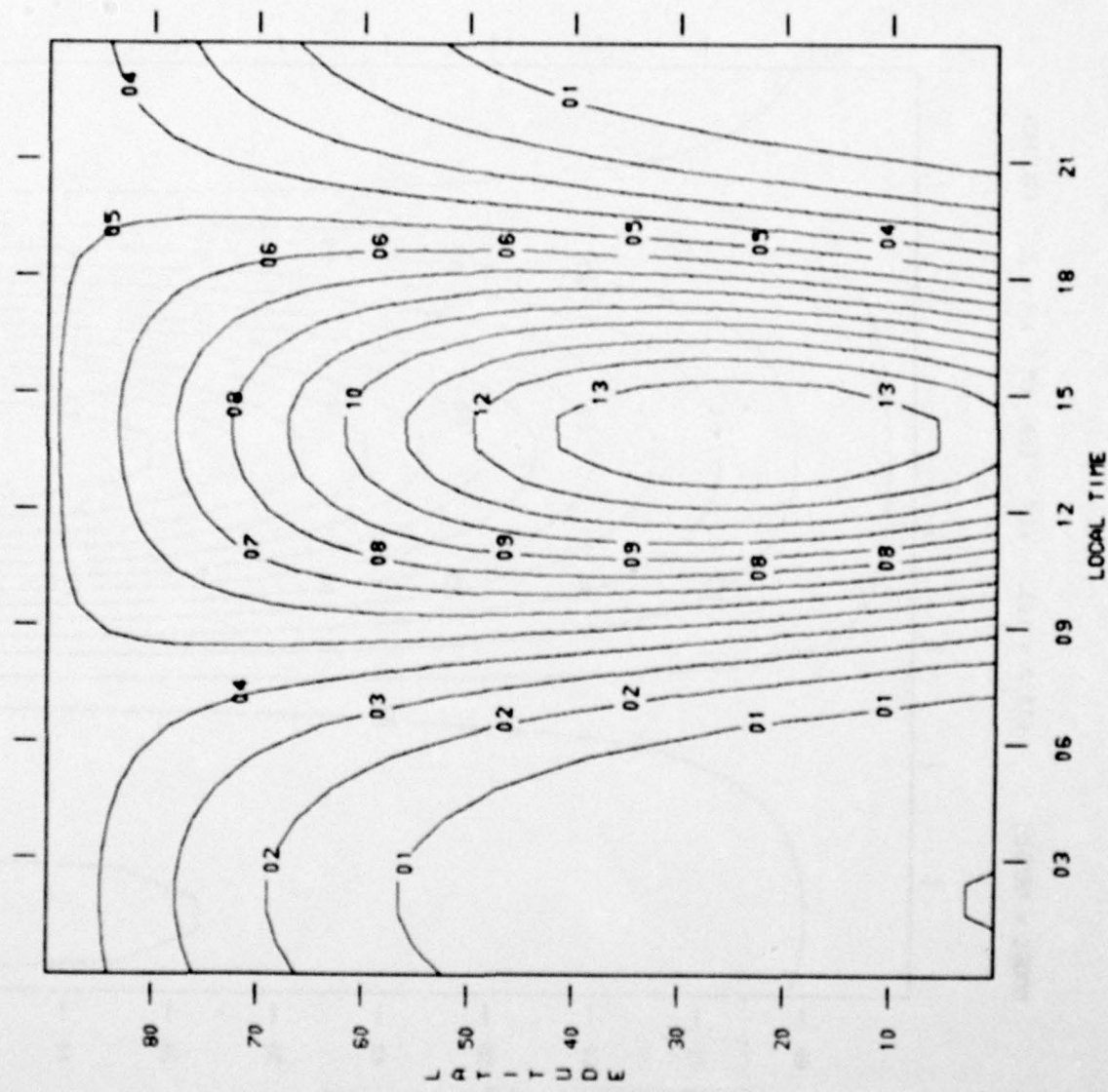
MODEL = DENSEL F10.7 = 125. ALT = 180. KM KP = 2. EQUINOX



CM/CM=3

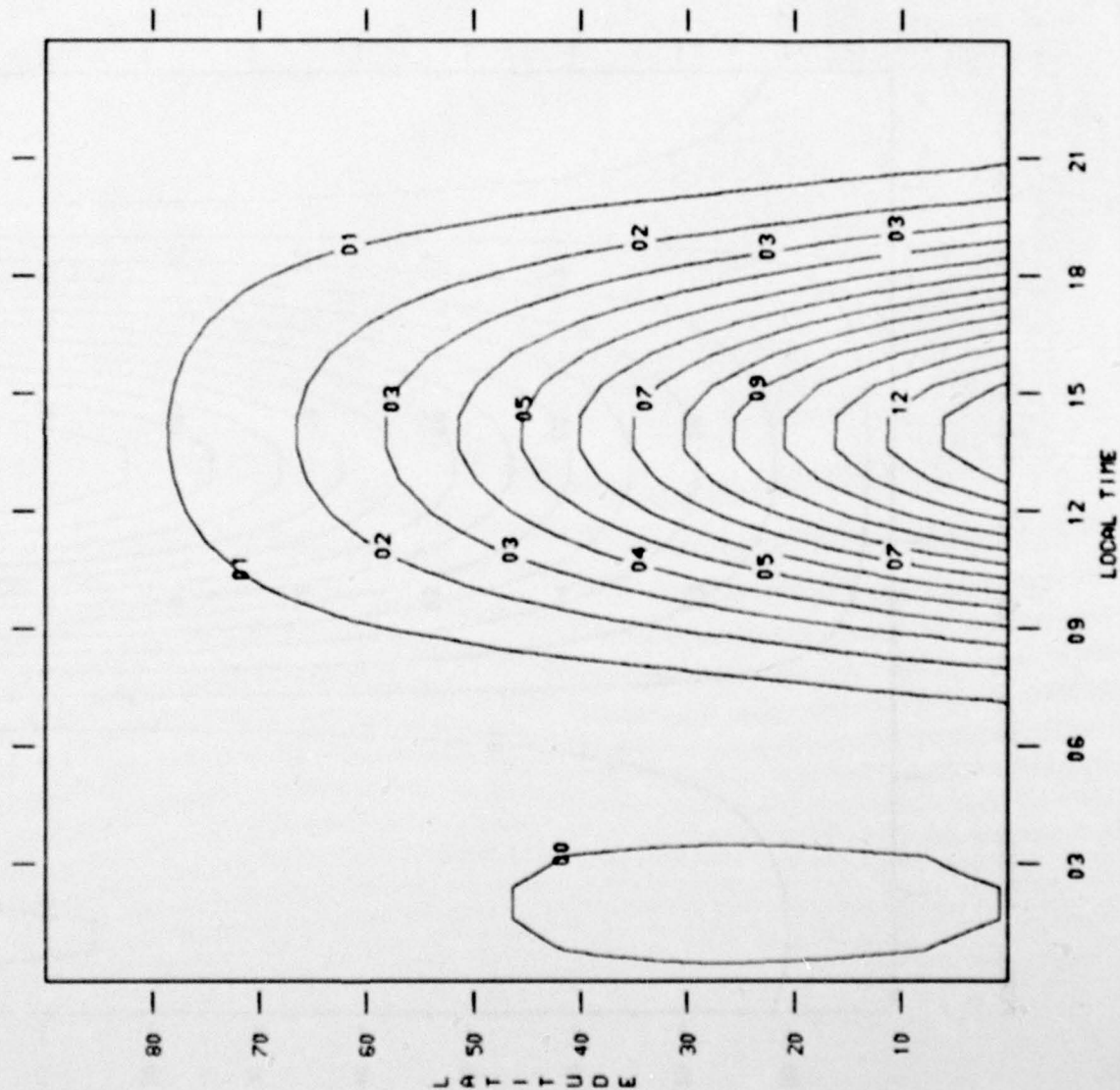
- 14 = 5.35E-13
- 13 = 5.30E-13
- 12 = 5.25E-13
- 11 = 5.21E-13
- 10 = 5.16E-13
- 09 = 5.12E-13
- 08 = 5.07E-13
- 07 = 5.02E-13
- 06 = 4.98E-13
- 05 = 4.93E-13
- 04 = 4.89E-13
- 03 = 4.84E-13
- 02 = 4.79E-13
- 01 = 4.75E-13
- 00 = 4.70E-13

MODEL = DENSEL F10.7 = 125. ALT = 180. KM KP = 2. SUMMER



- GM/Crit=3
- 14 = 5.35E-13
 - 13 = 5.30E-13
 - 12 = 5.26E-13
 - 11 = 5.21E-13
 - 10 = 5.16E-13
 - 09 = 5.12E-13
 - 08 = 5.07E-13
 - 07 = 5.02E-13
 - 06 = 4.98E-13
 - 05 = 4.93E-13
 - 04 = 4.89E-13
 - 03 = 4.84E-13
 - 02 = 4.79E-13
 - 01 = 4.75E-13
 - 00 = 4.70E-13

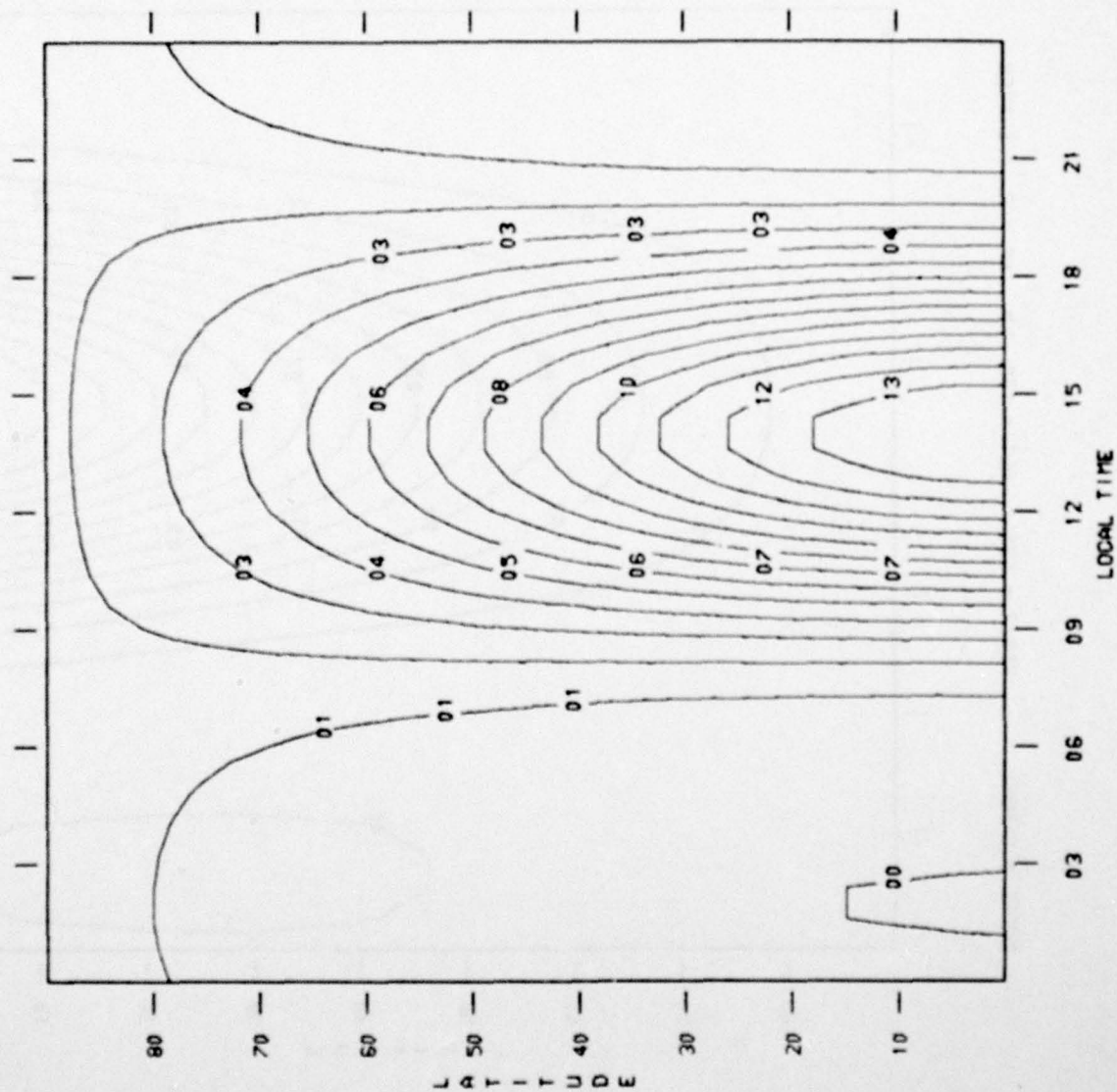
MODEL = DENSEL F10.7 = 125. ALT = 180. KM KP = 2. WINTER



GM/CN1003

- 14 = 5.27E-13
- 13 = 5.23E-13
- 12 = 5.19E-13
- 11 = 5.15E-13
- 10 = 5.11E-13
- 09 = 5.07E-13
- 08 = 5.03E-13
- 07 = 4.99E-13
- 06 = 4.95E-13
- 05 = 4.90E-13
- 04 = 4.86E-13
- 03 = 4.82E-13
- 02 = 4.78E-13
- 01 = 4.74E-13
- 00 = 4.70E-13

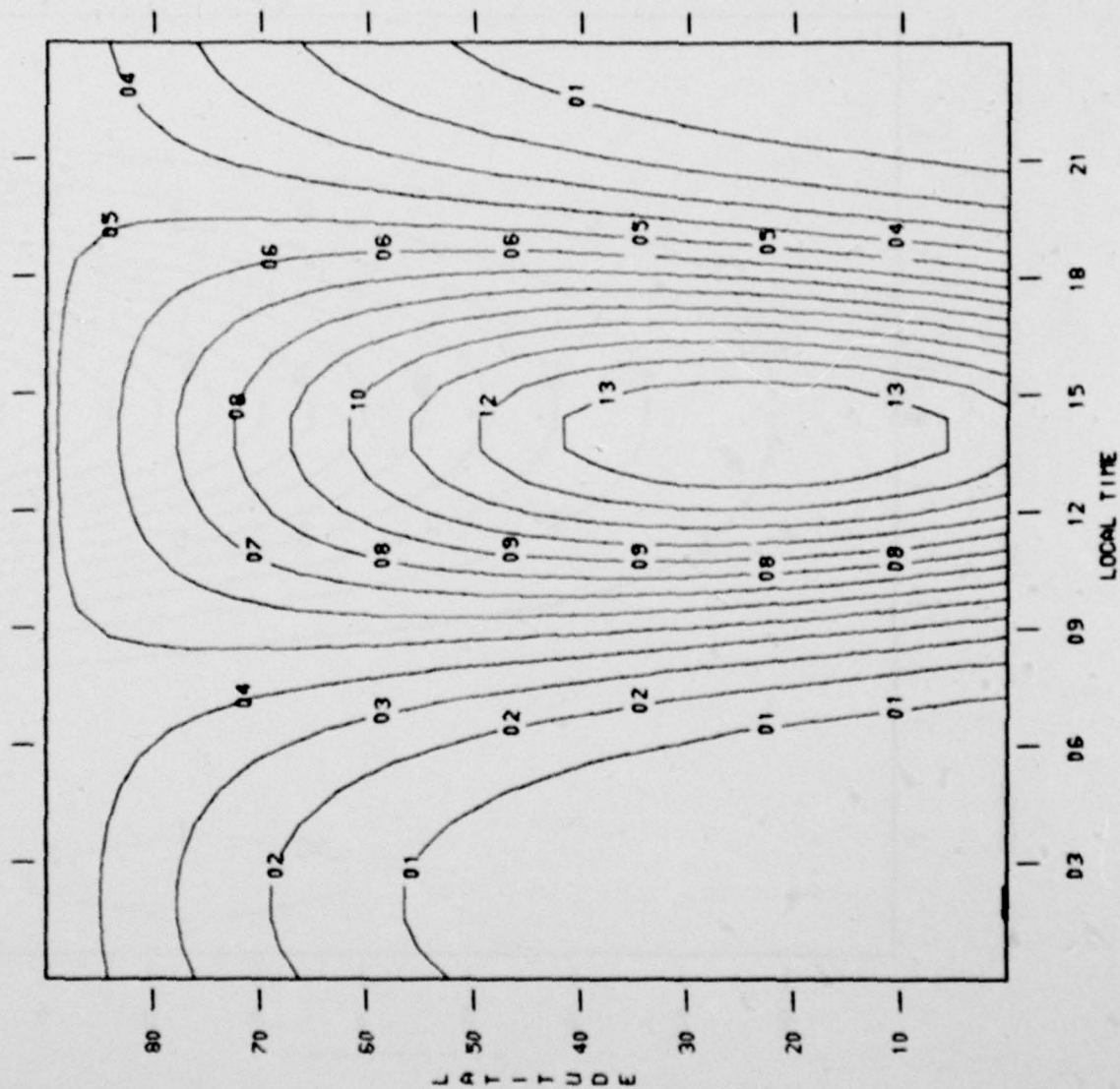
MODEL = DENSEL F10.7 = 125. ALT = 400. KM KP = 2. EQUINOX



CH/CH=3

- 14 = 6.80E-15
- 13 = 6.52E-15
- 12 = 6.25E-15
- 11 = 5.97E-15
- 10 = 5.69E-15
- 09 = 5.41E-15
- 08 = 5.13E-15
- 07 = 4.85E-15
- 06 = 4.57E-15
- 05 = 4.29E-15
- 04 = 4.01E-15
- 03 = 3.73E-15
- 02 = 3.46E-15
- 01 = 3.18E-15
- 00 = 2.90E-15

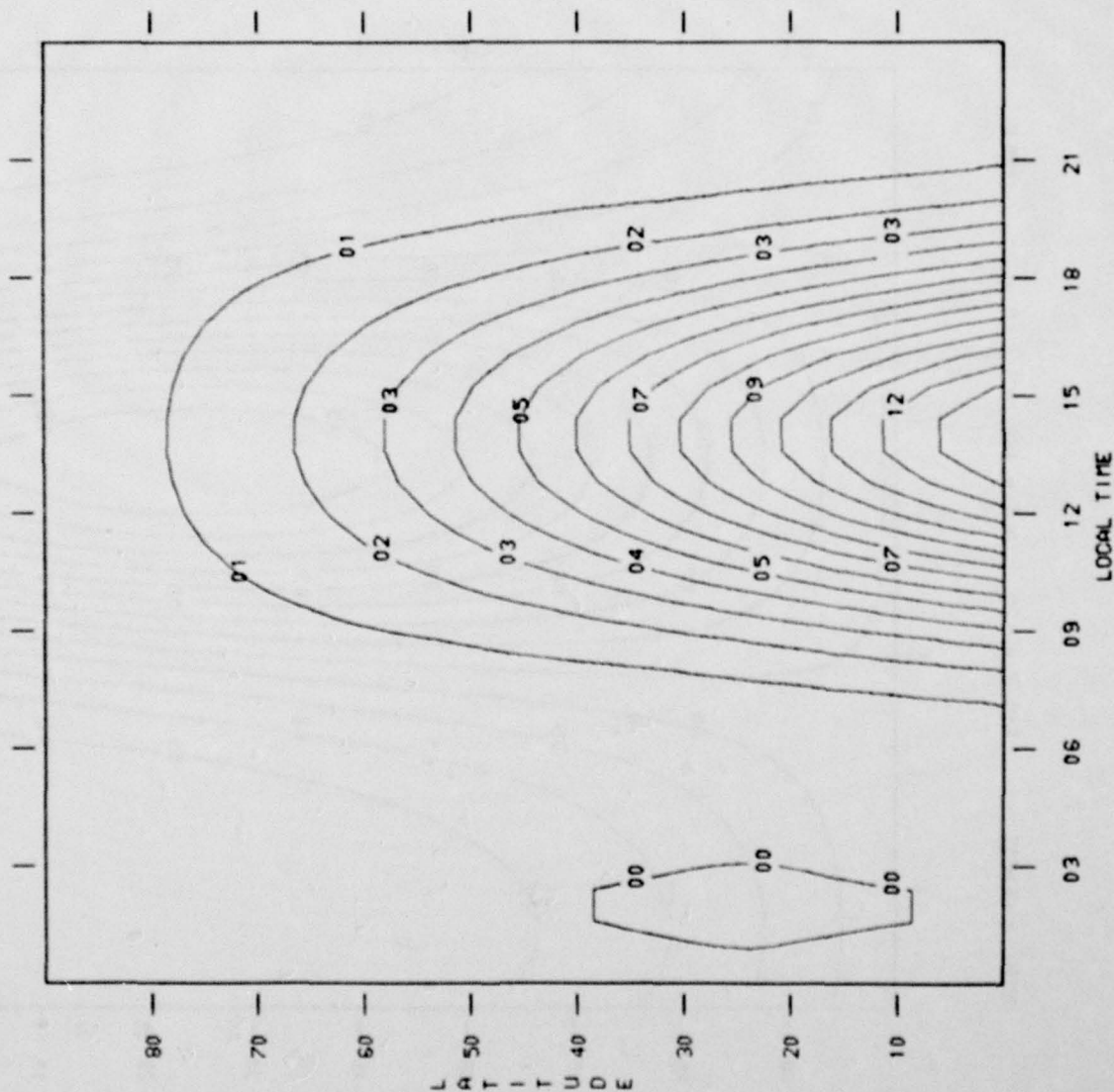
MODEL = DENSEL F10.7 = 125. ALT = 400. KM KP = 2. SUMMER



GM/CN=3

- 14 = 6.81E-15
- 13 = 6.53E-15
- 12 = 6.25E-15
- 11 = 5.97E-15
- 10 = 5.69E-15
- 09 = 5.41E-15
- 08 = 5.13E-15
- 07 = 4.85E-15
- 06 = 4.57E-15
- 05 = 4.29E-15
- 04 = 4.02E-15
- 03 = 3.74E-15
- 02 = 3.46E-15
- 01 = 3.18E-15
- 00 = 2.90E-15

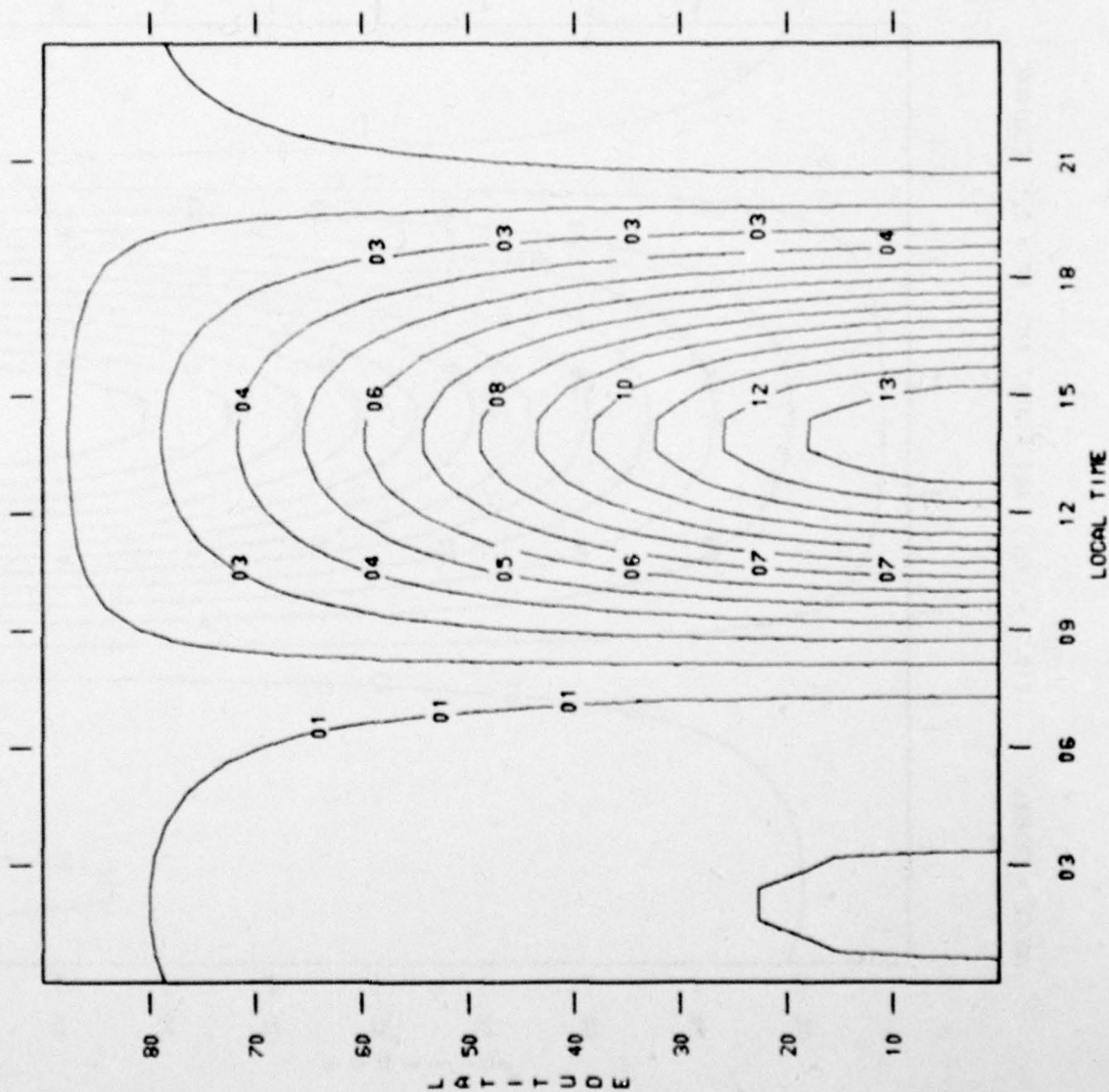
MODEL = DENSEL F10.7 = 125. ALT = 400. KM KP = 2. WINTER



CH/CHW3

- 14 = 7.34E-15
- 13 = 6.09E-15
- 12 = 5.85E-15
- 11 = 5.60E-15
- 10 = 5.36E-15
- 09 = 5.11E-15
- 08 = 4.87E-15
- 07 = 4.62E-15
- 06 = 4.37E-15
- 05 = 4.13E-15
- 04 = 3.88E-15
- 03 = 3.64E-15
- 02 = 3.39E-15
- 01 = 3.14E-15
- 00 = 2.90E-15

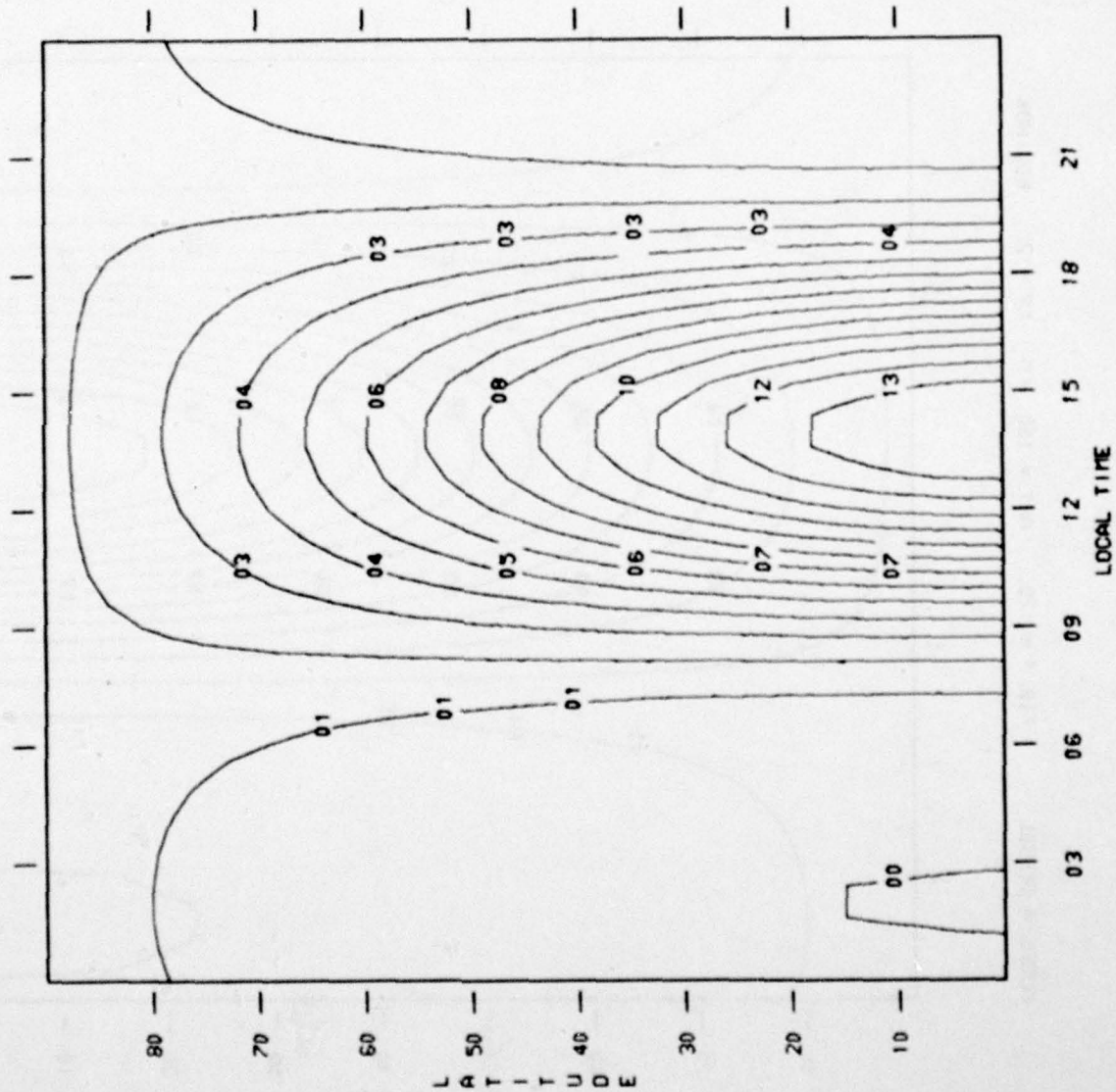
MODEL = DENSEL F10.7 = 70. ALT = 180. KM KP = 2. EQUINOX



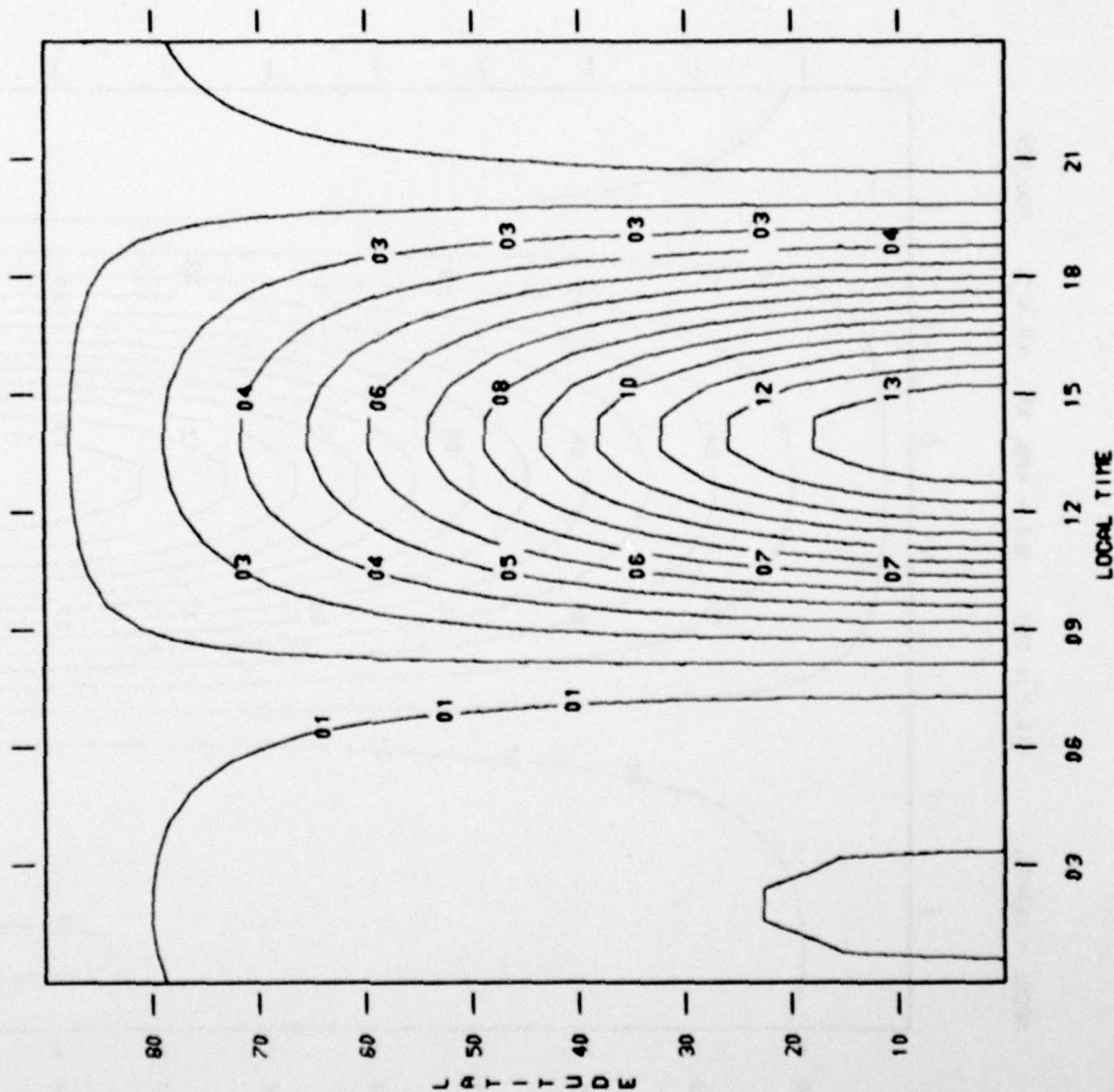
CH/CHmax3

14 = 3.83E-13
13 = 3.80E-13
12 = 3.76E-13
11 = 3.73E-13
10 = 3.70E-13
09 = 3.66E-13
08 = 3.63E-13
07 = 3.60E-13
06 = 3.57E-13
05 = 3.53E-13
04 = 3.50E-13
03 = 3.47E-13
02 = 3.43E-13
01 = 3.40E-13
00 = 3.37E-13

MODEL = DENSEL F10.7 = 70. ALT = 400. KM KP = 2. EQUINOX



MODEL = DENSEL F10.7 = 180. ALT = 180. KM KP = 2. EDUINDX



CM/CHW=3

14 = 6.86E-13

13 = 6.80E-13

12 = 6.75E-13

11 = 6.69E-13

10 = 6.63E-13

09 = 6.57E-13

08 = 6.51E-13

07 = 6.45E-13

06 = 6.39E-13

05 = 6.33E-13

04 = 6.27E-13

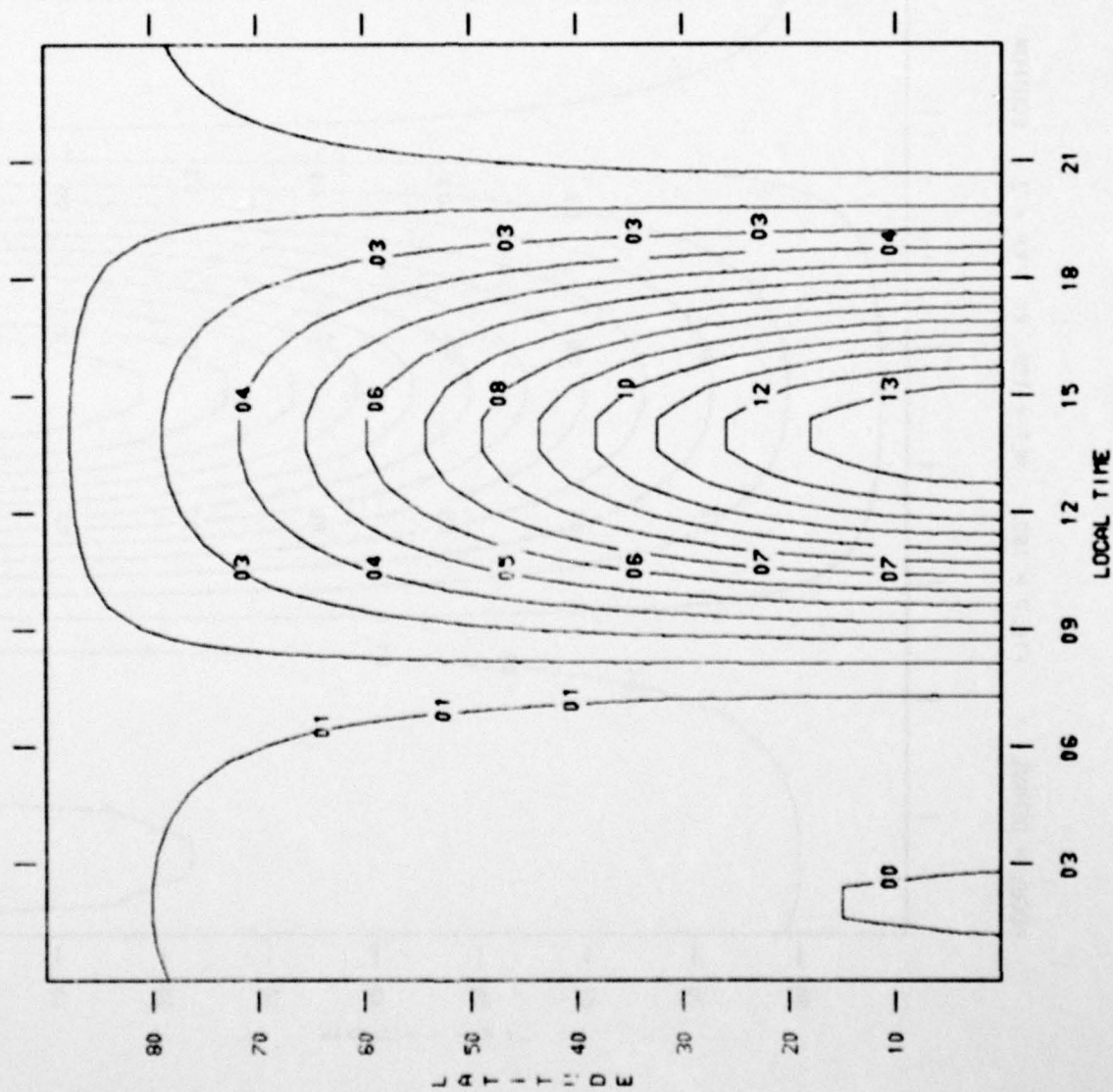
03 = 6.21E-13

02 = 6.15E-13

01 = 6.09E-13

00 = 6.04E-13

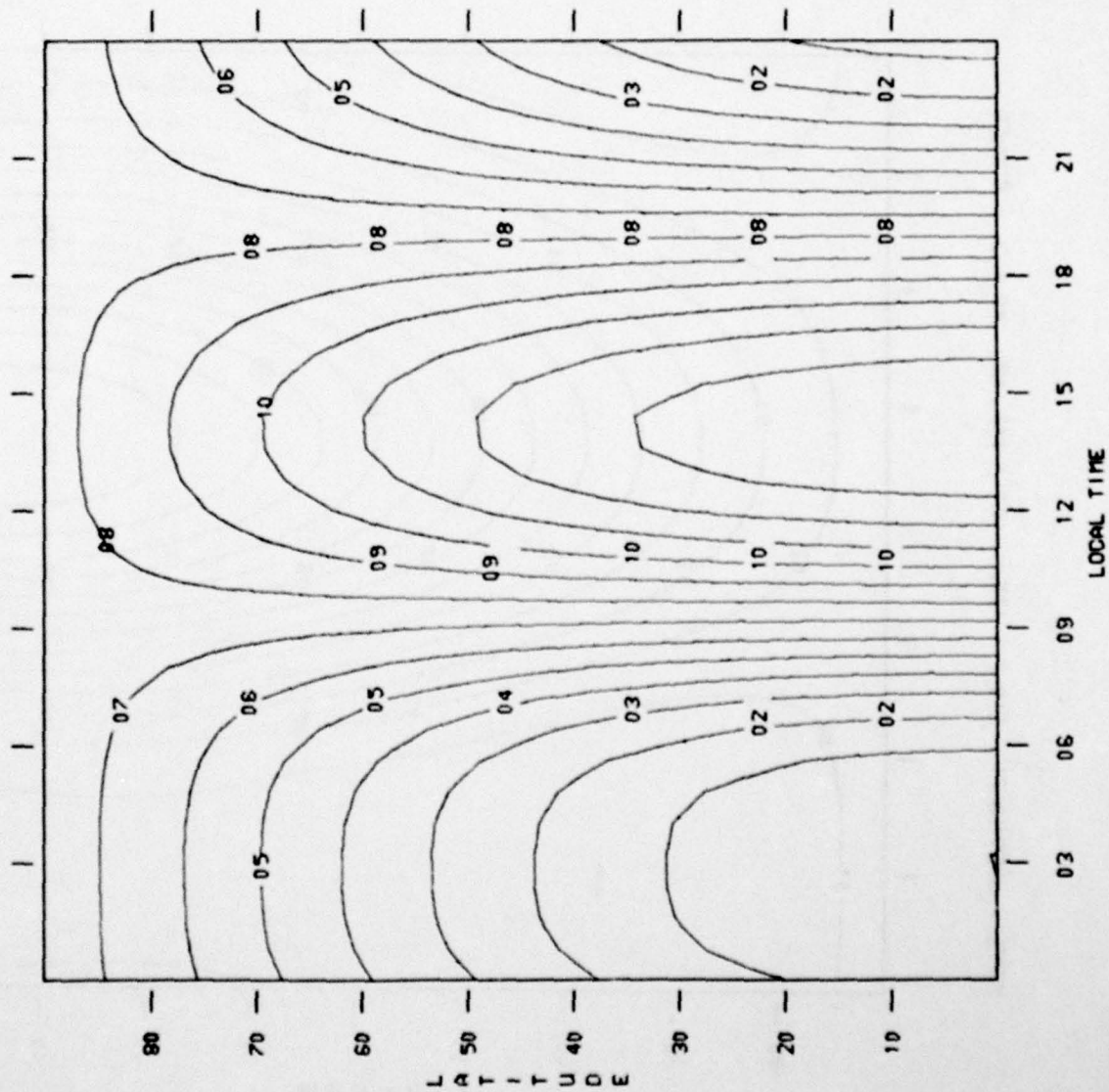
MODEL = DENSEL F10.7 = 180. ALT = 400. KM KP = 2. EQUINOX



CM/CHW3

14 = 9.80E-15
13 = 9.40E-15
12 = 8.99E-15
11 = 8.59E-15
10 = 8.19E-15
09 = 7.79E-15
08 = 7.39E-15
07 = 6.99E-15
06 = 6.58E-15
05 = 6.18E-15
04 = 5.78E-15
03 = 5.38E-15
02 = 4.98E-15
01 = 4.57E-15
00 = 4.17E-15

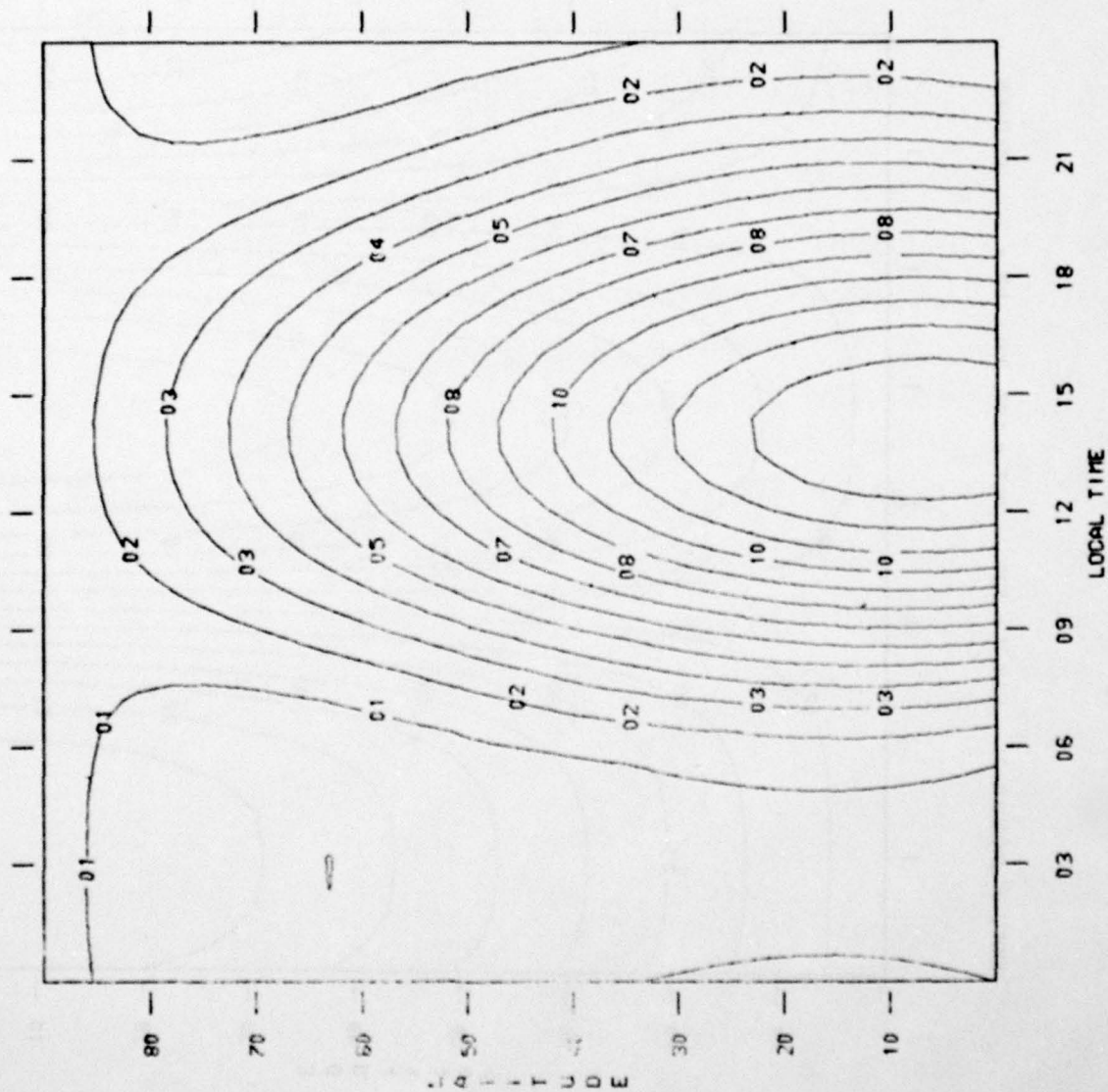
MODEL = JACCHIA 71 F10.7 = 125. ALT = 140. KM KP = 2. EQUINOX



CH/CH103

- 14 = 4.37E-12
- 13 = 4.33E-12
- 12 = 4.30E-12
- 11 = 4.27E-12
- 10 = 4.24E-12
- 09 = 4.21E-12
- 08 = 4.18E-12
- 07 = 4.15E-12
- 06 = 4.12E-12
- 05 = 4.09E-12
- 04 = 4.06E-12
- 03 = 4.03E-12
- 02 = 4.00E-12
- 01 = 3.97E-12
- 00 = 3.94E-12

MODEL = JACCHIA 71 F10.7 = 125. ALT = 140. KM KP = 2. SUMMER



GM/CH=3

14 =	3.86E-12
13 =	3.83E-12
12 =	3.80E-12
11 =	3.78E-12
10 =	3.75E-12
09 =	3.73E-12
08 =	3.70E-12
07 =	3.67E-12
06 =	3.65E-12
05 =	3.62E-12
04 =	3.60E-12
03 =	3.57E-12
02 =	3.54E-12
01 =	3.52E-12
00 =	3.49E-12

AD-A075 748

AEROSPACE CORP EL SEGUNDO CA SPACE SCIENCES LAB

F/G 4/1

A SURVEY OF CURRENTLY IMPORTANT EMPIRICAL THERMOSPHERIC MODELS.(U)

SEP 79 D R HICKMAN , B K CHING , C J RICE

F04701-78-C-0079

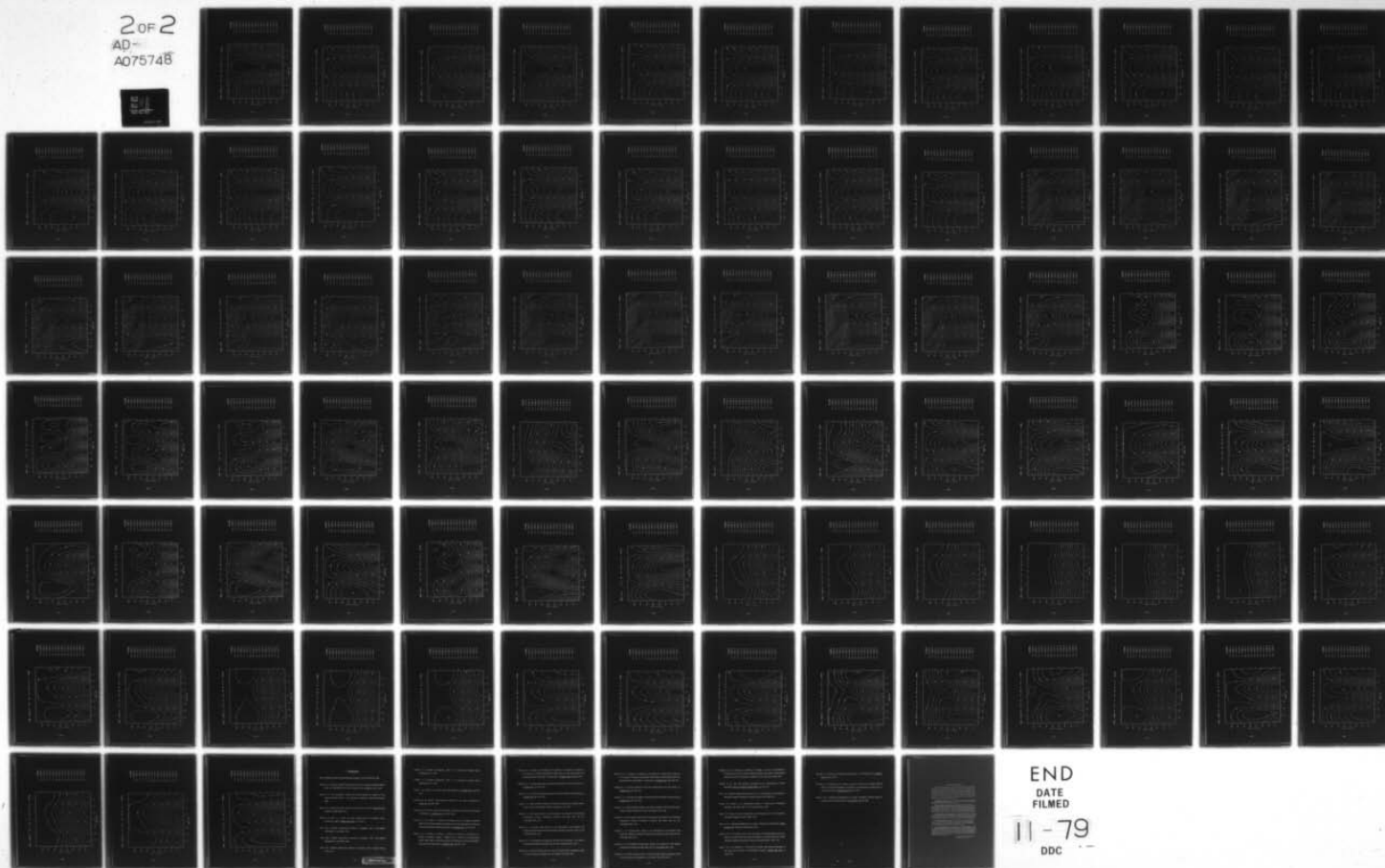
UNCLASSIFIED

TR-0079(4960-04)-2

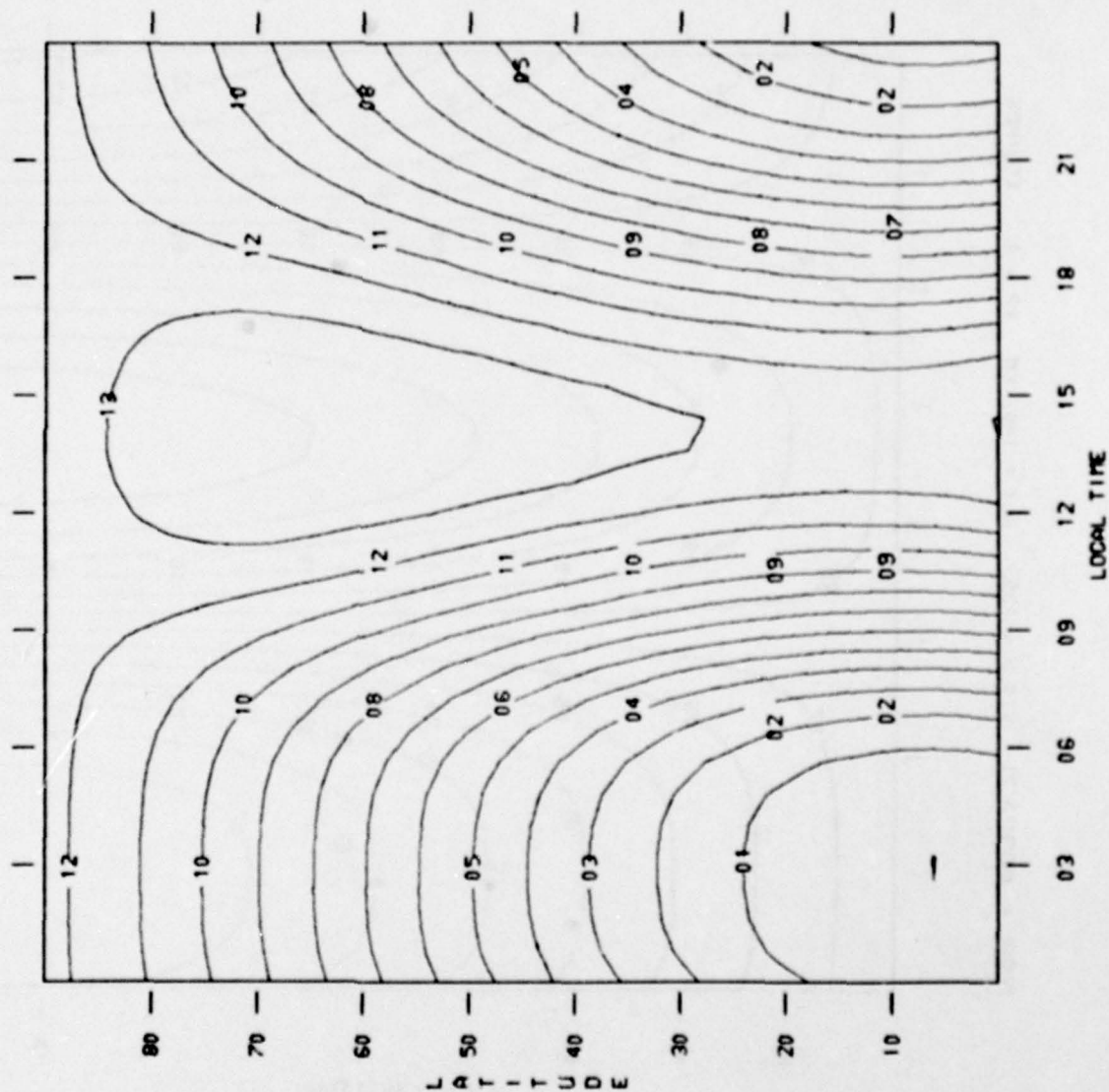
SAMSO-TR-79-57

NL

2 OF 2
AD-A075748



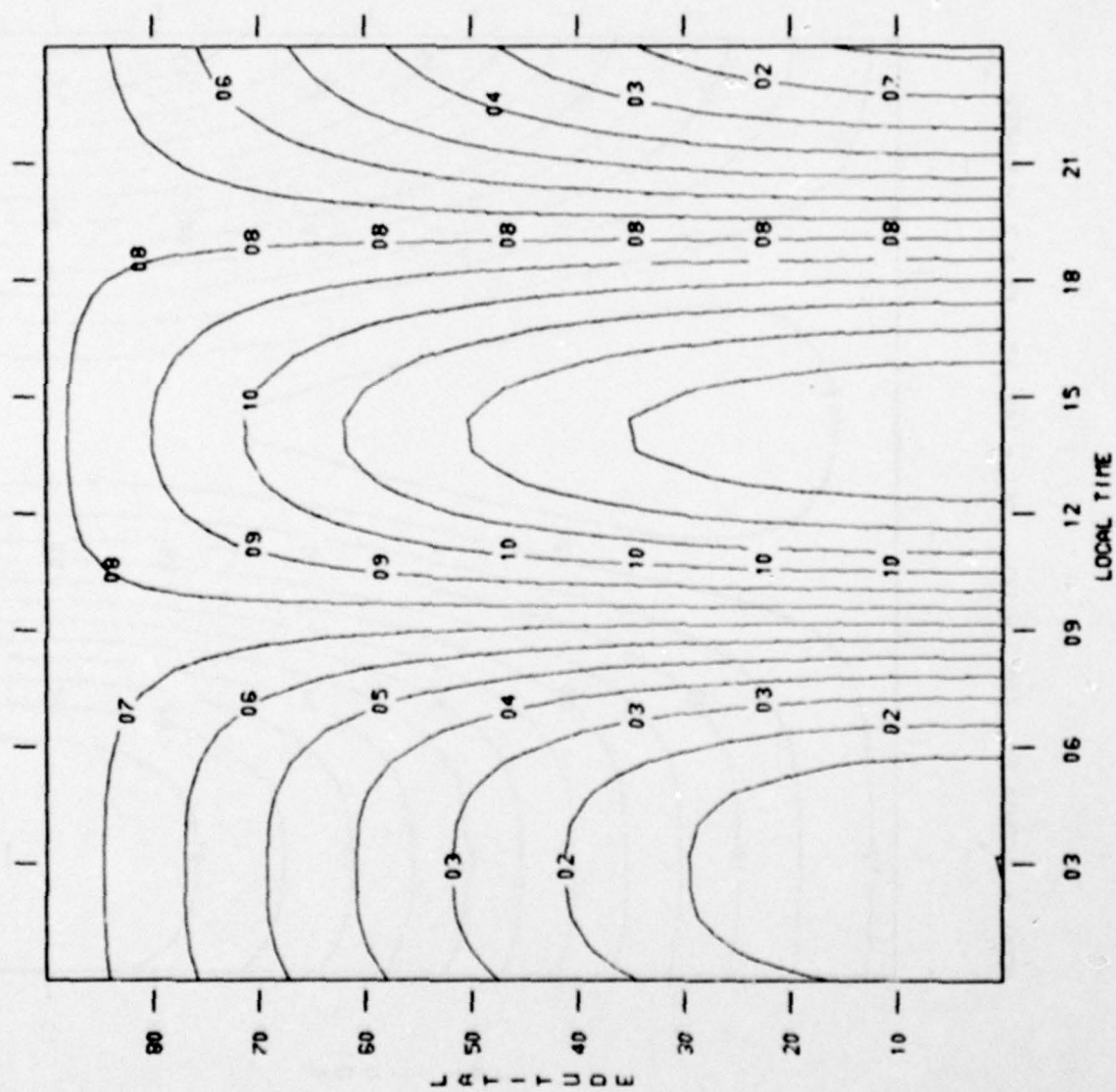
MODEL = JACCHIA 71 F10.7 = 125. ALT = 140. KM KP = 2. WINTER



CH/CHW3

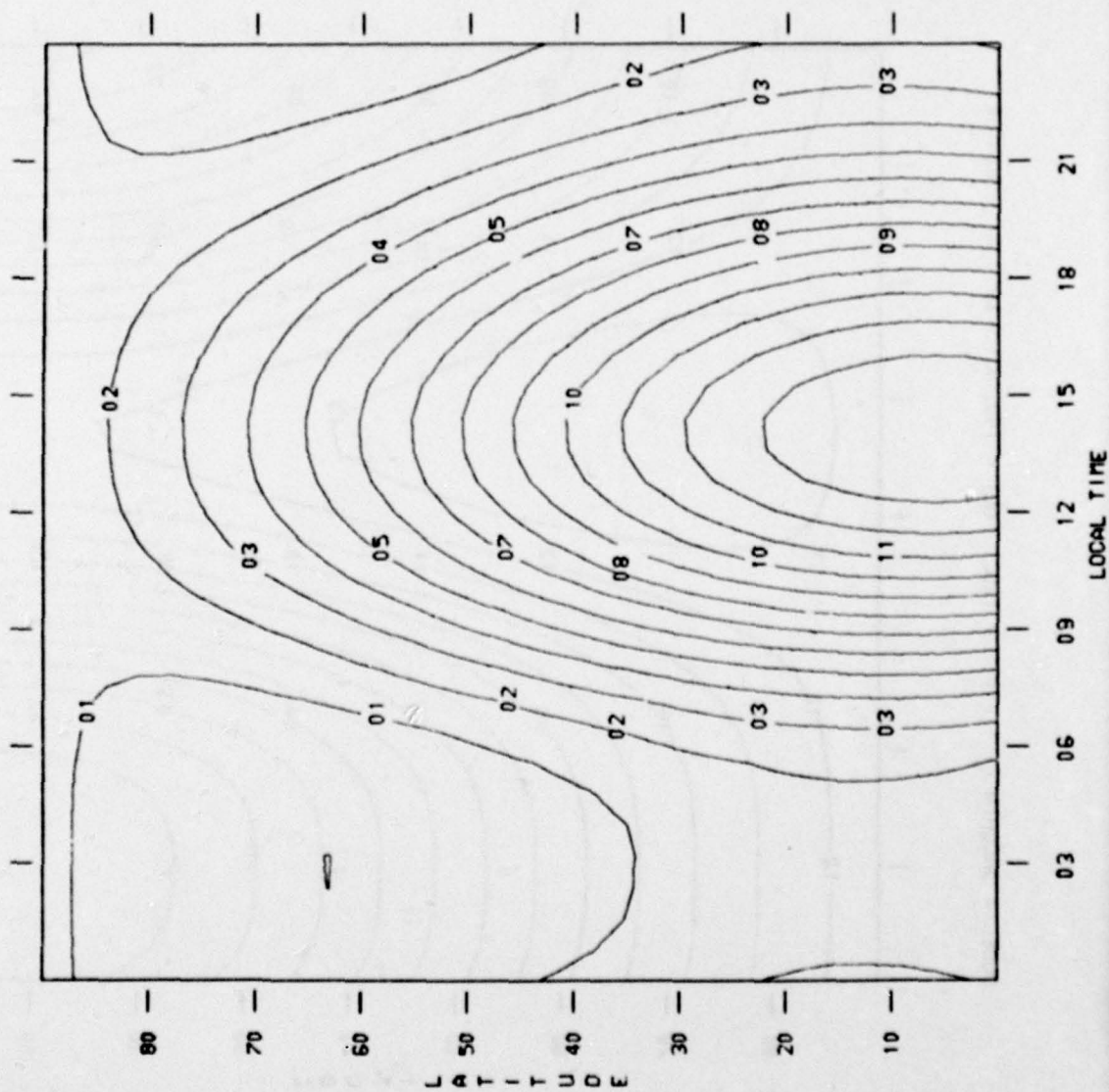
- 14 = 4.10E-12
- 13 = 4.07E-12
- 12 = 4.04E-12
- 11 = 4.01E-12
- 10 = 3.98E-12
- 09 = 3.95E-12
- 08 = 3.93E-12
- 07 = 3.90E-12
- 06 = 3.87E-12
- 05 = 3.84E-12
- 04 = 3.81E-12
- 03 = 3.78E-12
- 02 = 3.75E-12
- 01 = 3.72E-12
- 00 = 3.70E-12

MODEL = JACCHIA 71 F10.7 = 125. ALT = 140. KM KP = 6. EQUINOX



CM/Critv3
 14 = 5.03E-12
 13 = 5.00E-12
 12 = 4.97E-12
 11 = 4.94E-12
 10 = 4.91E-12
 09 = 4.88E-12
 08 = 4.84E-12
 07 = 4.81E-12
 06 = 4.78E-12
 05 = 4.75E-12
 04 = 4.72E-12
 03 = 4.69E-12
 02 = 4.65E-12
 01 = 4.62E-12
 00 = 4.59E-12

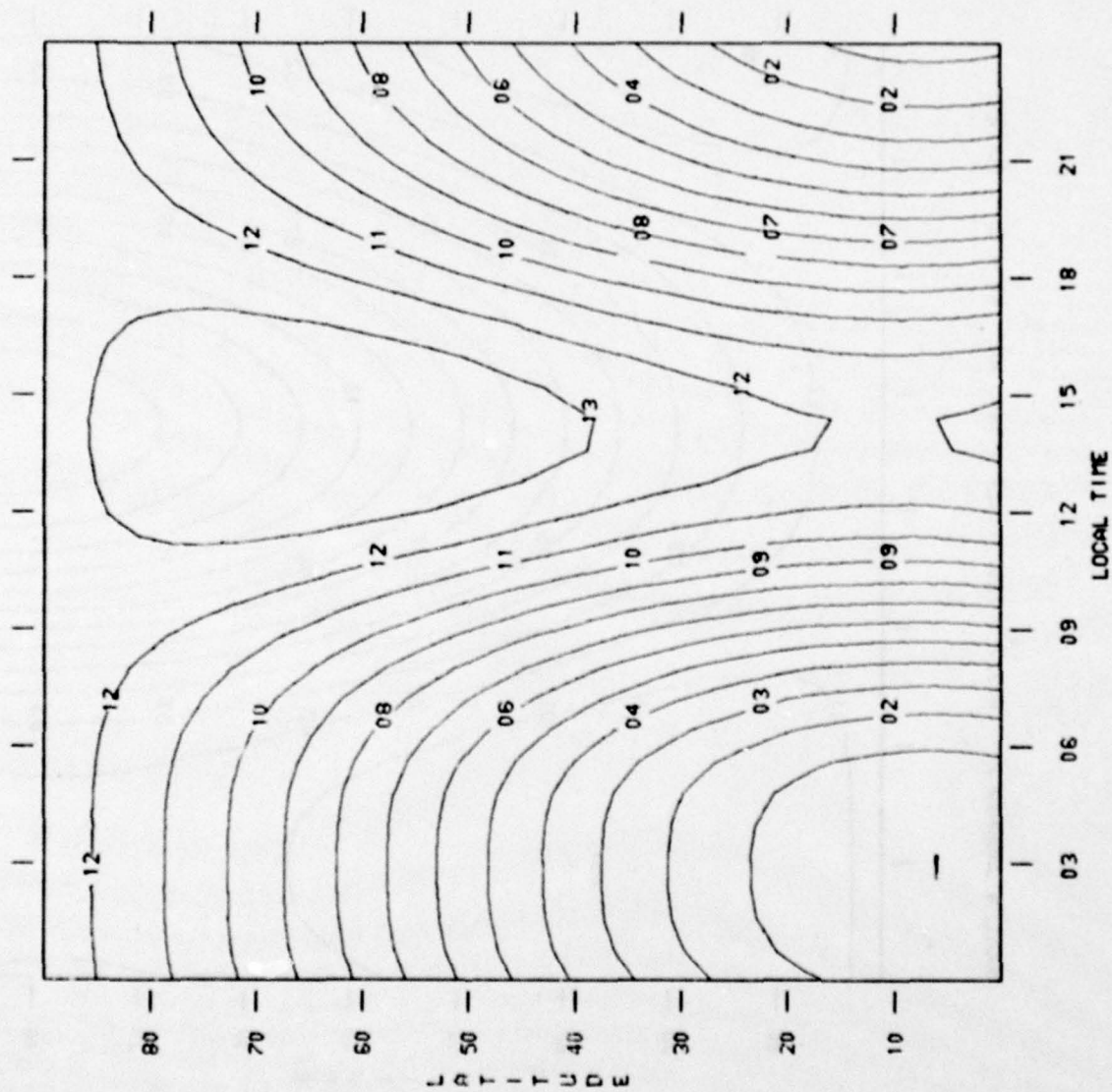
MODEL = JACCHIA 71 F10.7 = 125. ALT = 140. KM KP = 6. SUMMER



GM/CHEW3

14 =	4.45E-12
13 =	4.42E-12
12 =	4.39E-12
11 =	4.36E-12
10 =	4.33E-12
09 =	4.30E-12
08 =	4.28E-12
07 =	4.25E-12
06 =	4.22E-12
05 =	4.19E-12
04 =	4.16E-12
03 =	4.13E-12
02 =	4.10E-12
01 =	4.08E-12
00 =	4.05E-12

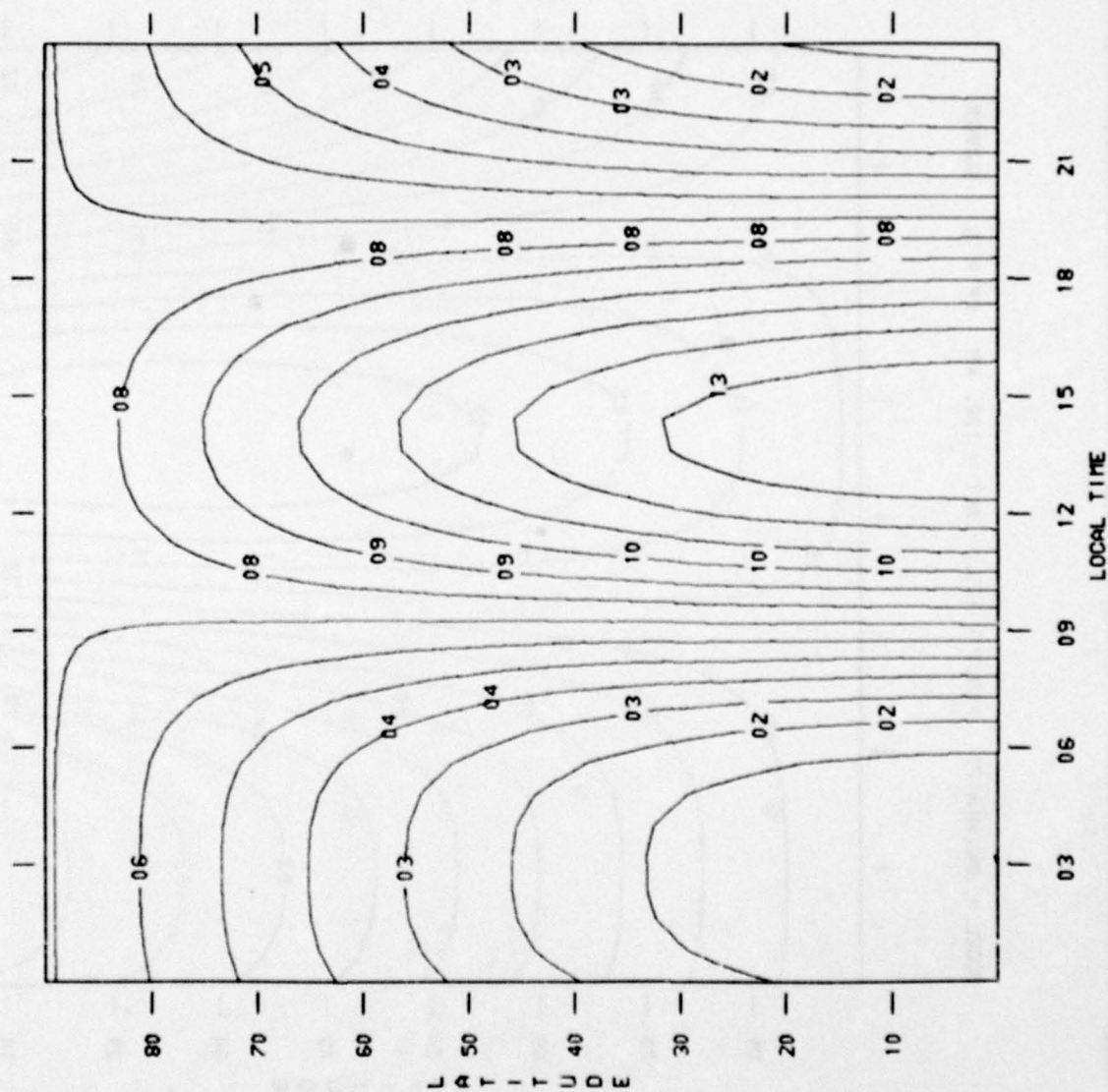
MODEL = JACCHIA 71 F10.7 = 125. ALT = 140. KM KP = 6. WINTER



GM/CN003

- 14 = 4.75E-12
- 13 = 4.72E-12
- 12 = 4.69E-12
- 11 = 4.66E-12
- 10 = 4.63E-12
- 09 = 4.59E-12
- 08 = 4.56E-12
- 07 = 4.53E-12
- 06 = 4.50E-12
- 05 = 4.47E-12
- 04 = 4.44E-12
- 03 = 4.41E-12
- 02 = 4.37E-12
- 01 = 4.34E-12
- 00 = 4.31E-12

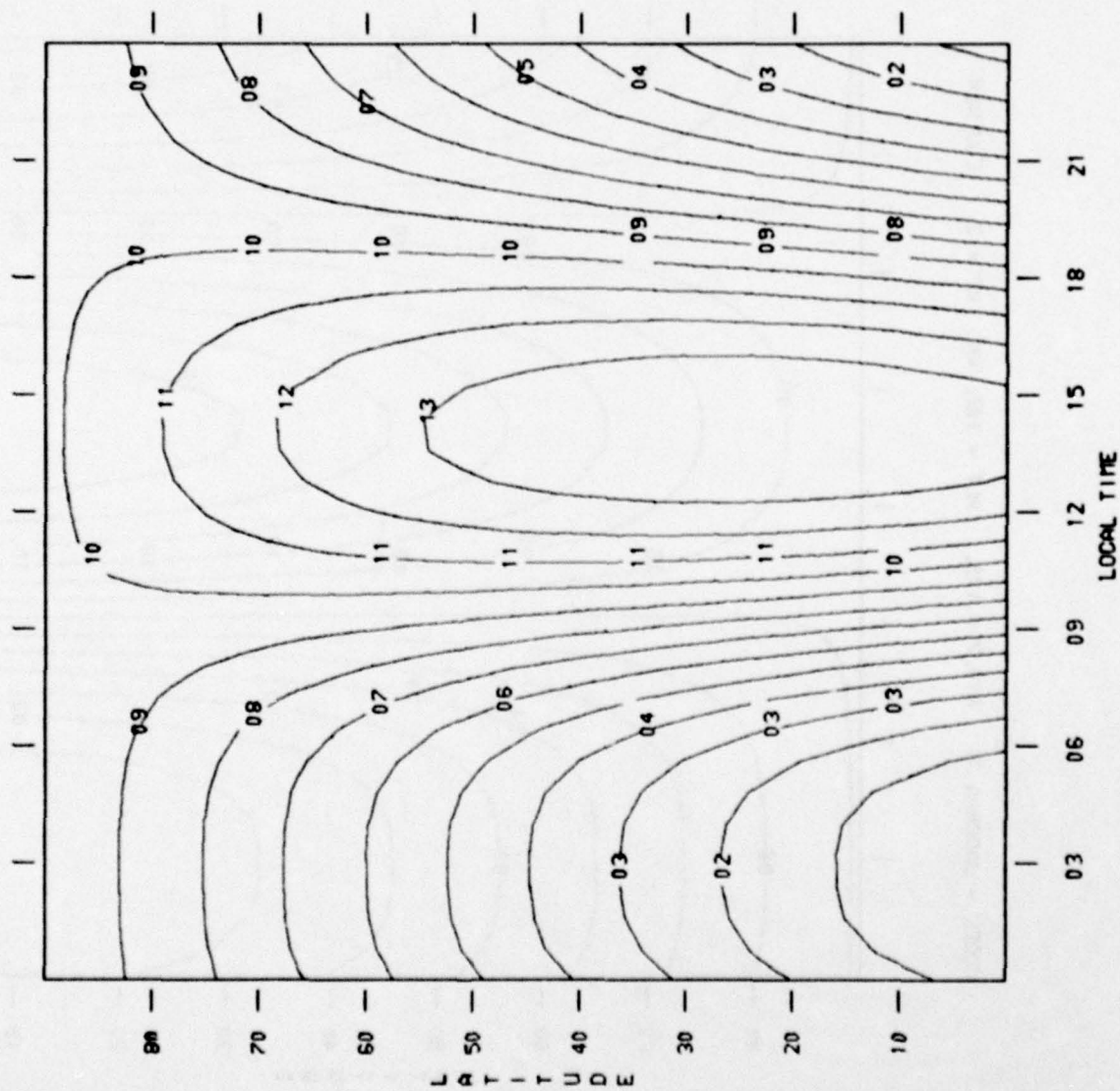
MODEL = JACCHIA 71 F10.7 = 125. ALT = 180. KM KP = 2. EQUINOX



GM/CHE#3

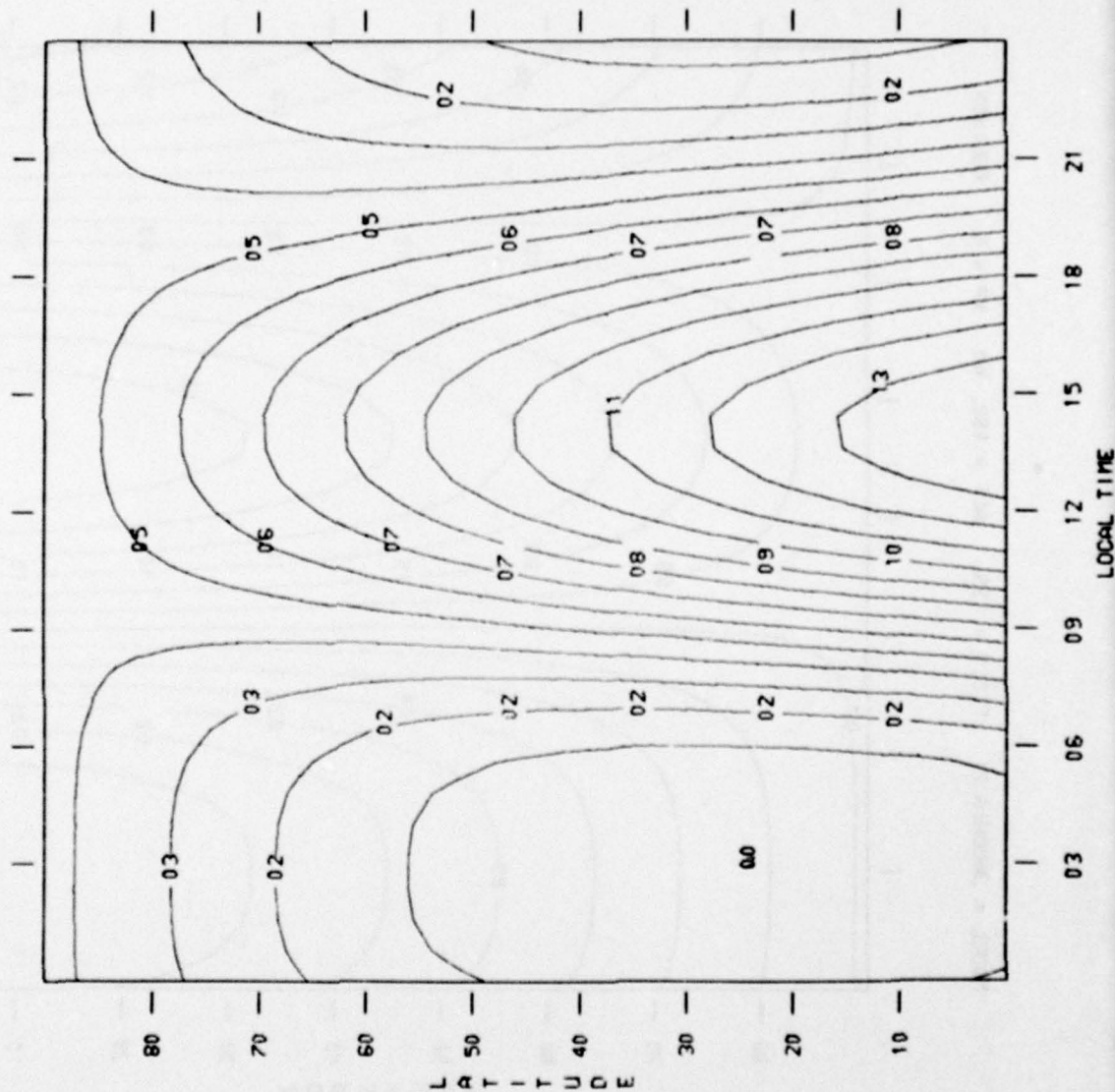
- 14 = 6.41E-13
- 13 = 6.31E-13
- 12 = 6.21E-13
- 11 = 6.11E-13
- 10 = 6.01E-13
- 09 = 5.91E-13
- 08 = 5.81E-13
- 07 = 5.71E-13
- 06 = 5.61E-13
- 05 = 5.51E-13
- 04 = 5.41E-13
- 03 = 5.31E-13
- 02 = 5.21E-13
- 01 = 5.10E-13
- 00 = 5.00E-13

MODEL = JACCHIA 71 F10.7 = 125. ALT = 180. KM KP = 2. SUMMER



GM/CH#3
 14 = 5.52E-13
 13 = 5.44E-13
 12 = 5.35E-13
 11 = 5.27E-13
 10 = 5.19E-13
 09 = 5.10E-13
 08 = 5.02E-13
 07 = 4.94E-13
 06 = 4.85E-13
 05 = 4.77E-13
 04 = 4.68E-13
 03 = 4.60E-13
 02 = 4.52E-13
 01 = 4.43E-13
 00 = 4.35E-13

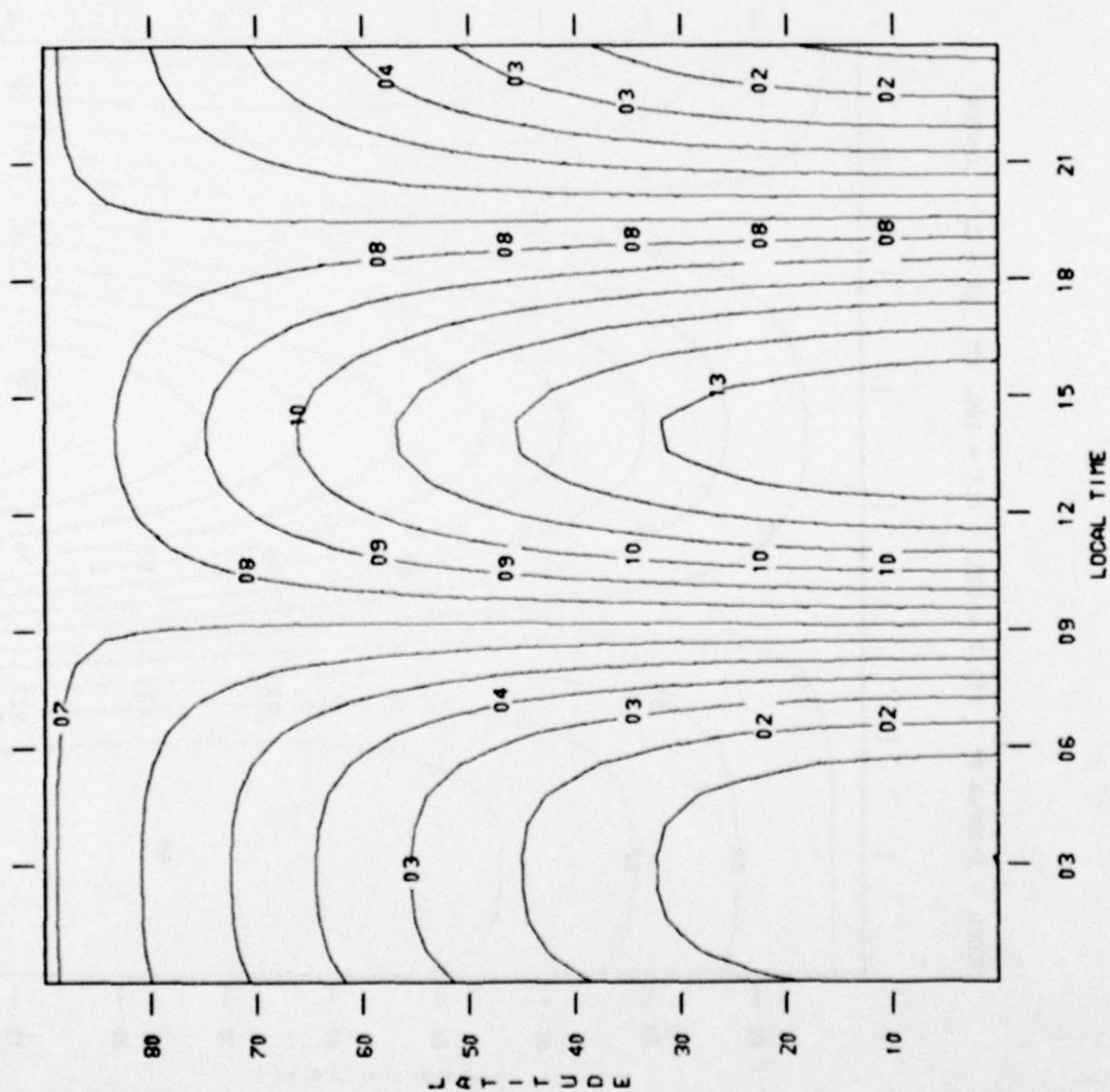
MODEL = JACCHIA 71 F10.7 = 125. ALT = 180. KM KP = 2. WINTER



GM/CHew3

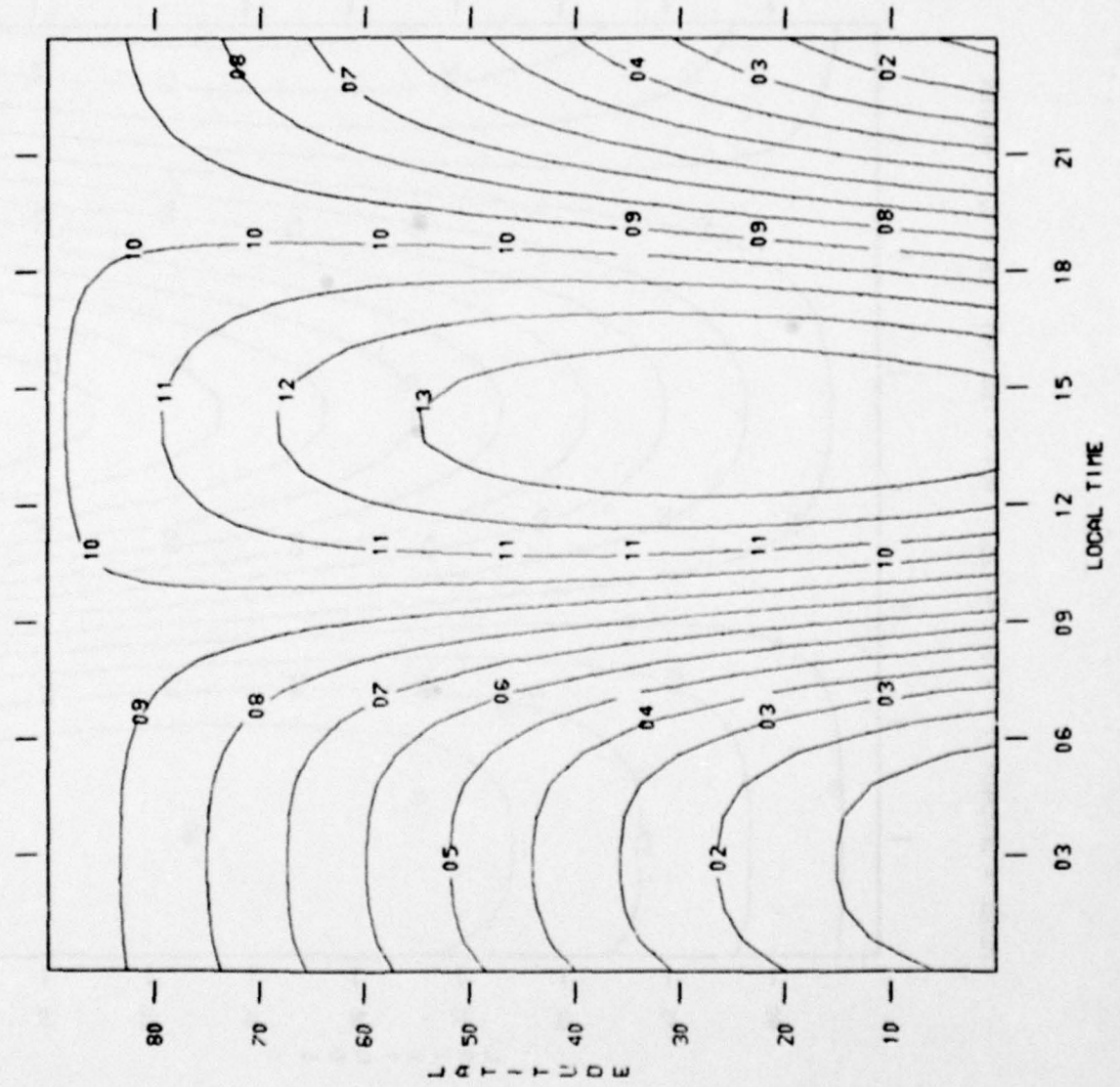
14 = 5.86E-13
13 = 5.77E-13
12 = 5.68E-13
11 = 5.59E-13
10 = 5.50E-13
09 = 5.41E-13
08 = 5.33E-13
07 = 5.24E-13
06 = 5.15E-13
05 = 5.06E-13
04 = 4.97E-13
03 = 4.88E-13
02 = 4.79E-13
01 = 4.70E-13
00 = 4.61E-13

MODEL = JACCHIA 71 F10.7 = 125. ALT = 180. KM KP = 6. EQUINOX



CM/CH=3
 14 = 7.59E-13
 13 = 7.48E-13
 12 = 7.38E-13
 11 = 7.28E-13
 10 = 7.17E-13
 09 = 7.07E-13
 08 = 6.96E-13
 07 = 6.86E-13
 06 = 6.76E-13
 05 = 6.65E-13
 04 = 6.55E-13
 03 = 6.44E-13
 02 = 6.34E-13
 01 = 6.24E-13
 00 = 6.13E-13

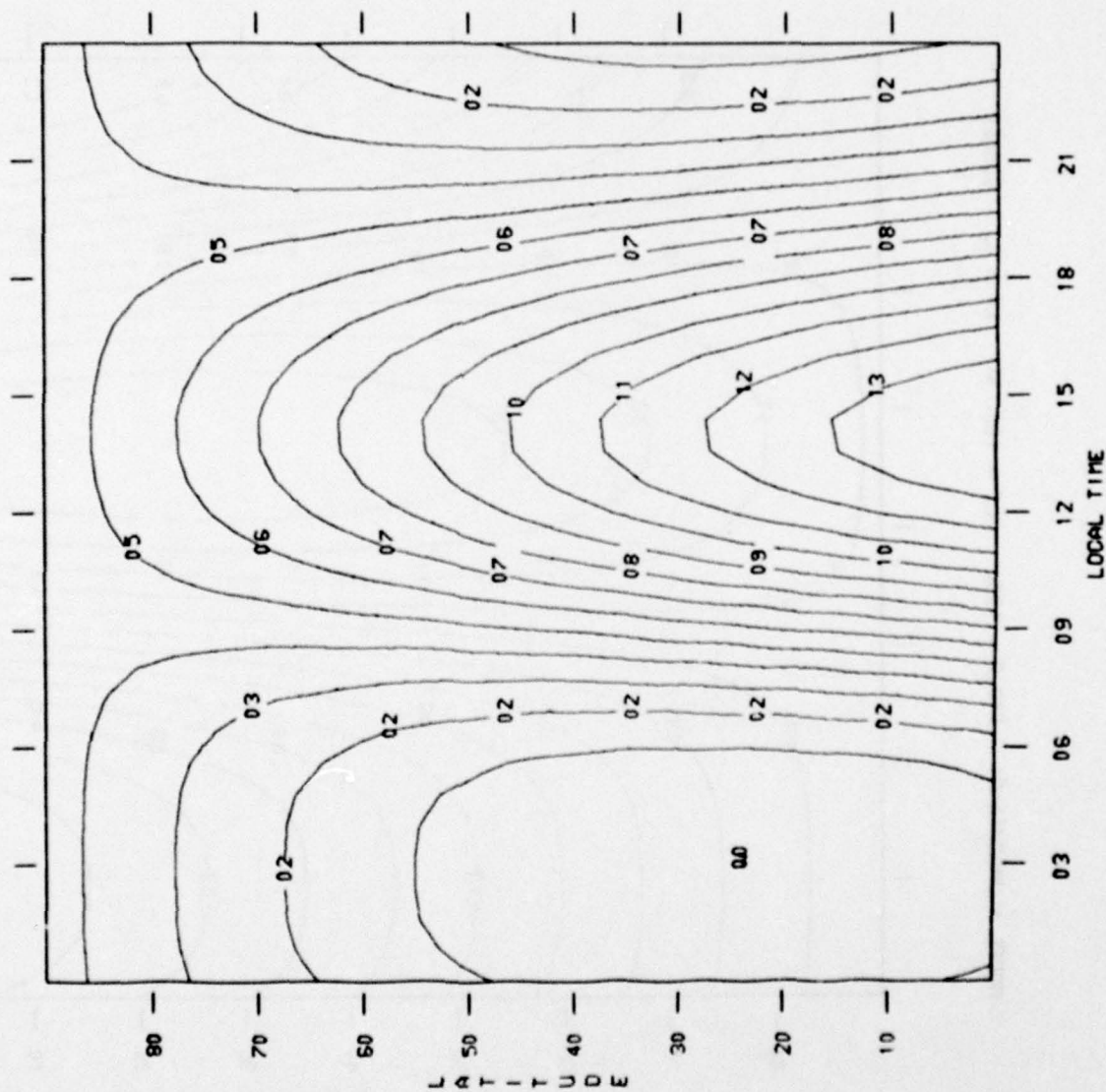
MODEL = JACCHIA 71 F10.7 = 125. ALT = 180. KM KP = 6. SUMMER



CH/CH103

- 14 = 6.53E-13
- 13 = 6.45E-13
- 12 = 6.36E-13
- 11 = 6.28E-13
- 10 = 6.19E-13
- 09 = 6.10E-13
- 08 = 6.02E-13
- 07 = 5.93E-13
- 06 = 5.84E-13
- 05 = 5.76E-13
- 04 = 5.67E-13
- 03 = 5.58E-13
- 02 = 5.50E-13
- 01 = 5.41E-13
- 00 = 5.32E-13

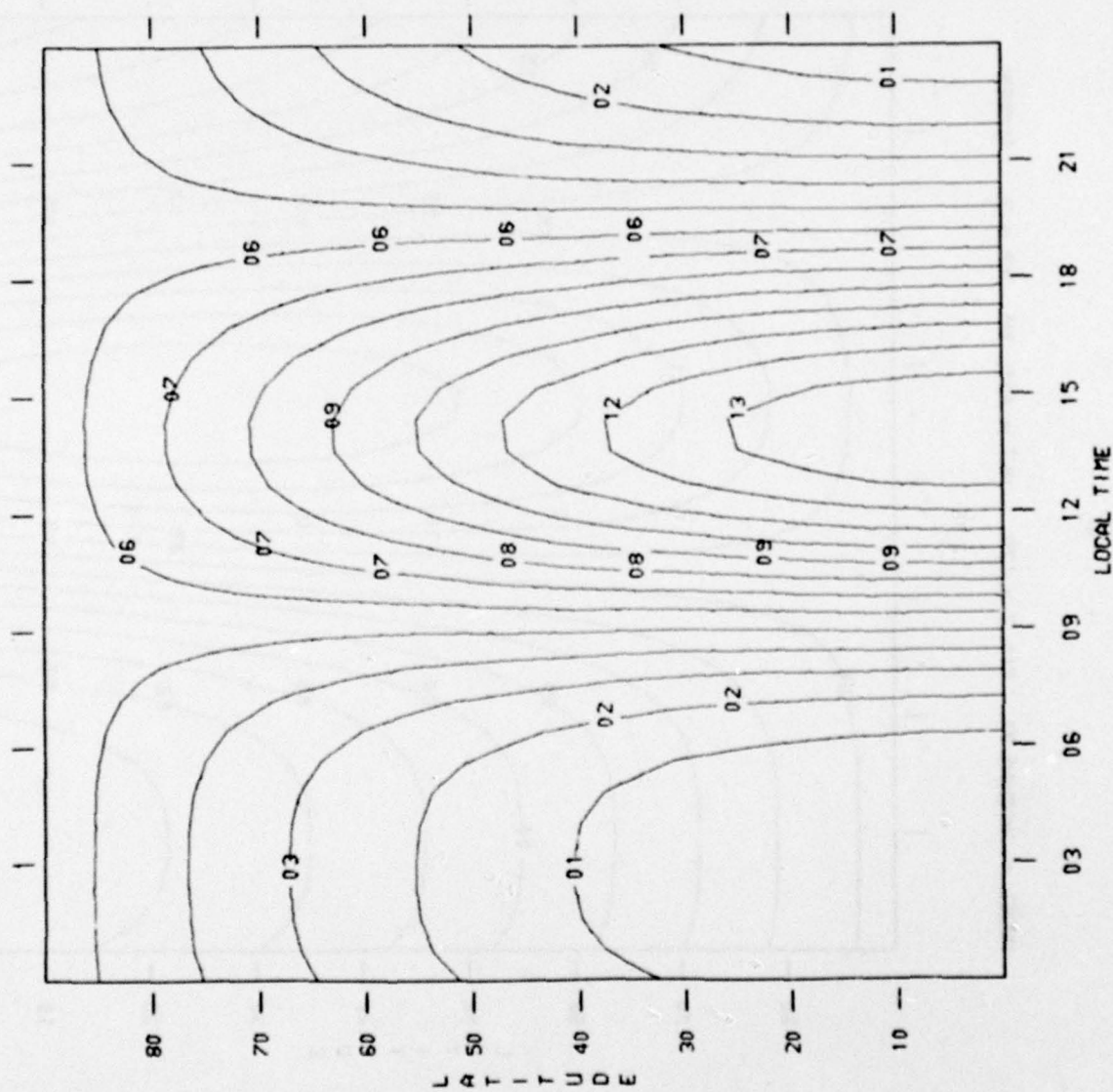
MODEL = JACCHIA 71 F10.7 = 125. ALT = 180. KM KP = 6. WINTER



GM/DTM=3

- 14 = 6.95E-13
- 13 = 6.85E-13
- 12 = 6.76E-13
- 11 = 6.67E-13
- 10 = 6.58E-13
- 09 = 6.48E-13
- 08 = 6.39E-13
- 07 = 6.30E-13
- 06 = 6.21E-13
- 05 = 6.11E-13
- 04 = 6.02E-13
- 03 = 5.93E-13
- 02 = 5.84E-13
- 01 = 5.74E-13
- 00 = 5.65E-13

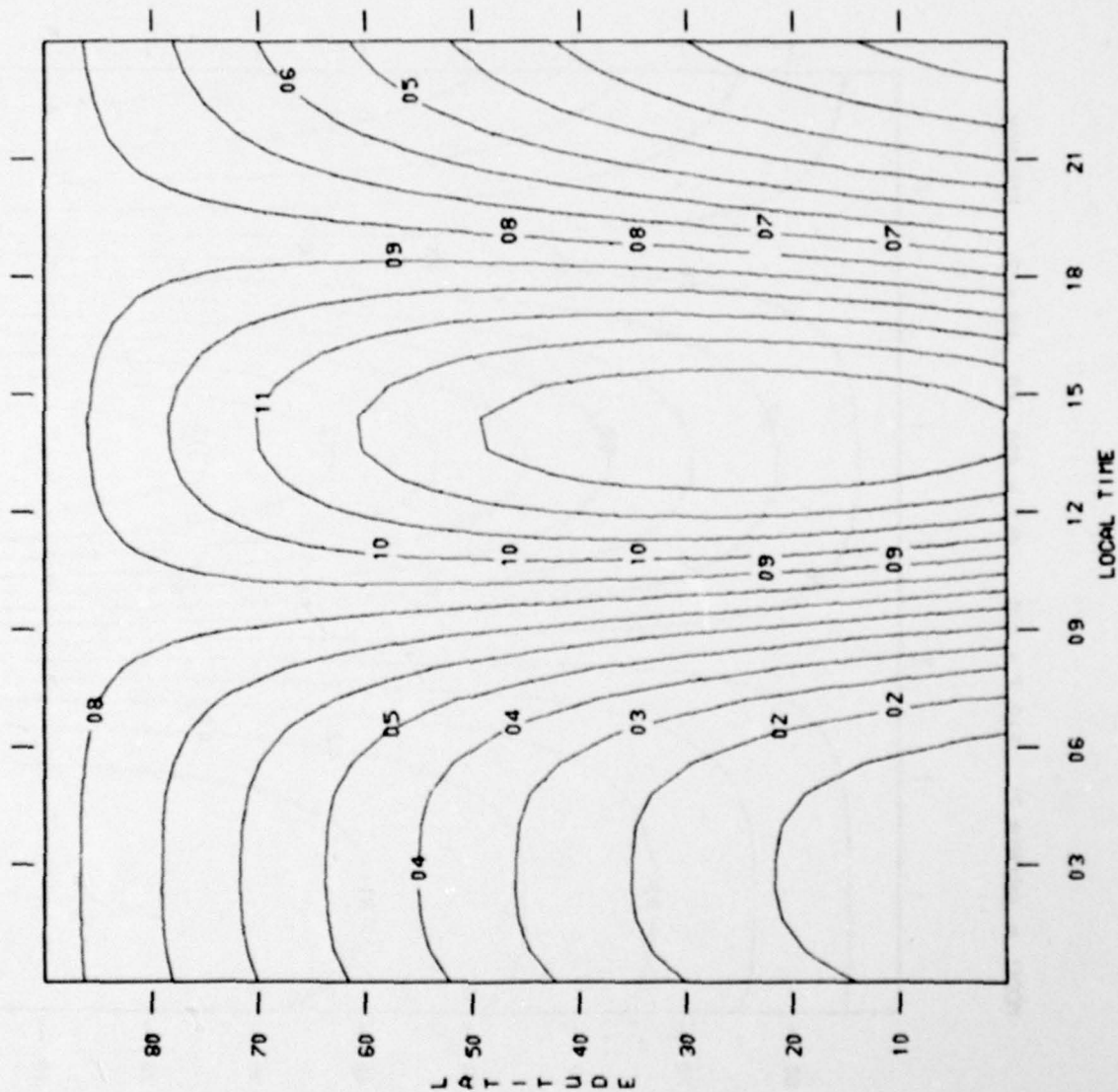
MODEL = JACCHIA 71 F10.7 = 125. ALT = 400. KM KP = 2. EQUINOX



CH/CH1003

- 14 = 5.49E-15
- 13 = 5.22E-15
- 12 = 4.96E-15
- 11 = 4.70E-15
- 10 = 4.43E-15
- 09 = 4.17E-15
- 08 = 3.90E-15
- 07 = 3.64E-15
- 06 = 3.38E-15
- 05 = 3.11E-15
- 04 = 2.85E-15
- 03 = 2.58E-15
- 02 = 2.32E-15
- 01 = 2.06E-15
- 00 = 1.79E-15

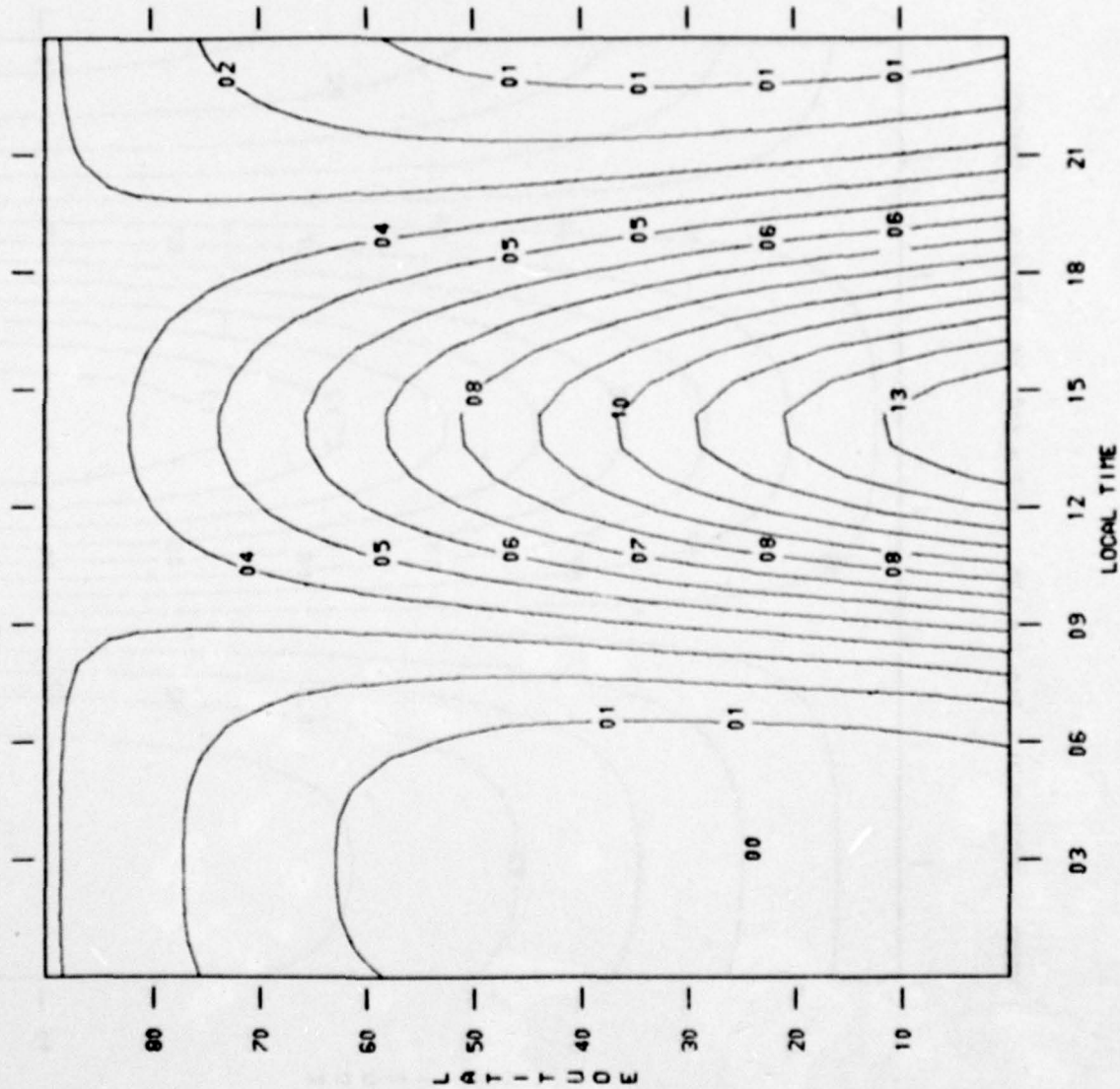
MODEL = JACCHIA 71 F10.7 = 125. ALT = 400. KM KP = 2. SUMMER



GM/CN1003

- 14 = 3.86E-15
- 13 = 3.68E-15
- 12 = 3.50E-15
- 11 = 3.32E-15
- 10 = 3.14E-15
- 09 = 2.96E-15
- 08 = 2.77E-15
- 07 = 2.59E-15
- 06 = 2.41E-15
- 05 = 2.23E-15
- 04 = 2.05E-15
- 03 = 1.86E-15
- 02 = 1.68E-15
- 01 = 1.50E-15
- 00 = 1.32E-15

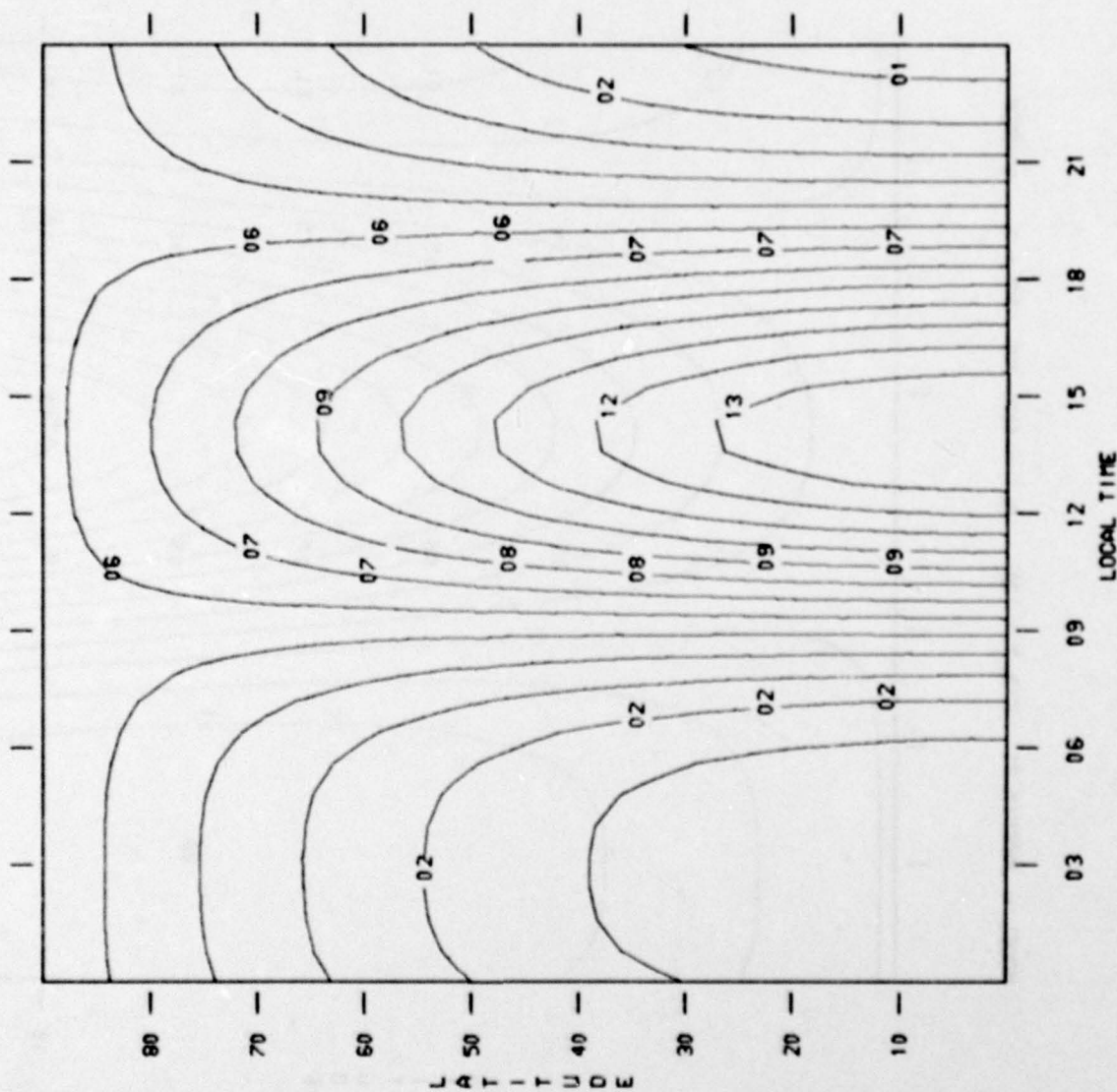
MODEL = JACCHIA 71 F10.7 = 125. ALT = 400. KM KP = 2. WINTER



GM/CHW3

- 14 = 4.35E-15
- 13 = 4.15E-15
- 12 = 3.94E-15
- 11 = 3.74E-15
- 10 = 3.53E-15
- 09 = 3.33E-15
- 08 = 3.12E-15
- 07 = 2.92E-15
- 06 = 2.71E-15
- 05 = 2.51E-15
- 04 = 2.30E-15
- 03 = 2.10E-15
- 02 = 1.89E-15
- 01 = 1.69E-15
- 00 = 1.48E-15

MODEL = JACCHIA 71 F10.7 = 125. ALT = 400. KM KP = 5. EQUINOX

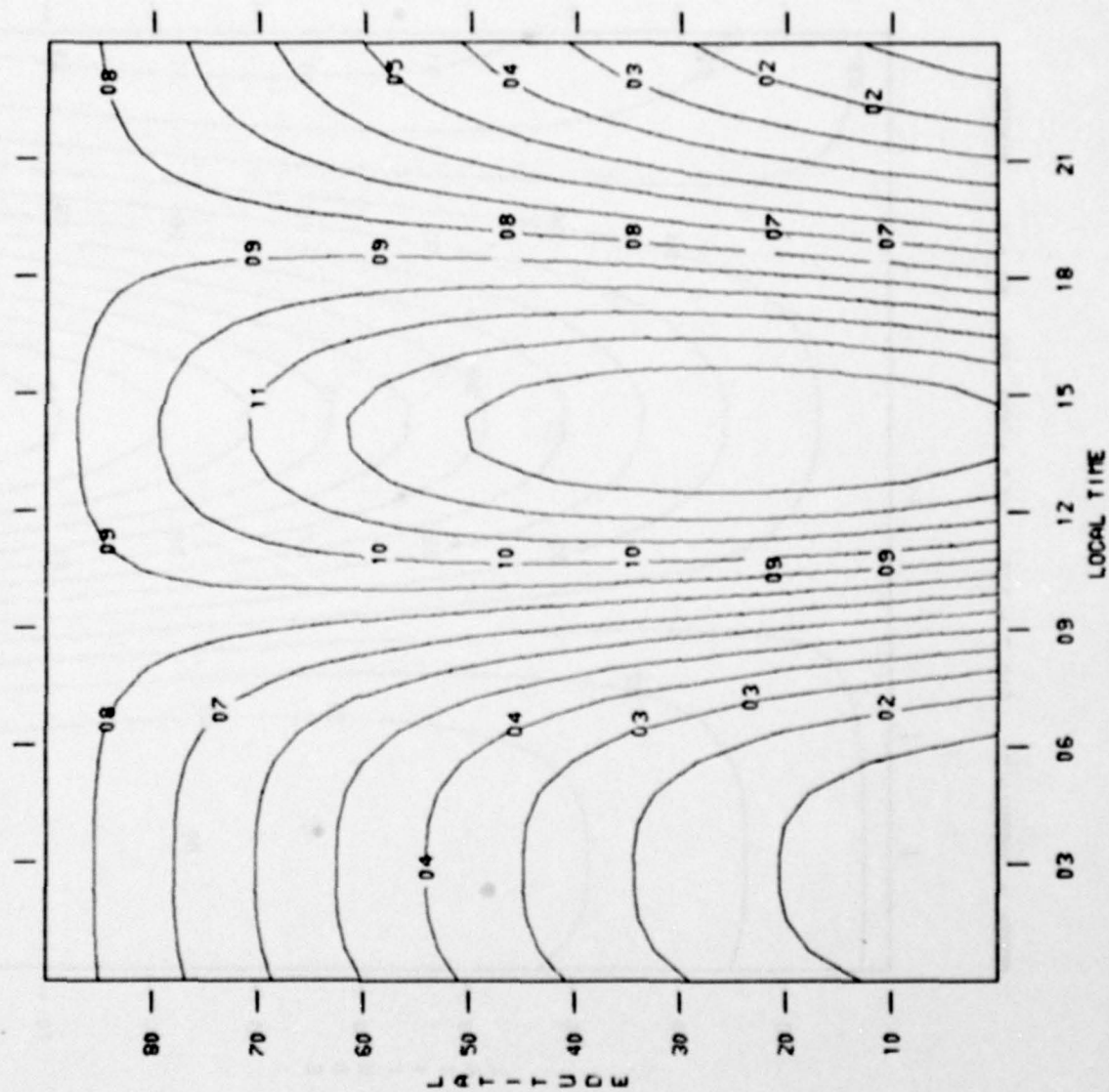


GM/CN=03

- 14 = 7.73E-15
- 13 = 7.38E-15
- 12 = 7.04E-15
- 11 = 6.70E-15
- 10 = 6.35E-15
- 09 = 6.01E-15
- 08 = 5.67E-15
- 07 = 5.32E-15
- 06 = 4.98E-15
- 05 = 4.64E-15
- 04 = 4.29E-15
- 03 = 3.95E-15
- 02 = 3.61E-15
- 01 = 3.26E-15
- 00 = 2.92E-15

L A T I T U D E

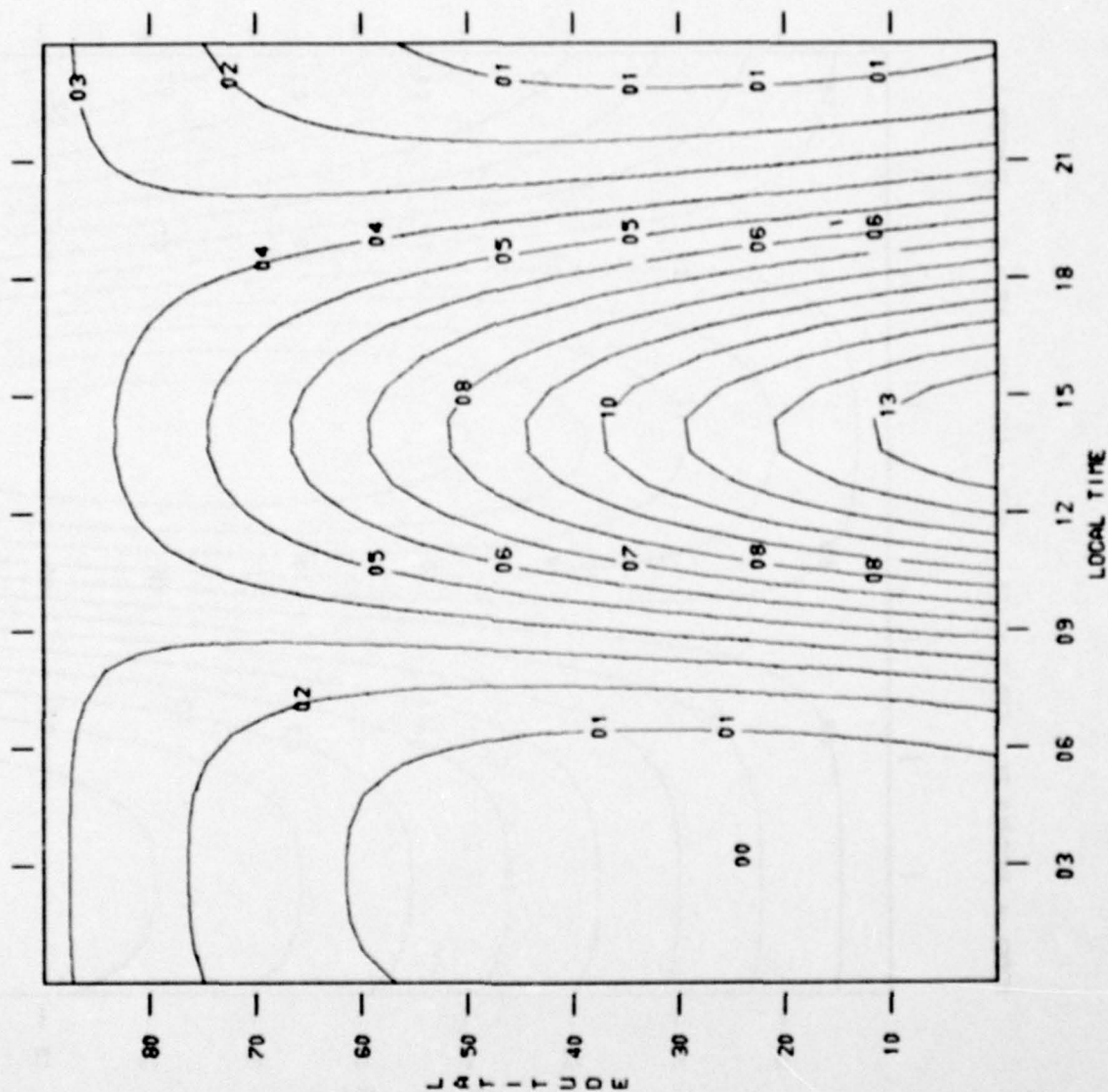
MODEL = JAOCHIA 71 F10.7 = 125. ALT = 400. KM KP = 6. SUMMER



CM/Chow3

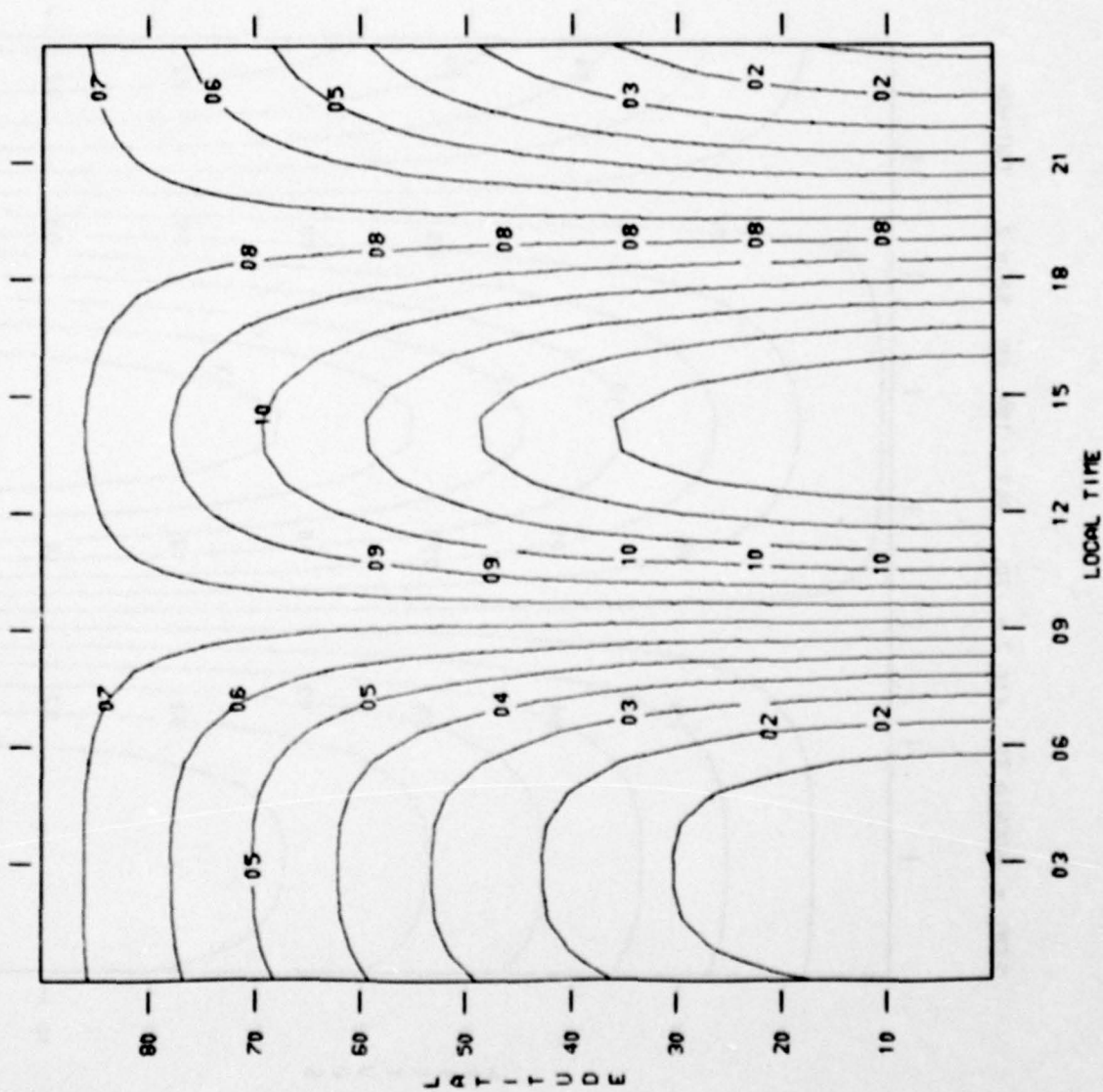
- 14 = 5.44E-15
- 13 = 5.21E-15
- 12 = 4.97E-15
- 11 = 4.73E-15
- 10 = 4.50E-15
- 09 = 4.26E-15
- 08 = 4.02E-15
- 07 = 3.79E-15
- 06 = 3.55E-15
- 05 = 3.32E-15
- 04 = 3.08E-15
- 03 = 2.84E-15
- 02 = 2.61E-15
- 01 = 2.37E-15
- 00 = 2.14E-15

MODEL = JACCHIA 71 F10.7 = 125. ALT = 400. KM KP = 6. WINTER



CM/CHW03
 14 = 6.18E-15
 13 = 5.91E-15
 12 = 5.64E-15
 11 = 5.37E-15
 10 = 5.10E-15
 09 = 4.83E-15
 08 = 4.56E-15
 07 = 4.30E-15
 06 = 4.03E-15
 05 = 3.76E-15
 04 = 3.49E-15
 03 = 3.22E-15
 02 = 2.95E-15
 01 = 2.68E-15
 00 = 2.41E-15

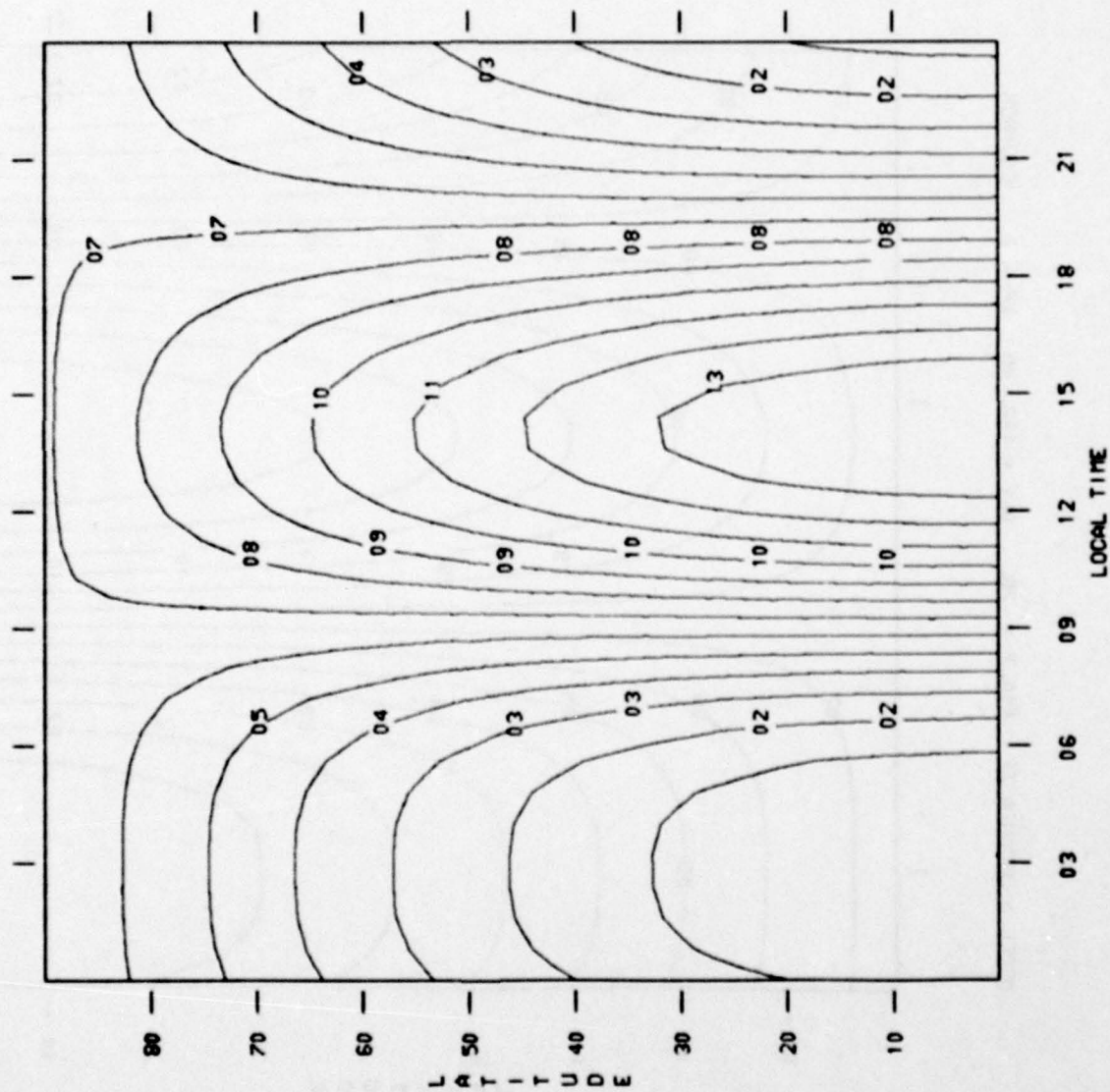
MODEL = JACCHIA 71 F10.7 = 70. ALT = 140. KM KP = 2. EQUINOX



CM/CH=3

- 14 = 3.94E-12
- 13 = 3.91E-12
- 12 = 3.88E-12
- 11 = 3.84E-12
- 10 = 3.81E-12
- 09 = 3.77E-12
- 08 = 3.74E-12
- 07 = 3.71E-12
- 06 = 3.67E-12
- 05 = 3.64E-12
- 04 = 3.60E-12
- 03 = 3.57E-12
- 02 = 3.54E-12
- 01 = 3.50E-12
- 00 = 3.47E-12

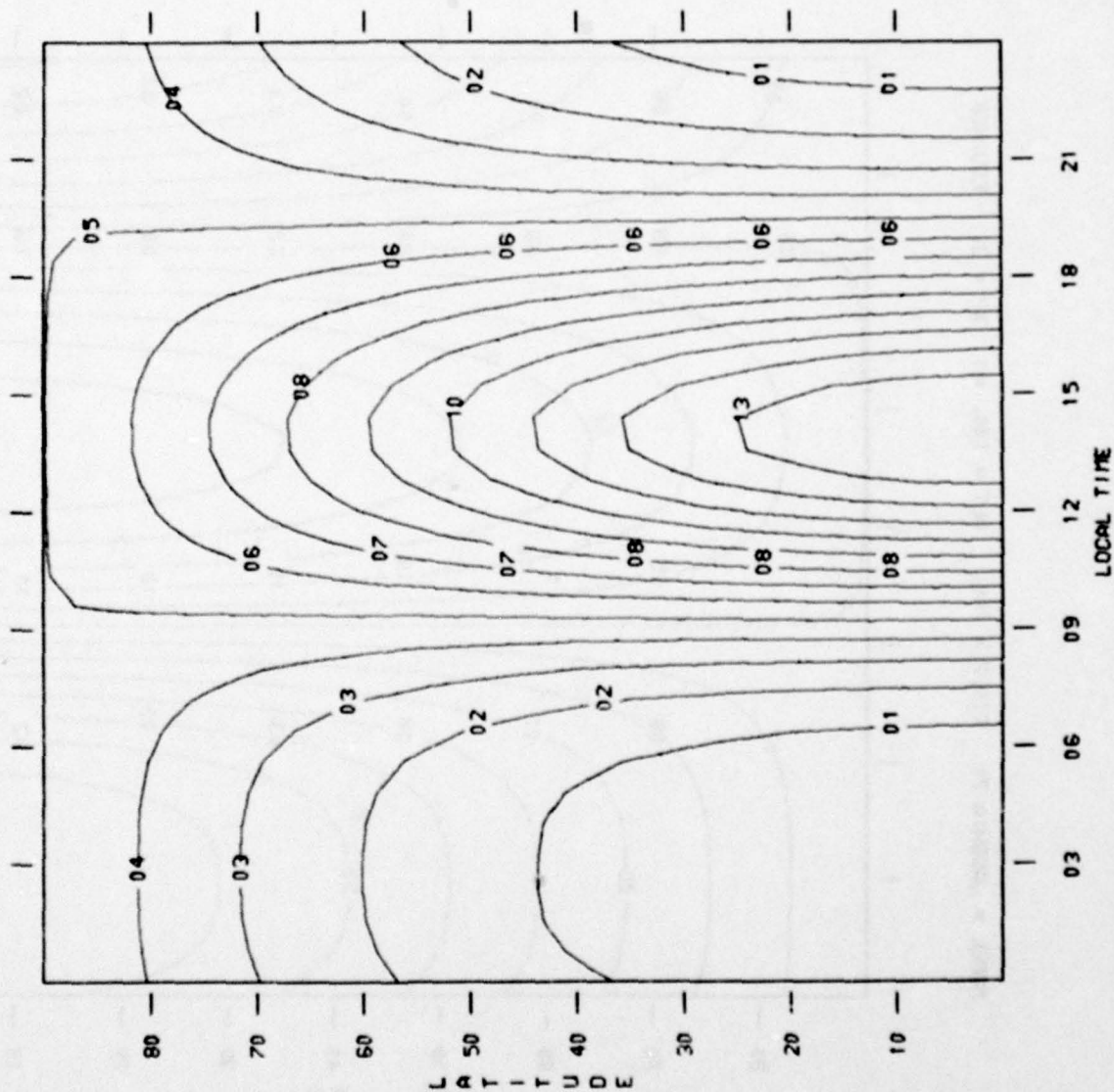
MODEL = JACCHIA 71 F10.7 = 70. ALT = 180. KM KP = 2. EQUINOX



CH/CN=3

- 14 = 5.02E-13
- 13 = 4.92E-13
- 12 = 4.82E-13
- 11 = 4.72E-13
- 10 = 4.62E-13
- 09 = 4.52E-13
- 08 = 4.42E-13
- 07 = 4.31E-13
- 06 = 4.21E-13
- 05 = 4.11E-13
- 04 = 4.01E-13
- 03 = 3.91E-13
- 02 = 3.81E-13
- 01 = 3.71E-13
- 00 = 3.61E-13

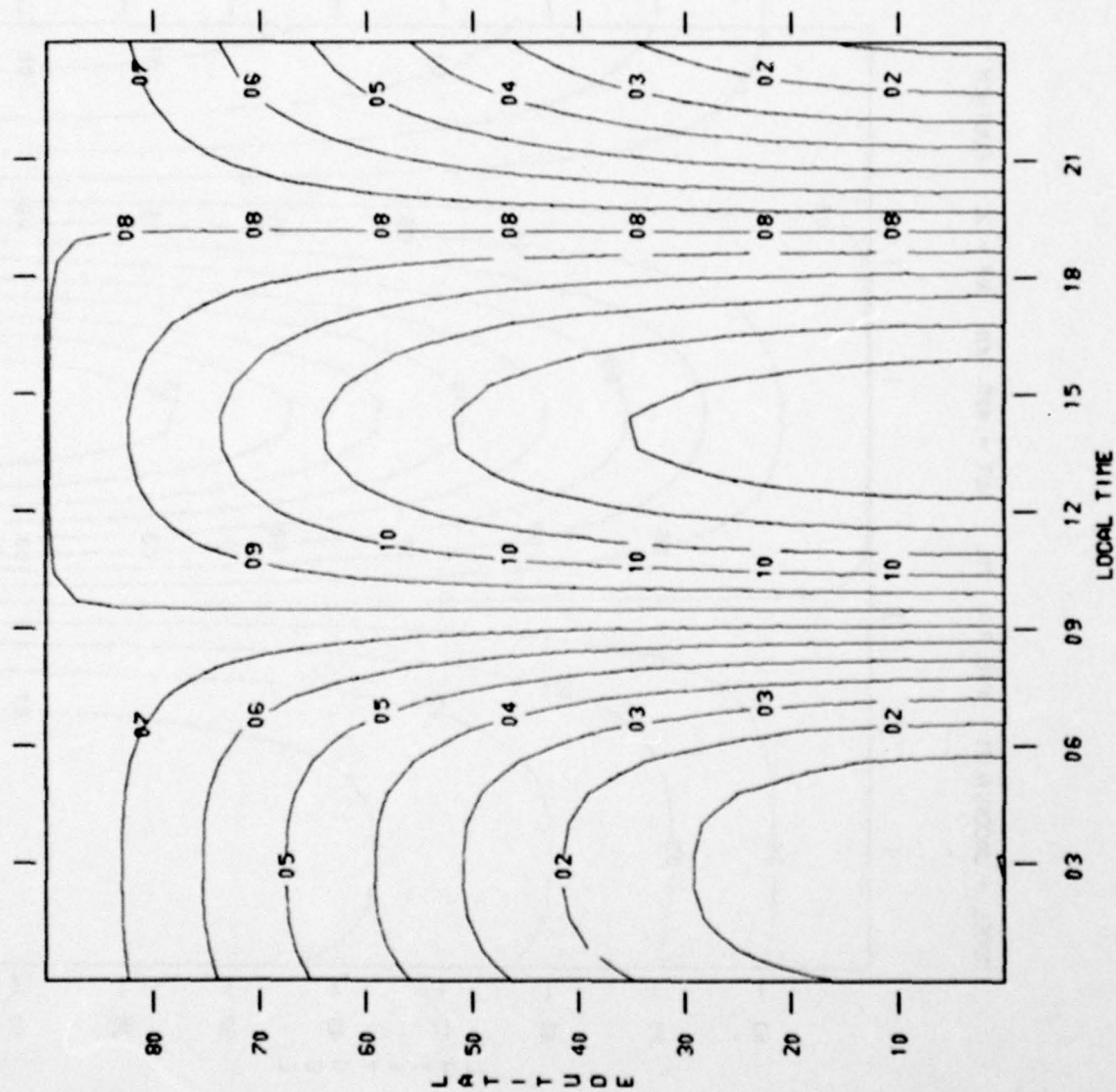
MODEL = JACCHIA 71 F10.7 = 70. ALT = 400. KM KP = 2. EQUINOX



CH/CH103

- 14 = 1.83E-15
- 13 = 1.73E-15
- 12 = 1.63E-15
- 11 = 1.53E-15
- 10 = 1.43E-15
- 09 = 1.33E-15
- 08 = 1.23E-15
- 07 = 1.13E-15
- 06 = 1.03E-15
- 05 = 9.32E-16
- 04 = 8.32E-16
- 03 = 7.33E-16
- 02 = 6.34E-16
- 01 = 5.34E-16
- 00 = 4.35E-16

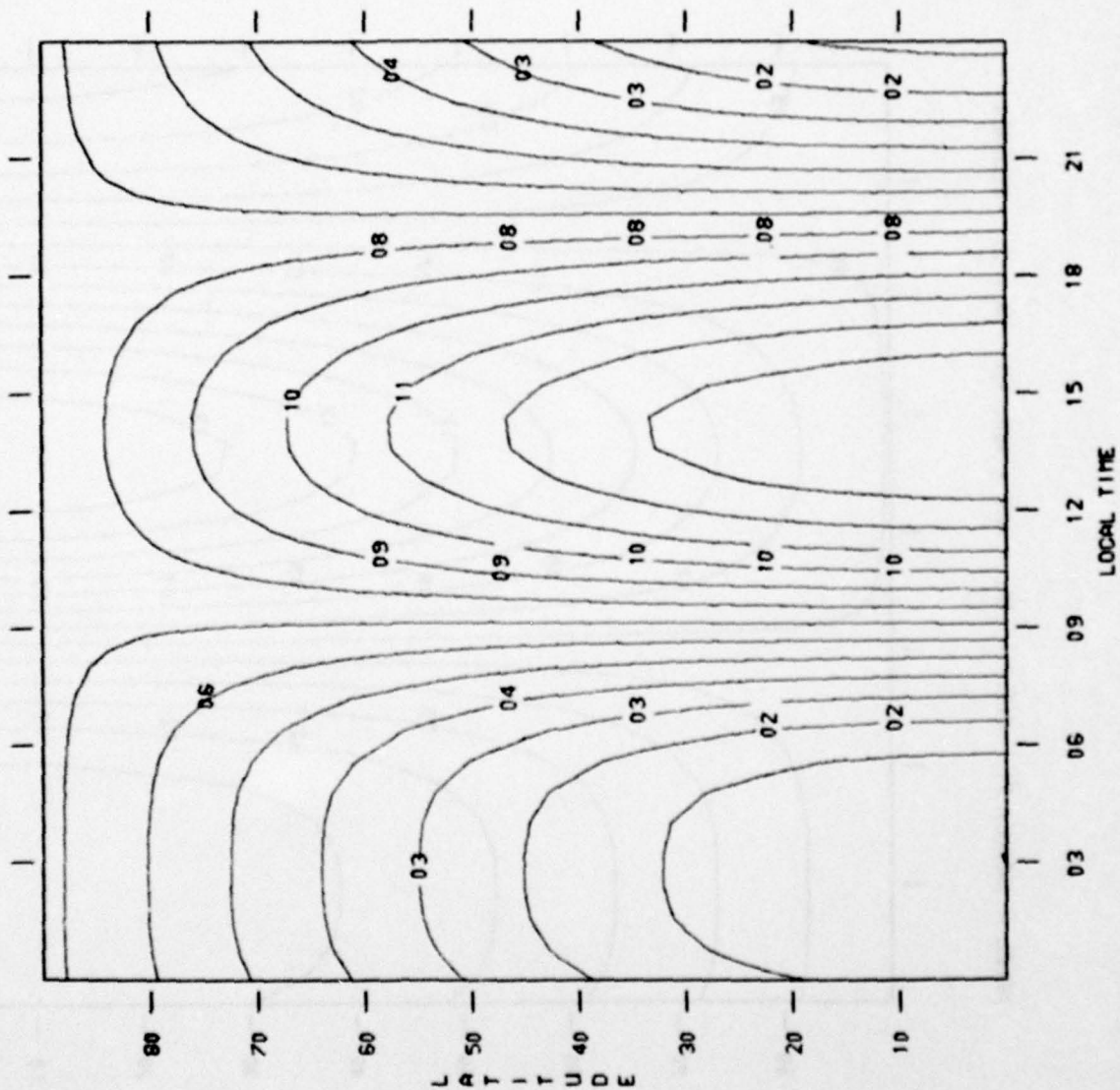
MODEL = JACCHIA 71 F10.7 = 180. ALT = 140. KM KP = 2. EQUINOX



GM/CH=3

14 =	4.66E-12
13 =	4.63E-12
12 =	4.61E-12
11 =	4.58E-12
10 =	4.55E-12
09 =	4.52E-12
08 =	4.50E-12
07 =	4.47E-12
06 =	4.44E-12
05 =	4.41E-12
04 =	4.38E-12
03 =	4.36E-12
02 =	4.33E-12
01 =	4.30E-12
00 =	4.27E-12

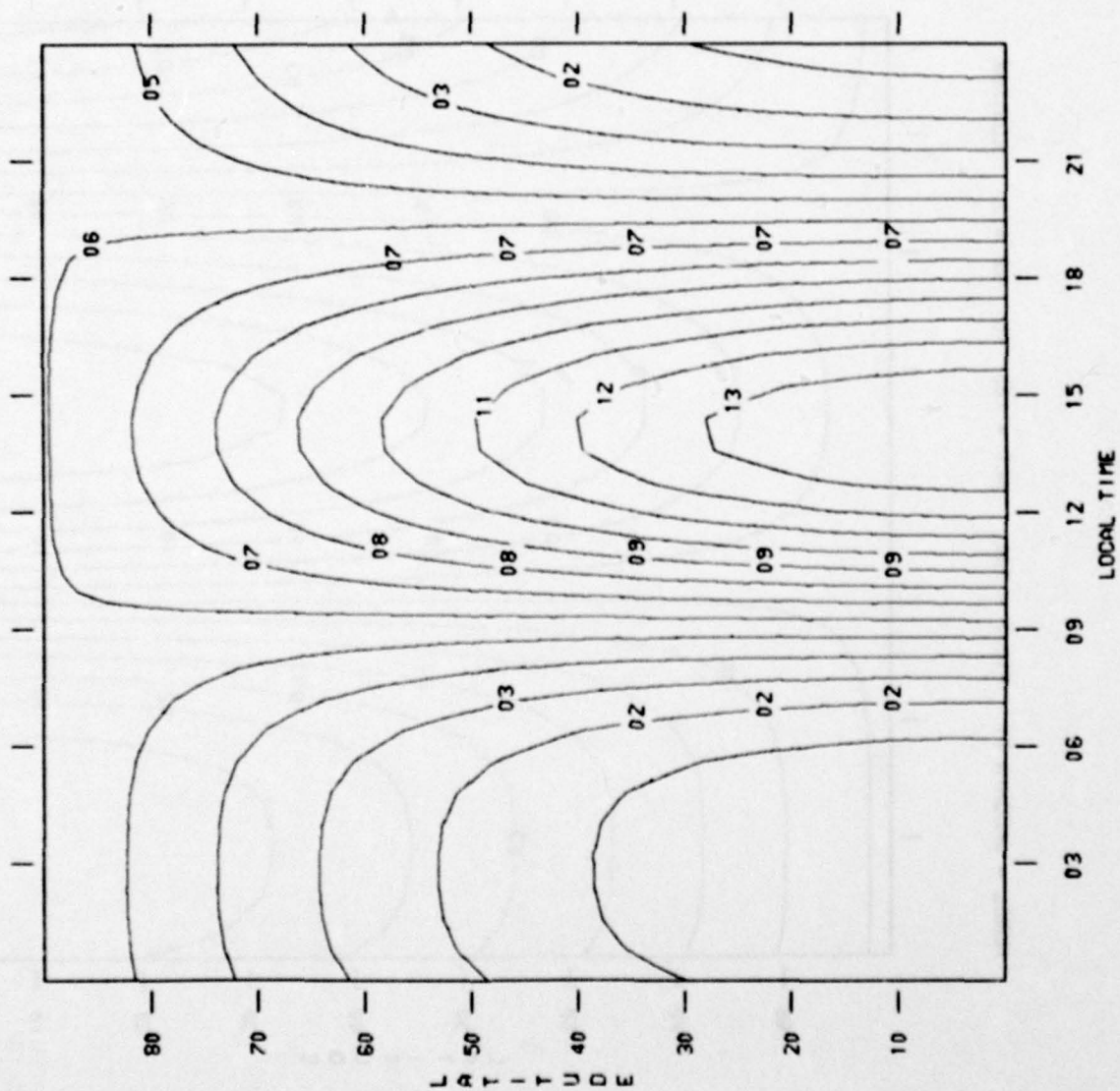
MODEL = JACCHIA 71 F10.7 = 180. ALT = 180. KM KP = 2. EQUINOX



GHz/Chirp3

14 =	7.42E-13
13 =	7.32E-13
12 =	7.23E-13
11 =	7.14E-13
10 =	7.04E-13
09 =	6.95E-13
08 =	6.86E-13
07 =	6.77E-13
06 =	6.67E-13
05 =	6.58E-13
04 =	6.49E-13
03 =	6.39E-13
02 =	6.30E-13
01 =	6.21E-13
00 =	6.12E-13

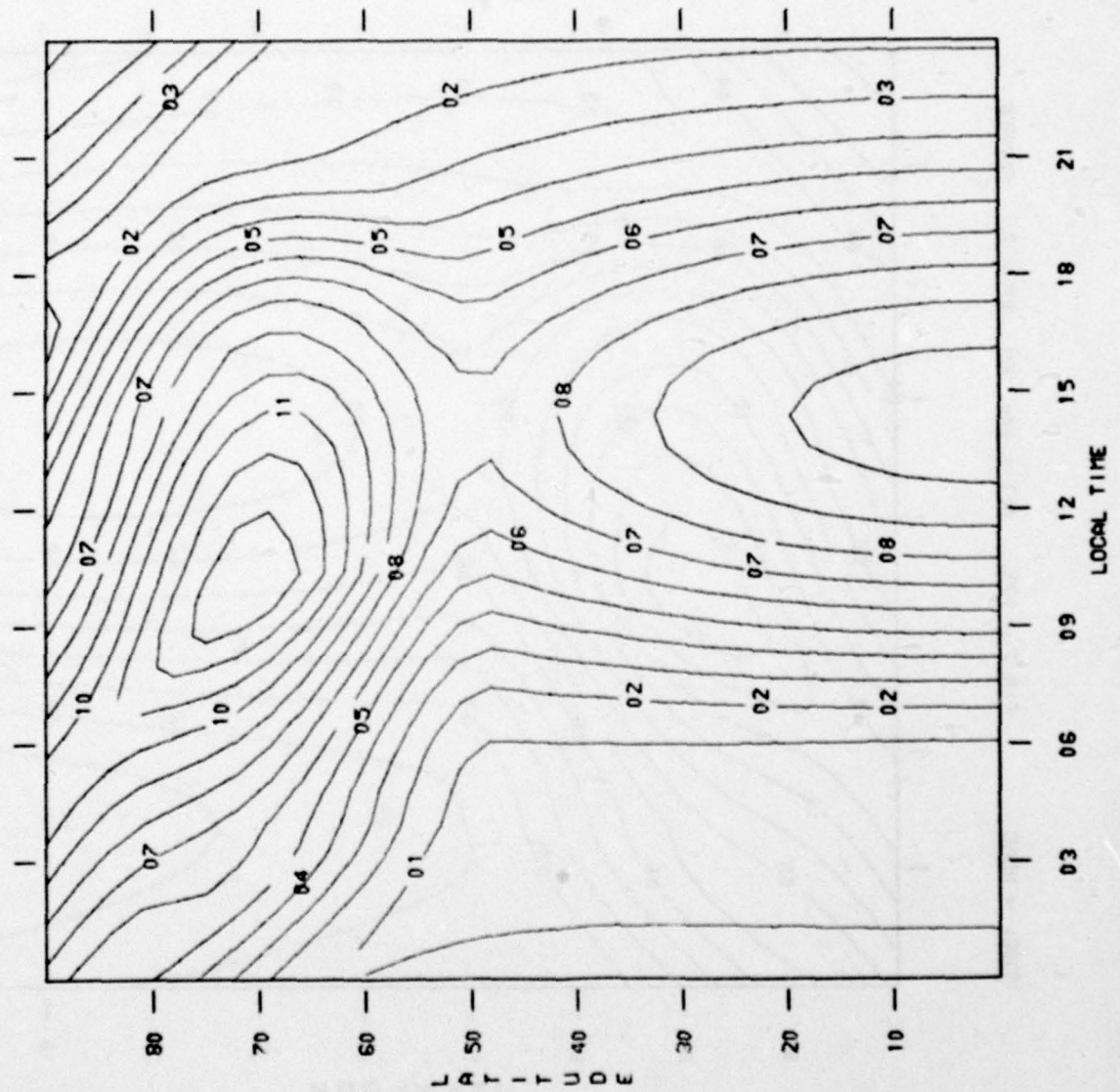
MODEL = JACCHIA 71 F10.7 = 180. ALT = 400. KM KP = 2. EQUINOX



CH/CHmax3

- 14 = 1.09E-14
- 13 = 1.04E-14
- 12 = 9.97E-15
- 11 = 9.51E-15
- 10 = 9.05E-15
- 09 = 8.58E-15
- 08 = 8.12E-15
- 07 = 7.65E-15
- 06 = 7.19E-15
- 05 = 6.73E-15
- 04 = 6.26E-15
- 03 = 5.80E-15
- 02 = 5.33E-15
- 01 = 4.87E-15
- 00 = 4.41E-15

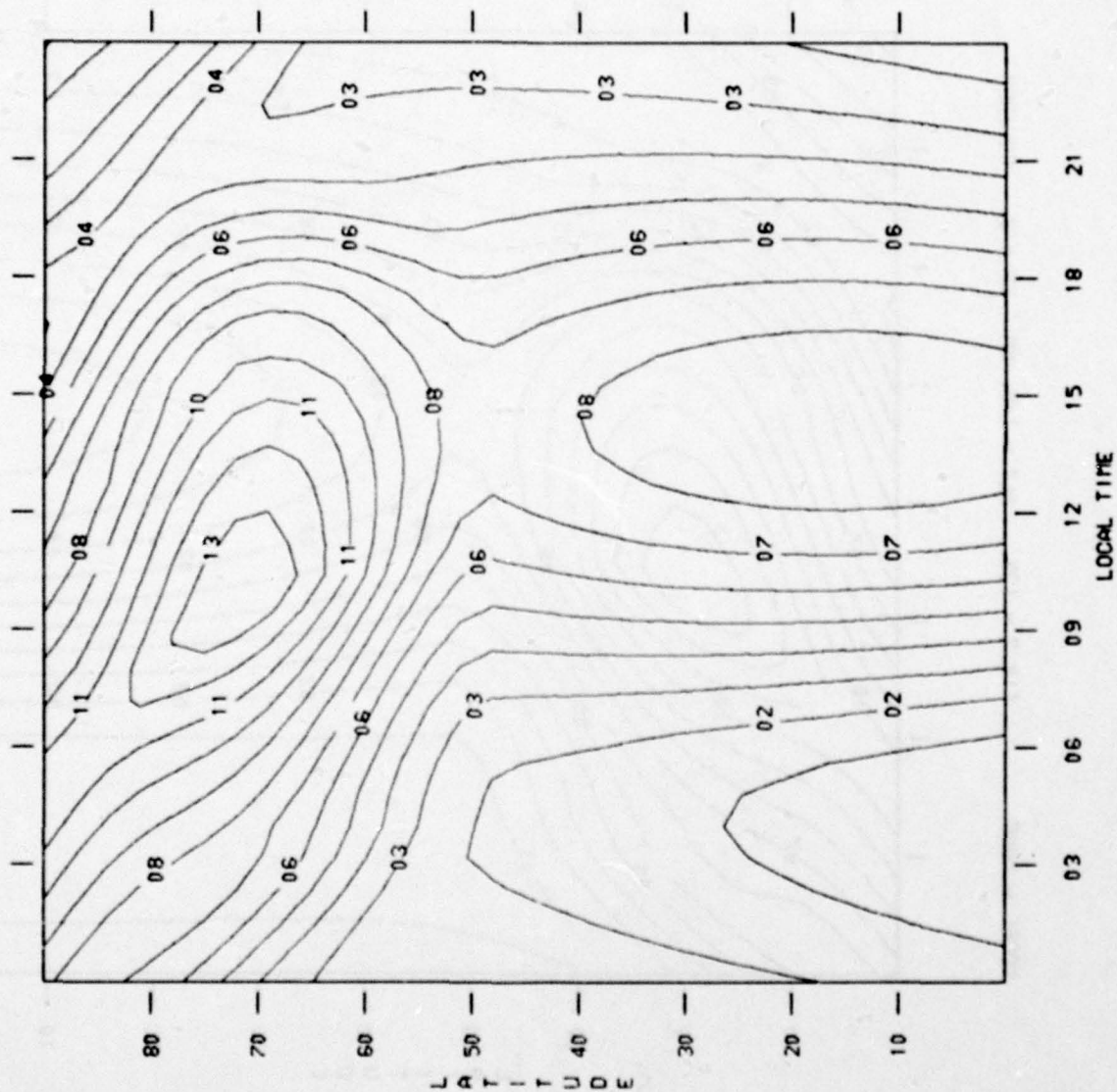
MODEL = MDAC F10.7 = 125. ALT = 140. KM KP = 2. EQUINOX



CM/CHW3

14 = 5.05E-12
 13 = 4.98E-12
 12 = 4.91E-12
 11 = 4.85E-12
 10 = 4.78E-12
 09 = 4.71E-12
 08 = 4.65E-12
 07 = 4.58E-12
 06 = 4.52E-12
 05 = 4.45E-12
 04 = 4.38E-12
 03 = 4.32E-12
 02 = 4.25E-12
 01 = 4.18E-12
 00 = 4.12E-12

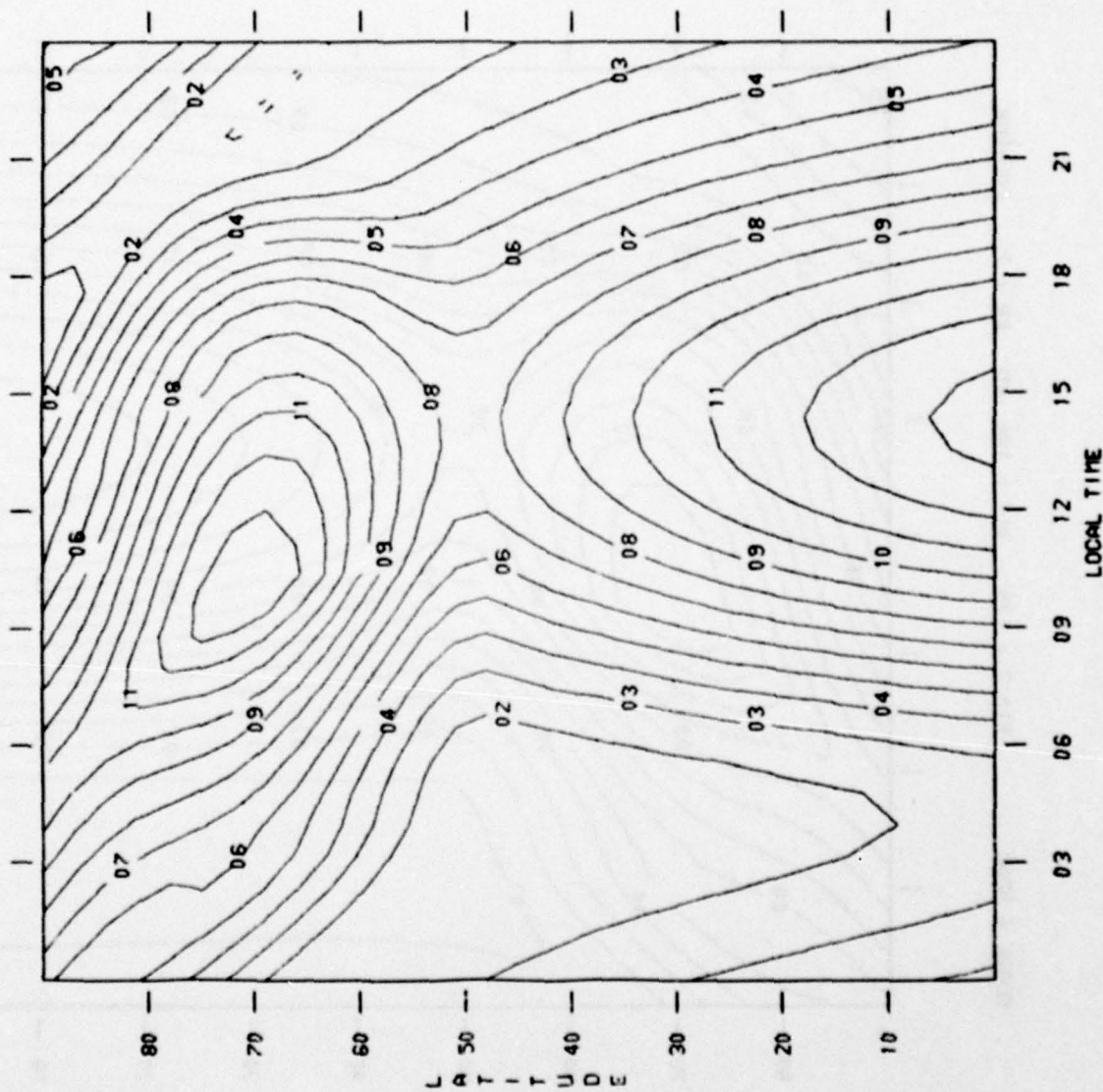
MODEL = MD&C F10.7 = 125. ALT = 140. KM KP = 2. SUMMER



GM/CN03

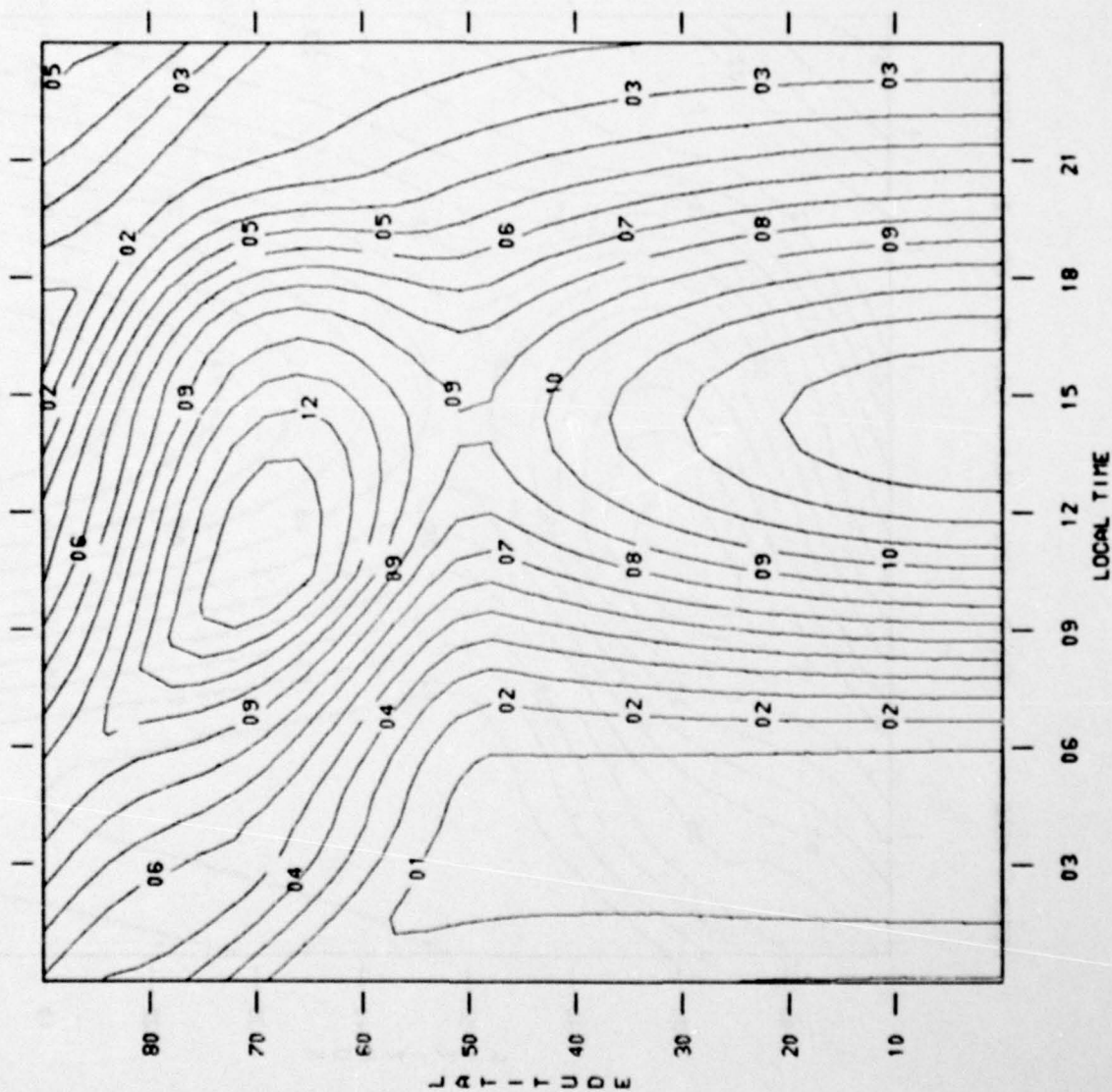
- 14 = 4.48E-12
- 13 = 4.41E-12
- 12 = 4.34E-12
- 11 = 4.27E-12
- 10 = 4.21E-12
- 09 = 4.14E-12
- 08 = 4.07E-12
- 07 = 4.00E-12
- 06 = 3.93E-12
- 05 = 3.86E-12
- 04 = 3.79E-12
- 03 = 3.72E-12
- 02 = 3.65E-12
- 01 = 3.58E-12
- 00 = 3.51E-12

MODEL = MODC F10.7 = 125. ALT = 140. KM KP = 2. WINTER

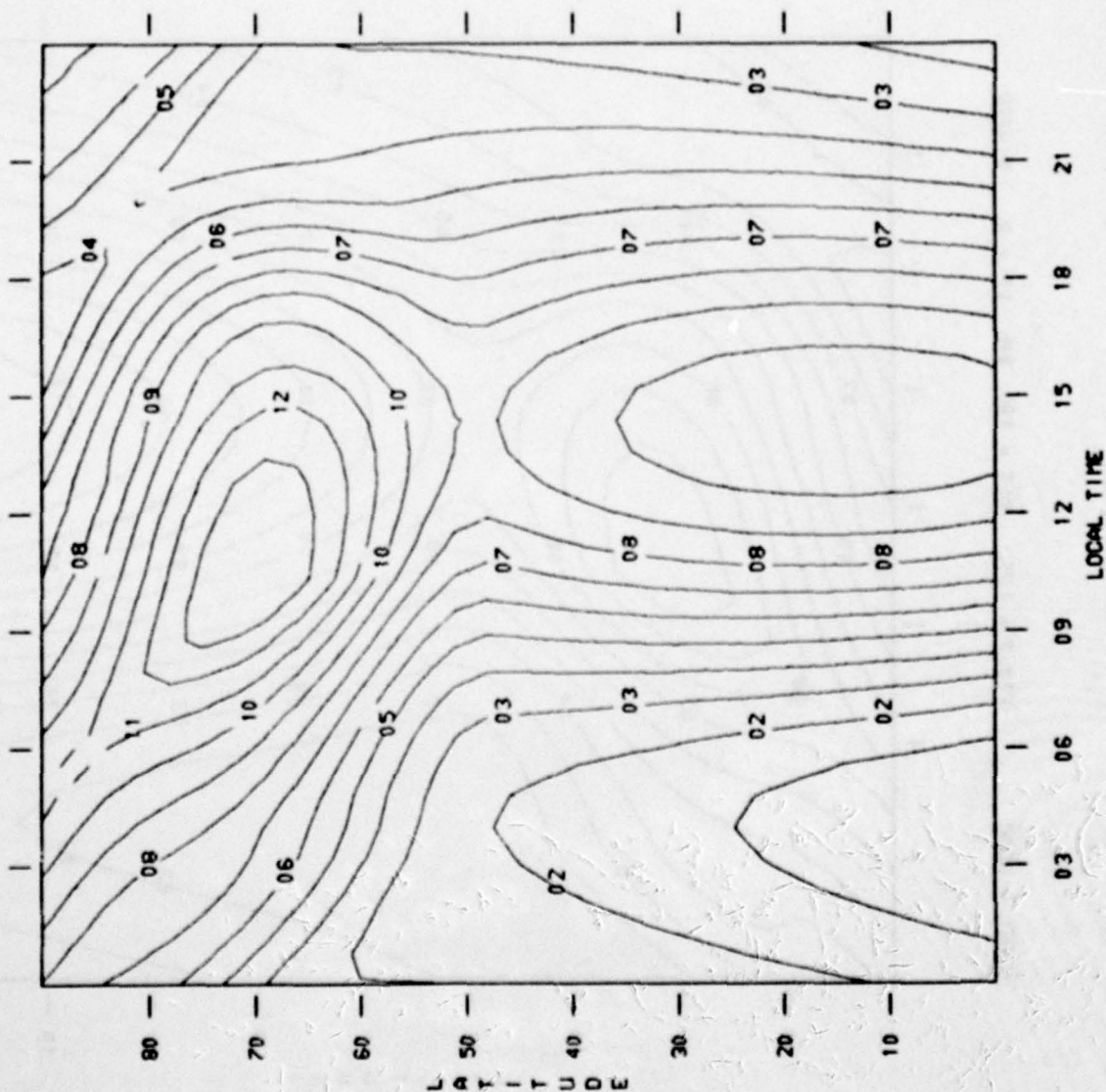


CM/CHW3
 14 = 4.46E-12
 13 = 4.41E-12
 12 = 4.35E-12
 11 = 4.29E-12
 10 = 4.23E-12
 09 = 4.17E-12
 08 = 4.12E-12
 07 = 4.06E-12
 06 = 4.00E-12
 05 = 3.94E-12
 04 = 3.88E-12
 03 = 3.83E-12
 02 = 3.77E-12
 01 = 3.71E-12
 00 = 3.65E-12

MODEL = MDAC F10.7 = 125. ALT = 180. KM KP = 2. EQUINOX



MODEL = MDAC F10.7 = 125. ALT = 180. KM KP = 2. SUMMER

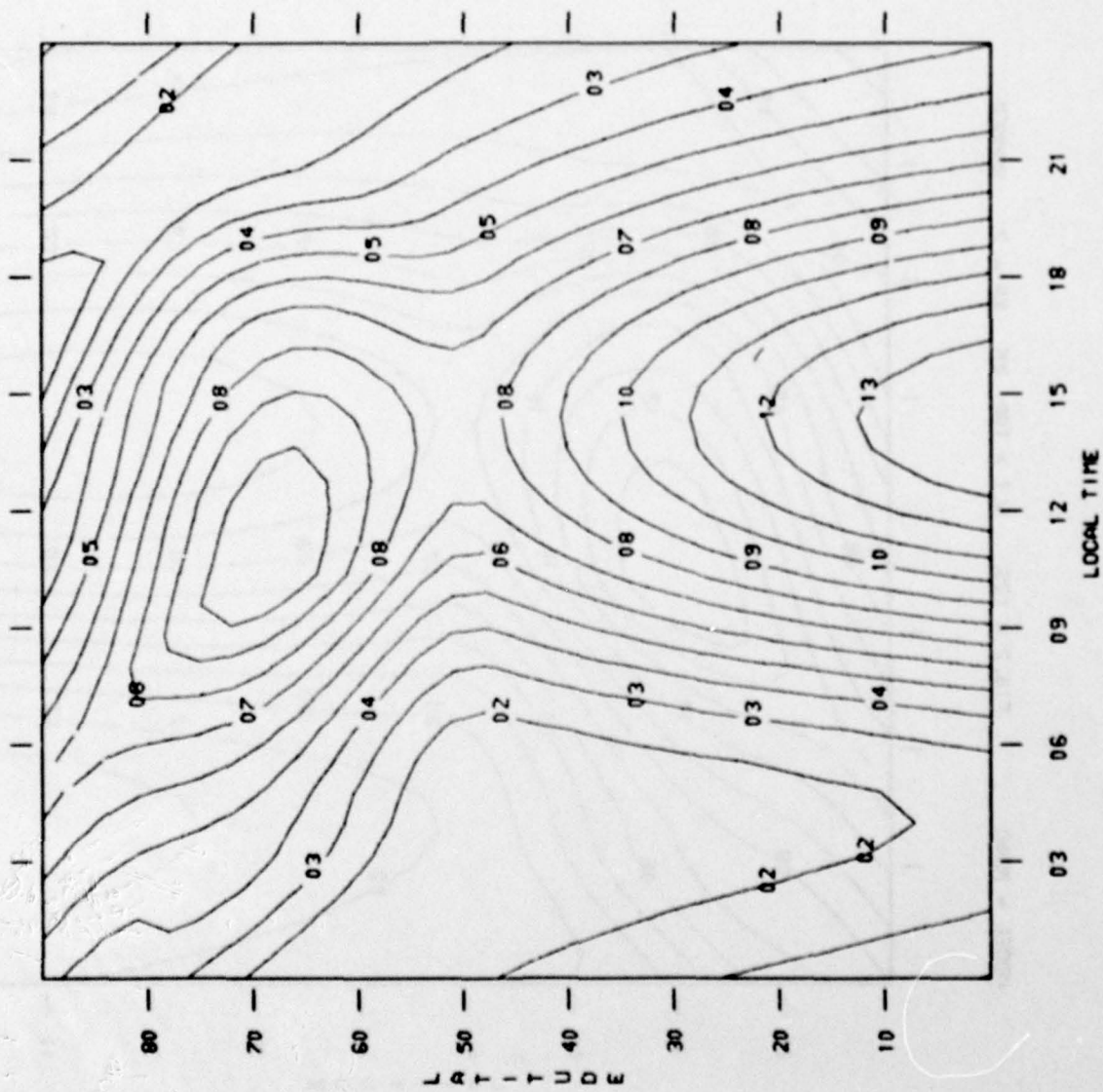


GM/CITE=3

- 14 = 6.64E-13
- 13 = 6.44E-13
- 12 = 6.25E-13
- 11 = 6.06E-13
- 10 = 5.87E-13
- 09 = 5.67E-13
- 08 = 5.48E-13
- 07 = 5.29E-13
- 06 = 5.09E-13
- 05 = 4.90E-13
- 04 = 4.71E-13
- 03 = 4.51E-13
- 02 = 4.32E-13
- 01 = 4.13E-13
- 00 = 3.94E-13

L A T I T U D E

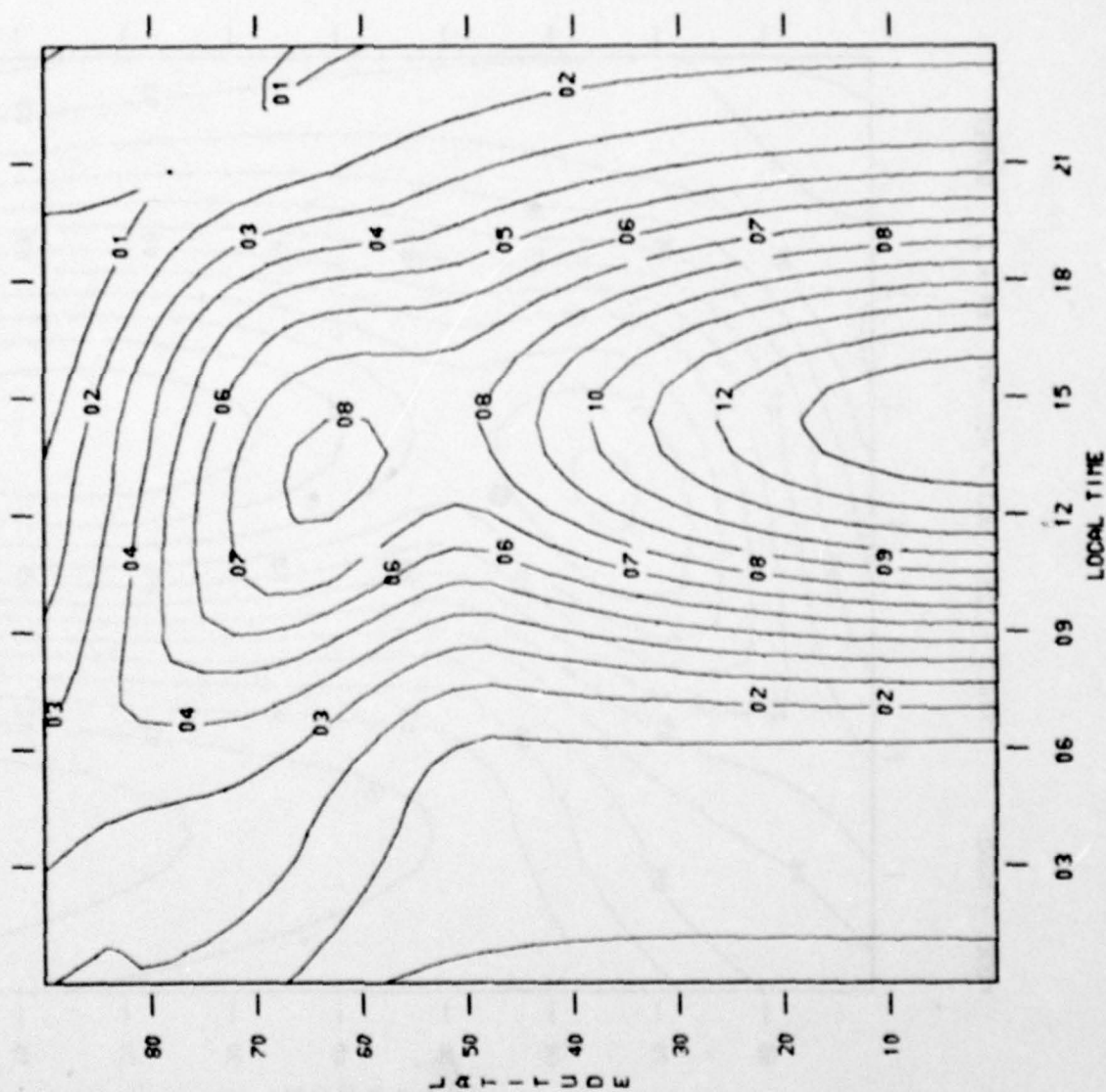
MODEL = M00C F10.7 = 125. ALT = 180. KM KP = 2. WINTER



GM/Chaw3

14 =	6.56E-13
13 =	6.37E-13
12 =	6.18E-13
11 =	6.00E-13
10 =	5.81E-13
09 =	5.62E-13
08 =	5.43E-13
07 =	5.24E-13
06 =	5.05E-13
05 =	4.86E-13
04 =	4.67E-13
03 =	4.49E-13
02 =	4.30E-13
01 =	4.11E-13
00 =	3.92E-13

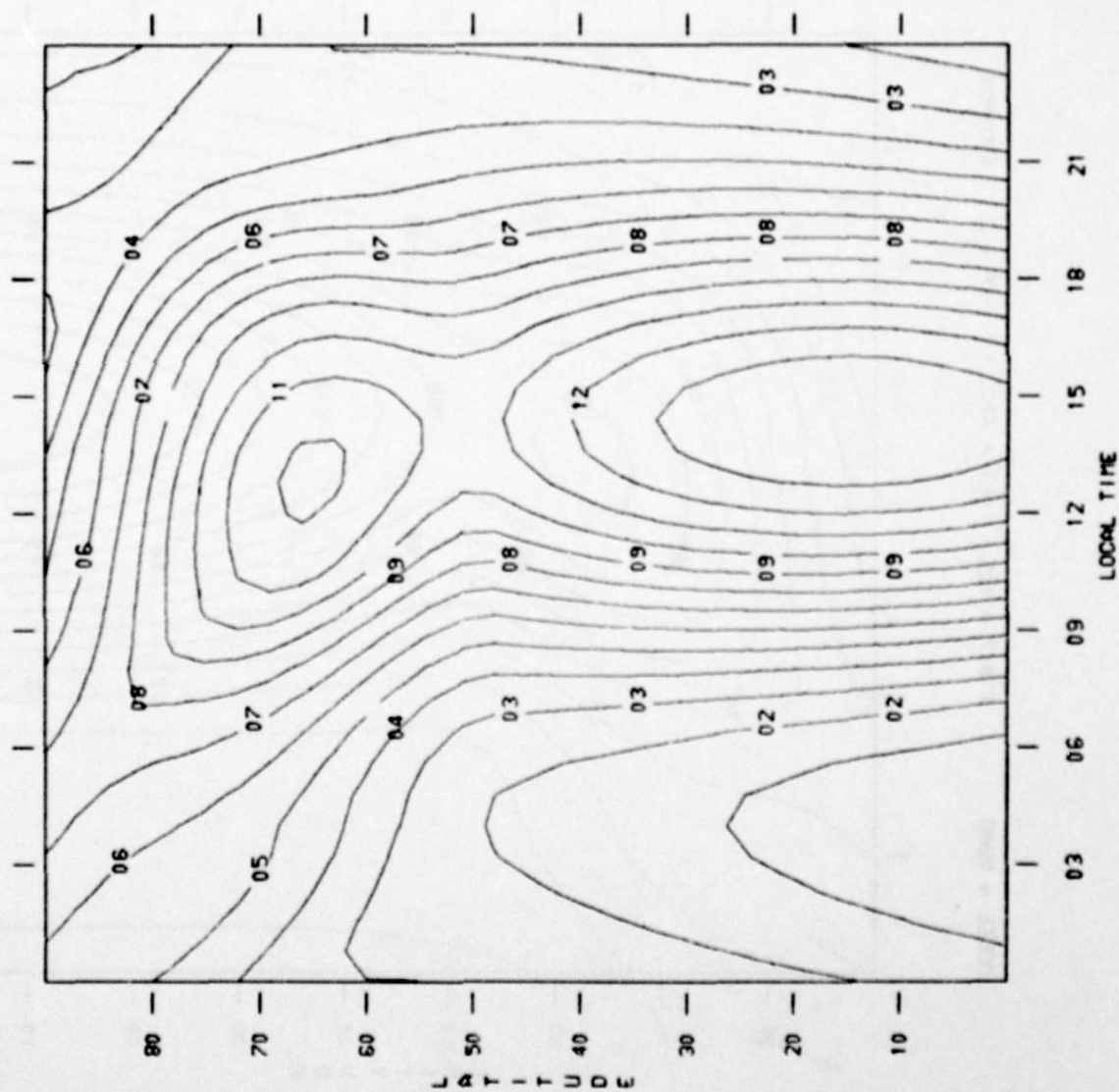
MODEL = M04C F10.7 = 125. ALT = 400. KM KP = 2. EQUINOX



CM/CH03

14 =	5.21E-15
13 =	4.96E-15
12 =	4.72E-15
11 =	4.47E-15
10 =	4.23E-15
09 =	3.98E-15
08 =	3.74E-15
07 =	3.49E-15
06 =	3.25E-15
05 =	3.00E-15
04 =	2.76E-15
03 =	2.51E-15
02 =	2.27E-15
01 =	2.02E-15
00 =	1.78E-15

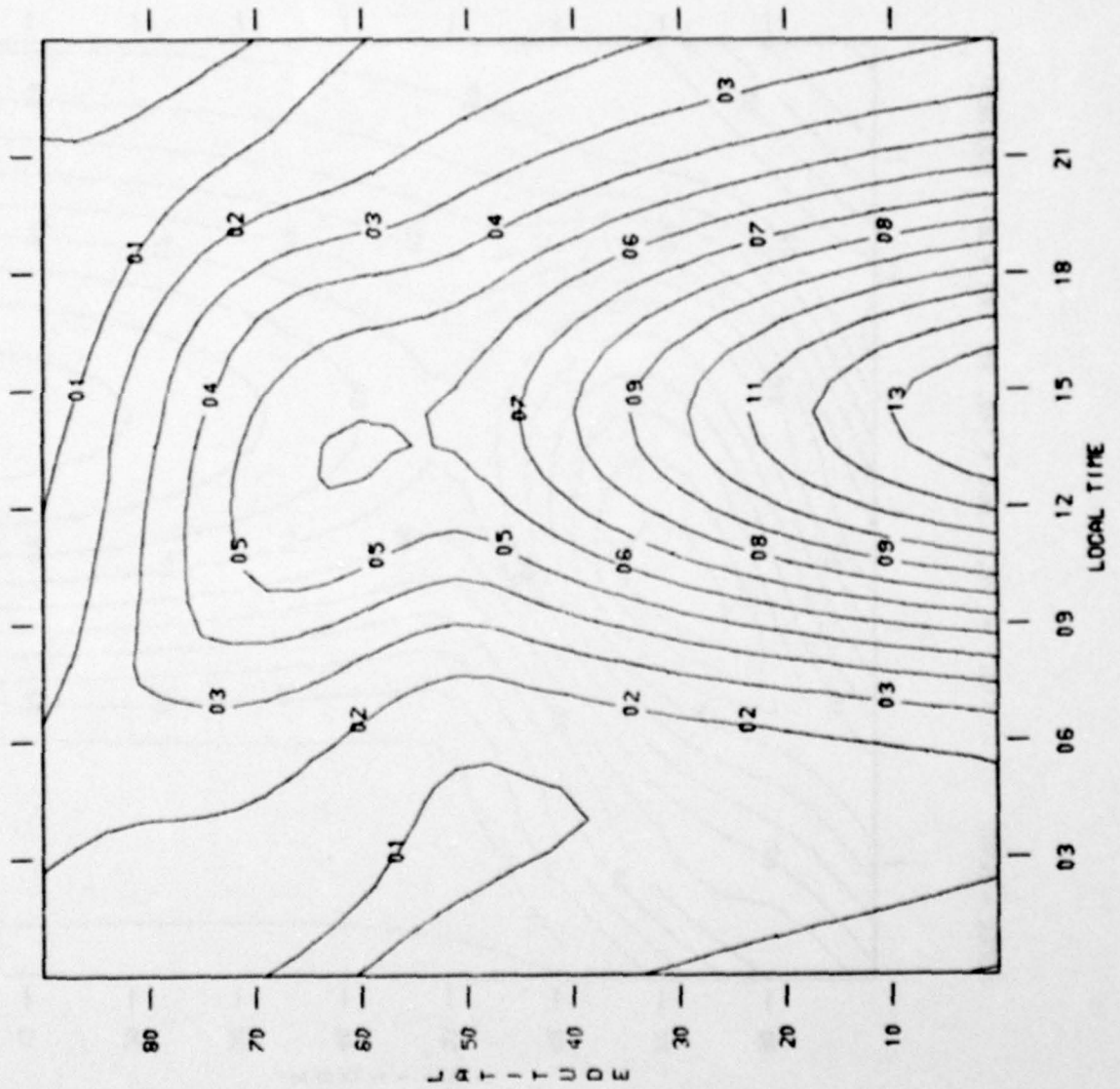
MODEL = MD4C F10.7 = 125. ALT = 400. KM KP = 2. SUMMER



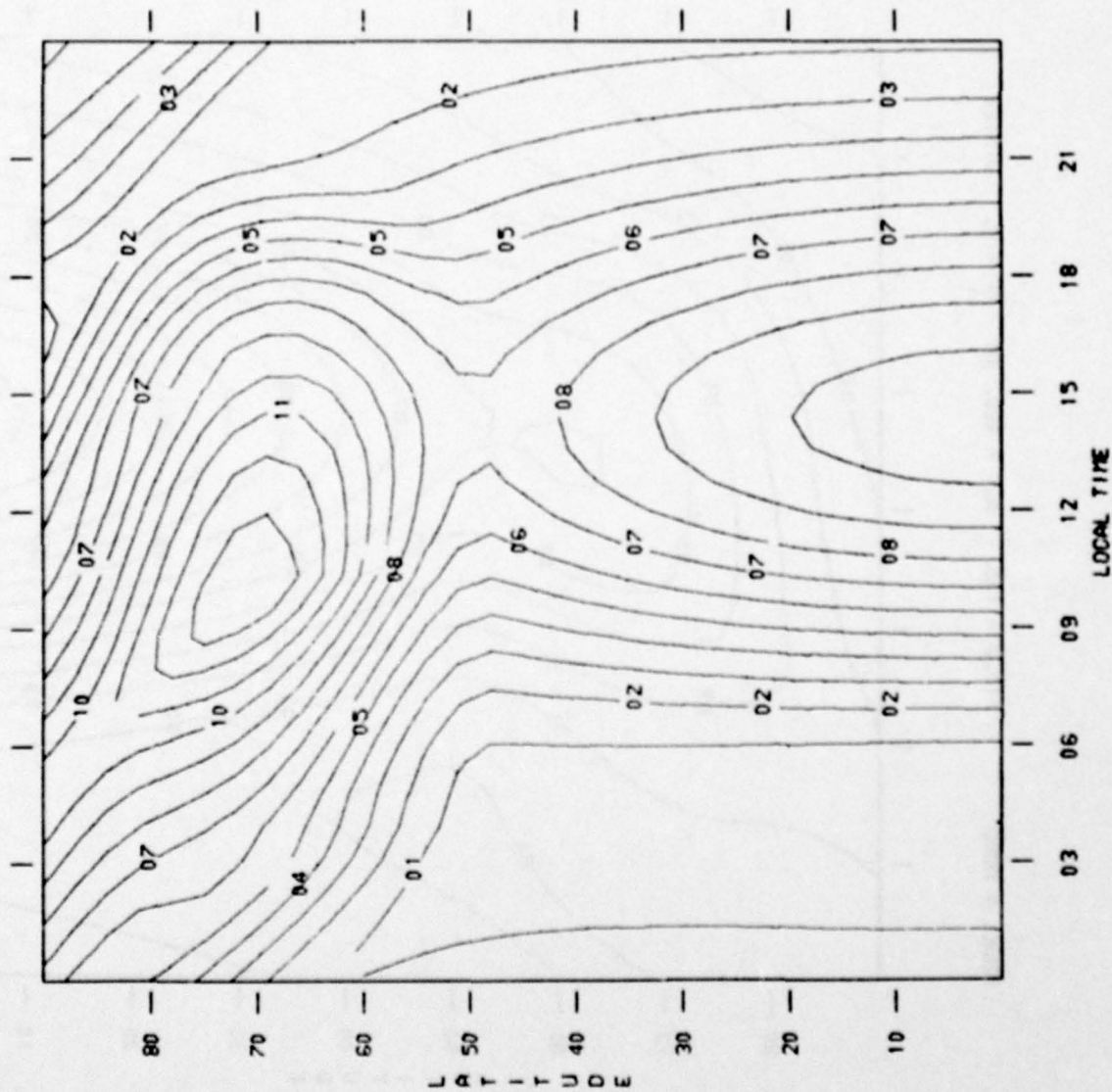
GM/CN003

- 14 = 3.39E-15
- 13 = 3.23E-15
- 12 = 3.07E-15
- 11 = 2.91E-15
- 10 = 2.75E-15
- 09 = 2.59E-15
- 08 = 2.43E-15
- 07 = 2.27E-15
- 06 = 2.10E-15
- 05 = 1.94E-15
- 04 = 1.78E-15
- 03 = 1.62E-15
- 02 = 1.46E-15
- 01 = 1.30E-15
- 00 = 1.14E-15

MODEL = M0AC F10.7 = 125. ALT = 400. KM KP = 2. WINTER



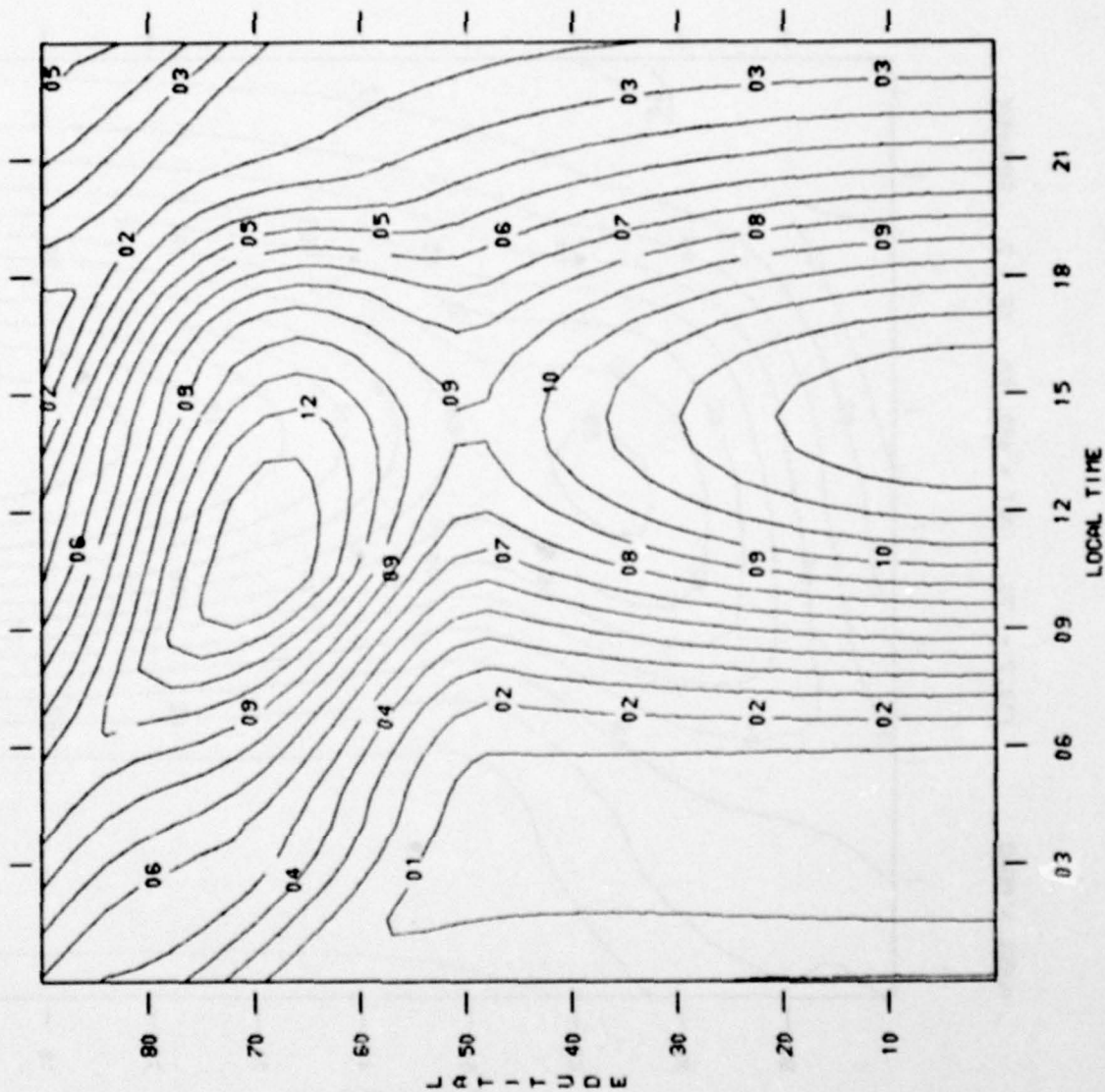
MODEL = MDAC F10.7 = 70. ALT = 140. KM KP = 2. EQUINOX



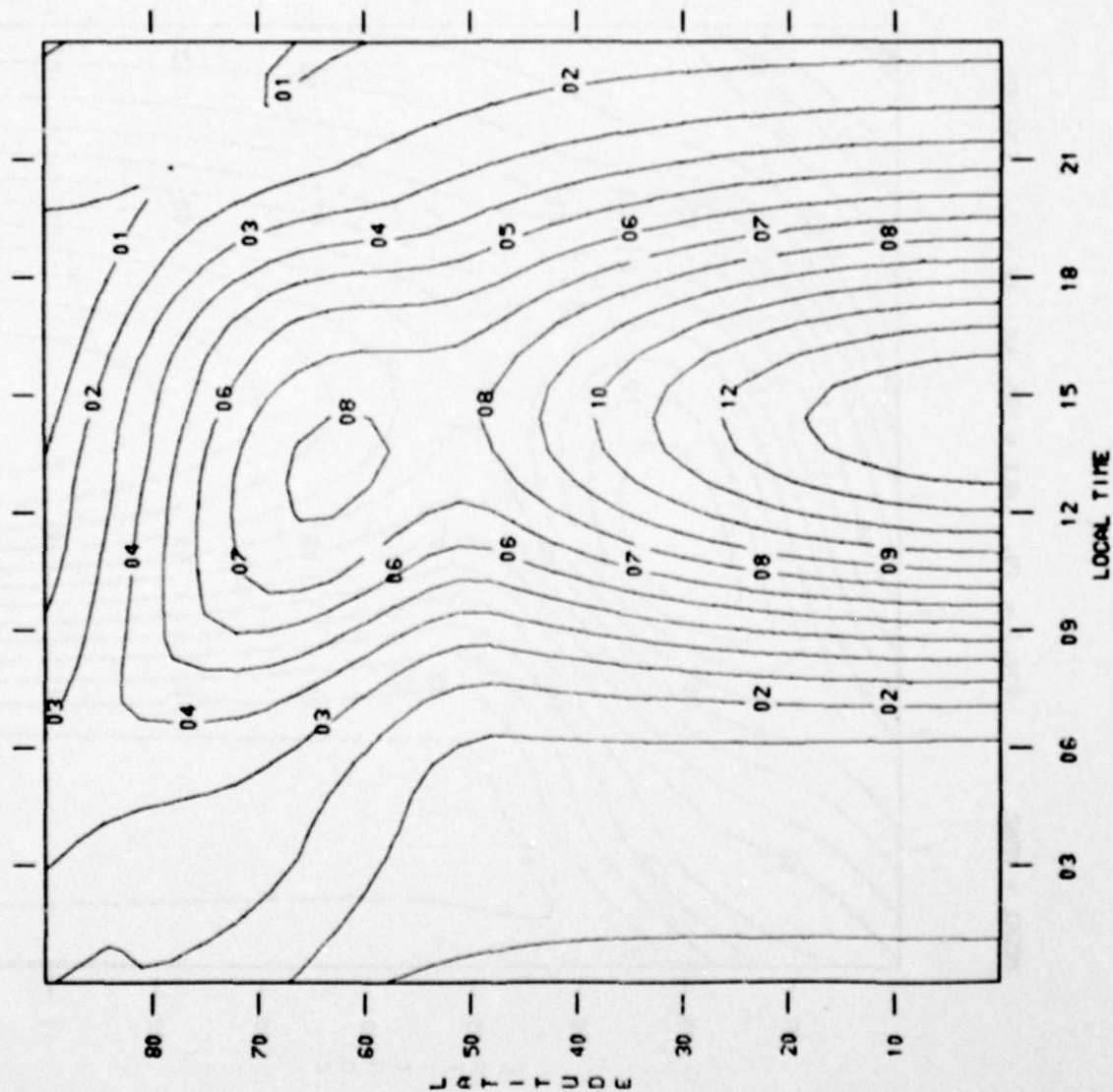
GM/CN=3

- 14 = 4.00E-12
- 13 = 3.95E-12
- 12 = 3.90E-12
- 11 = 3.84E-12
- 10 = 3.79E-12
- 09 = 3.74E-12
- 08 = 3.69E-12
- 07 = 3.63E-12
- 06 = 3.58E-12
- 05 = 3.53E-12
- 04 = 3.48E-12
- 03 = 3.42E-12
- 02 = 3.37E-12
- 01 = 3.32E-12
- 00 = 3.27E-12

MODEL = MDAC F10.7 = 70. ALT = 180. KM KP = 2. EQUINOX



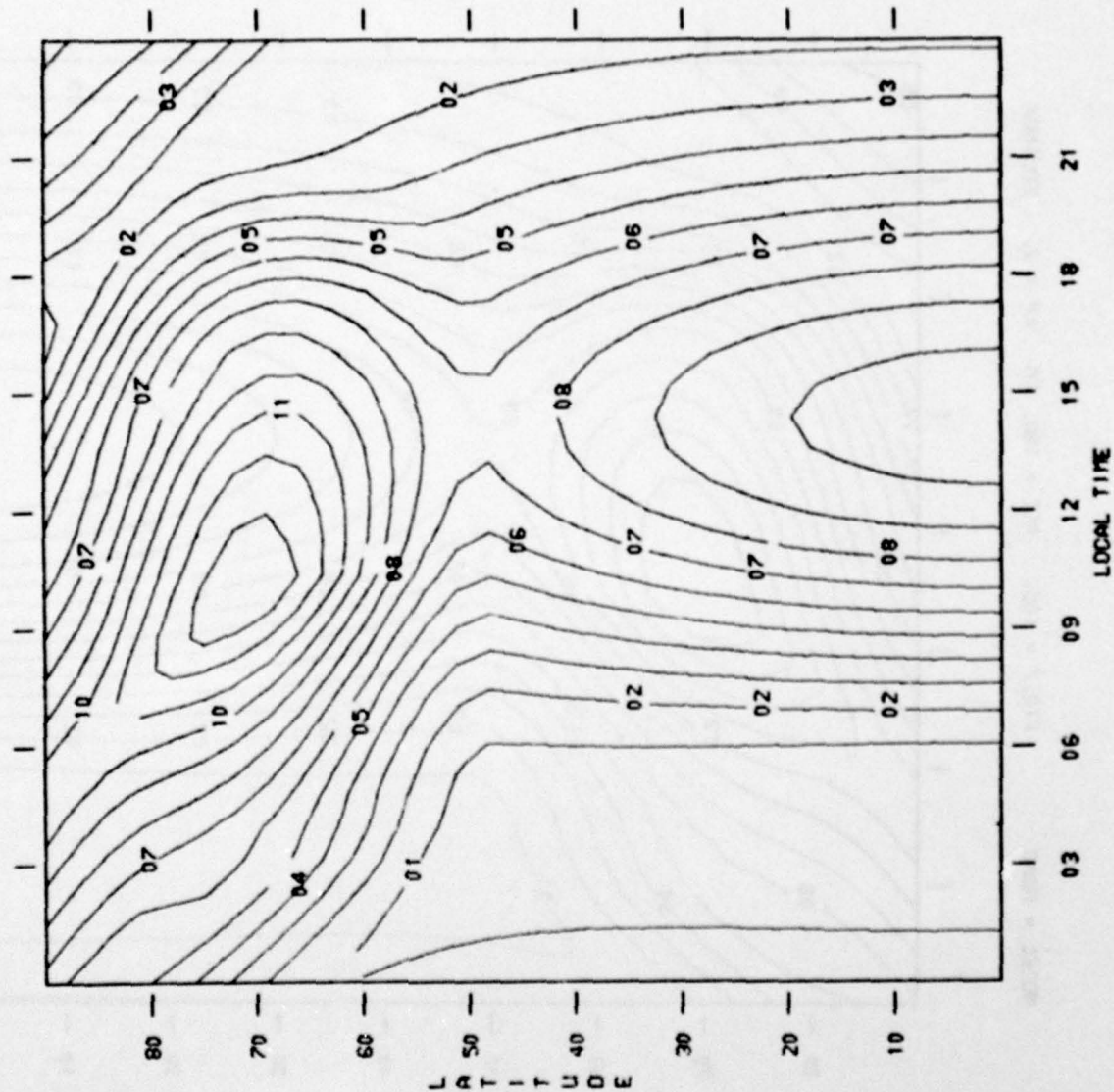
MODEL = MD6C F10.7 = 70. ALT = 400. KM KP = 2. EQUINOX



GM/CN=3

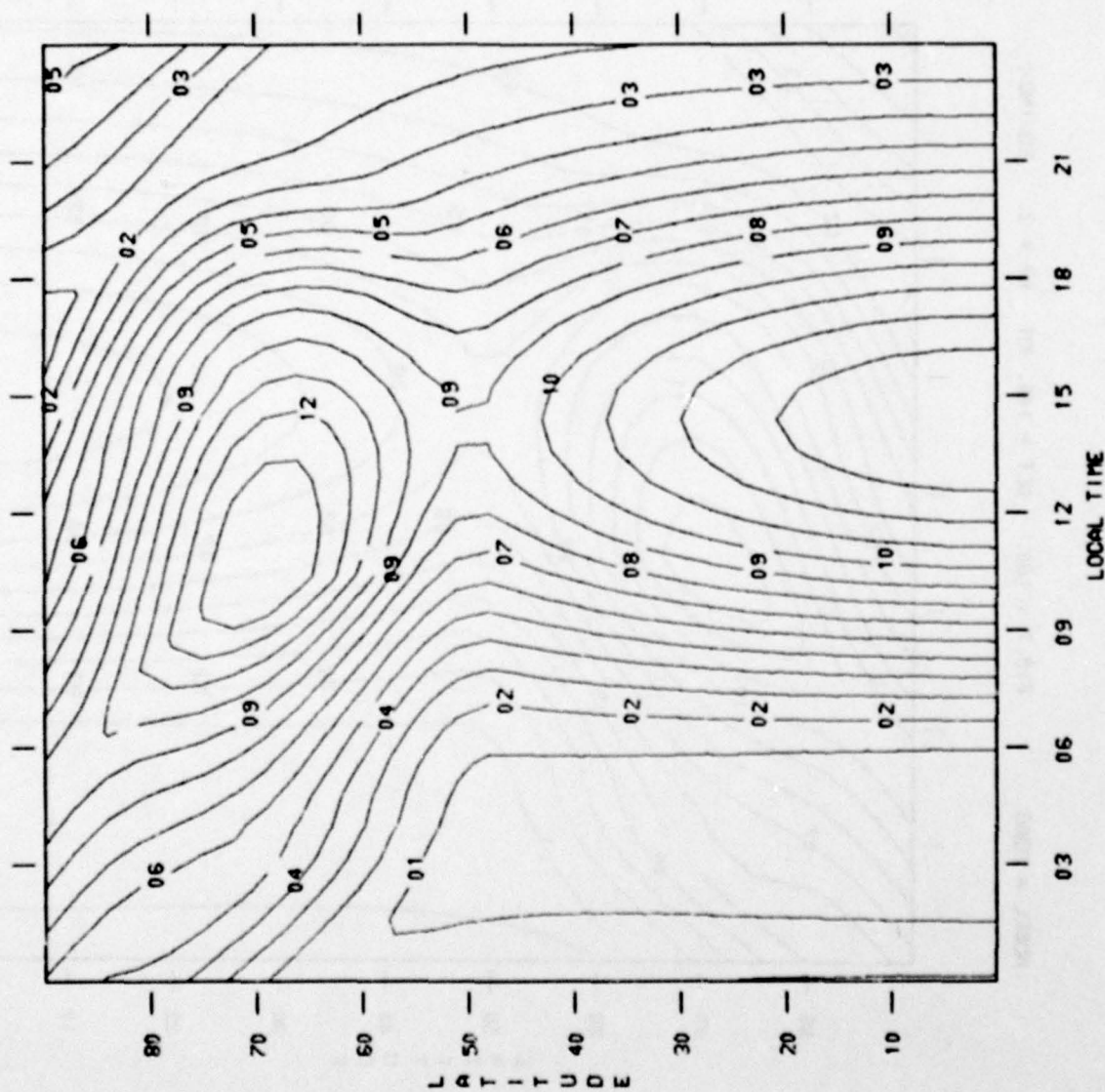
- 14 = 1.66E-15
- 13 = 1.58E-15
- 12 = 1.50E-15
- 11 = 1.42E-15
- 10 = 1.35E-15
- 09 = 1.27E-15
- 08 = 1.19E-15
- 07 = 1.11E-15
- 06 = 1.03E-15
- 05 = 9.56E-16
- 04 = 8.78E-16
- 03 = 8.00E-16
- 02 = 7.22E-16
- 01 = 6.44E-16
- 00 = 5.66E-16

MODEL = MOAC F10.7 = 180. ALT = 140. KM KP = 2. EQUINOX



GM/CN=03
 14 = 5.87E-12
 13 = 5.79E-12
 12 = 5.71E-12
 11 = 5.63E-12
 10 = 5.56E-12
 09 = 5.48E-12
 08 = 5.40E-12
 07 = 5.33E-12
 06 = 5.25E-12
 05 = 5.17E-12
 04 = 5.10E-12
 03 = 5.02E-12
 02 = 4.94E-12
 01 = 4.86E-12
 00 = 4.79E-12

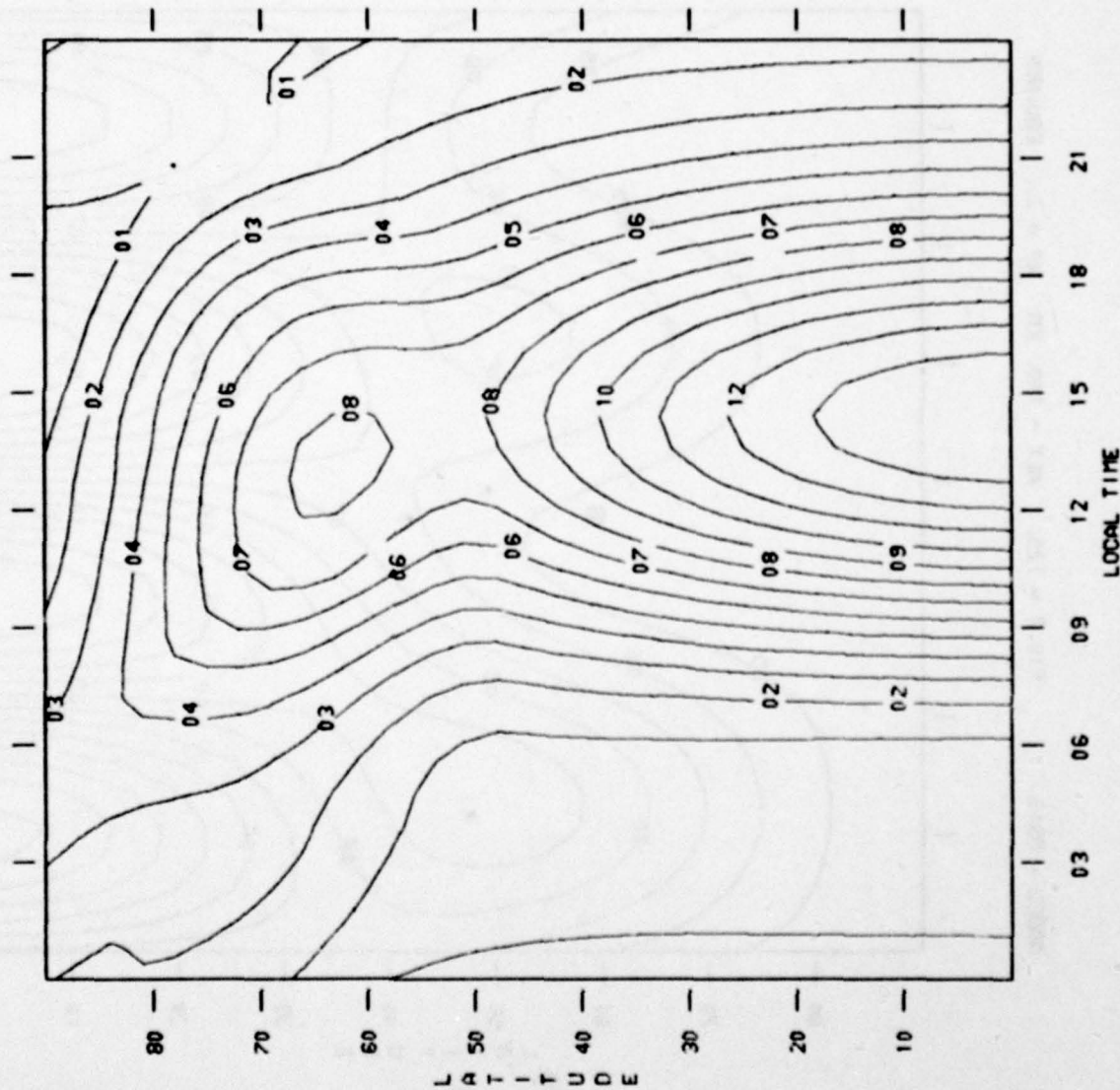
MODEL = MD4C F10.7 = 180. ALT = 180. KM KP = 2. EQUINOX



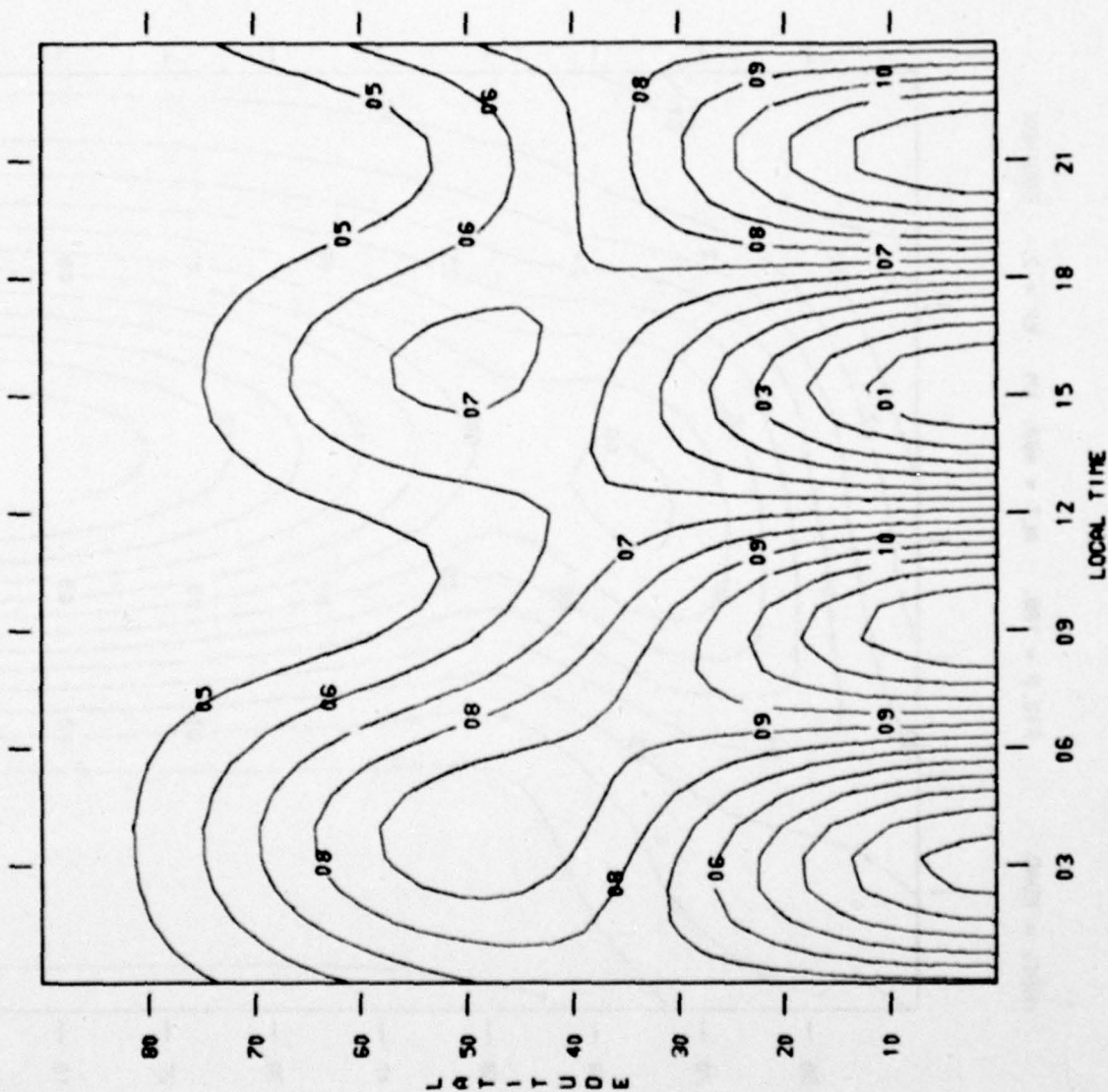
GM/CN003

- 14 = 1.01E-12
- 13 = 9.86E-13
- 12 = 9.62E-13
- 11 = 9.37E-13
- 10 = 9.12E-13
- 09 = 8.88E-13
- 08 = 8.63E-13
- 07 = 8.39E-13
- 06 = 8.14E-13
- 05 = 7.90E-13
- 04 = 7.65E-13
- 03 = 7.41E-13
- 02 = 7.16E-13
- 01 = 6.92E-13
- 00 = 6.67E-13

MODEL = MDAC F10.7 = 180. ALT = 400. KM KP = 2. EQUINOX



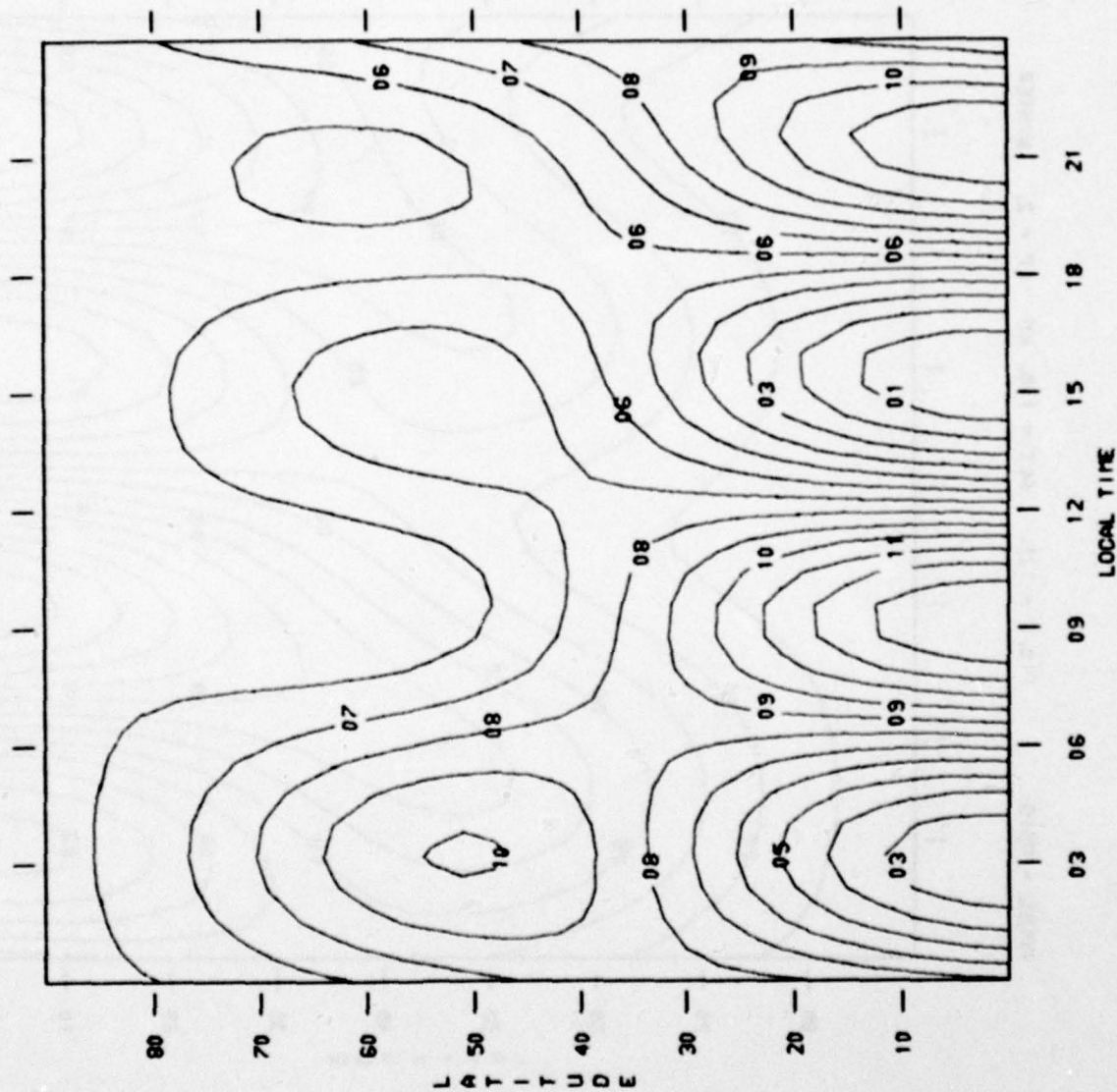
MODEL = MSIS F10.7 = 125. ALT = 140. KM KP = 2. EQUINOX



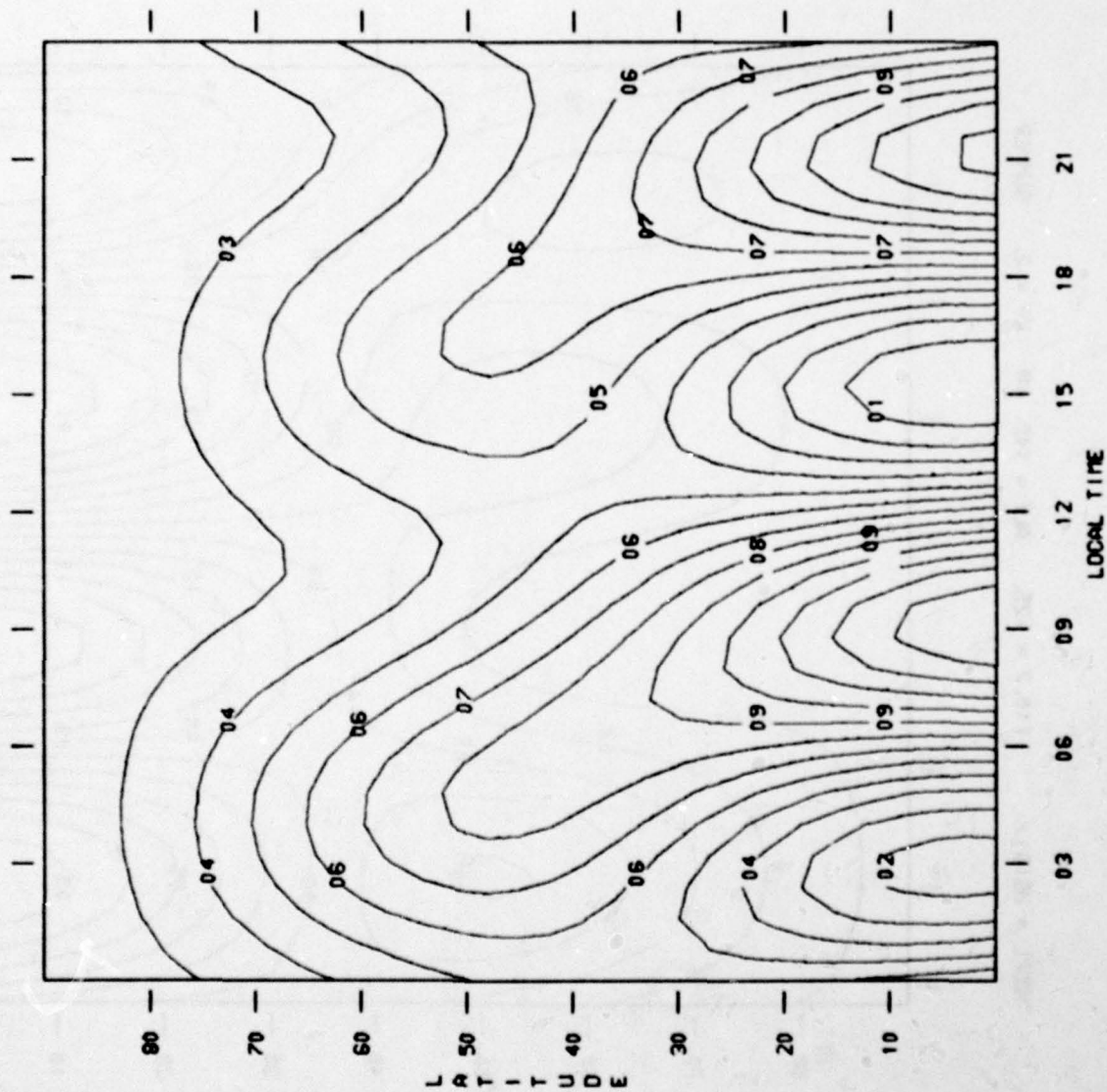
GM/CN=03

- 14 = 3.91E-12
- 13 = 3.84E-12
- 12 = 3.78E-12
- 11 = 3.71E-12
- 10 = 3.65E-12
- 09 = 3.58E-12
- 08 = 3.51E-12
- 07 = 3.45E-12
- 06 = 3.38E-12
- 05 = 3.32E-12
- 04 = 3.25E-12
- 03 = 3.19E-12
- 02 = 3.12E-12
- 01 = 3.06E-12
- 00 = 2.99E-12

MODEL = MSIS F10.7 = 125. ALT = 140. KM KP = 2. SUNSP



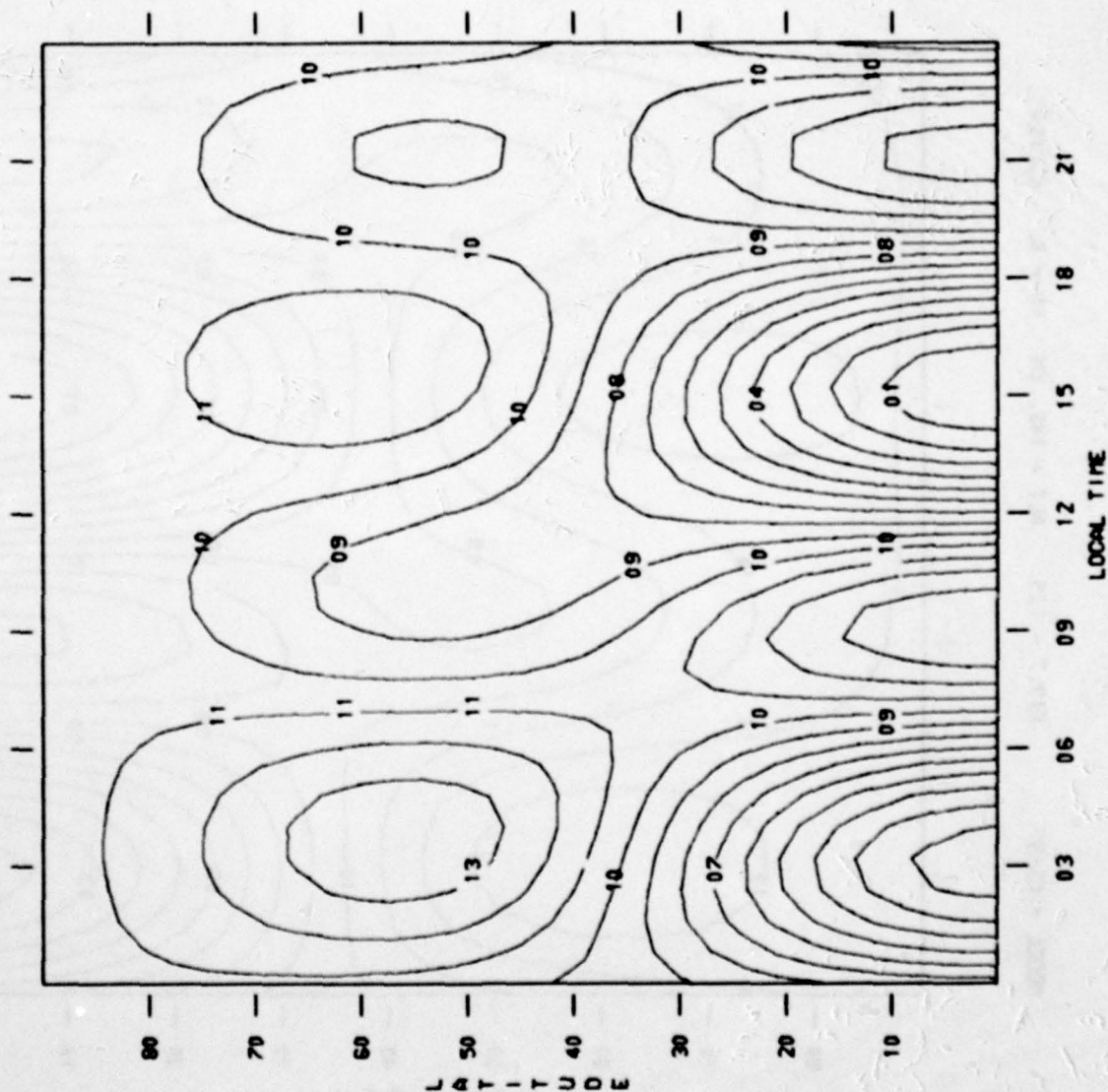
MODEL = MSIS F10.7 = 125. ALT = 140. KM KP = 2. WINTER



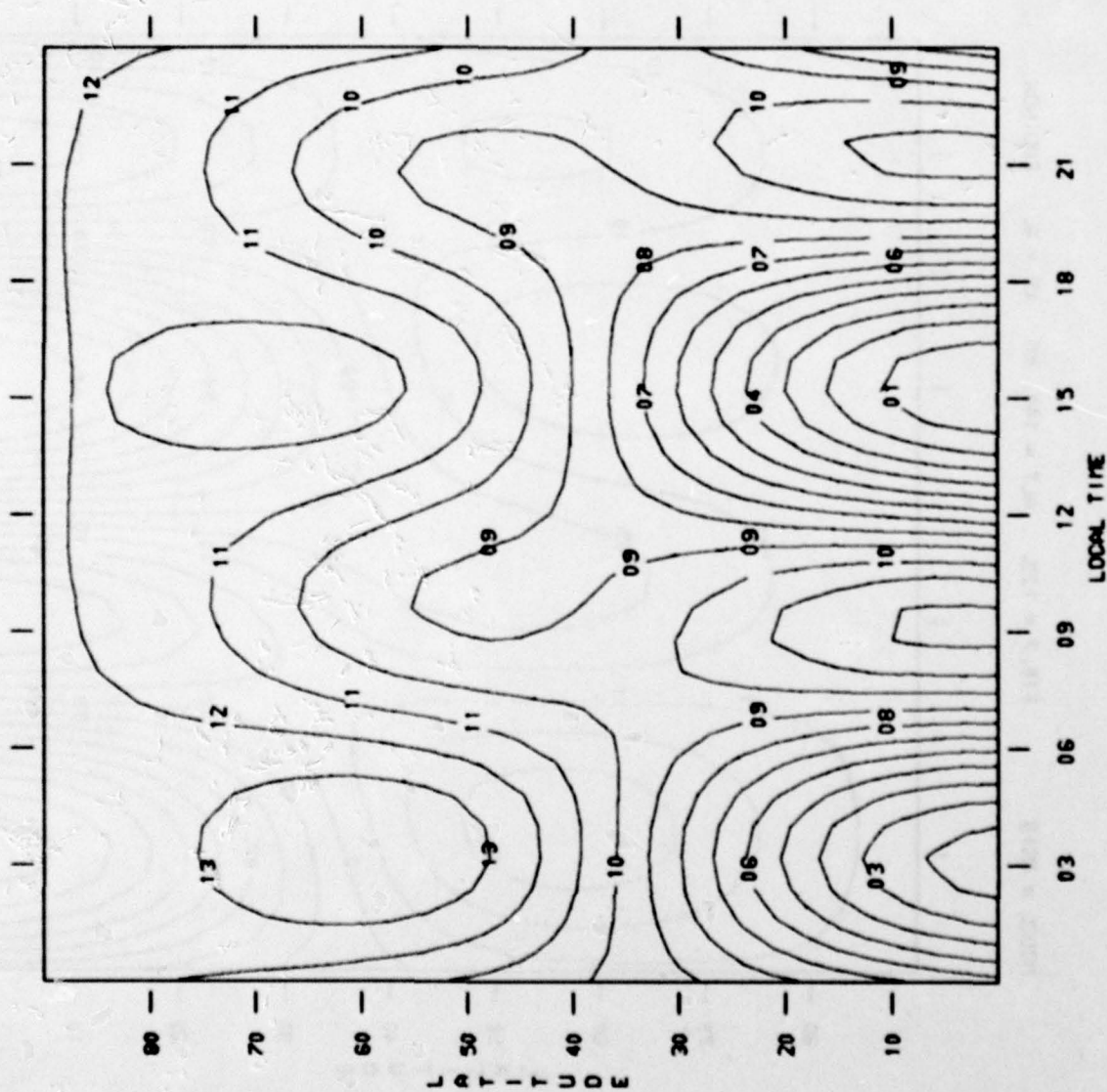
CM/CHW3

- 14 = 3.50E-12
- 13 = 3.44E-12
- 12 = 3.38E-12
- 11 = 3.32E-12
- 10 = 3.26E-12
- 09 = 3.20E-12
- 08 = 3.14E-12
- 07 = 3.08E-12
- 06 = 3.03E-12
- 05 = 2.97E-12
- 04 = 2.91E-12
- 03 = 2.85E-12
- 02 = 2.79E-12
- 01 = 2.73E-12
- 00 = 2.67E-12

MODEL = MSIS F10.7 = 125. ALT = 140. KM KP = 6. EQUINOX



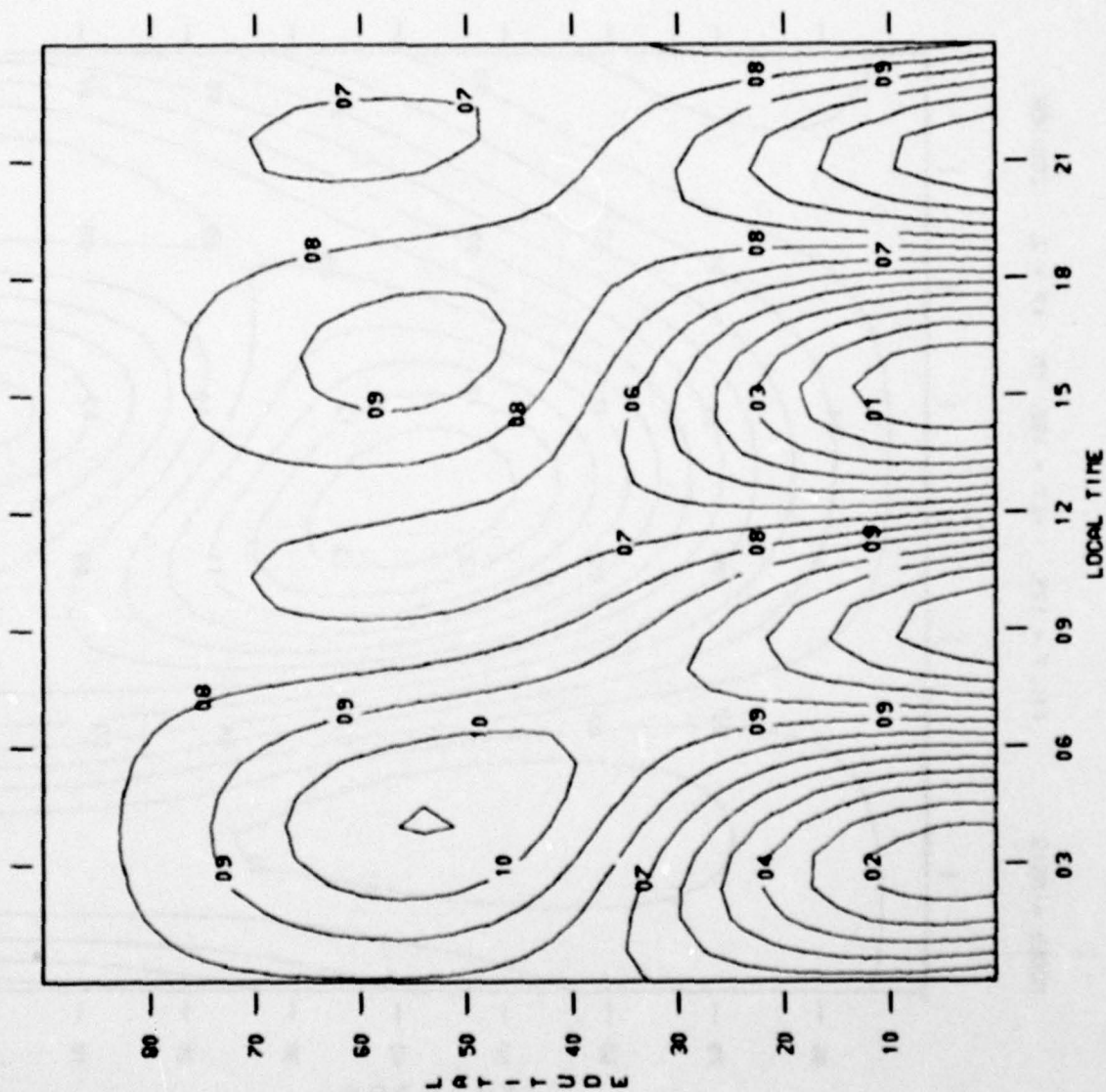
MODEL = MSIS F10.7 = 125. ALT = 140. KM KP = 6. SUMMER



GT/CN03

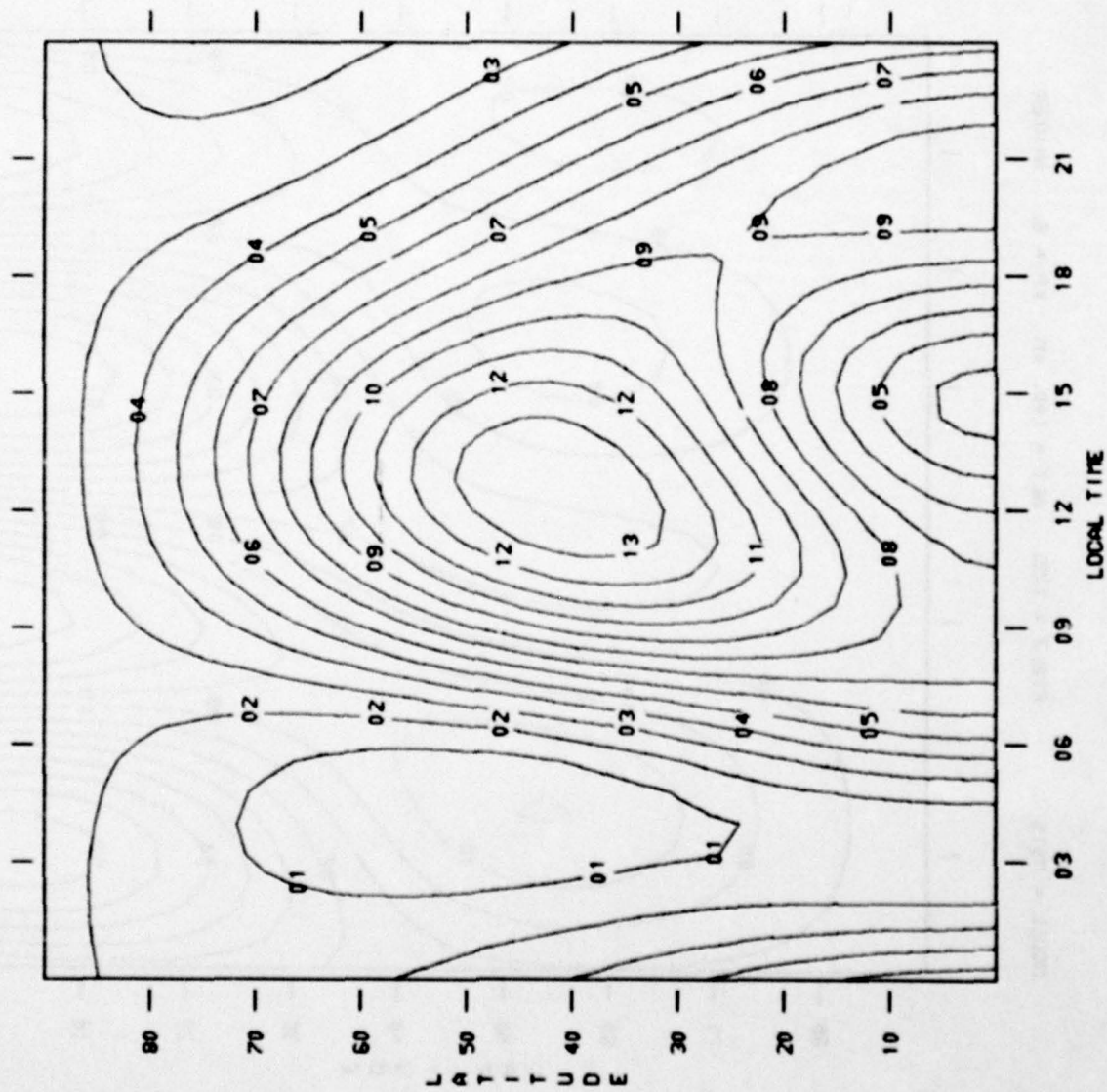
- 14 = 3.90E-12
- 13 = 3.82E-12
- 12 = 3.75E-12
- 11 = 3.68E-12
- 10 = 3.60E-12
- 09 = 3.53E-12
- 08 = 3.45E-12
- 07 = 3.38E-12
- 06 = 3.30E-12
- 05 = 3.23E-12
- 04 = 3.15E-12
- 03 = 3.08E-12
- 02 = 3.01E-12
- 01 = 2.93E-12
- 00 = 2.86E-12

MODEL = MSIS F10.7 = 125. ALT = 140. KM KP = 6. WINTER

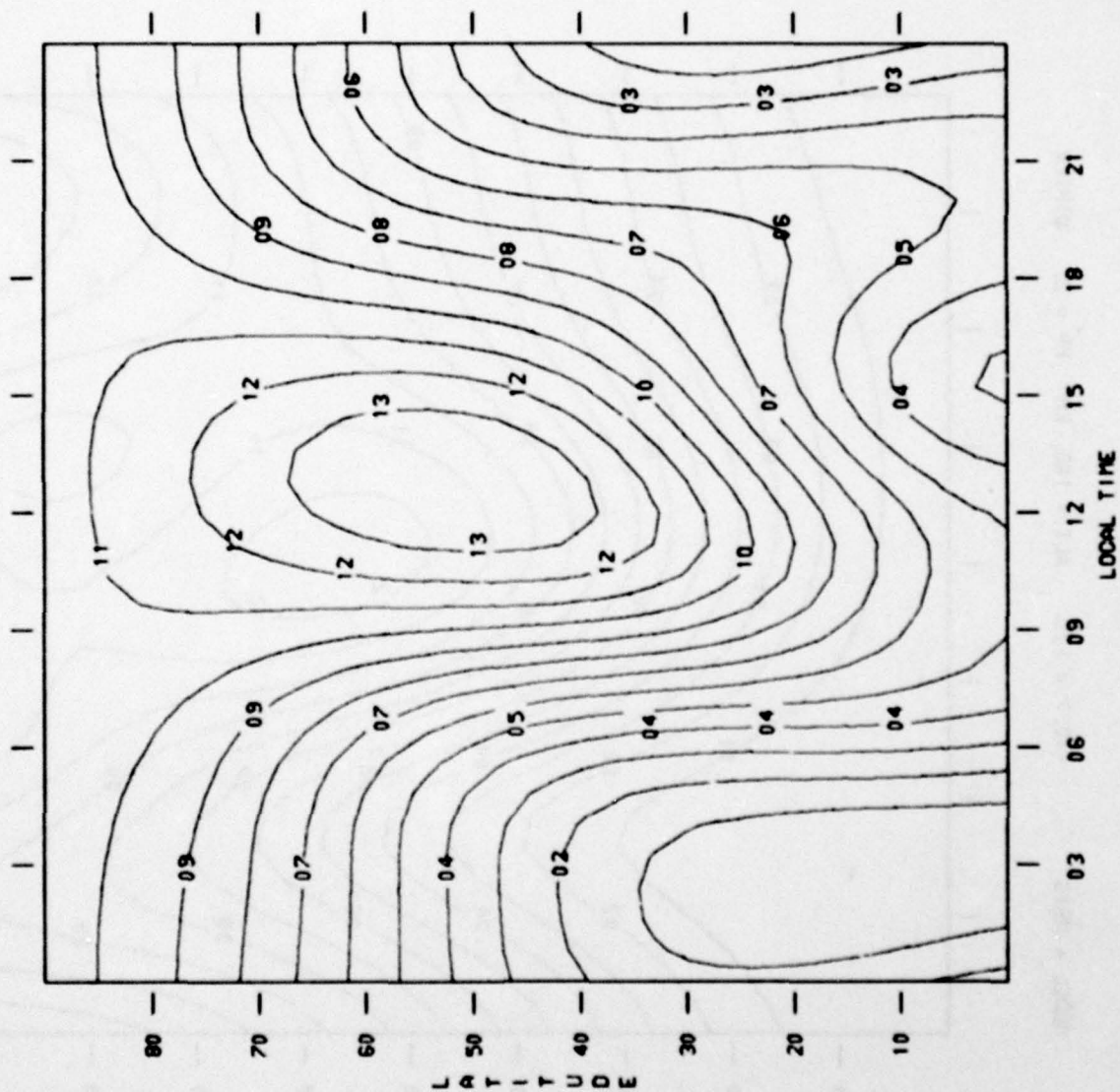


CM/Chaw3
 14 = 3.74E-12
 13 = 3.67E-12
 12 = 3.61E-12
 11 = 3.54E-12
 10 = 3.48E-12
 09 = 3.42E-12
 08 = 3.35E-12
 07 = 3.29E-12
 06 = 3.22E-12
 05 = 3.16E-12
 04 = 3.10E-12
 03 = 3.03E-12
 02 = 2.97E-12
 01 = 2.90E-12
 00 = 2.84E-12

MODEL = MSIS F10.7 = 125. ALT = 180. KM KP = 2. EQUINOX



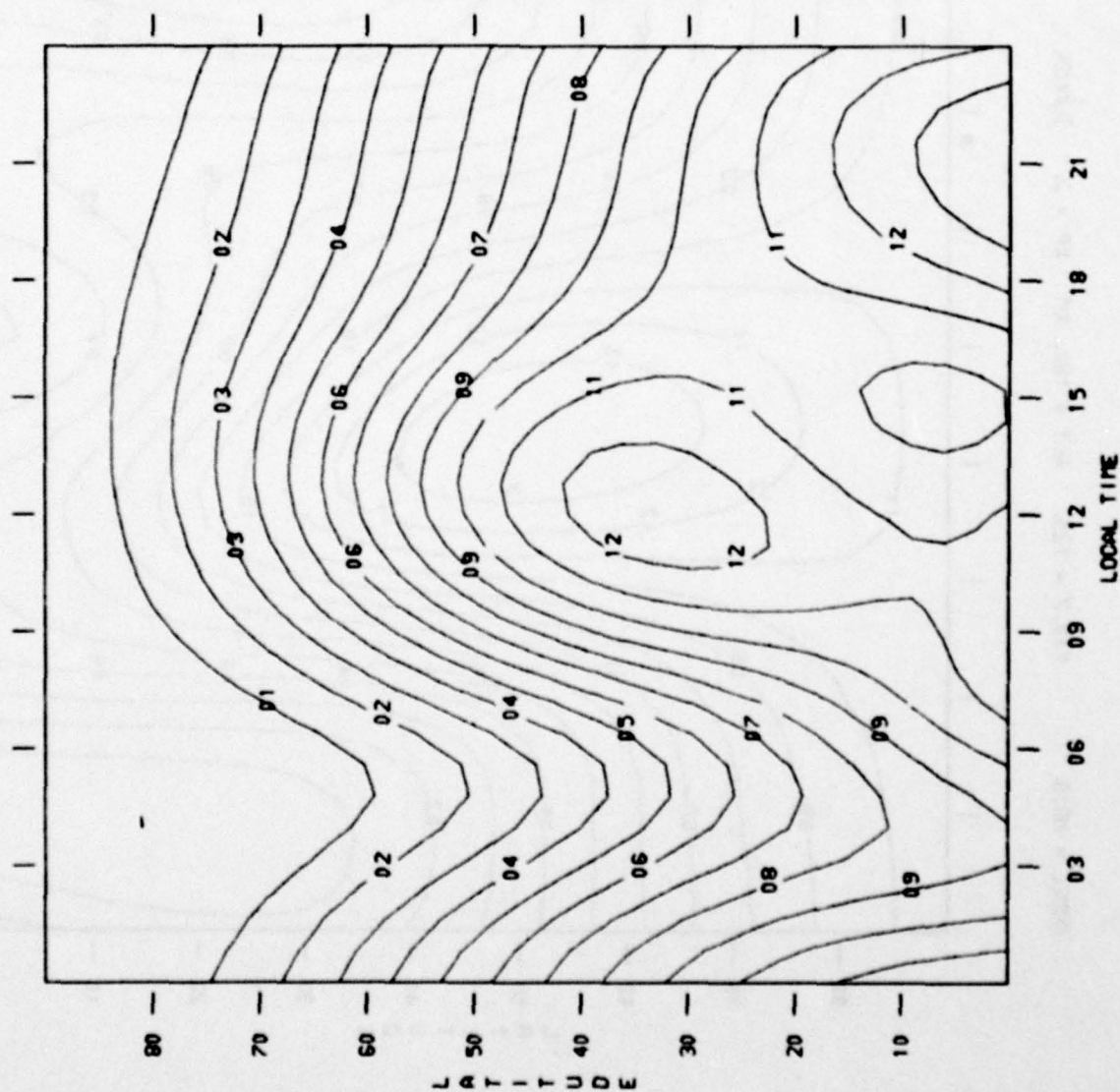
MODEL = MSIS F10.7 = 125. ALT = 180. KM KP = 2. SUMMER



GM/CN=3

- 14 = 5.43E-13
- 13 = 5.37E-13
- 12 = 5.31E-13
- 11 = 5.25E-13
- 10 = 5.18E-13
- 09 = 5.12E-13
- 08 = 5.06E-13
- 07 = 5.00E-13
- 06 = 4.93E-13
- 05 = 4.87E-13
- 04 = 4.81E-13
- 03 = 4.75E-13
- 02 = 4.68E-13
- 01 = 4.62E-13
- 00 = 4.56E-13

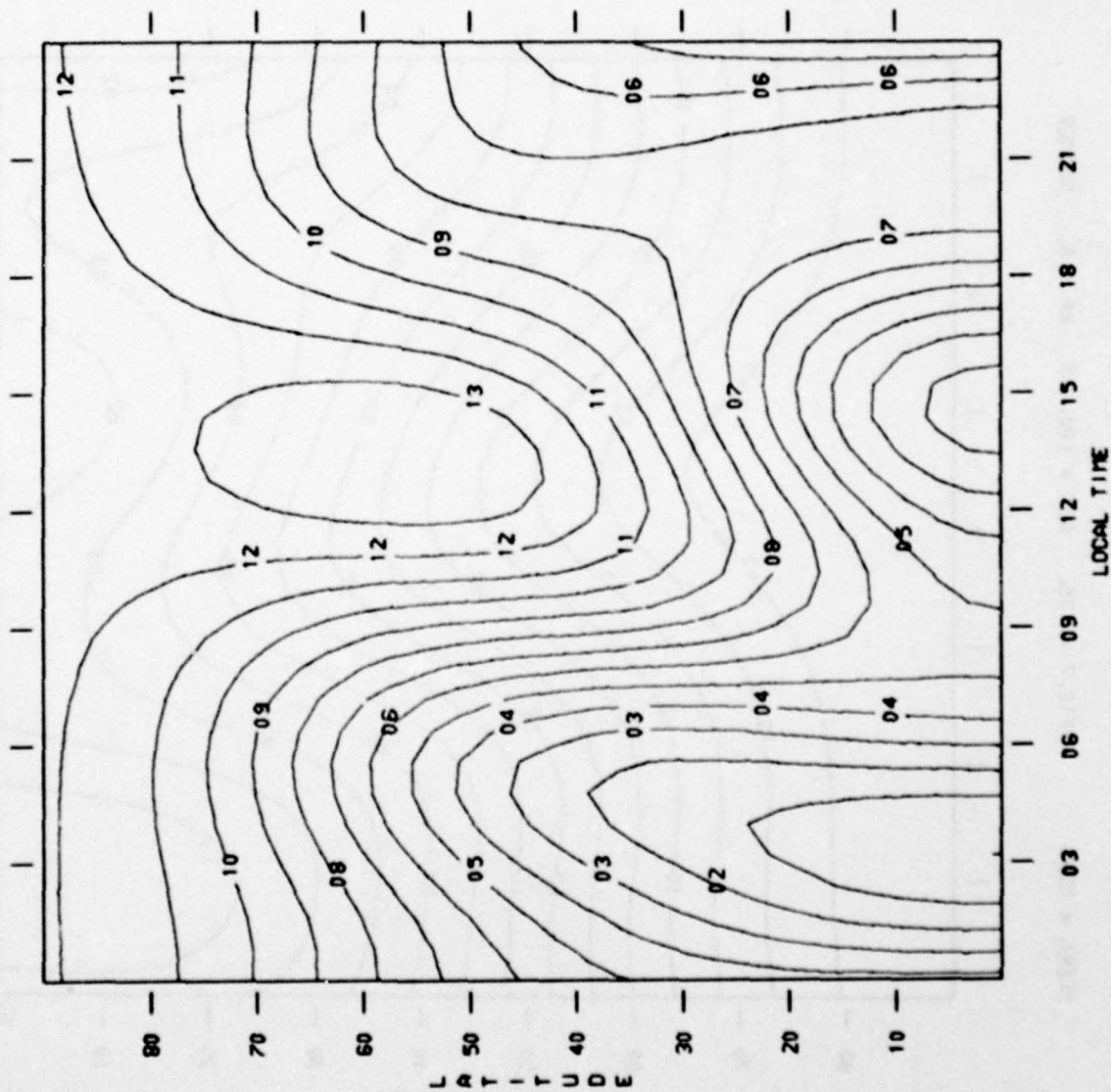
MODEL = MSIS F10.7 = 125. ALT = 180. KM KP = 2. WINTER



GM/CN03

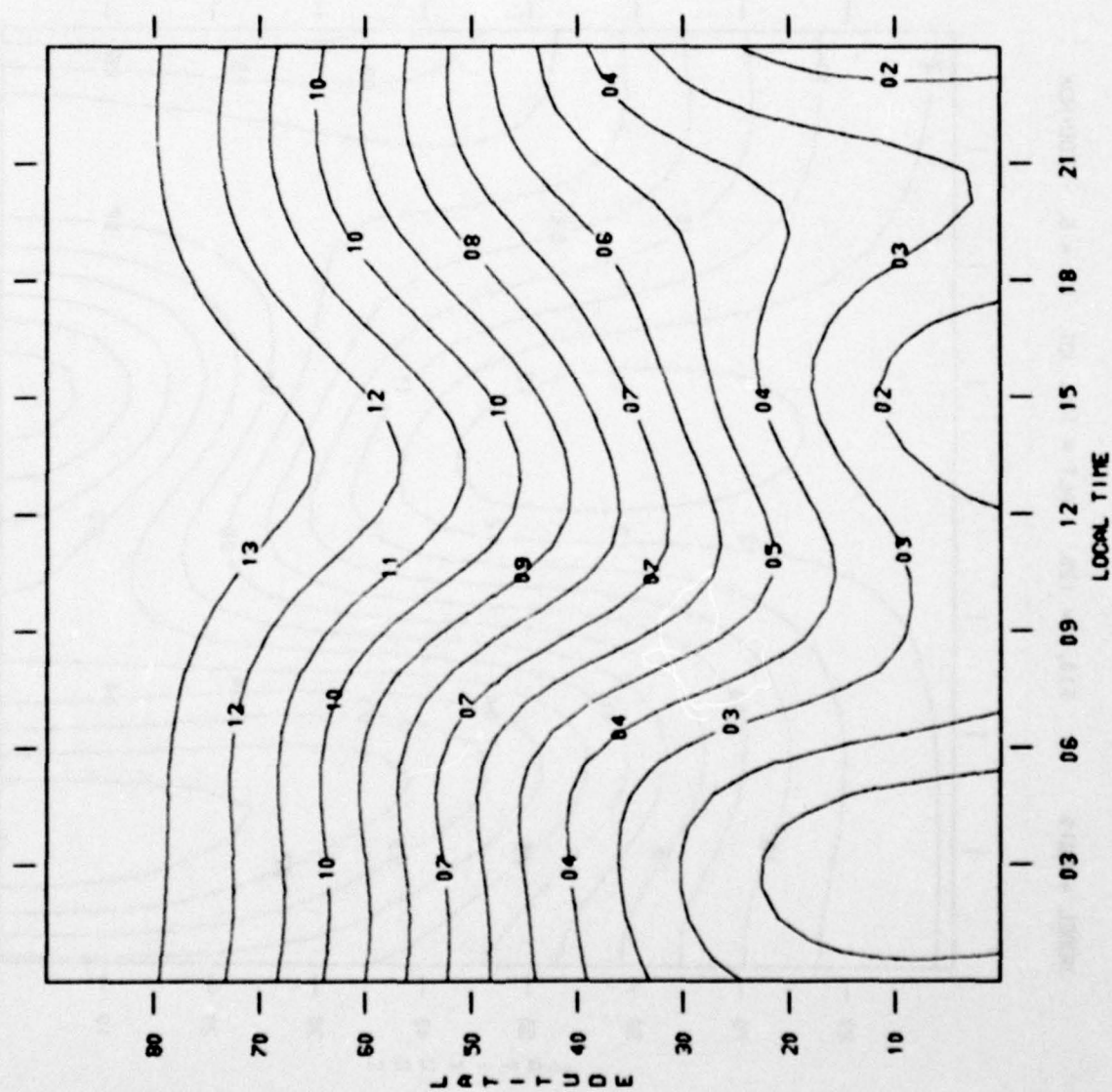
14 = 5.11E-13
 13 = 5.04E-13
 12 = 4.97E-13
 11 = 4.90E-13
 10 = 4.83E-13
 09 = 4.76E-13
 08 = 4.69E-13
 07 = 4.62E-13
 06 = 4.54E-13
 05 = 4.47E-13
 04 = 4.40E-13
 03 = 4.33E-13
 02 = 4.26E-13
 01 = 4.19E-13
 00 = 4.12E-13

MODEL = MSIS F10.7 = 125. ALT = 180. KM KP = 6. EQUINOX



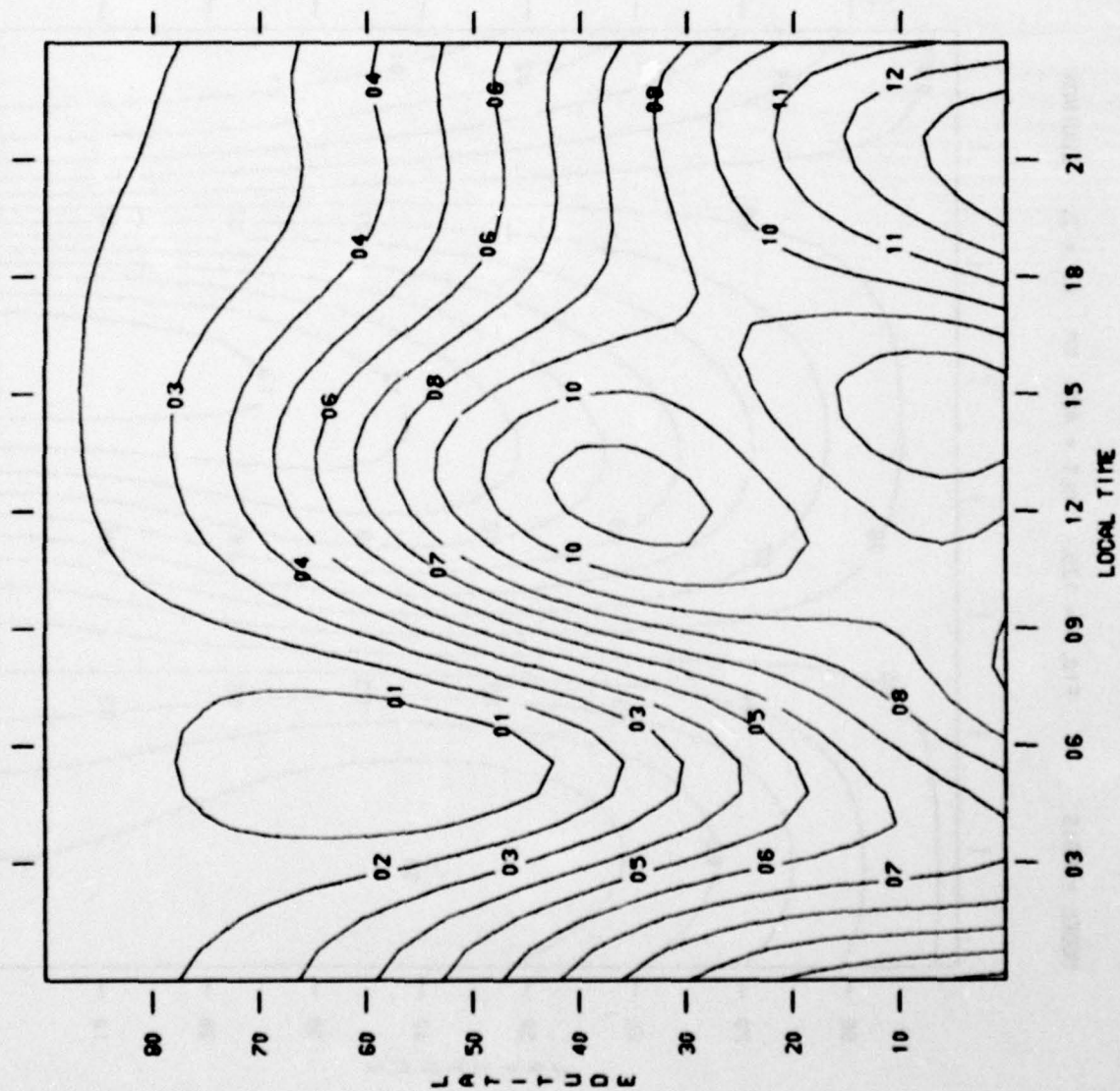
CM/CHW3
14 = 7.10E-13
13 = 7.04E-13
12 = 6.97E-13
11 = 6.90E-13
10 = 6.83E-13
09 = 6.77E-13
08 = 6.70E-13
07 = 6.63E-13
06 = 6.56E-13
05 = 6.49E-13
04 = 6.43E-13
03 = 6.36E-13
02 = 6.29E-13
01 = 6.22E-13
00 = 6.16E-13

MODEL = MSIS F10.7 = 125, ALT = 180. KM KP = 6. SUMMER



GM/CN=3
 14 = 7.05E-13
 13 = 6.92E-13
 12 = 6.78E-13
 11 = 6.65E-13
 10 = 6.52E-13
 09 = 6.39E-13
 08 = 6.25E-13
 07 = 6.12E-13
 06 = 5.99E-13
 05 = 5.85E-13
 04 = 5.72E-13
 03 = 5.59E-13
 02 = 5.45E-13
 01 = 5.32E-13
 00 = 5.19E-13

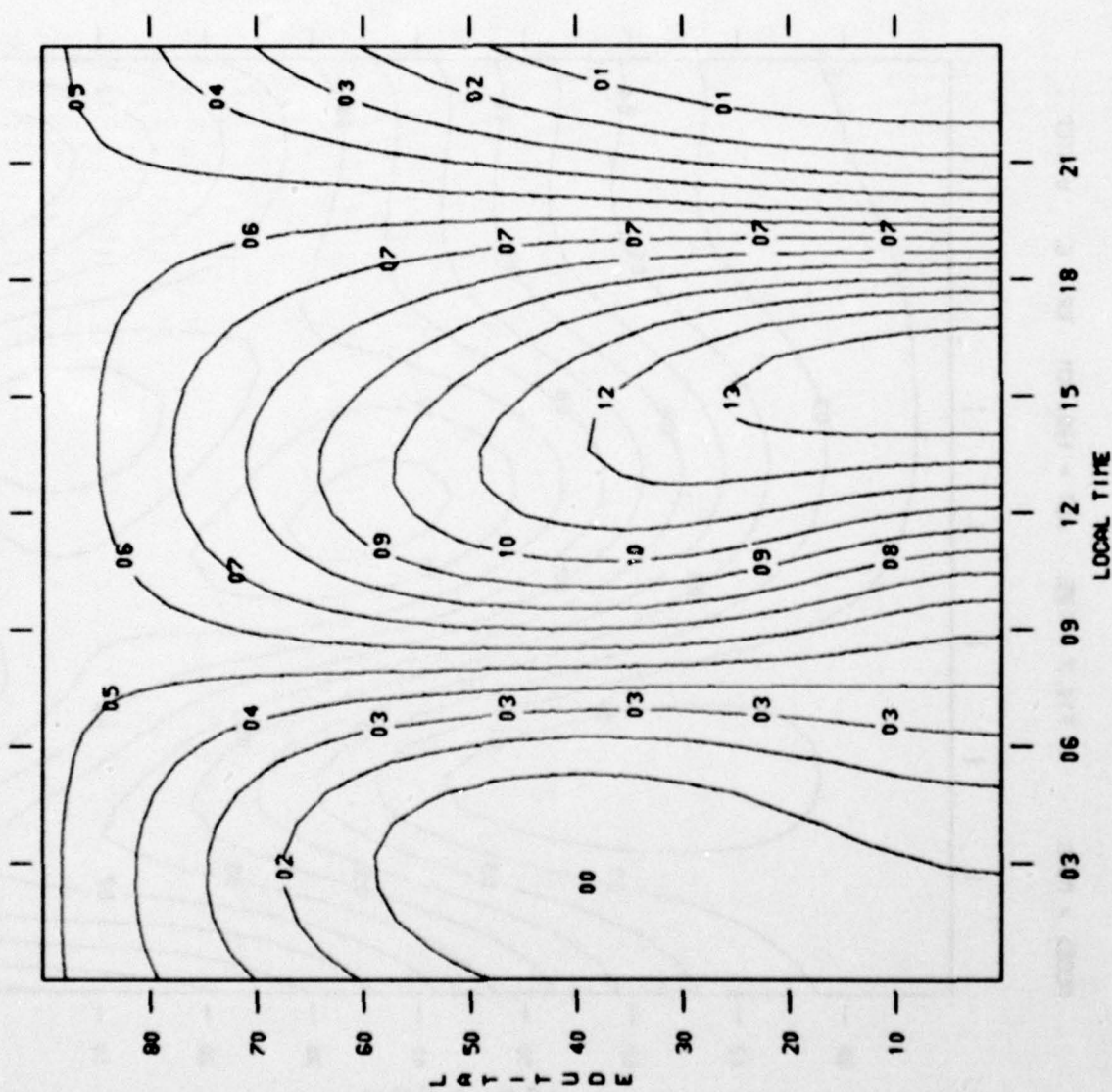
MODEL = MSIS F10.7 = 125. ALT = 180. KM KP = 6. WINTER



CH/CHEW3

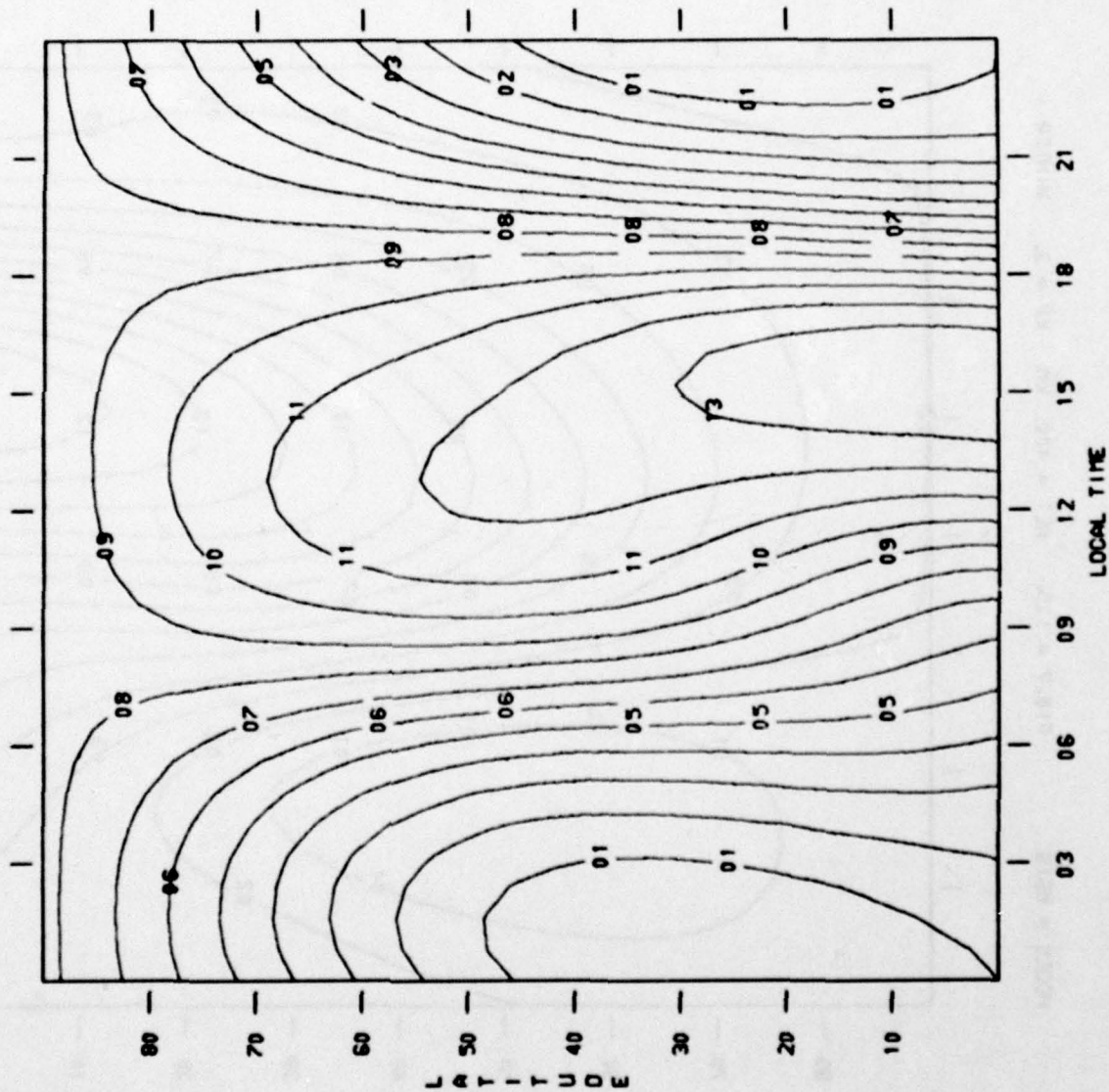
14 = 5.90E-13
 13 = 5.84E-13
 12 = 5.77E-13
 11 = 5.71E-13
 10 = 5.65E-13
 09 = 5.58E-13
 08 = 5.52E-13
 07 = 5.45E-13
 06 = 5.39E-13
 05 = 5.33E-13
 04 = 5.26E-13
 03 = 5.20E-13
 02 = 5.14E-13
 01 = 5.07E-13
 00 = 5.01E-13

MODEL = MSIS F10.7 = 125. ALT = 400. KM KP = 2. EQUINOX



GN/CN/3
14 = 5.53E-15
13 = 5.27E-15
12 = 5.02E-15
11 = 4.77E-15
10 = 4.52E-15
09 = 4.27E-15
08 = 4.02E-15
07 = 3.76E-15
06 = 3.51E-15
05 = 3.26E-15
04 = 3.01E-15
03 = 2.76E-15
02 = 2.50E-15
01 = 2.25E-15
00 = 2.00E-15

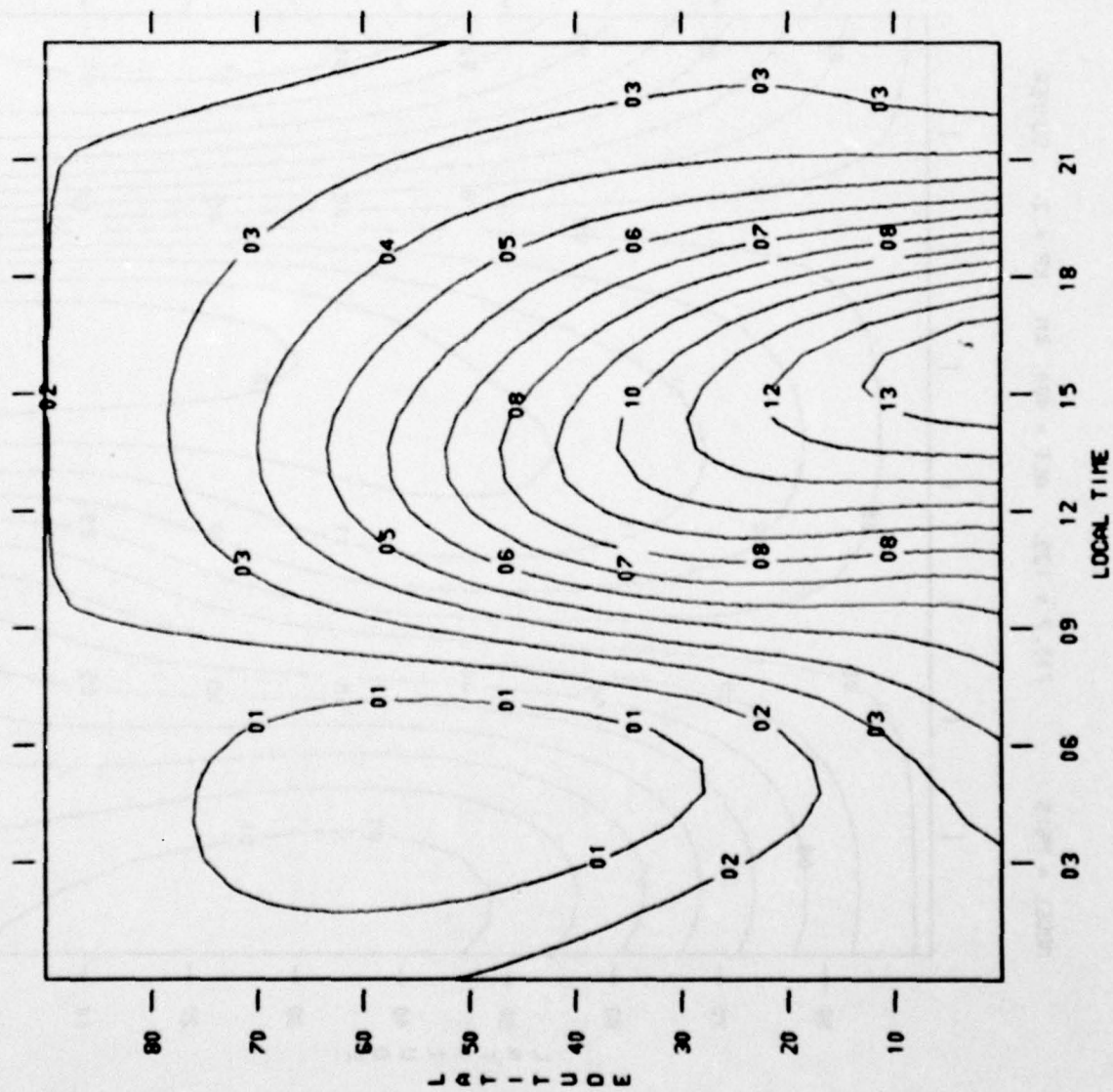
MODEL = MSIS F10.7 = 125. ALT = 400. KM KP = 2. SUMMER



CH/CHmax3

- 14 = 4.25E-15
- 13 = 4.03E-15
- 12 = 3.82E-15
- 11 = 3.60E-15
- 10 = 3.38E-15
- 09 = 3.16E-15
- 08 = 2.95E-15
- 07 = 2.73E-15
- 06 = 2.51E-15
- 05 = 2.29E-15
- 04 = 2.08E-15
- 03 = 1.86E-15
- 02 = 1.64E-15
- 01 = 1.42E-15
- 00 = 1.21E-15

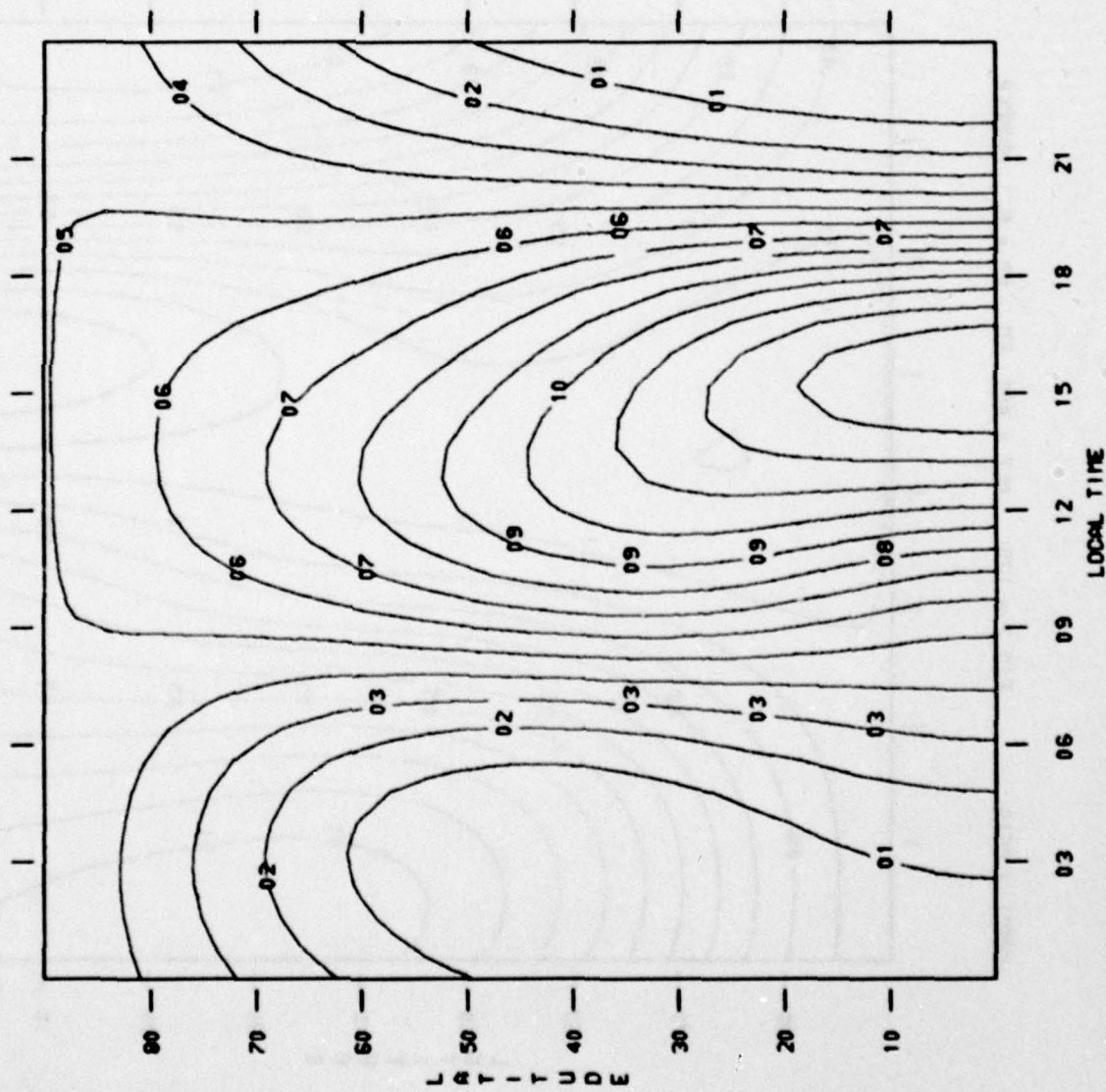
MODEL = MSIS F10.7 = 125. ALT = 400. KM KP = 2. WINTER



CM/Chow3

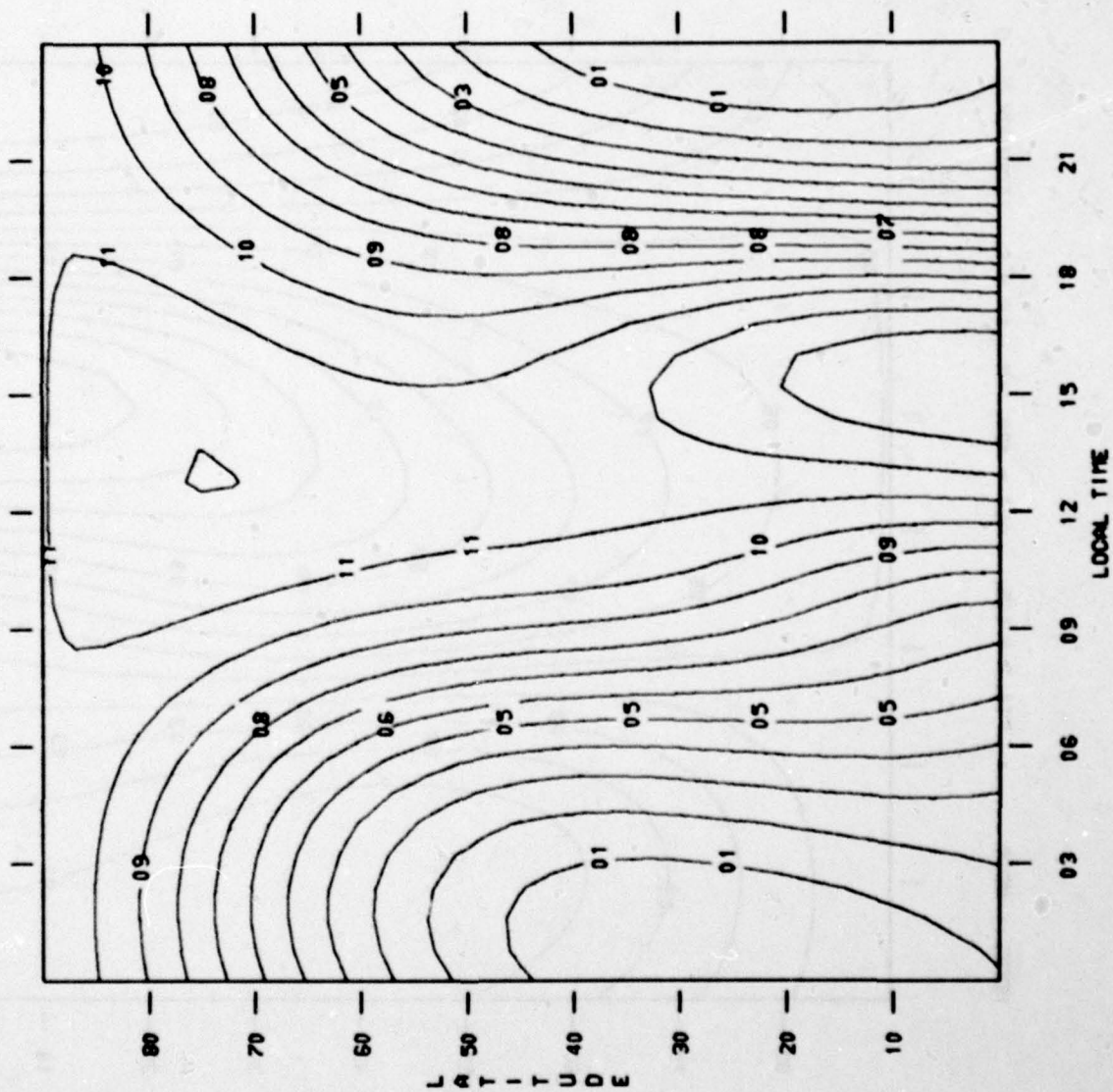
- 14 = 4.96E-15
- 13 = 4.70E-15
- 12 = 4.45E-15
- 11 = 4.19E-15
- 10 = 3.94E-15
- 09 = 3.68E-15
- 08 = 3.43E-15
- 07 = 3.17E-15
- 06 = 2.92E-15
- 05 = 2.66E-15
- 04 = 2.41E-15
- 03 = 2.15E-15
- 02 = 1.90E-15
- 01 = 1.64E-15
- 00 = 1.39E-15

MODEL = MSIS F10.7 = 125. ALT = 400. KM KP = 6. EQUINOX

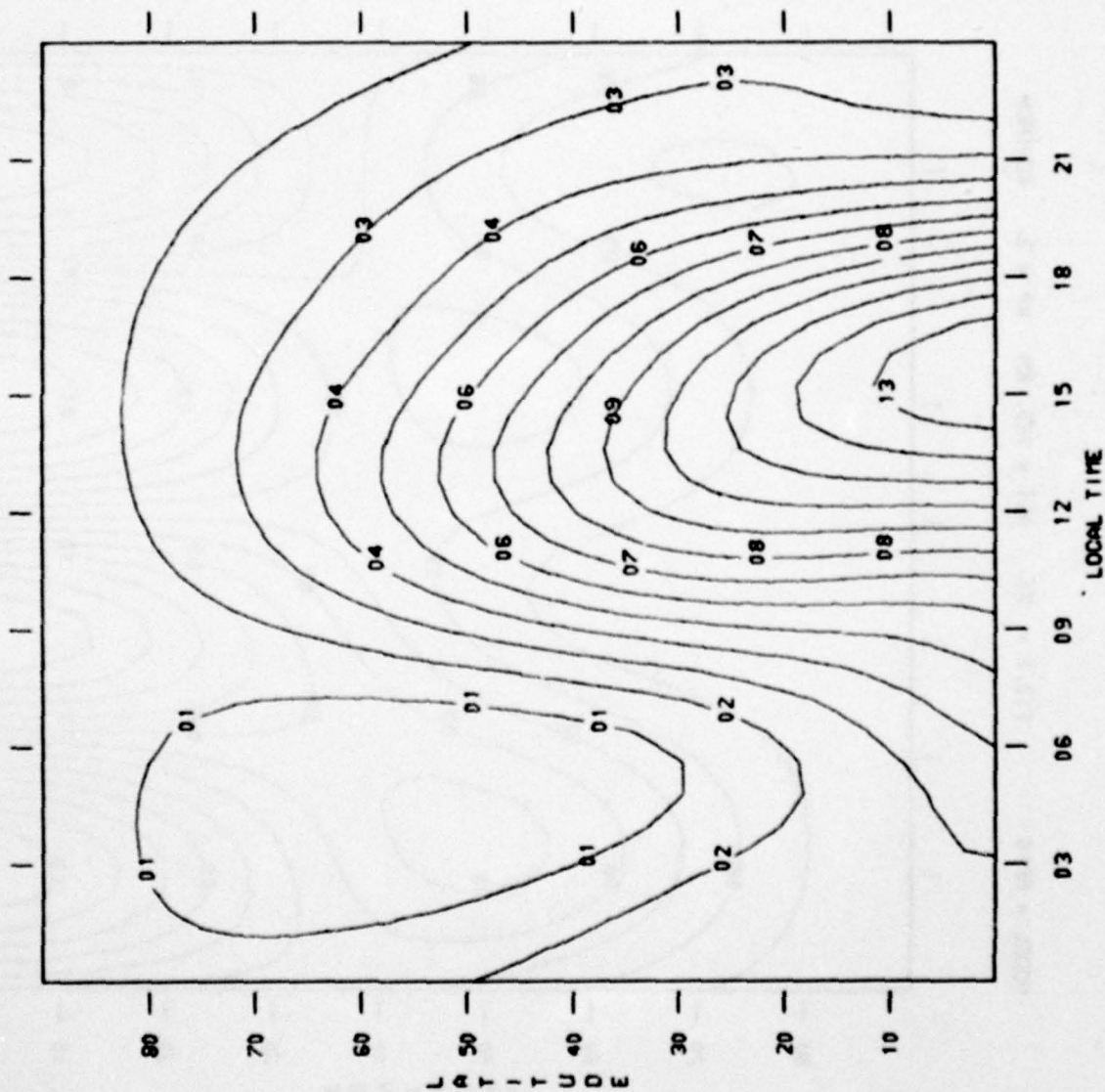


CM/CN=3
 14 = 7.87E-15
 13 = 7.53E-15
 12 = 7.18E-15
 11 = 6.84E-15
 10 = 6.49E-15
 09 = 6.15E-15
 08 = 5.81E-15
 07 = 5.46E-15
 06 = 5.12E-15
 05 = 4.77E-15
 04 = 4.43E-15
 03 = 4.08E-15
 02 = 3.74E-15
 01 = 3.39E-15
 00 = 3.05E-15

MODEL = MSIS F10.7 = 125. ALT = 400. KM KP = 6. SUMMER



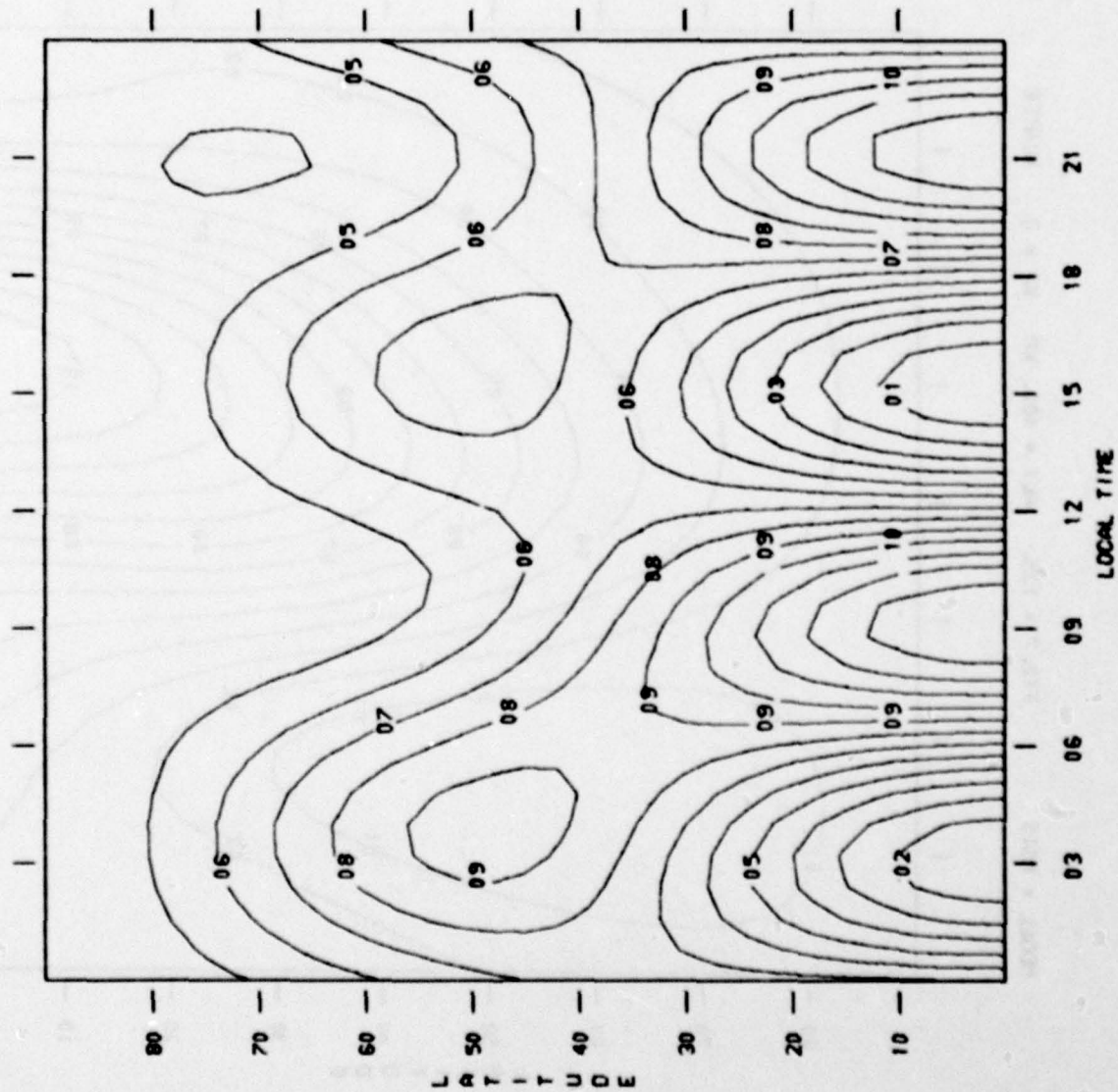
MODEL = MSIS F10.7 = 125. ALT = 400. KM KP = 6. WINTER



CM/CN=3

14 =	7.05E-15
13 =	6.70E-15
12 =	6.36E-15
11 =	6.01E-15
10 =	5.66E-15
09 =	5.31E-15
08 =	4.97E-15
07 =	4.62E-15
06 =	4.27E-15
05 =	3.93E-15
04 =	3.58E-15
03 =	3.23E-15
02 =	2.89E-15
01 =	2.54E-15
00 =	2.19E-15

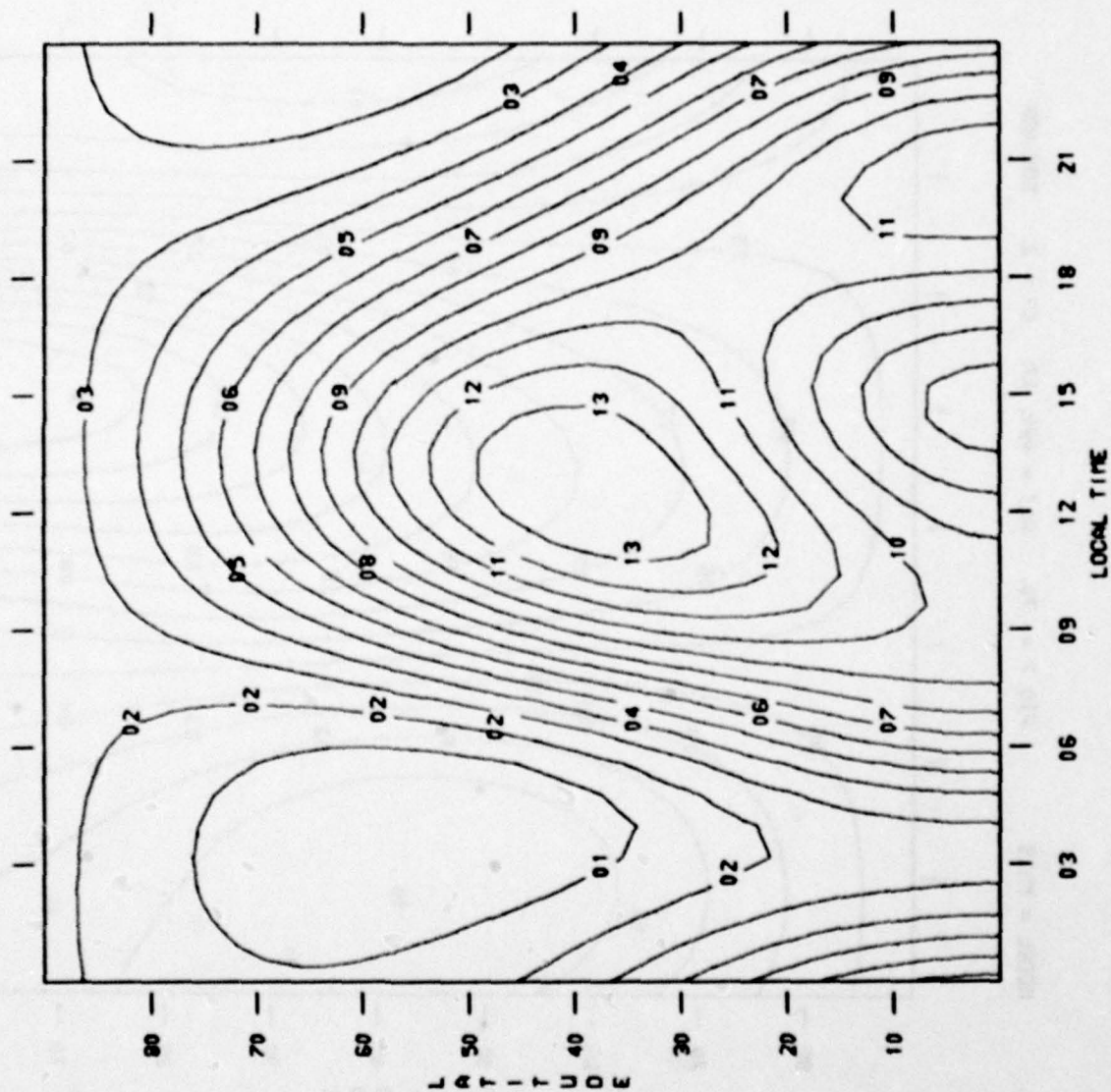
MODEL = MSIS F10.7 = 70. ALT = 140. KM KP = 2. EQUINOX



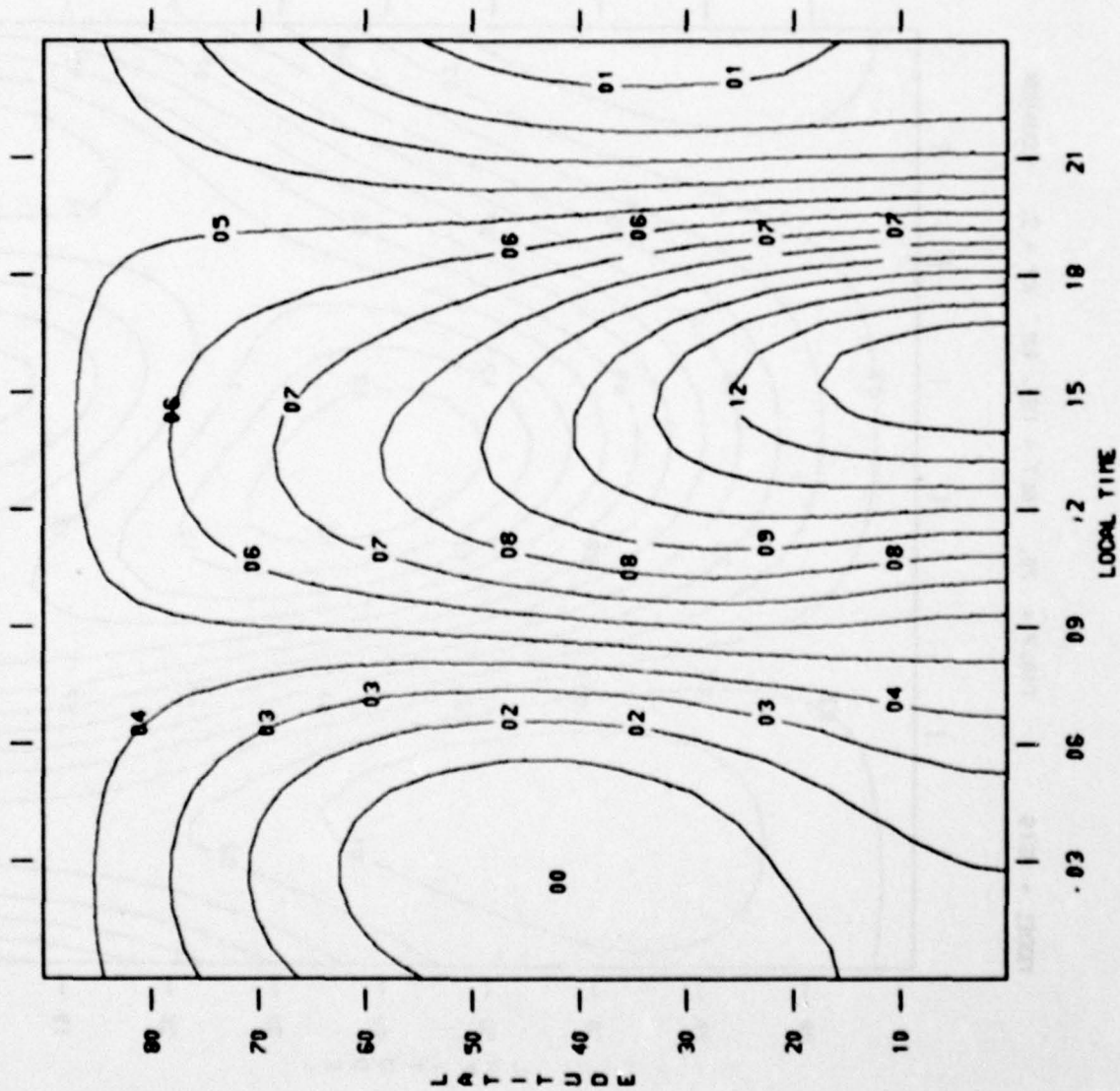
GM/CN=3

- 14 = 3.93E-12
- 13 = 3.87E-12
- 12 = 3.81E-12
- 11 = 3.75E-12
- 10 = 3.69E-12
- 09 = 3.62E-12
- 08 = 3.56E-12
- 07 = 3.50E-12
- 06 = 3.43E-12
- 05 = 3.37E-12
- 04 = 3.31E-12
- 03 = 3.25E-12
- 02 = 3.19E-12
- 01 = 3.12E-12
- 00 = 3.06E-12

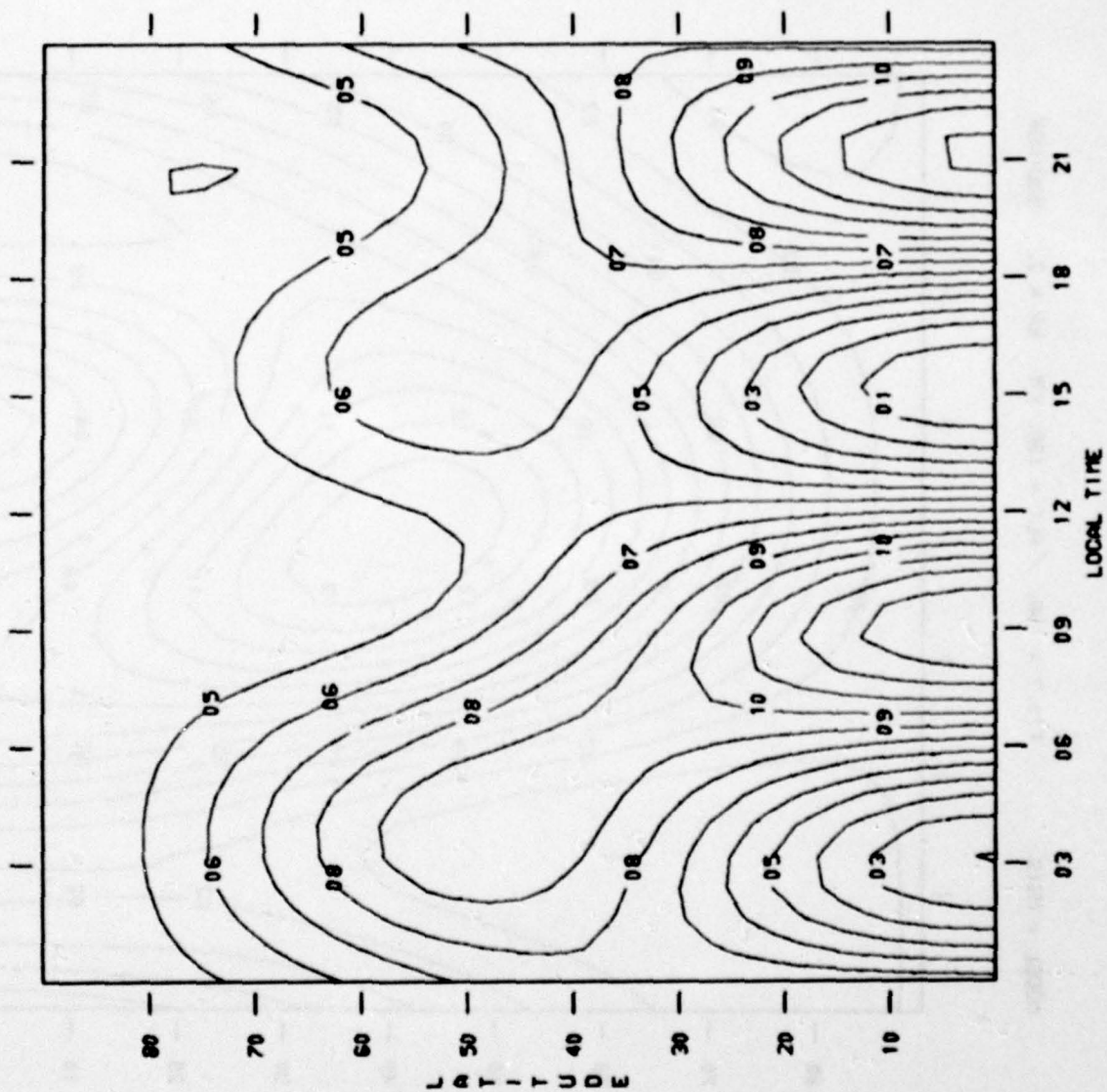
MODEL = MSIS F10.7 = 70. ALT = 180. KM KP = 2. EQUINOX



MODEL = MSIS F10.7 = 70. ALT = 400. KM KP = 2. EQUINOX



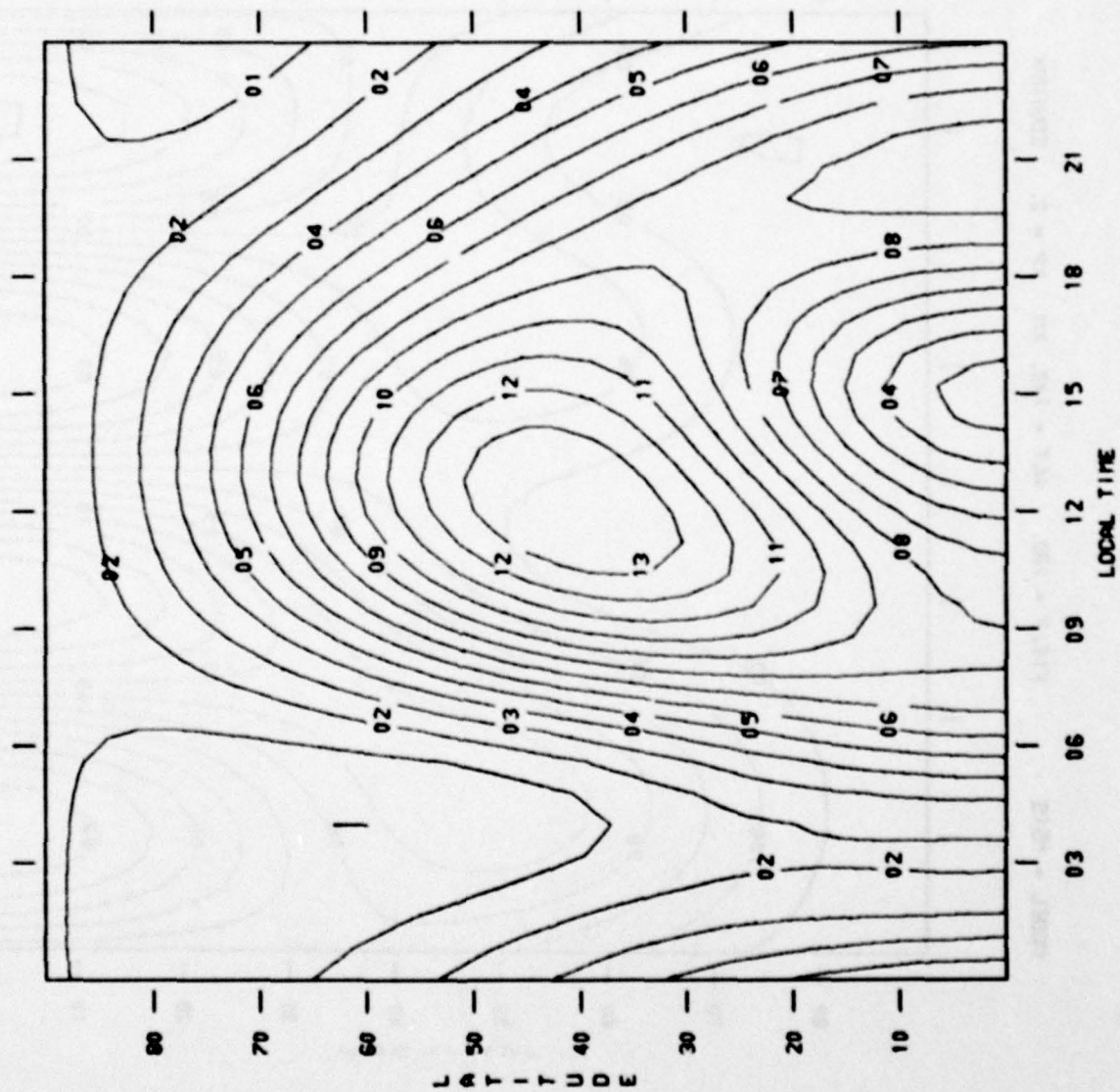
MODEL = MSIS F10.7 = 180. ALT = 140. KM KP = 2. EQUINOX



GM/CN=3

- 14 = 3.88E-12
- 13 = 3.81E-12
- 12 = 3.74E-12
- 11 = 3.68E-12
- 10 = 3.61E-12
- 09 = 3.54E-12
- 08 = 3.47E-12
- 07 = 3.40E-12
- 06 = 3.34E-12
- 05 = 3.27E-12
- 04 = 3.20E-12
- 03 = 3.13E-12
- 02 = 3.06E-12
- 01 = 3.00E-12
- 00 = 2.93E-12

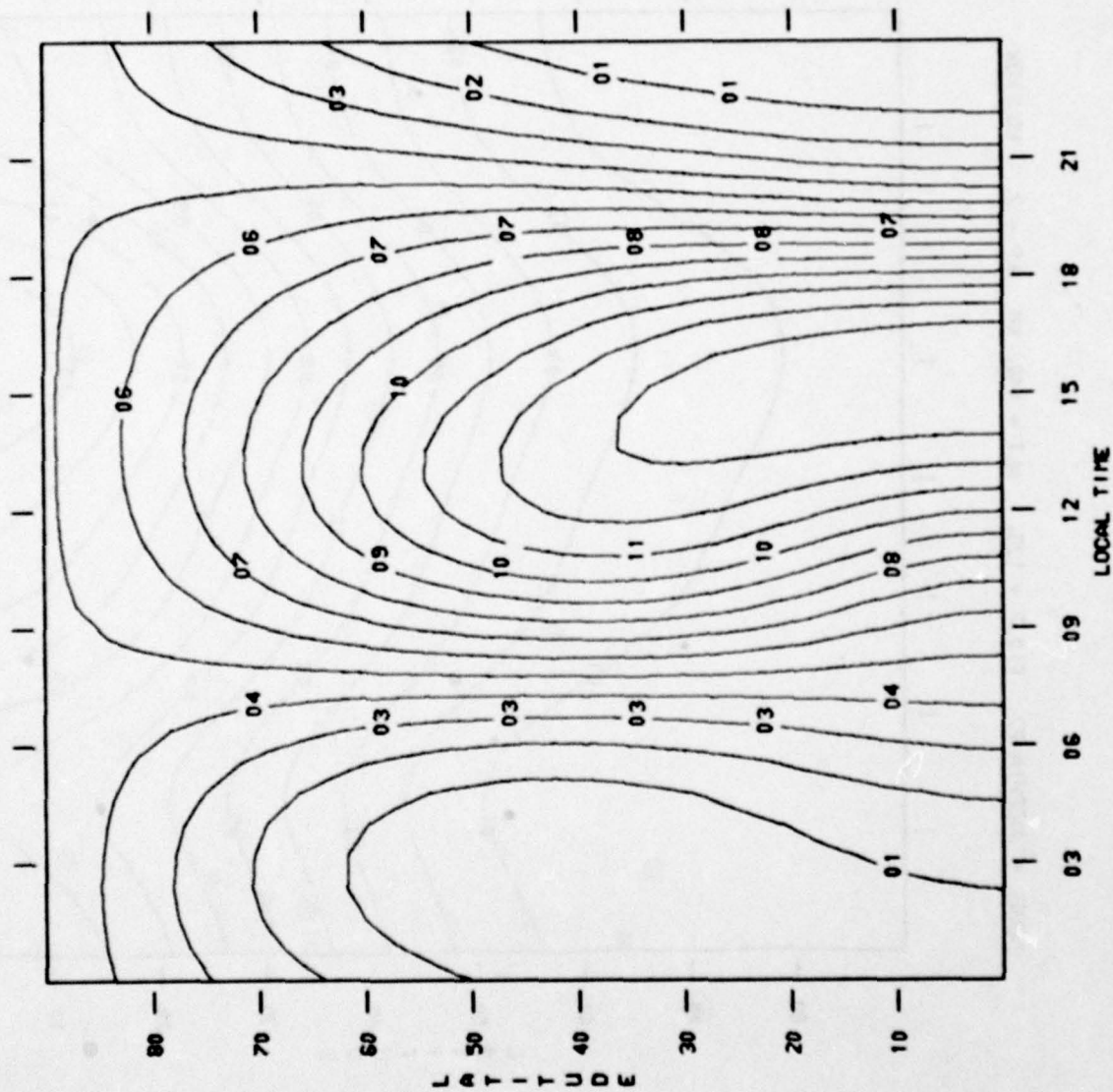
MODEL = MSIS F10.7 = 180. ALT = 180. KM KP = 2. EQUINOX



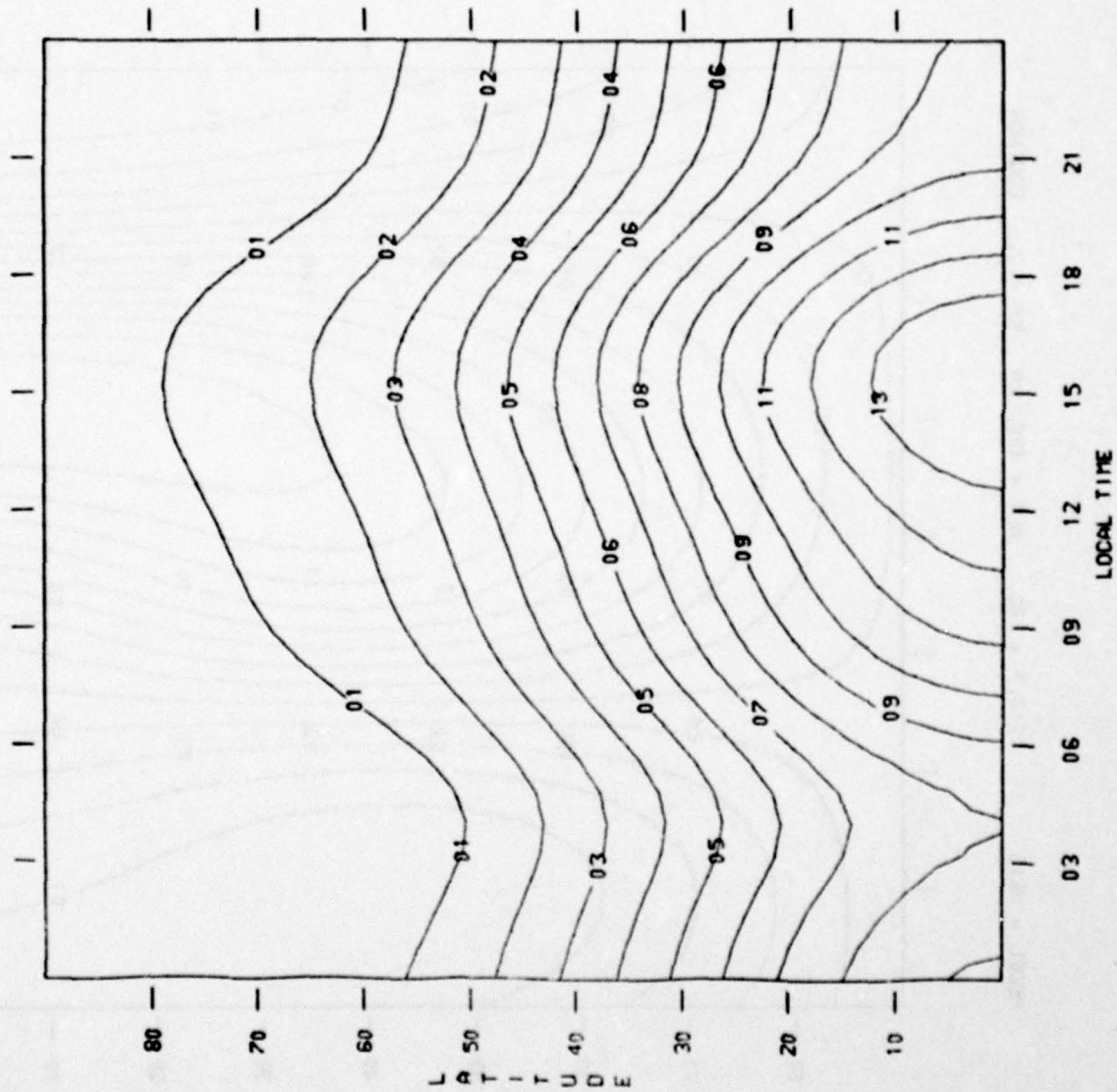
GM/CN=3

- 14 = 6.76E-13
- 13 = 6.70E-13
- 12 = 6.64E-13
- 11 = 6.58E-13
- 10 = 6.52E-13
- 09 = 6.47E-13
- 08 = 6.41E-13
- 07 = 6.35E-13
- 06 = 6.29E-13
- 05 = 6.23E-13
- 04 = 6.17E-13
- 03 = 6.11E-13
- 02 = 6.05E-13
- 01 = 5.99E-13
- 00 = 5.93E-13

MODEL = MSIS F10.7 = 180. ALT = 400. KM KP = 2. EQUINOX



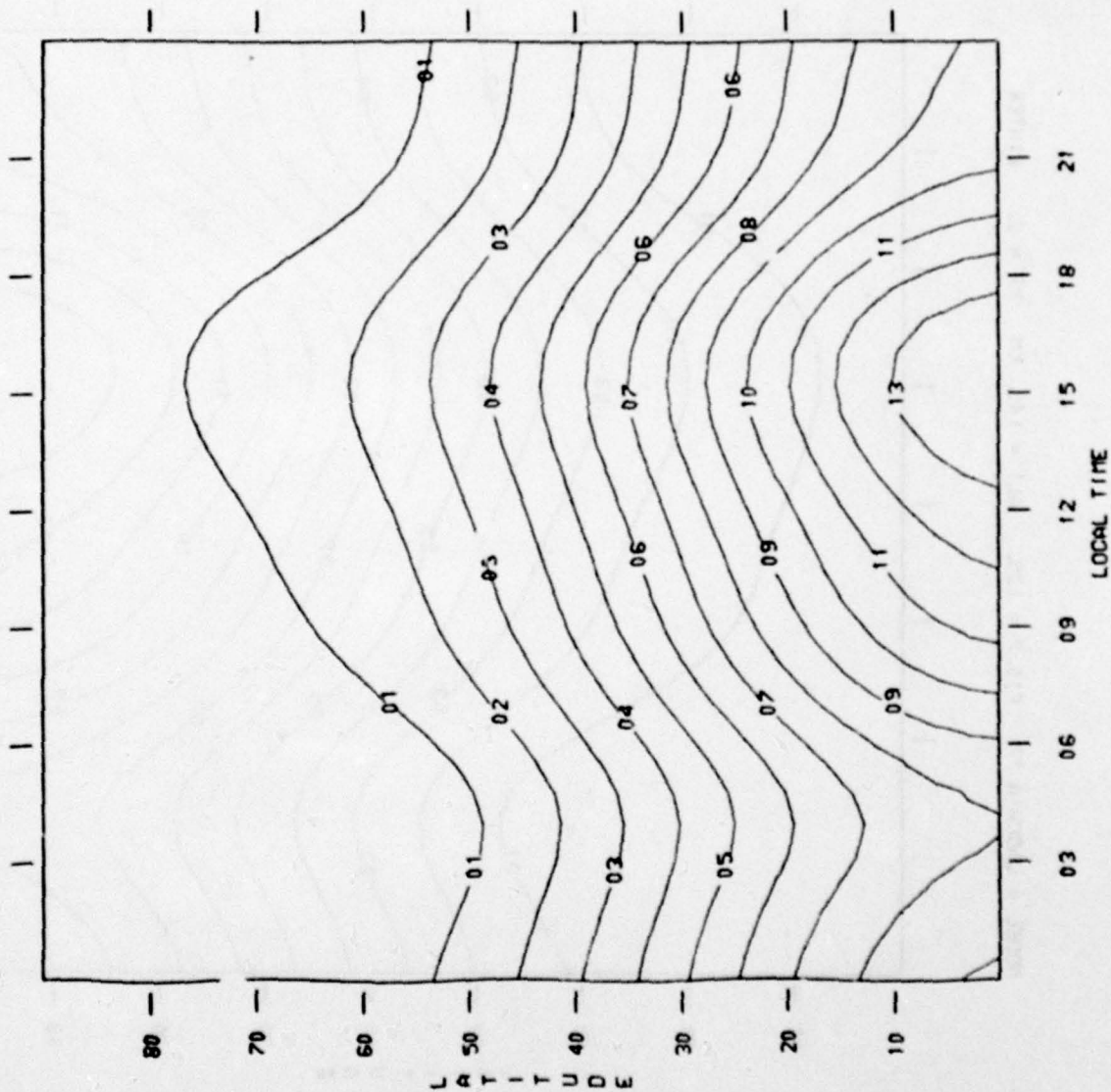
MODEL = JACCHIA 77 F10.7 = 125. ALT = 140. KM KP = 2. EQUINOX



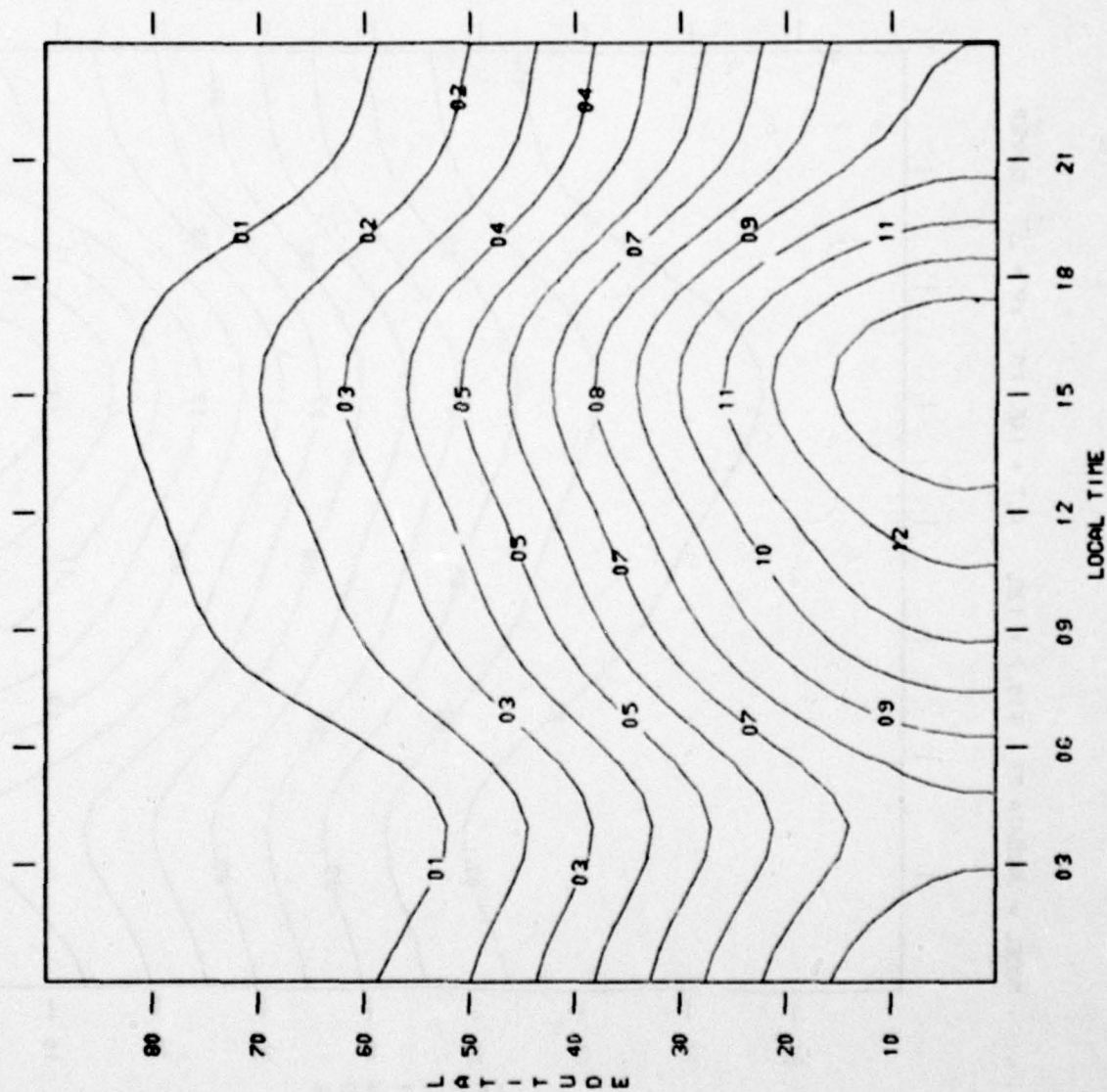
GM/Crime3

- 14 = 4.63E-12
- 13 = 4.56E-12
- 12 = 4.50E-12
- 11 = 4.43E-12
- 10 = 4.36E-12
- 09 = 4.30E-12
- 08 = 4.23E-12
- 07 = 4.16E-12
- 06 = 4.10E-12
- 05 = 4.03E-12
- 04 = 3.97E-12
- 03 = 3.90E-12
- 02 = 3.83E-12
- 01 = 3.77E-12
- 00 = 3.70E-12

MODEL = JACCHIA 77 F10.7 = 125. ALT = 140. KM KP = 2. SUMMER



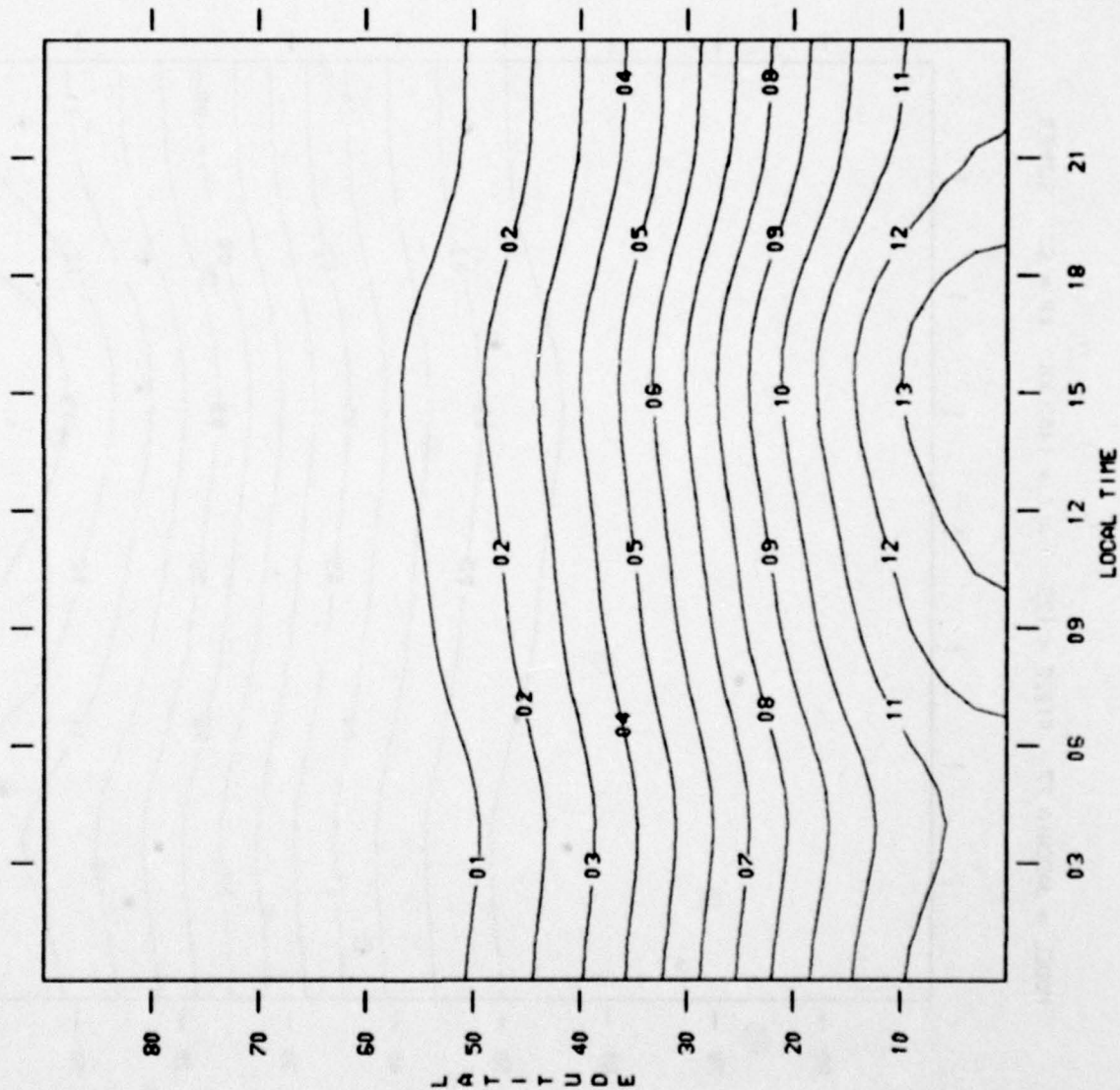
MODEL = JACCHIA 77 F10.7 = 125. ALT = 140. KM KP = 2. WINTER



GM/Crime3

- 14 = 4.30E-12
- 13 = 4.24E-12
- 12 = 4.18E-12
- 11 = 4.12E-12
- 10 = 4.06E-12
- 09 = 4.00E-12
- 08 = 3.94E-12
- 07 = 3.88E-12
- 06 = 3.82E-12
- 05 = 3.76E-12
- 04 = 3.70E-12
- 03 = 3.64E-12
- 02 = 3.58E-12
- 01 = 3.52E-12
- 00 = 3.46E-12

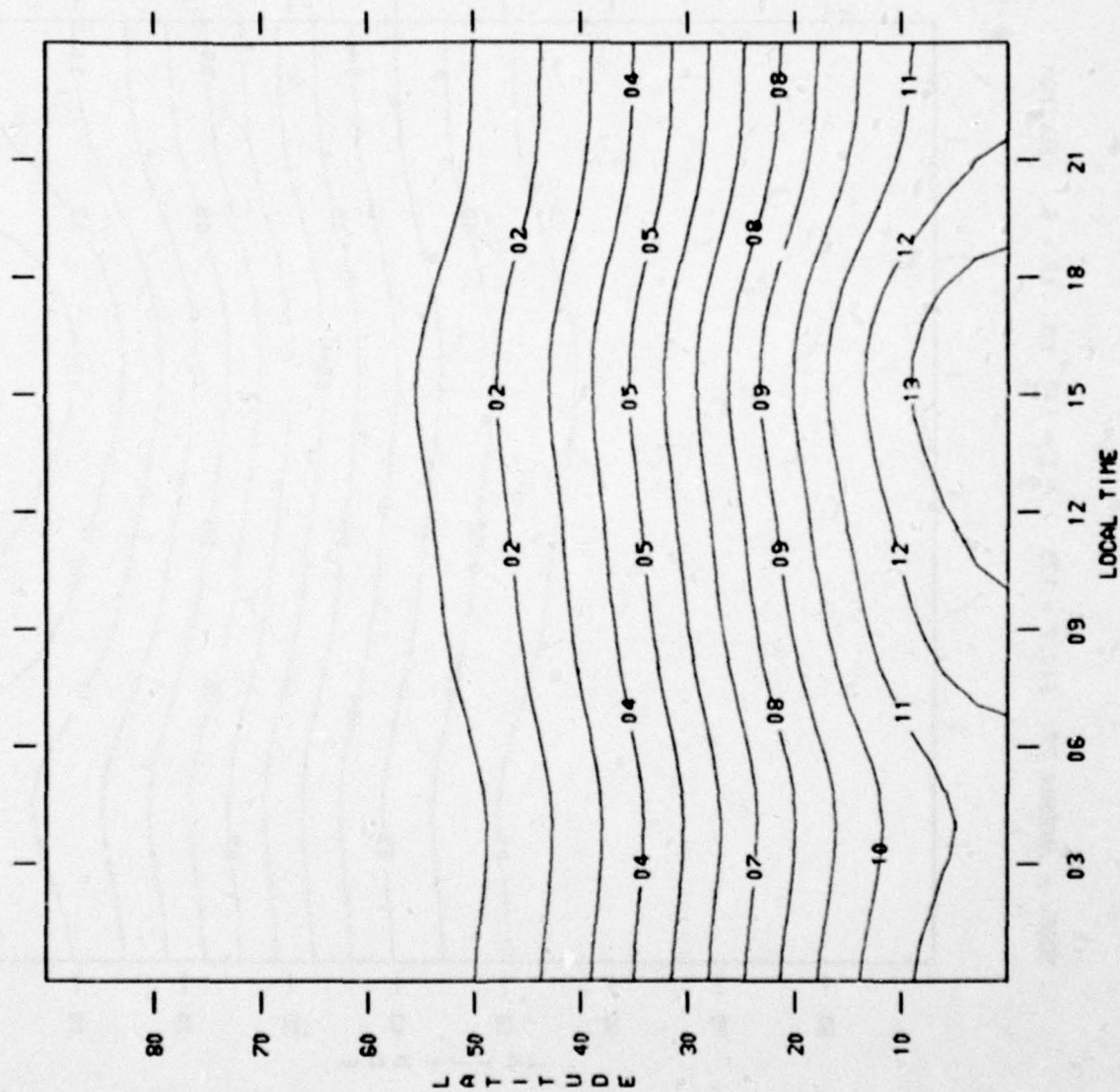
MODEL = JACCHIA 77 F10.7 = 125. ALT = 140. KM KP = 6. EQUINOX



CM/CHW=3

- 14 = 6.84E-12
- 13 = 6.62E-12
- 12 = 6.40E-12
- 11 = 6.18E-12
- 10 = 5.96E-12
- 09 = 5.74E-12
- 08 = 5.53E-12
- 07 = 5.31E-12
- 06 = 5.09E-12
- 05 = 4.87E-12
- 04 = 4.65E-12
- 03 = 4.43E-12
- 02 = 4.22E-12
- 01 = 4.00E-12
- 00 = 3.78E-12

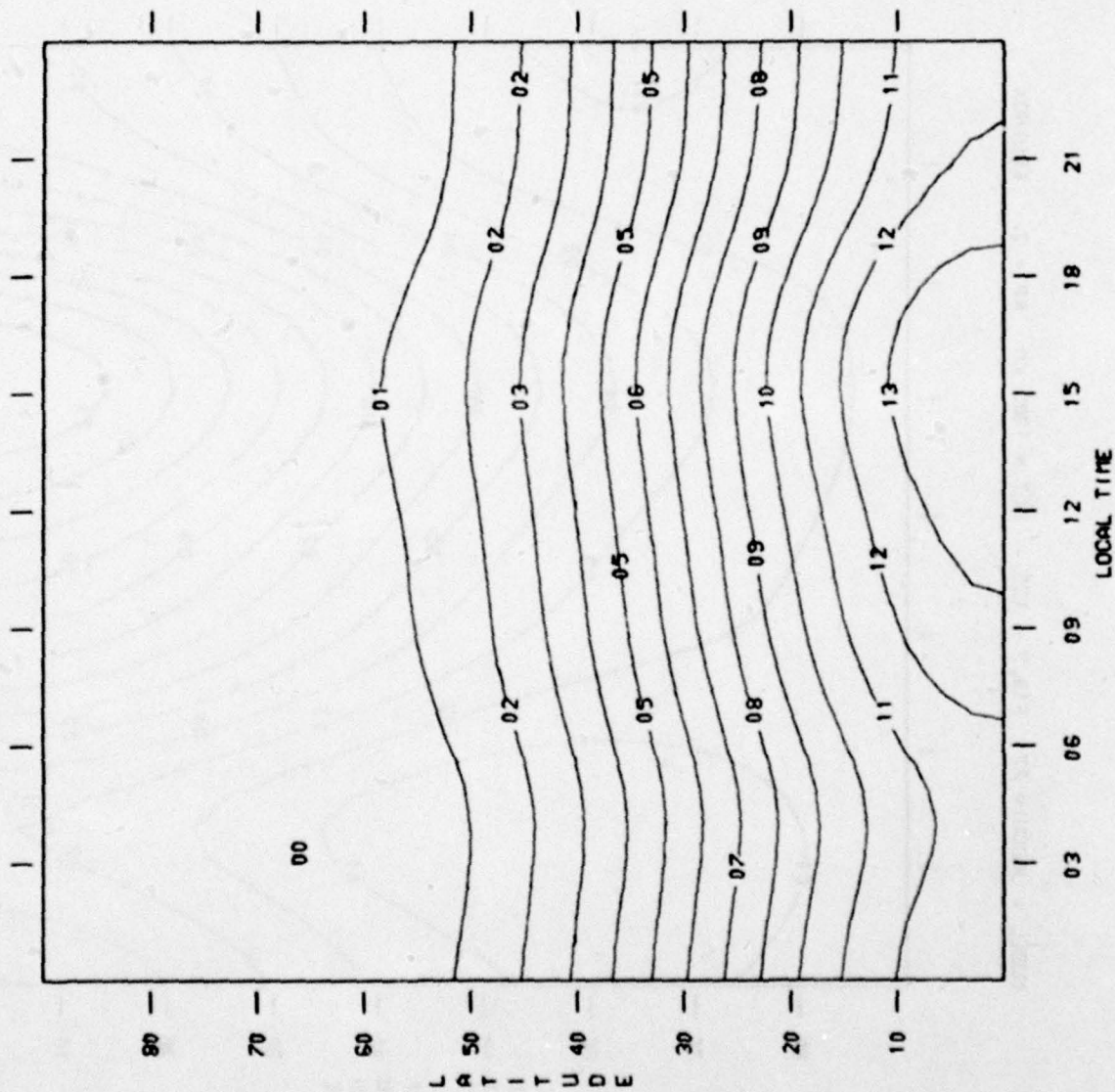
MODEL = JACCHIA 77 F10.7 = 125. ALT = 140. KM KP = 6. SUMMER



GM/CN003

- 14 = 5.98E-12
- 13 = 5.79E-12
- 12 = 5.60E-12
- 11 = 5.41E-12
- 10 = 5.22E-12
- 09 = 5.04E-12
- 08 = 4.85E-12
- 07 = 4.66E-12
- 06 = 4.47E-12
- 05 = 4.28E-12
- 04 = 4.10E-12
- 03 = 3.91E-12
- 02 = 3.72E-12
- 01 = 3.53E-12
- 00 = 3.34E-12

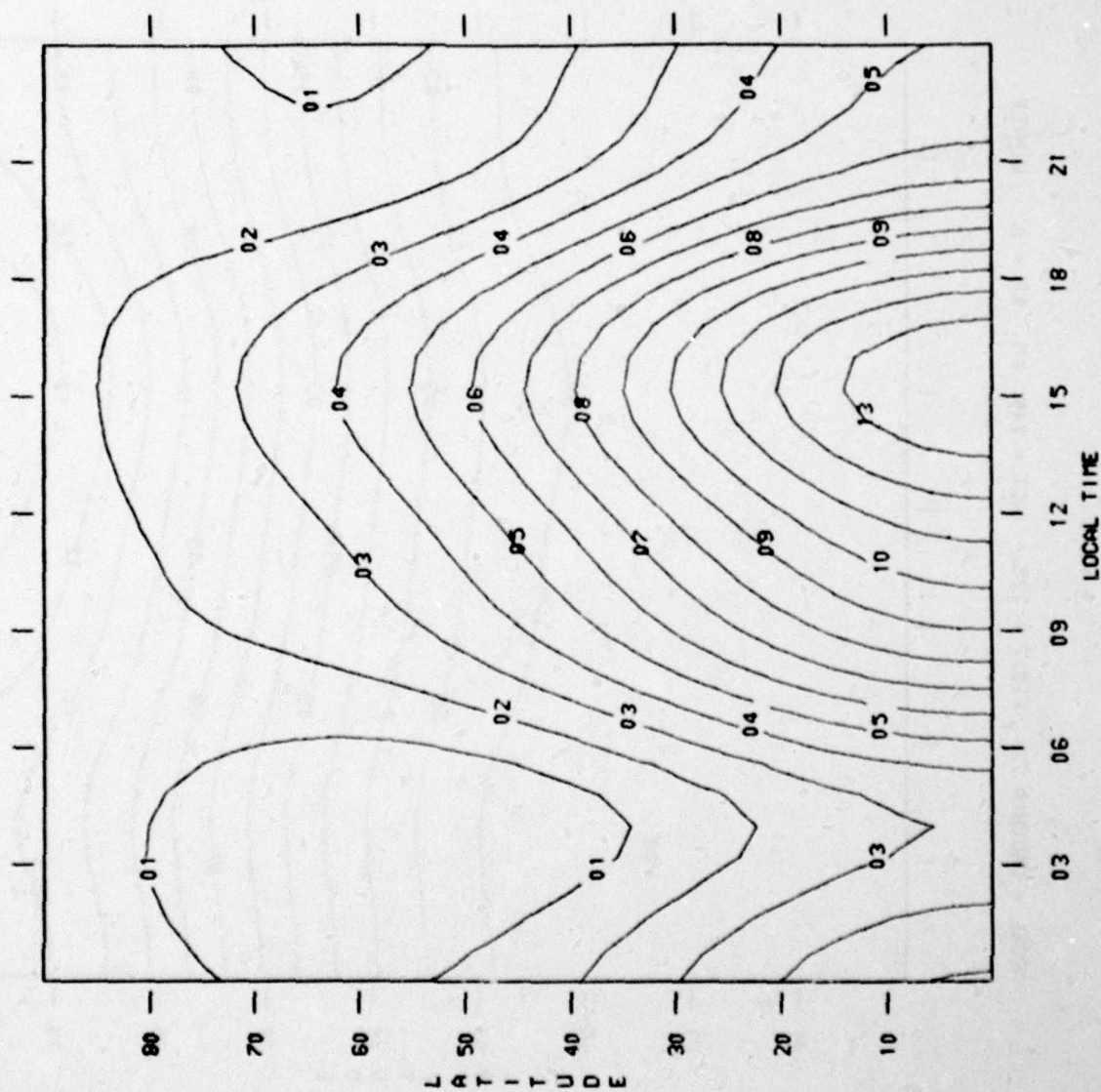
MODEL = JACCHIA 77 F10.7 = 125. ALT = 140. KM KP = 6. WINTER



GM/CN=3

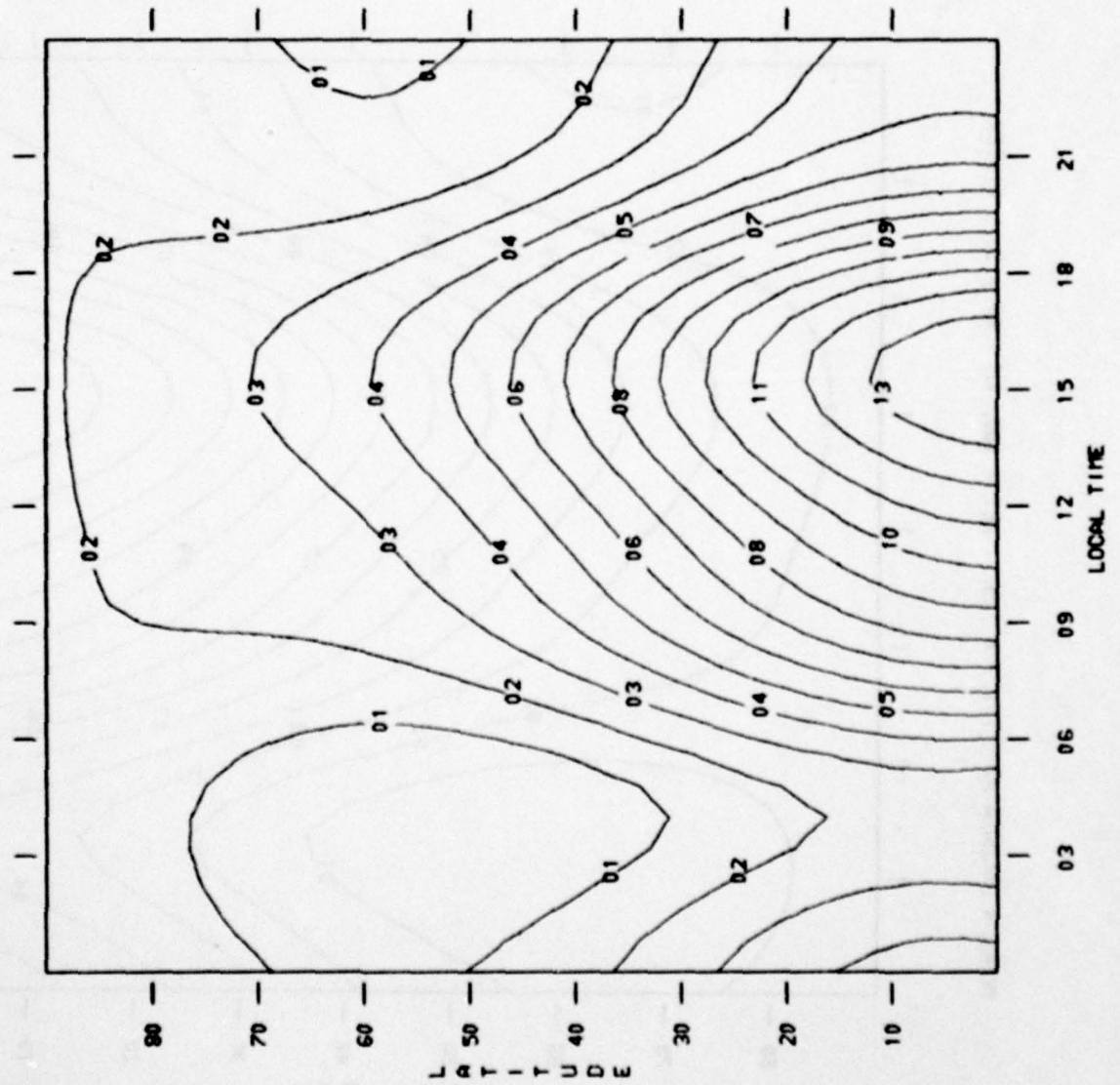
- 14 = 6.35E-12
- 13 = 6.15E-12
- 12 = 5.94E-12
- 11 = 5.74E-12
- 10 = 5.53E-12
- 09 = 5.33E-12
- 08 = 5.12E-12
- 07 = 4.92E-12
- 06 = 4.71E-12
- 05 = 4.51E-12
- 04 = 4.30E-12
- 03 = 4.10E-12
- 02 = 3.89E-12
- 01 = 3.68E-12
- 00 = 3.48E-12

MODEL = JACCHIA 77 F10.7 = 125. ALT = 180. KM KP = 2. EQUINOX



GM/CN=3
 14 = 7.13E-13
 13 = 6.99E-13
 12 = 6.85E-13
 11 = 6.71E-13
 10 = 6.57E-13
 09 = 6.43E-13
 08 = 6.29E-13
 07 = 6.15E-13
 06 = 6.01E-13
 05 = 5.87E-13
 04 = 5.72E-13
 03 = 5.58E-13
 02 = 5.44E-13
 01 = 5.30E-13
 00 = 5.16E-13

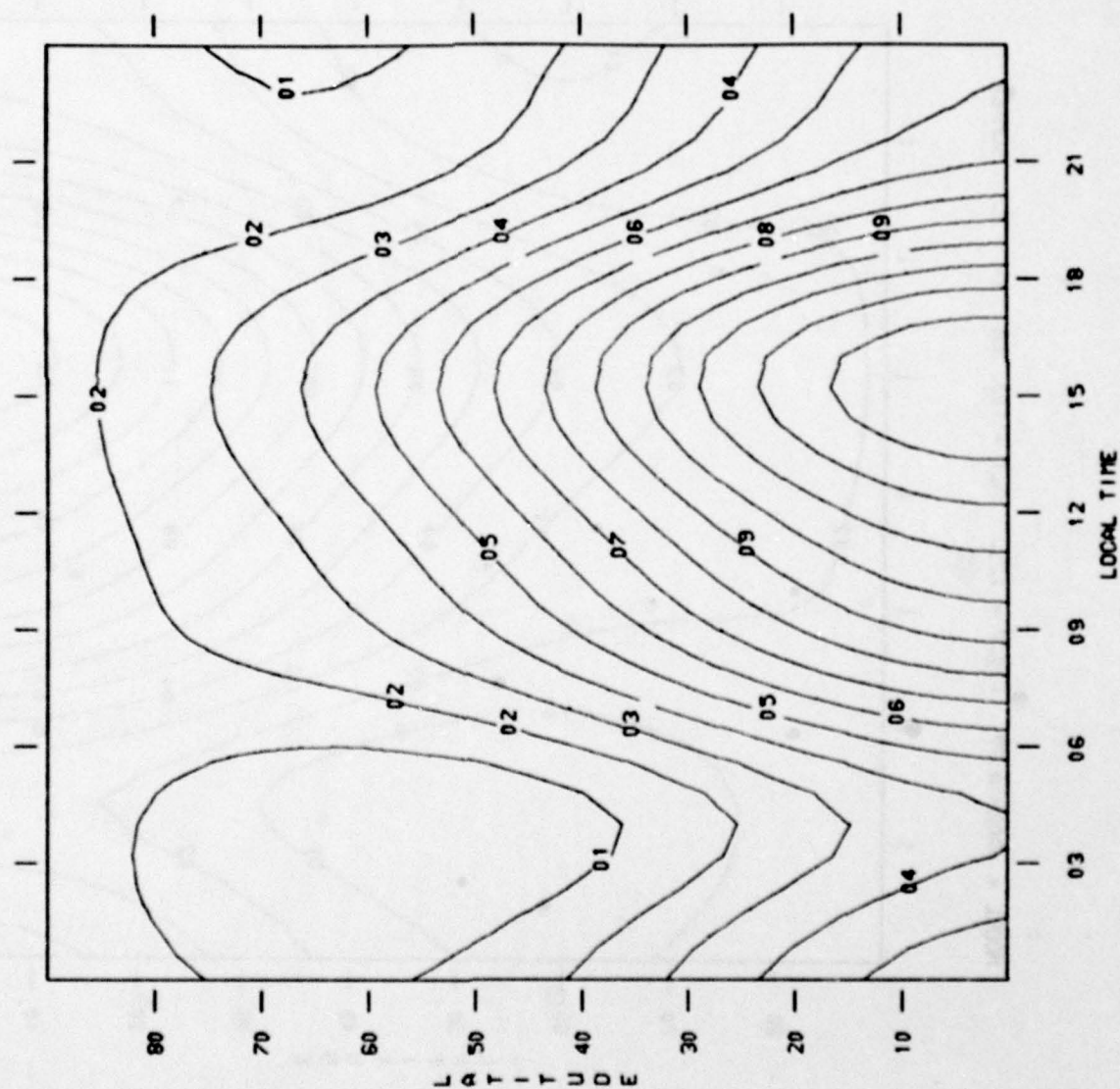
MODEL = JACCHIA 77 F10.7 = 125. ALT = 180. KM KP = 2. SUPER



CM/CNWS3

- 14 = 6.05E-13
- 13 = 5.94E-13
- 12 = 5.83E-13
- 11 = 5.72E-13
- 10 = 5.61E-13
- 09 = 5.50E-13
- 08 = 5.39E-13
- 07 = 5.28E-13
- 06 = 5.17E-13
- 05 = 5.06E-13
- 04 = 4.95E-13
- 03 = 4.84E-13
- 02 = 4.73E-13
- 01 = 4.62E-13
- 00 = 4.51E-13

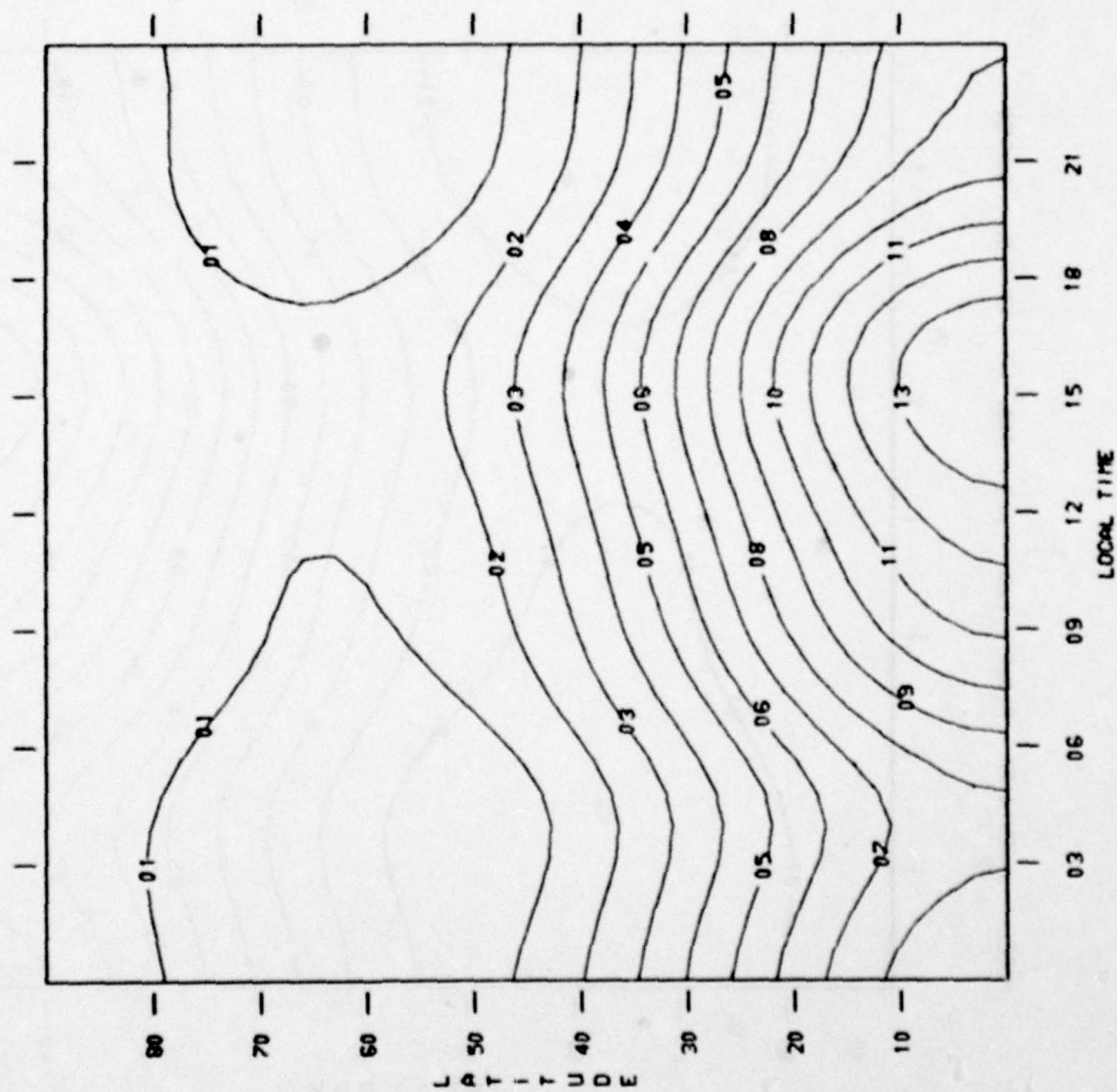
MODEL = JACCHIA 77 F10.7 = 125. ALT = 180. KM KP = 2. WINTER



Gr/Chm3

- 14 = 6.52E-13
- 13 = 6.38E-13
- 12 = 6.24E-13
- 11 = 6.10E-13
- 10 = 5.96E-13
- 09 = 5.83E-13
- 08 = 5.69E-13
- 07 = 5.55E-13
- 06 = 5.41E-13
- 05 = 5.27E-13
- 04 = 5.13E-13
- 03 = 4.99E-13
- 02 = 4.85E-13
- 01 = 4.71E-13
- 00 = 4.57E-13

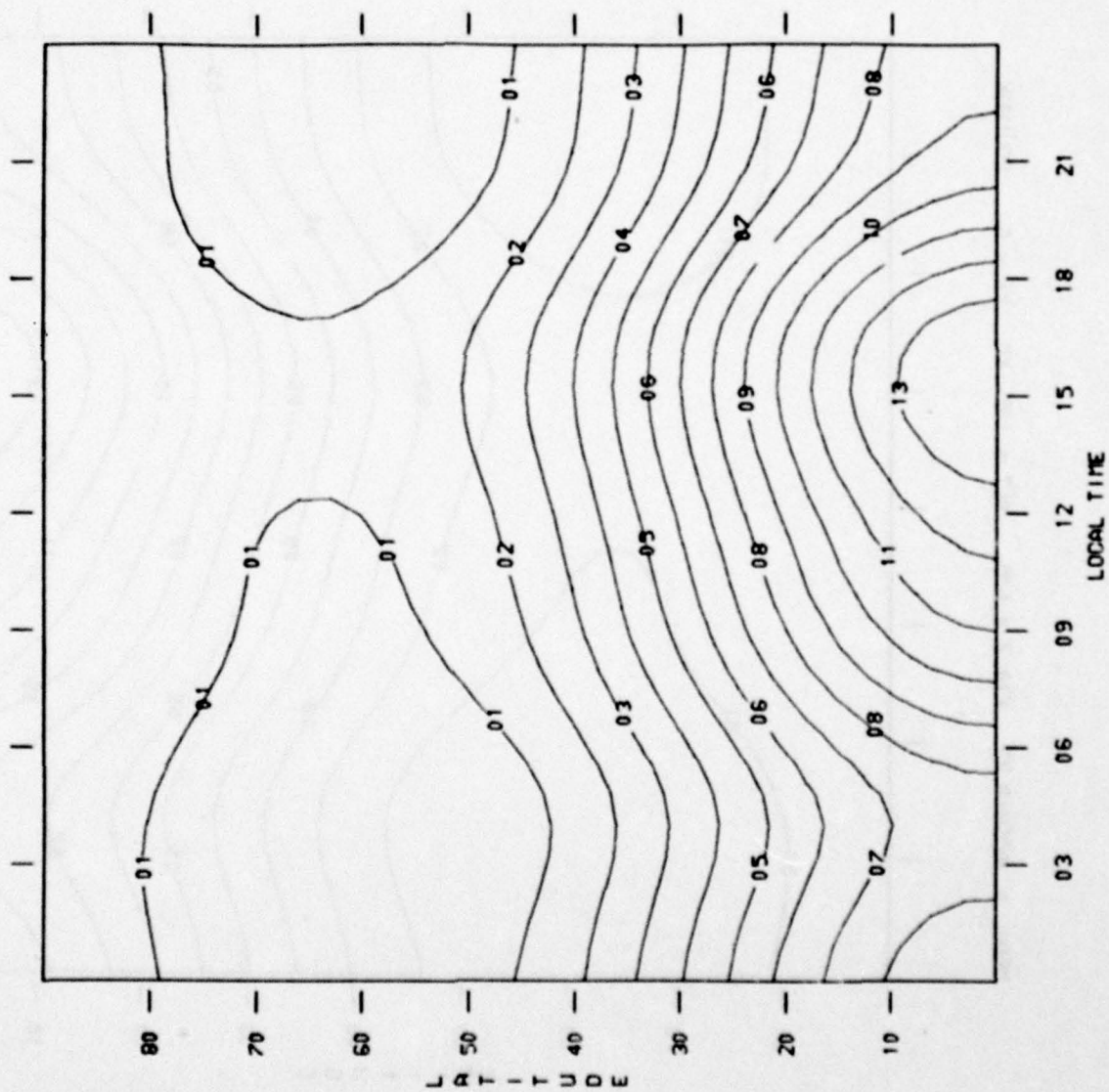
MODEL = JACCHIA 77 F10.7 = 125. ALT = 180. KM KP = 6. EQUINOX



GM/Critm3

- 14 = 1.05E-12
- 13 = 1.02E-12
- 12 = 9.80E-13
- 11 = 9.44E-13
- 10 = 9.07E-13
- 09 = 8.71E-13
- 08 = 8.34E-13
- 07 = 7.98E-13
- 06 = 7.61E-13
- 05 = 7.25E-13
- 04 = 6.88E-13
- 03 = 6.51E-13
- 02 = 6.15E-13
- 01 = 5.78E-13
- 00 = 5.42E-13

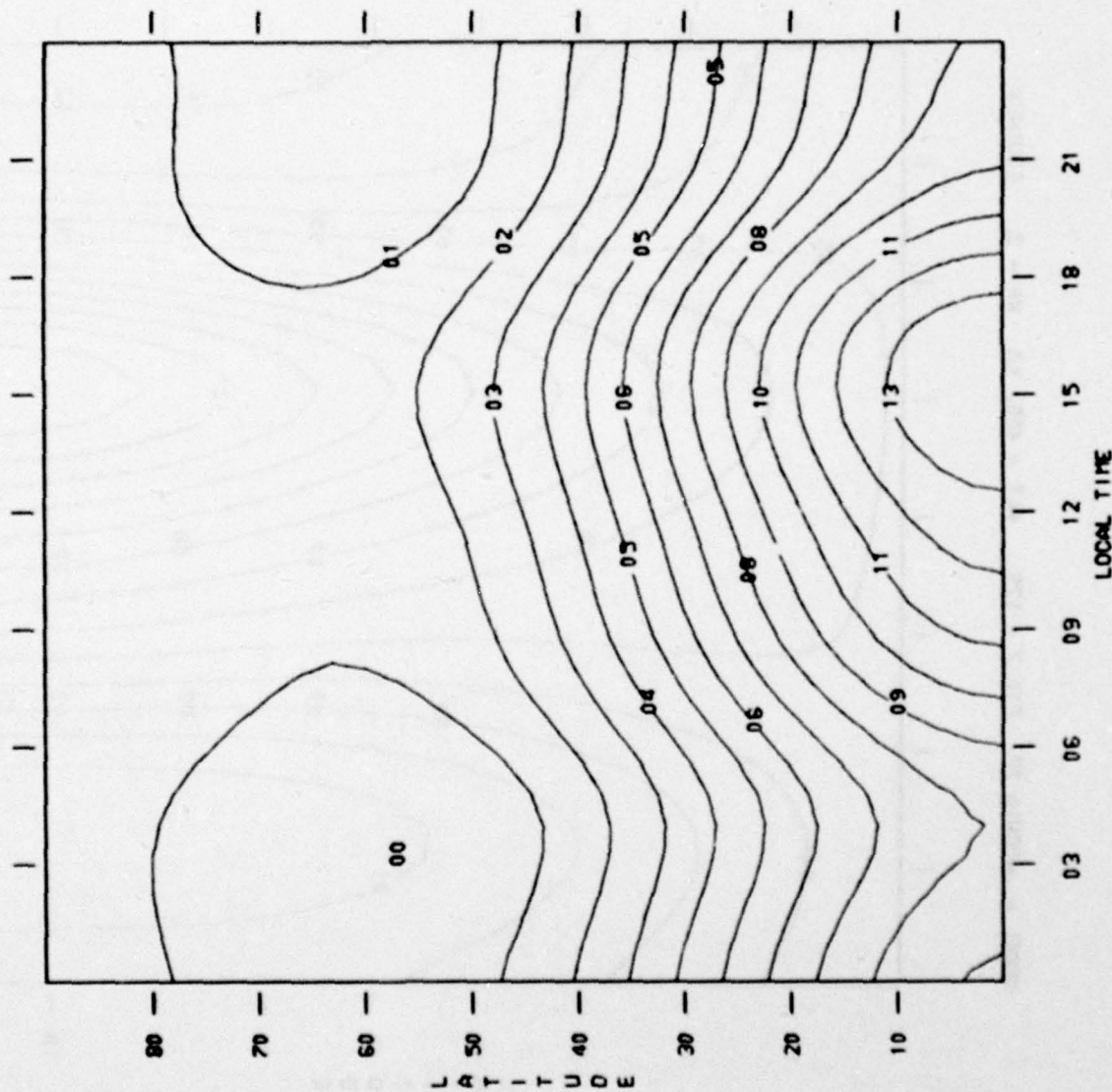
MODEL = JACCHIA 77 F10.7 = 125. ALT = 180. KM KP = 6. SUMMER



GM/CNWS3

14 = 8.94E-13
 13 = 8.64E-13
 12 = 8.34E-13
 11 = 8.05E-13
 10 = 7.75E-13
 09 = 7.45E-13
 08 = 7.16E-13
 07 = 6.86E-13
 06 = 6.57E-13
 05 = 6.27E-13
 04 = 5.97E-13
 03 = 5.68E-13
 02 = 5.38E-13
 01 = 5.09E-13
 00 = 4.79E-13

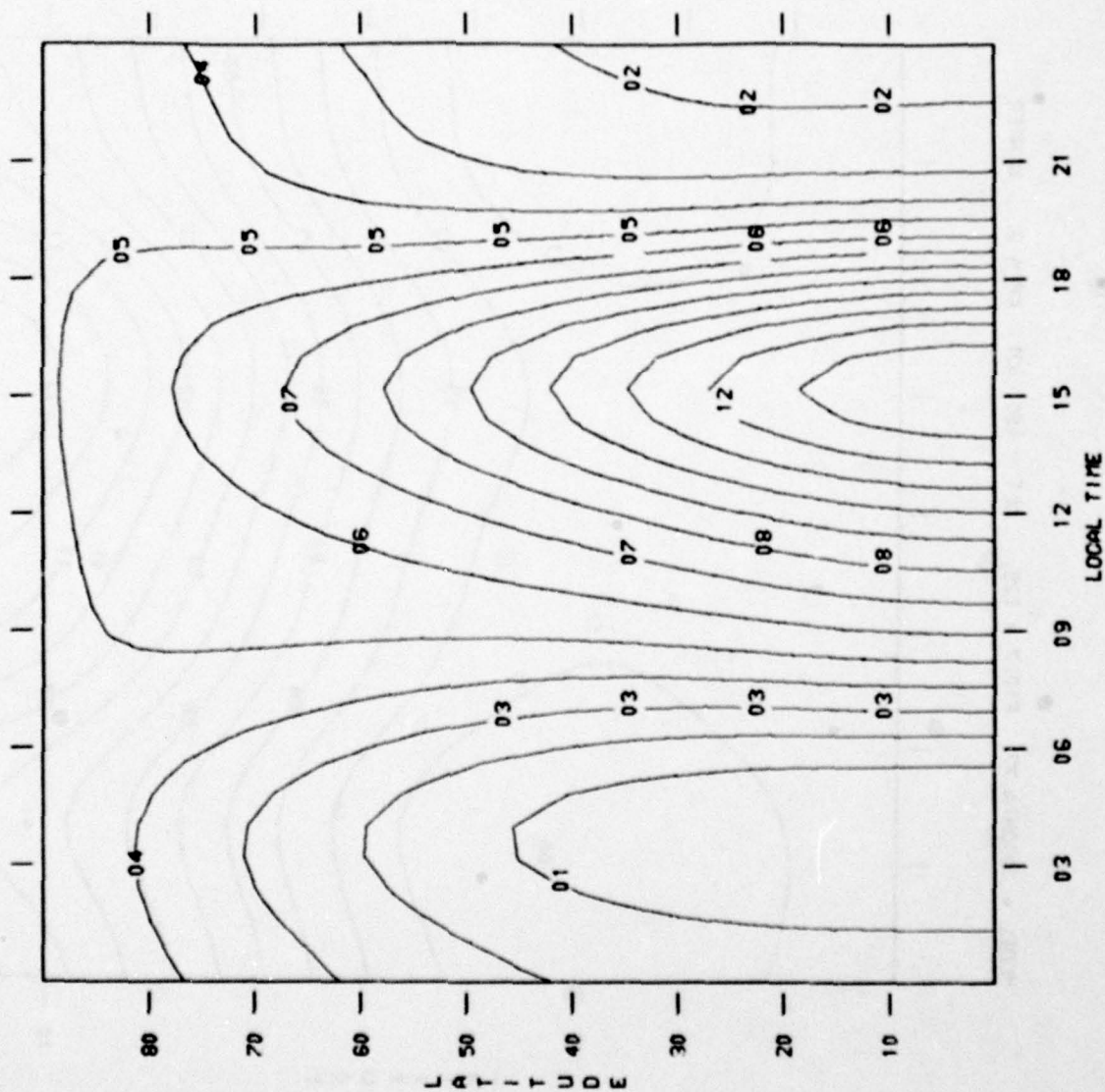
MODEL = JACCHIA 77 F10.7 = 125. ALT = 180. KM KP = 6. WINTER



CH/CHW3

- 14 = 9.63E-13
- 13 = 9.28E-13
- 12 = 8.93E-13
- 11 = 8.58E-13
- 10 = 8.23E-13
- 09 = 7.88E-13
- 08 = 7.53E-13
- 07 = 7.18E-13
- 06 = 6.83E-13
- 05 = 6.48E-13
- 04 = 6.13E-13
- 03 = 5.78E-13
- 02 = 5.43E-13
- 01 = 5.08E-13
- 00 = 4.74E-13

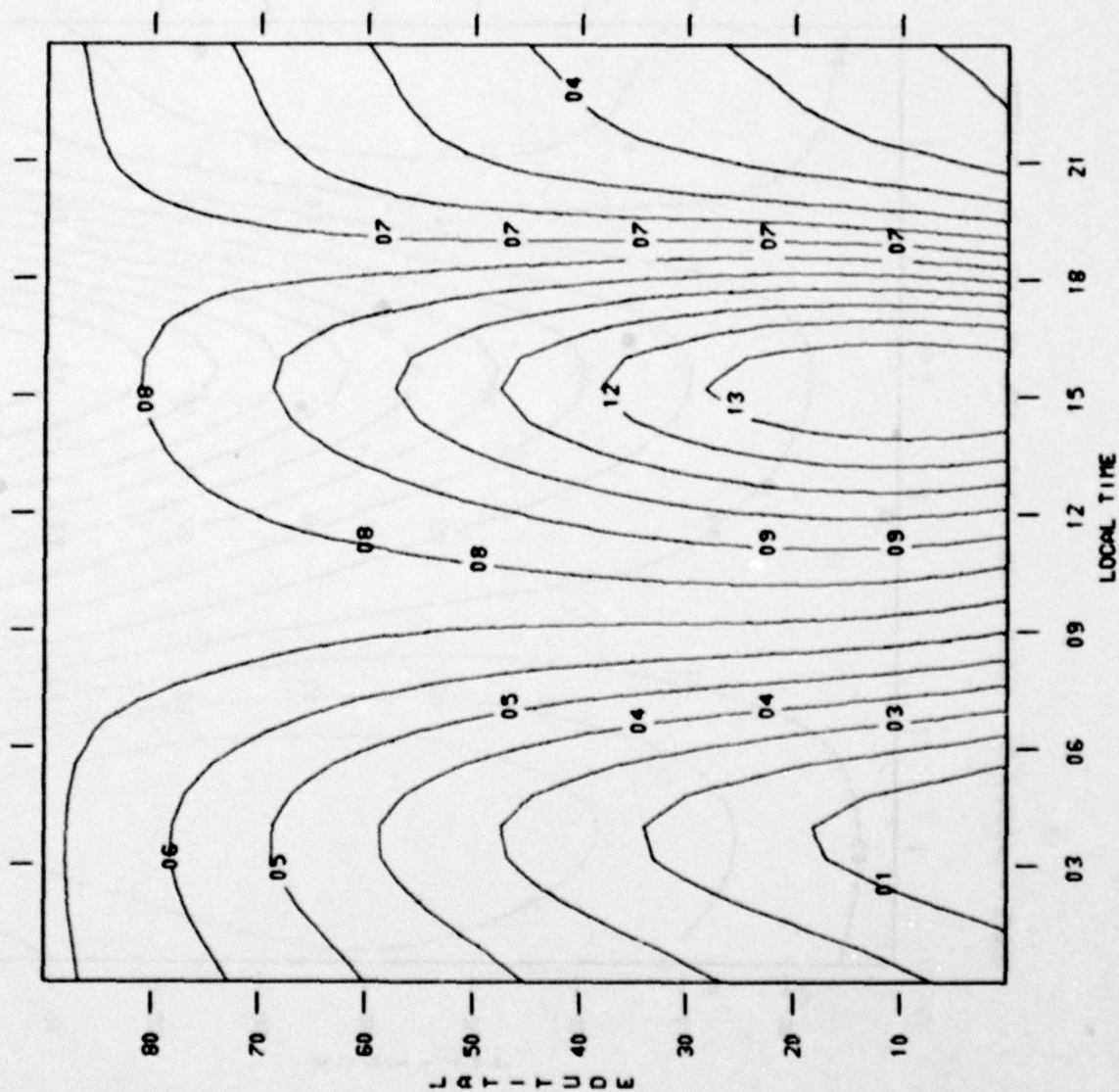
MODEL = JACCHIA 77 F10.7 = 125. ALT = 400. KM KP = 2. EQUINOX



CM/Chaw3

- 14 = 5.79E-15
- 13 = 5.51E-15
- 12 = 5.23E-15
- 11 = 4.95E-15
- 10 = 4.66E-15
- 09 = 4.38E-15
- 08 = 4.10E-15
- 07 = 3.82E-15
- 06 = 3.53E-15
- 05 = 3.25E-15
- 04 = 2.97E-15
- 03 = 2.69E-15
- 02 = 2.40E-15
- 01 = 2.12E-15
- 00 = 1.84E-15

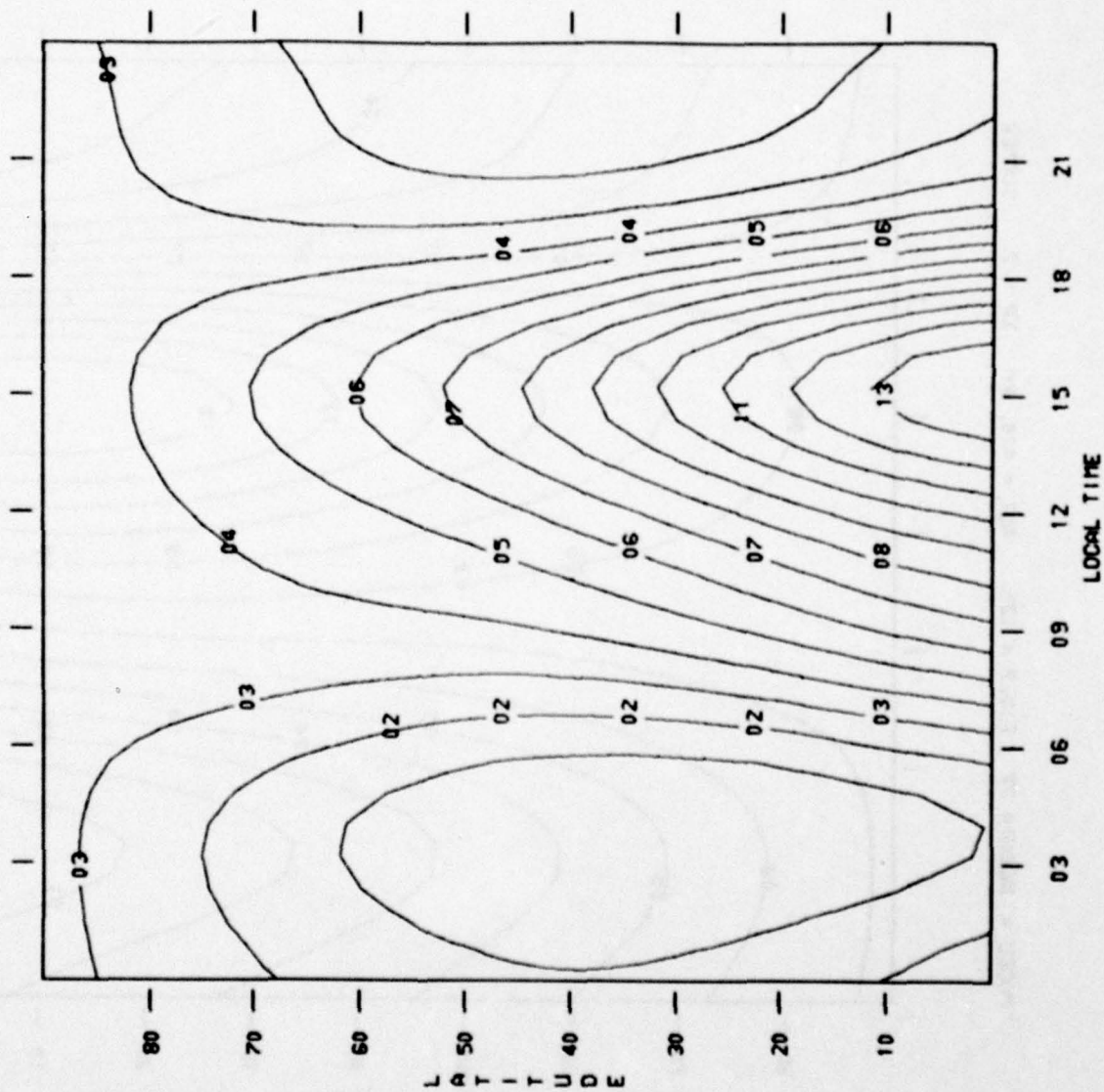
MODEL = JACCHIA 77 F10.7 = 125. ALT = 400. KM KP = 2. SUMMER



CM/CMW3

- 14 = 4.27E-15
- 13 = 4.06E-15
- 12 = 3.85E-15
- 11 = 3.64E-15
- 10 = 3.44E-15
- 09 = 3.23E-15
- 08 = 3.02E-15
- 07 = 2.81E-15
- 06 = 2.60E-15
- 05 = 2.39E-15
- 04 = 2.18E-15
- 03 = 1.97E-15
- 02 = 1.76E-15
- 01 = 1.55E-15
- 00 = 1.34E-15

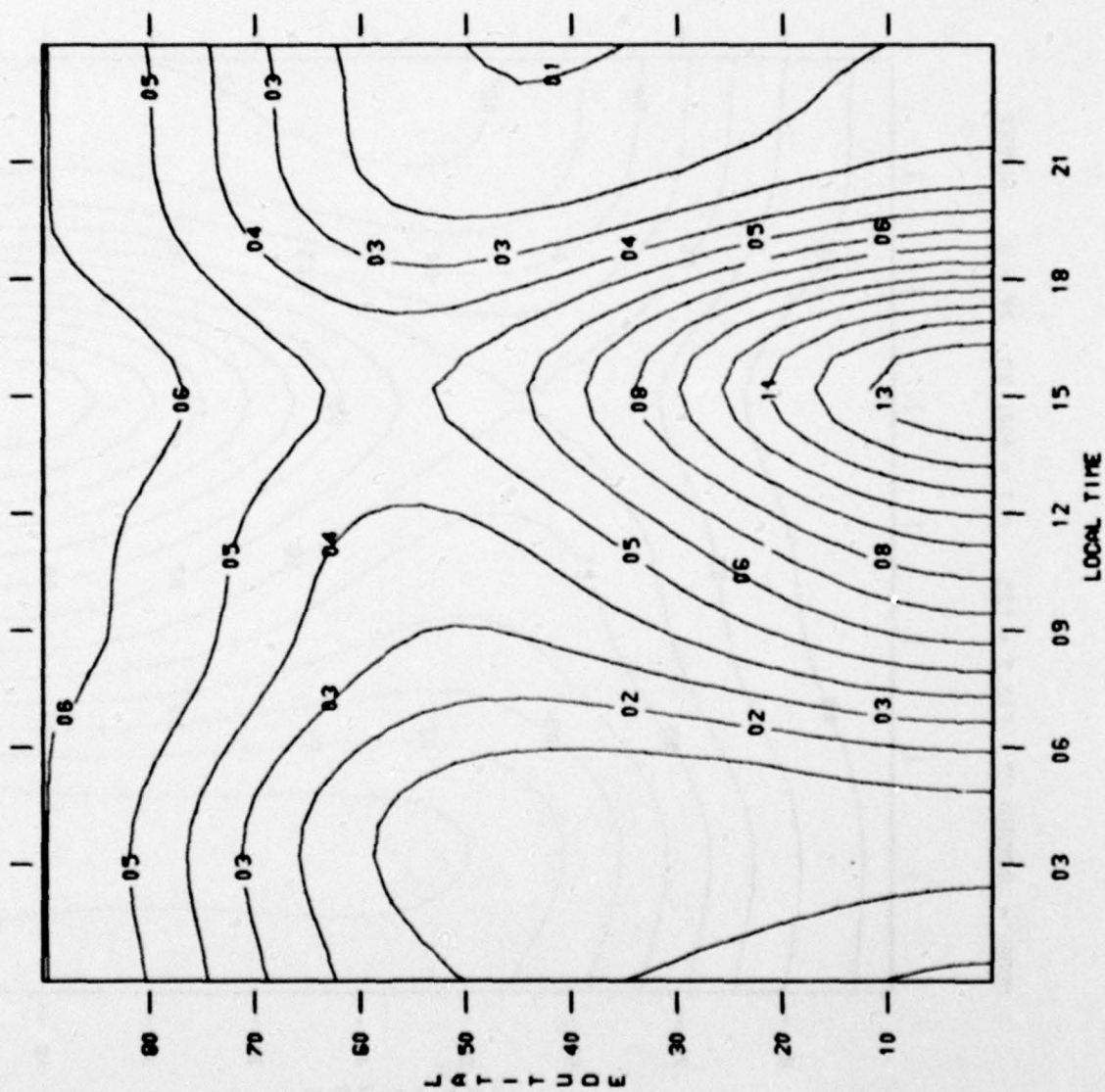
MODEL = JACCHIA 77 F10.7 = 125. ALT = 400. KM KP = 2. WINTER



GM/CN=03

14 =	4.88E-15
13 =	4.62E-15
12 =	4.36E-15
11 =	4.11E-15
10 =	3.85E-15
09 =	3.59E-15
08 =	3.34E-15
07 =	3.08E-15
06 =	2.82E-15
05 =	2.57E-15
04 =	2.31E-15
03 =	2.05E-15
02 =	1.80E-15
01 =	1.54E-15
00 =	1.28E-15

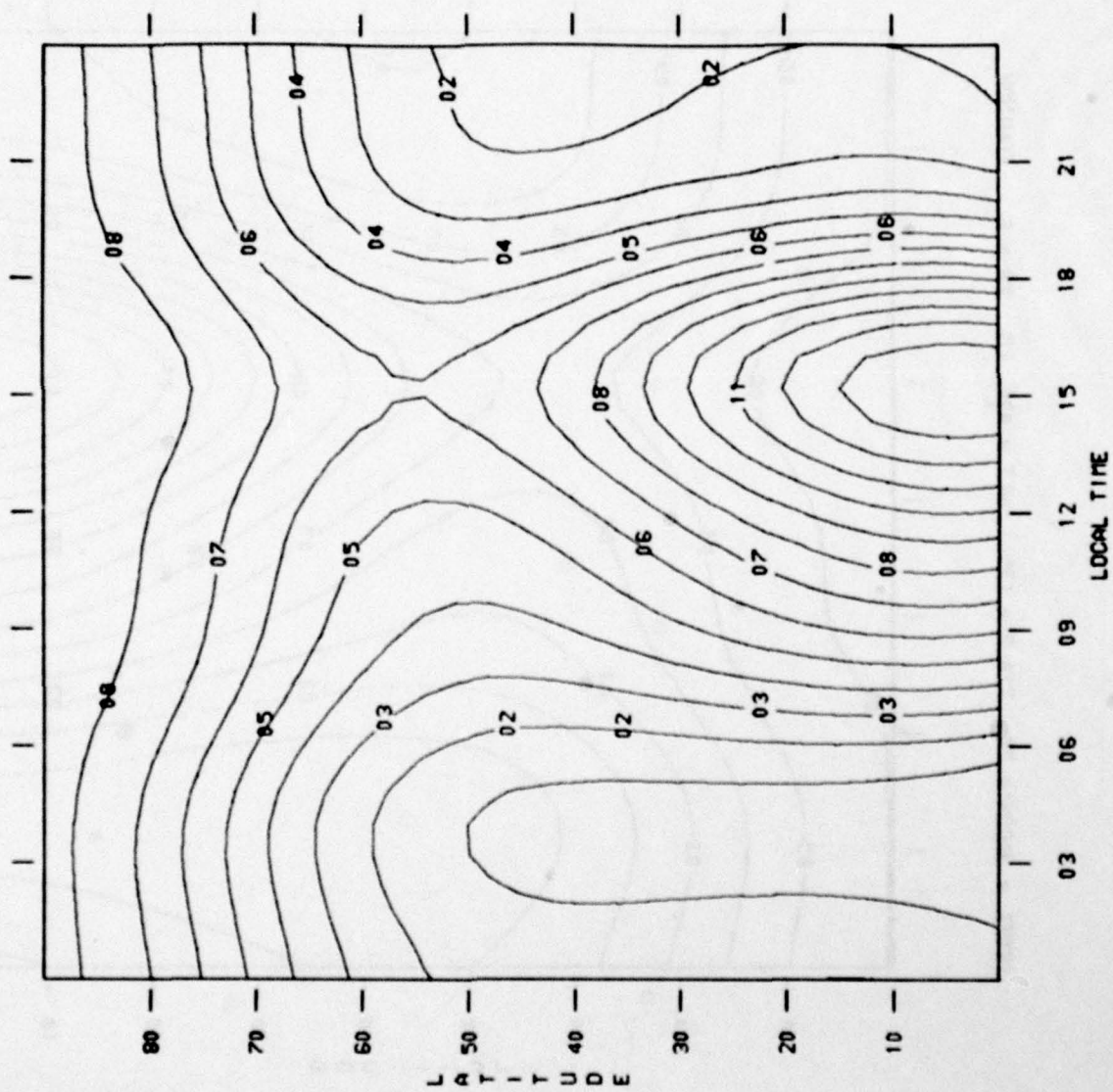
MODEL = JACCHIA 77 F10.7 = 125. ALT = 400. KM KP = 6. EQUINOX



GM/CN=3

- 14 = 8.56E-15
- 13 = 8.12E-15
- 12 = 7.69E-15
- 11 = 7.25E-15
- 10 = 6.81E-15
- 09 = 6.38E-15
- 08 = 5.94E-15
- 07 = 5.50E-15
- 06 = 5.07E-15
- 05 = 4.63E-15
- 04 = 4.19E-15
- 03 = 3.76E-15
- 02 = 3.32E-15
- 01 = 2.88E-15
- 00 = 2.44E-15

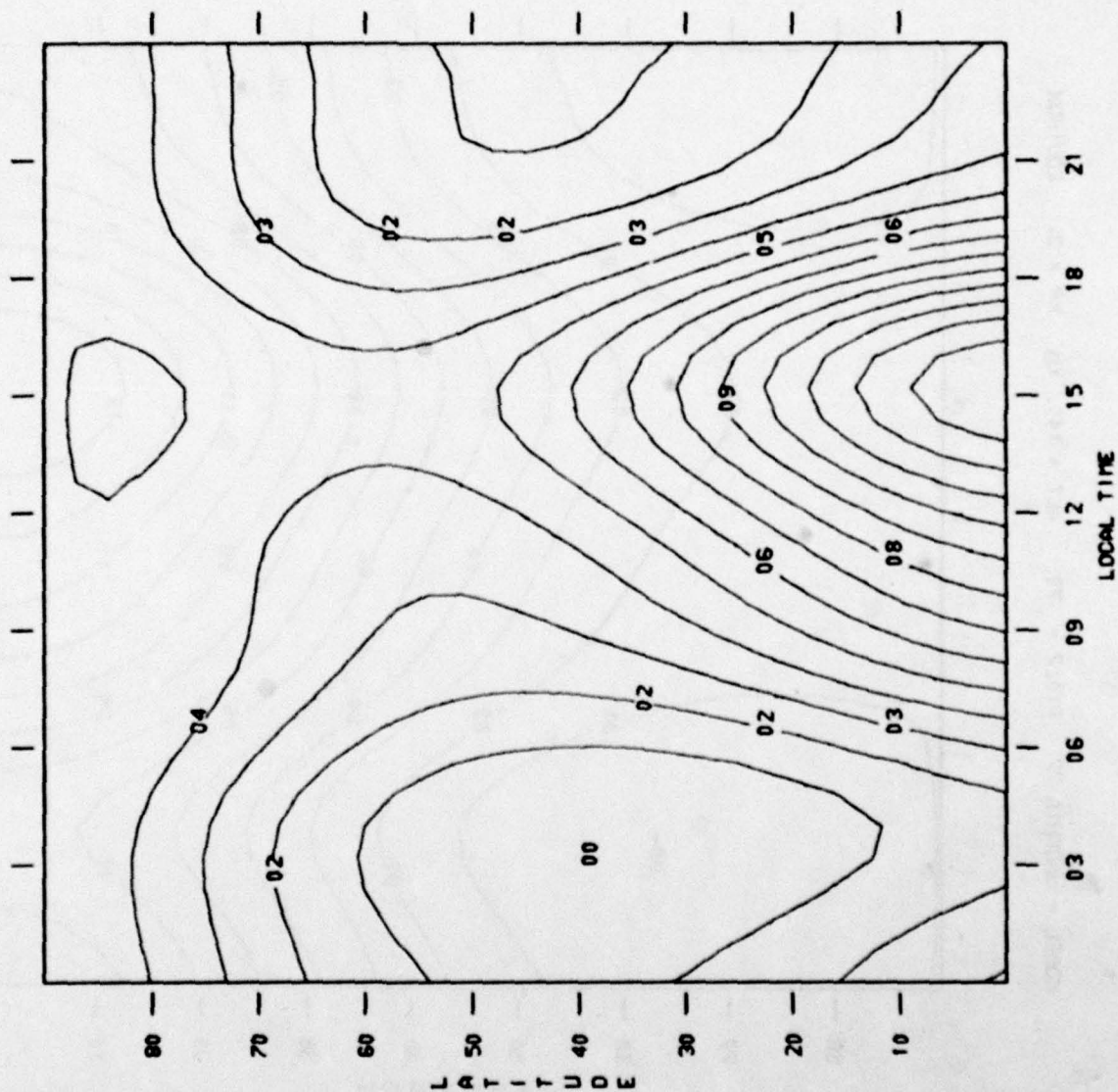
MODEL = JACCHIA 77 F10.7 = 125. ALT = 400. KM KP = 6. SUMMER



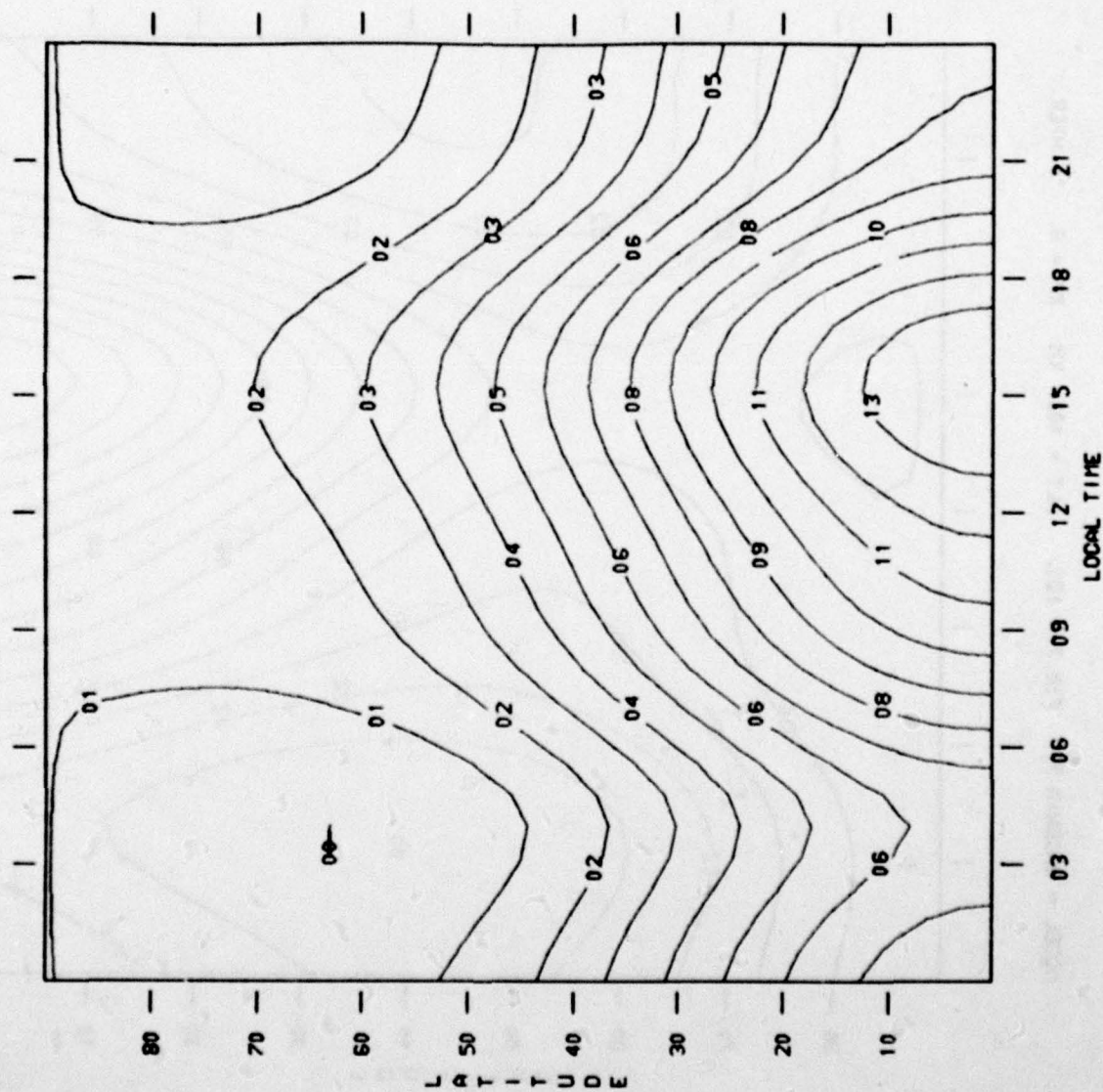
CH/CHW3

- 14 = 6.27E-15
- 13 = 5.96E-15
- 12 = 5.65E-15
- 11 = 5.35E-15
- 10 = 5.04E-15
- 09 = 4.73E-15
- 08 = 4.43E-15
- 07 = 4.12E-15
- 06 = 3.82E-15
- 05 = 3.51E-15
- 04 = 3.20E-15
- 03 = 2.90E-15
- 02 = 2.59E-15
- 01 = 2.28E-15
- 00 = 1.98E-15

MODEL = JACCHIA 77 F10.7 = 125. ALT = 400. KM KP = 6. WINTER



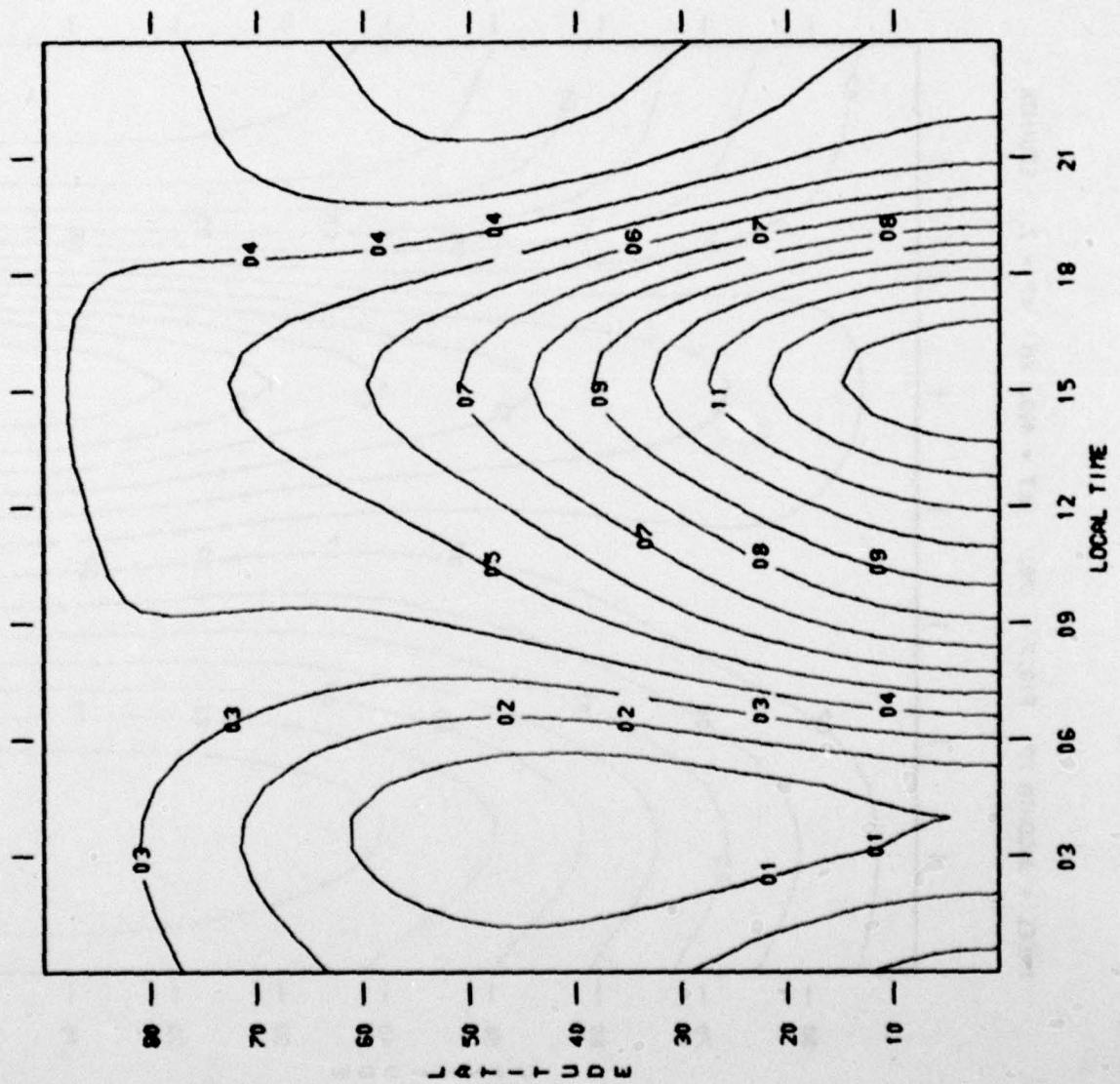
MODEL = JACCHIA 77 F10.7 = 70. ALT = 140. KM KP = 2. EQUINOX



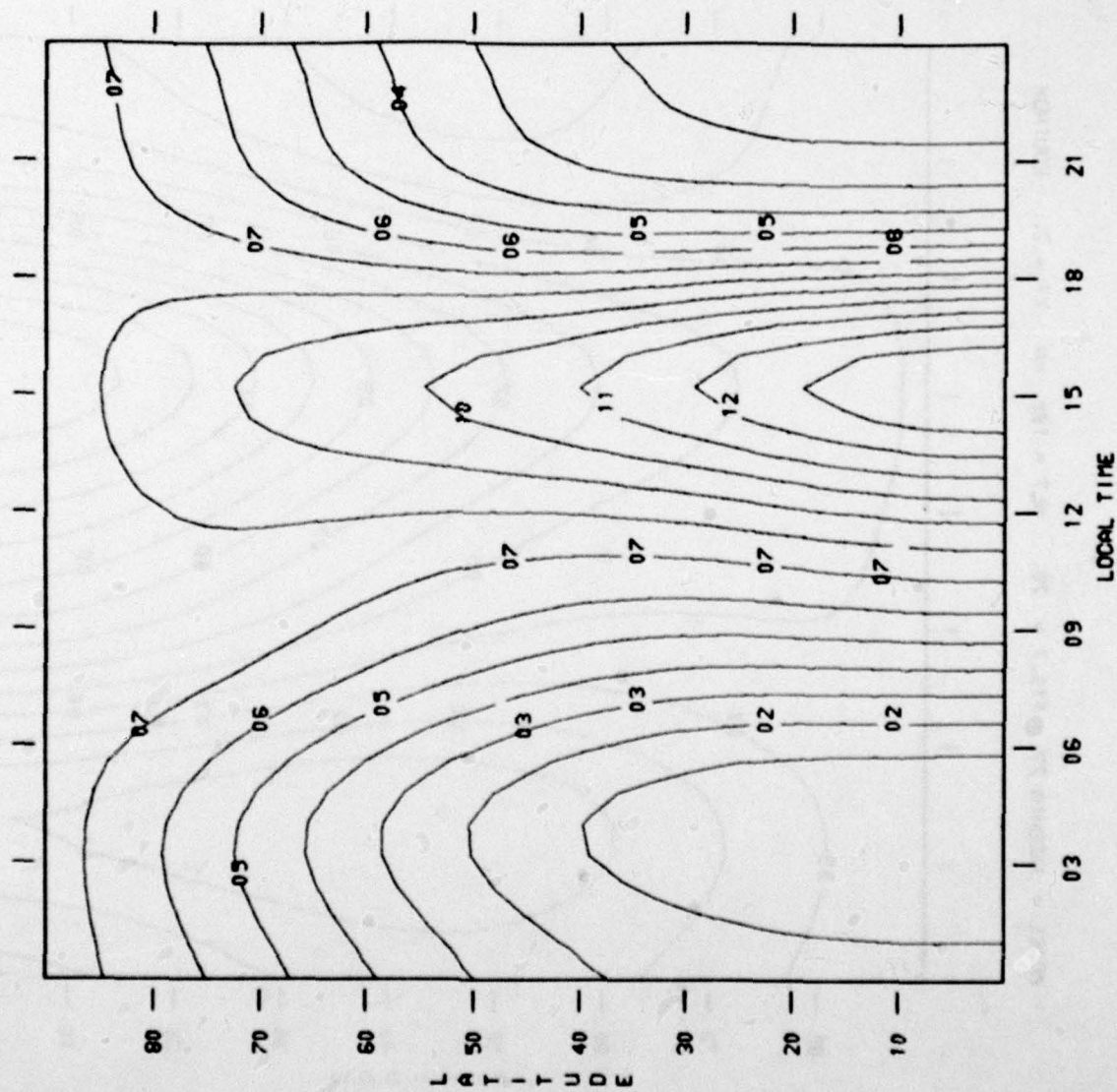
CM/CHW3

- 14 = 4.20E-12
- 13 = 4.14E-12
- 12 = 4.08E-12
- 11 = 4.02E-12
- 10 = 3.96E-12
- 09 = 3.90E-12
- 08 = 3.84E-12
- 07 = 3.78E-12
- 06 = 3.72E-12
- 05 = 3.65E-12
- 04 = 3.59E-12
- 03 = 3.53E-12
- 02 = 3.47E-12
- 01 = 3.41E-12
- 00 = 3.35E-12

MODEL = JACCHIA 77 F10.7 = 70. ALT = 180. KM KP = 2. EQUINOX



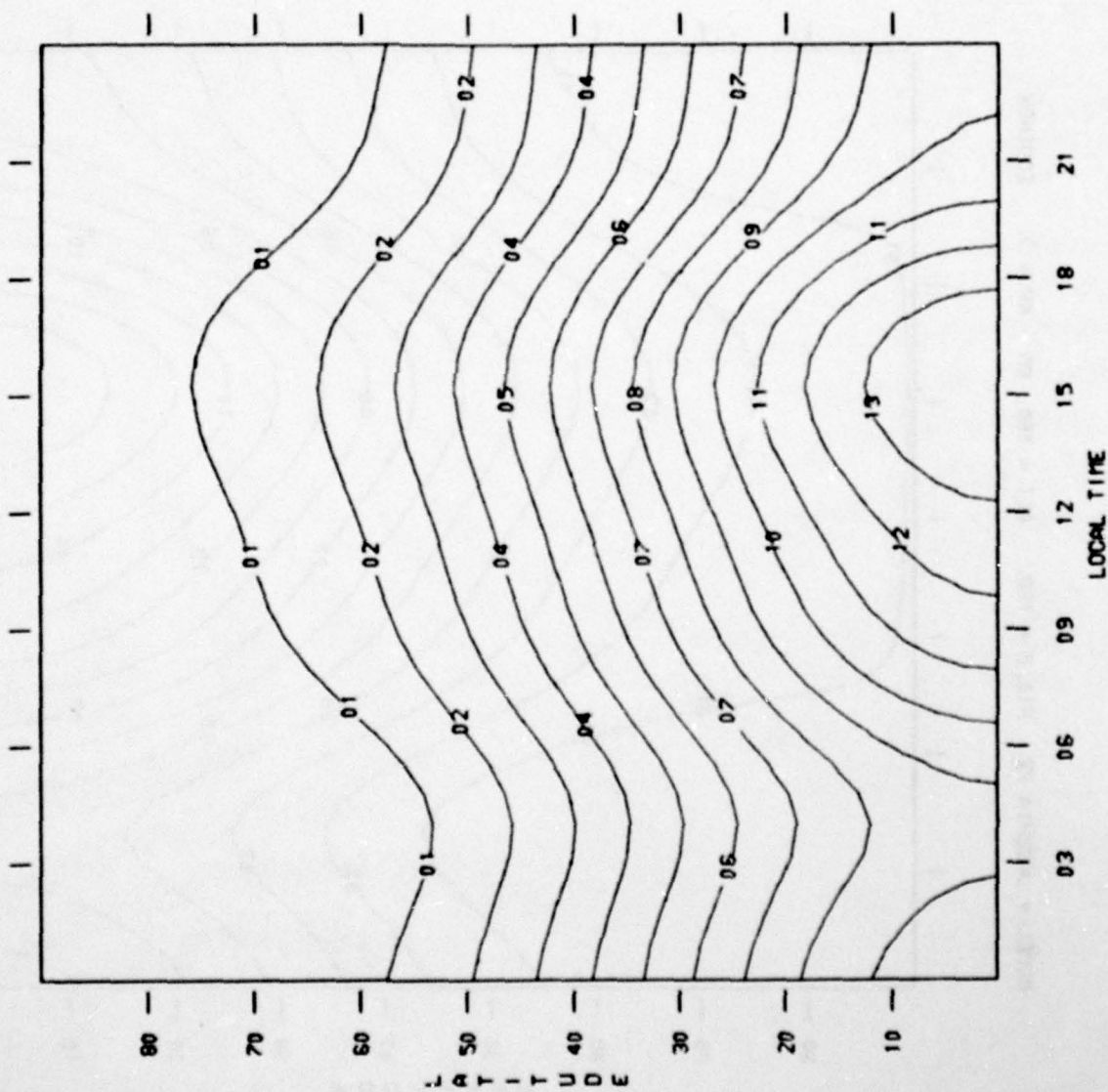
MODEL = JACCHIA 77 F10.7 = 70. ALT = 400. KM KP = 2. EQUINOX



GM/CN=3

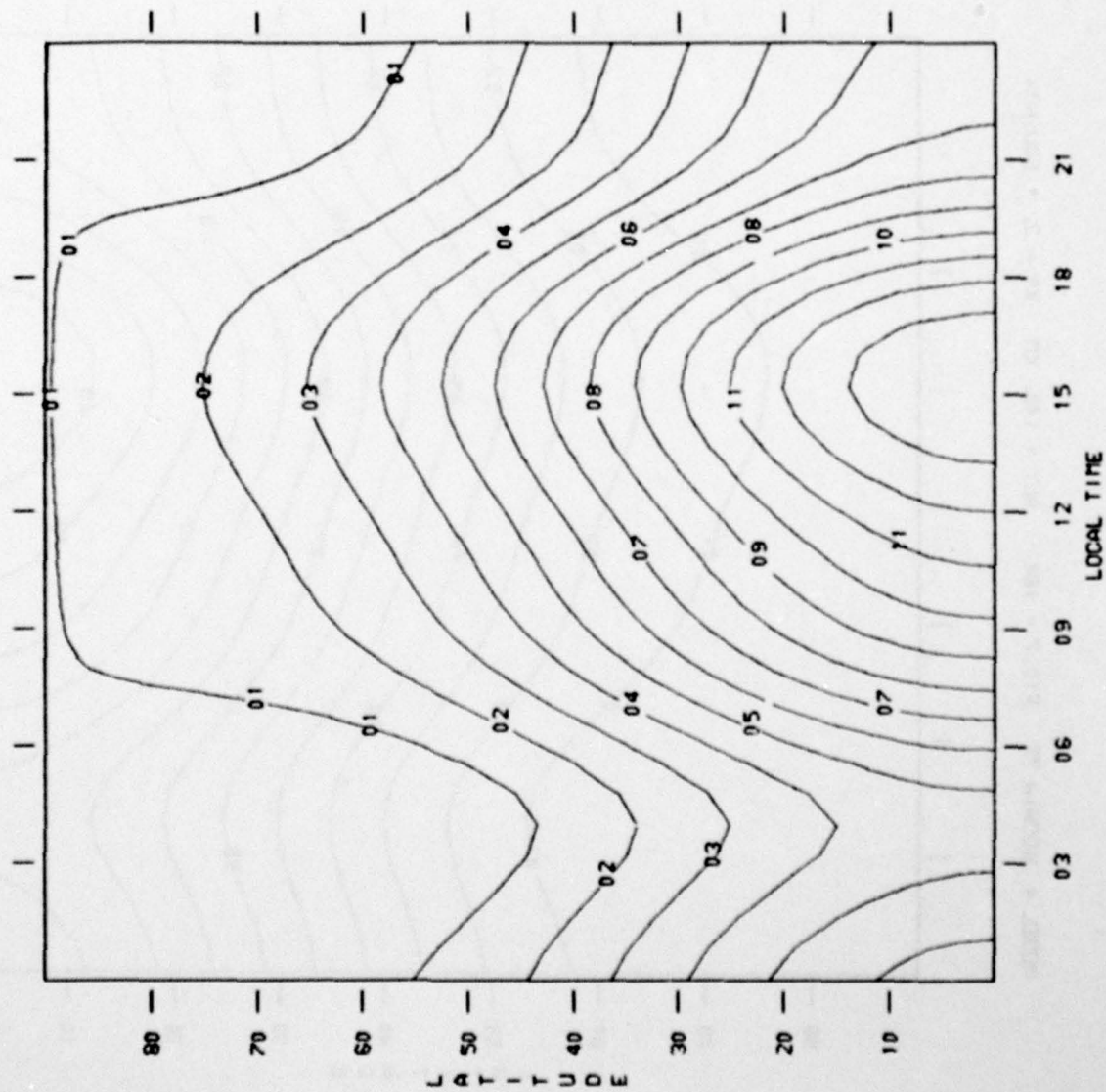
14 = 1.70E-15
 13 = 1.60E-15
 12 = 1.51E-15
 11 = 1.41E-15
 10 = 1.32E-15
 09 = 1.22E-15
 08 = 1.13E-15
 07 = 1.03E-15
 06 = 9.40E-16
 05 = 8.45E-16
 04 = 7.50E-16
 03 = 6.56E-16
 02 = 5.61E-16
 01 = 4.66E-16
 00 = 3.71E-16

MODEL = JACCHIA 77 F10.7 = 180. ALT = 140. KM KP = 2. EQUINOX



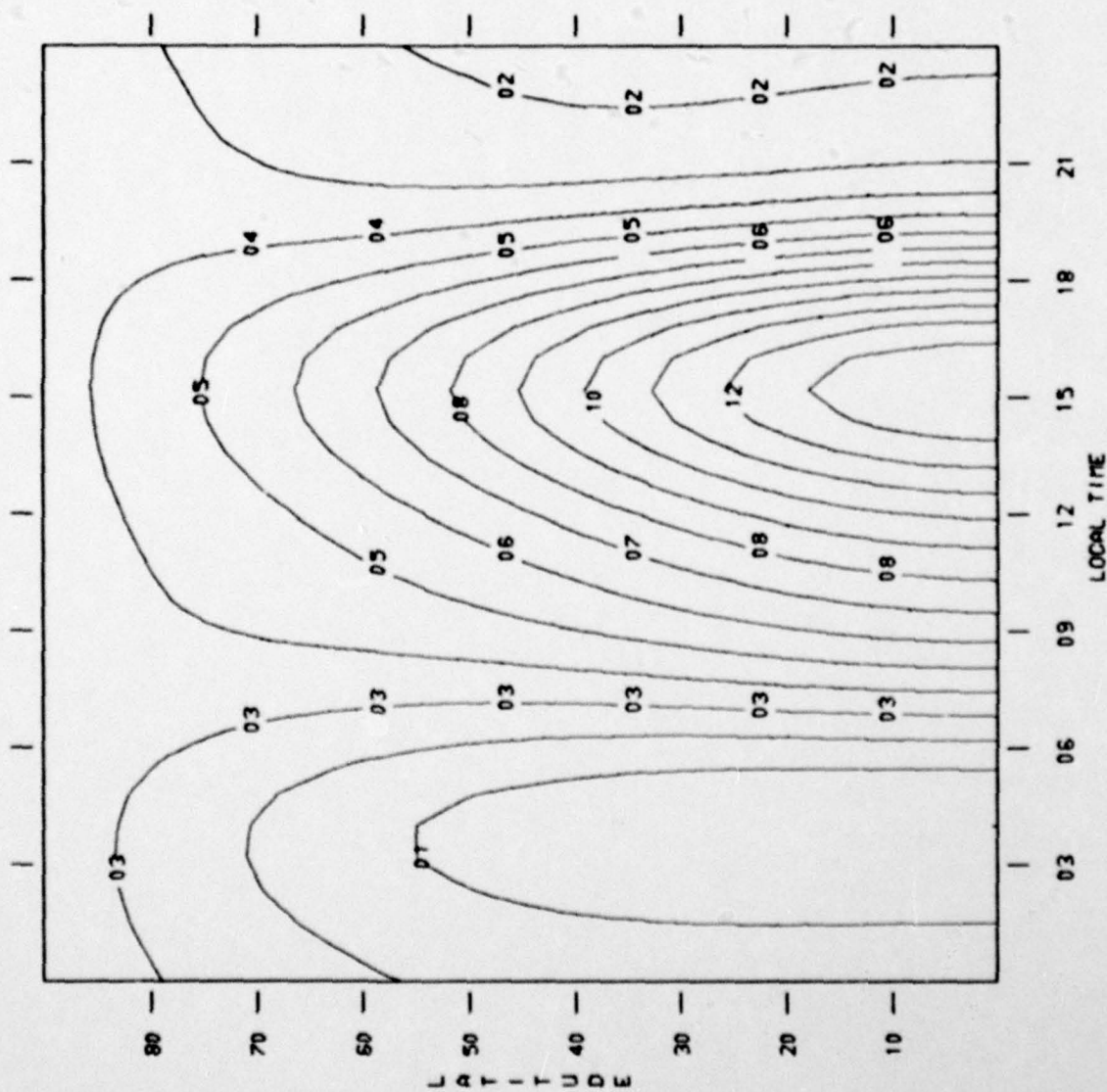
14 = 4.87E-12
 13 = 4.81E-12
 12 = 4.74E-12
 11 = 4.67E-12
 10 = 4.60E-12
 09 = 4.53E-12
 08 = 4.46E-12
 07 = 4.39E-12
 06 = 4.32E-12
 05 = 4.25E-12
 04 = 4.18E-12
 03 = 4.11E-12
 02 = 4.04E-12
 01 = 3.97E-12
 00 = 3.90E-12

MODEL = JACCHIA 77 F10.7 = 180. ALT = 180. KM KP = 2. EQUINOX



CM/CITE3
14 = 8.09E-13
13 = 7.94E-13
12 = 7.79E-13
11 = 7.64E-13
10 = 7.49E-13
09 = 7.34E-13
08 = 7.19E-13
07 = 7.03E-13
06 = 6.88E-13
05 = 6.73E-13
04 = 6.58E-13
03 = 6.43E-13
02 = 6.28E-13
01 = 6.13E-13
00 = 5.98E-13

MODEL = JACCHIA 77 F10.7 = 180. ALT = 400. KM KP = 2. EQUINOX



CM/CHW3

- 14 = 1.09E-14
- 13 = 1.04E-14
- 12 = 9.94E-15
- 11 = 9.46E-15
- 10 = 8.98E-15
- 09 = 8.50E-15
- 08 = 8.02E-15
- 07 = 7.54E-15
- 06 = 7.06E-15
- 05 = 6.58E-15
- 04 = 6.10E-15
- 03 = 5.62E-15
- 02 = 5.14E-15
- 01 = 4.66E-15
- 00 = 4.18E-15

V. REFERENCES

Anon., Geophysical Model, Lockheed Missiles and Space Co. Rep. SS-T61-43, 1961.

Bruce, R. W., "A Survey of Model Atmospheres Used in the Analysis of Satellite Orbits,"
Rept. No. TOR-469(5540-10)-2, The Aerospace Corp., El Segundo, Calif., 1965.

Bruce, R. W., "An Atmospheric Density Model Recommended for Analyses of Low
Altitude Satellite Orbits," The Aerospace Corporation, TOR-1001(2110-01)-8,
1966.

Bruce, R. W., "Upper Atmosphere Density Determined from LOGACS," Space Res. XII,
Akademie-Verlag, Berlin, 1972.

Ching, B. K., and V. L. Carter, "Ion Gauge Measurements of Latitudinal Density
Variations at Night," Geophys. Res. Lett., 1, 93, 1974.

CIRA 1961, COSPAR International Reference Atmosphere, 1961, North-Holland
Publishing Co., Amsterdam, 1961.

CIRA 1965, COSPAR International Reference Atmosphere, 1965, North-Holland
Publishing Co., Amsterdam, 1965.

CIRA 1972, COSPAR International Reference Atmosphere, 1972, Akademie-Verlag,
Berlin, 1972.

COESA, U. S. Standard Atmosphere, 1962, U. S. Government Printing Office, Washington, D. C., 1962.

COESA, U. S. Standard Atmosphere, 1976, U. S. Government Printing Office, Washington, D. C., 1976.

Frank, L. A., "Plasma in the Earth's Polar Magnetosphere," J. Geophys. Res., 76, 5202, 1971.

Harris, I. and W. Priester, "Time-Dependent Structure of the Upper Atmosphere," J. Atmos. Sci., 19, 286, 1962a.

Harris, I. and W. Priester, "Theoretical Models for the Solar-Cycle Variation of the Upper Atmosphere," J. Geophys. Res., 67, 4585, 1962b.

Hedin, A. E., H. G. Mayr, C. A. Reber, N. W. Spencer and G. R. Carignan, "Empirical Model of Global Thermospheric Temperature and Composition Based on Data from the OGO-6 Quadrupole Mass Spectrometer," J. Geophys. Res., 79, 215, 1974.

Hedin, A. E., J. E. Salah, J. V. Evans, C. A. Reber, G. P. Newton, N. W. Spencer, D. C. Kayser, D. Alcayde, P. Bauer, L. Cogger, and J. P. McClure, "A Global Thermospheric Model Based on Mass Spectrometer and Incoherent Scatter Data MSIS 1. N₂ Density and Temperature," J. Geophys. Res., 82, 2139, 1977.

- Hedin, A. E., C. A. Reber, G. P. Newton, N. W. Spencer, H. C. Brinton, H. G. Mayr and W. E. Potter, "A Global Thermospheric Model Based on Mass Spectrometer and Incoherent Scatter Data MSIS 2. Composition," J. Geophys. Res., 82, 2148, 1977.
- Heikkila, W. J., "Auroral Emissions and Particle Precipitation in the Noon Sector," J. Geophys. Res., 77, 4100, 1972.
- Jacchia, L. G., "A Variable Atmospheric Density Model From Satellite Accelerations," J. Geophys. Res., 65, 2775, 1960.
- Jacchia, L. G., "Static Diffusion Models of the Upper Atmosphere with Empirical Temperature Profiles," Smithsonian Contrib. Astrophys., 8, 215, 1965.
- Jacchia, L. G. "New Static Models of the Thermosphere and Exosphere with Empirical Temperature Profiles," Smithsonian Astrophys. Obs. Spec. Rep. No. 313, Cambridge, Mass., 1970.
- Jacchia, L. G., "Revised Static Models of the Thermosphere and Exosphere with Empirical Temperature Profiles," Smithsonian Astrophys. Obs. Spec. Rep. No. 332, Cambridge, Mass., 1971.
- Jacchia, L. G., "Thermospheric Temperature, Density, and Composition: New Models," Smithsonian Astrophys. Obs. Spec. Rep. No. 375, Cambridge, Mass., 1977.
- Minzner, R. A., K.S.W. Champion and H. L. Pond, "The ARDC Model Atmosphere, 1959," Air Force Surveys in Geophysics No. 115, ARCRC-TR-59-267, 1959.

- Hedin, A. E., C. A. Reber, G. P. Newton, N. W. Spencer, H. C. Brinton, H. G. Mayr and W. E. Potter, "A Global Thermospheric Model Based on Mass Spectrometer and Incoherent Scatter Data MSIS 2. Composition," J. Geophys. Res., 82, 2148, 1977.
- Heikkila, W. J., "Auroral Emissions and Particle Precipitation in the Noon Sector," J. Geophys. Res., 77, 4100, 1972.
- Jacchia, L. G., "A Variable Atmospheric Density Model From Satellite Accelerations," J. Geophys. Res., 65, 2775, 1960.
- Jacchia, L. G., "Static Diffusion Models of the Upper Atmosphere with Empirical Temperature Profiles," Smithsonian Contrib. Astrophys., 8, 215, 1965.
- Jacchia, L. G. "New Static Models of the Thermosphere and Exosphere with Empirical Temperature Profiles," Smithsonian Astrophys. Obs. Spec. Rep. No. 313, Cambridge, Mass., 1970.
- Jacchia, L. G., "Revised Static Models of the Thermosphere and Exosphere with Empirical Temperature Profiles," Smithsonian Astrophys. Obs. Spec. Rep. No. 332, Cambridge, Mass., 1971.
- Jacchia, L. G., "Thermospheric Temperature, Density, and Composition: New Models," Smithsonian Astrophys. Obs. Spec. Rep. No. 375, Cambridge, Mass., 1977.
- Minzner, R. A., K.S.W. Champion and H. L. Pond, "The ARDC Model Atmosphere, 1959," Air Force Surveys in Geophysics No. 115, ARCRC-TR-59-267, 1959.

- Minzner, R. A., C. A. Reber, L. G. Jacchia, F. T. Huang, A. E. Cole, A. J. Keneshea, S. P. Zimmerman, and J. M. Forbes, "Defining Constants, Equations, and Abbreviated Tables of the 1975 U.S. Standard Atmosphere," NASA Tech. Rep. R-459, 1976.
- Minzner, R. A., "The 1976 Standard Atmosphere and Its Relationship to Earlier Standards," Revs. of Geophys. and Space Phys., 15, 375, 1977.
- Moe, O. K., "Indirect Energy Sources and Sinks in the Thermosphere and Mesosphere," McDonnell Douglas Astronautics Company, Report MDC-G2280, 1971.
- Nicolet, M., "Density of the Heterosphere Related to Temperature," Smithsonian Astrophys. Obs. Spec. Rep. No. 75, Cambridge, Mass., 1961.
- Olson, W. P., "Study of Particle Precipitation as an Energy Source in the Atmosphere," McDonnell Douglas Rep. MDC-G2281, 1971.
- Olson, W. P., "Corpuscular Radiation as an Upper Atmospheric Energy Source," Space Research XII, Akademie-Verlag, Berlin, 1972a.
- Olson, W. P., K. A. Pfitzer, and O. K. Moe, "Response of the Magnetosphere and Atmosphere to the Solar Wind," Final Scientific Report for Contract F44620-72-C-0084, McDonnell Douglas Astronautics Company, Huntington Beach, Calif., 1975.
- Sharp, L. R., D. R. Hickman, C. J. Rice and J. M. Straus, "The Altitude Dependence of the Local Time Variation of Thermospheric Density," Geophys. Res. Lett., in press, 1978.

von Zahn, U., "Neutral Air Density and Composition at 150 Kilometers," J. Geophys.

Res., 75, 5517, 1970.

von Zahn, U., W. Kohnlein, K. H. Fricke, U. Laux, H. Trinks and H. Volland, "ESRO-4

Model of Global Thermospheric Composition and Temperatures During Times of

Low Solar Activity," Geophys. Res. Lett., 4, 33, 1977.

Walker, J.C.G., "Analytical Representation of Upper Atmosphere Densities Based on

Jacchia's Static Diffusion Models," J. Atmos. Sci., 22, 462, 1965.

LABORATORY OPERATIONS

The Laboratory Operations of The Aerospace Corporation is conducting experimental and theoretical investigations necessary for the evaluation and application of scientific advances to new military concepts and systems. Versatility and flexibility have been developed to a high degree by the laboratory personnel in dealing with the many problems encountered in the nation's rapidly developing space and missile systems. Expertise in the latest scientific developments is vital to the accomplishment of tasks related to these problems. The laboratories that contribute to this research are:

Aerophysics Laboratory: Launch and reentry aerodynamics, heat transfer, reentry physics, chemical kinetics, structural mechanics, flight dynamics, atmospheric pollution, and high-power gas lasers.

Chemistry and Physics Laboratory: Atmospheric reactions and atmospheric optics, chemical reactions in polluted atmospheres, chemical reactions of excited species in rocket plumes, chemical thermodynamics, plasma and laser-induced reactions, laser chemistry, propulsion chemistry, space vacuum and radiation effects on materials, lubrication and surface phenomena, photo-sensitive materials and sensors, high precision laser ranging, and the application of physics and chemistry to problems of law enforcement and biomedicine.

Electronics Research Laboratory: Electromagnetic theory, devices, and propagation phenomena, including plasma electromagnetics; quantum electronics, lasers, and electro-optics; communication sciences, applied electronics, semiconducting, superconducting, and crystal device physics, optical and acoustical imaging; atmospheric pollution; millimeter wave and far-infrared technology.

Materials Sciences Laboratory: Development of new materials; metal matrix composites and new forms of carbon; test and evaluation of graphite and ceramics in reentry; spacecraft materials and electronic components in nuclear weapons environment; application of fracture mechanics to stress corrosion and fatigue-induced fractures in structural metals.

Space Sciences Laboratory: Atmospheric and ionospheric physics, radiation from the atmosphere, density and composition of the atmosphere, aurorae and airglow; magnetospheric physics, cosmic rays, generation and propagation of plasma waves in the magnetosphere; solar physics, studies of solar magnetic fields; space astronomy, x-ray astronomy; the effects of nuclear explosions, magnetic storms, and solar activity on the earth's atmosphere, ionosphere, and magnetosphere; the effects of optical, electromagnetic, and particulate radiations in space on space systems.

THE AEROSPACE CORPORATION
El Segundo, California